Synthesis and Evaluation of Modified Oximidine Analogues as
Anticancer Agents and of
Terephthalaldehyde-*bis*-Guanylhydrazones as Endotoxin
Sequestering Agents

BY

© 2009
Kriangsak Khownium

Submitted to the graduate degree program in Medicinal Chemistry
and the Graduate Faculty of the University of Kansas
in partial fulfillment of the requirements for the degree of
Doctor of Philosophy.

Dissertation Committee:

_____

Chair

_____

_____

_____

_____

Date Defended: _____

The Dissertation Committee for Kriangsak Khownium certifies that this is the
approved version of the following dissertation:

Synthesis and Evaluation of Modified Oximidine Analogues as Anticancer Agents and of Terephthalaldehyde-*bis*-Guanylhydrazones as Endotoxin Sequestering Agents

Dissertation Committee:

_____

Chair

_____

_____

_____

_____

Date Approved: _____

Abstract:

Synthesis and Evaluation of Modified Oximidine Analogues as
Anticancer Agents

Kriangsak Khownium

The University of Kansas, 2009

Chapter 1 – Design and Synthesis of a Core-Modified Oximidine Analogue

The natural products oximidine I and II are potent and selective anticancer agents at nanomolar concentrations. They were isolated in 1999 from the fermentation broth of *Pseudomonas sp.* Q52002 by Hayakawa and co-workers. Their structures and potent cytotoxicity are similar to the recently discovered natural products salicylihalamides, apicularens, and lobatamides, which are members of the benzolactone enamide family.

In order to explore the biological activity of oximidine II, we have investigated the formation of the triene macrocycle of oximidine using a RCM procedure, and the reductive copper-mediated macrocycle formation. We observed the limitation of RCM for the formation of the triene macrocycle. The chiral pool approach, using D-glucal, was explored as an alternative route to prepare the *cis*-diene for RCM. The reductive copper-mediate protocol provided a better result. To facilitate the preparation of oximidine analogs, we also have chosen a simplified scaffold based on a quantitative structure-activity relationship (QSAR) analysis using

the comparative molecular similarity indices analysis (CoMSIA) model reported by Georg et al. in 2006. We prepared by total synthesis oximidine analogues that carry a vinyl sulfone, a boronic acid and an α-keto oxadiazole instead of the enamide side chain.

Chapter 2 – Novel Oximidine Analogues with Improved Stability as Anticancer Agents

Structure-activity relationship (SAR) studies for the benzolactone enamide family, including oximidine II, have demonstrated that the enamide side chain is crucial for their anticancer activity. However, it is believed that the enamide will be labile under physiological conditions. *This has led to our hypothesis that the replacement of the enamide moiety with a stable warhead will allow the discovery of novel anticancer agents with improved pharmacokinetics.*

We selected three different warheads that are likely to be stable under physiological conditions and that could undergo nucleophilic addition like the enamide. All new analogs were tested for cell growth inhibition against four human cancer cell lines: leukemia (HL-60), breast (MCF-7), and melanoma (SK-MEL-28 and SK-MEL-5). The results showed that these analogs were micromolar inhibitors in the range of 20 μM – 60 μM, except for the α-keto oxadiazole that did not display cytotoxicity toward any of the cell lines.

Chapter 3 – Novel Endotoxin-Sequestering Compounds with Terepthalaldehyde-bis-Guanylhydrazone Scaffolds

Lipopolyamines bind to the lipid A moiety of lipopolysaccharide, a constituent of Gram-negative bacterial membranes, and neutralize its toxicity in animal models of endotoxic shock. In an effort to identify non-polyamine scaffolds with similar endotoxin-recognizing features, we had observed an unusually high frequency of hits containing guanylhydrazone scaffolds in high-throughput screens. We now describe the syntheses and preliminary structure-activity relationships in a homologous series of *bis*-guanylhydrazone compounds decorated with hydrophobic functionalities. These first-generation compounds bind and neutralize lipopolysaccharide with a potency comparable to that of polymyxin B, a peptide antibiotic known to sequester LPS.

Acknowledgements

The attractive course syllabus and the competitive research environment at KU were the key factors in my decision to join the graduate program here. During these years I have grown as a person and as a chemist, and here I would like to express my gratitude to all individuals that helped me in my journey. First and foremost, I would like to thank my family for their support and for being my role model of hard work. Their love and understanding have been the main driving force for pursuing my dream as a chemist. I am deeply grateful to my advisor Professor Gunda Georg for all her support and guidance. Her role has been pivotal in my graduate career.

I would like to express my gratitude to Professor Sunil David for his support during my work on the LPS project. I enjoyed working with the David's group Dr. Stewart Wood, Dr. Rajalakshmi Balakrishna, and Kelly Miller. I would like to thank Professor Gerald Lushington for his advice and the CoMSIA/QSAR analysis for the oximidine project.

I would like to express my gratitude to my dissertation committee members Professor Apurba Dutta, Professor Sunil David, Professor Jon Tunge and Professor Helena Malinakova for their critical role in this important step of my career. In particular, I would like to thank Professors Malinakova, and David to take the time to read my thesis and offer valuable suggestions. I also would like to thank my oral exam committee members Professor Paul Hanson, Professor Richard Givens, Professor Lester Mitscher and Professor Apurba Dutta.

I have enjoyed to do research both at the University of Kansas and the

To my Mom and Dad, and my Uncle

who always believed in hard work and the simple phrase

"The Knowledge is the Power"

Table of Contents

Chapter 1

Design and Synthesis of a Core-Modified Oximidine Analogue

Chapter 2

Novel Oximidine Analogues with Improved Stability as

Anticancer Agents

Chapter 3

Novel Endotoxin-Sequestering Compounds with

Terepthalaldehyde-bis-Guanylhydrazone Scaffolds

Chapter 4

Experimental

Chapter 5

Bibliography

List of Figures

List of Tables

List of Compounds

ix

List of Abbreviations

3D-QSAR – three-dimensional quantitative structure-activity relationship

AcC1 – acetyl chloride

atm – atmosphere

br – broad

(BAIB) – [bis(acetoxy)iodo]benzene

CoMFA – comparative molecular field analysis

CoMSIA – comparative molecular similarity indices analysis

CuTC – copper thiophene carboxylate

d – doublet

DEAD – diethyl azodicarboxylate

DDQ – 2,3-dichloro-4,5-dicyano-1,4-benzoquinone

DIBAL – diisobutylaluminum hydride

DIPEA – *N,N*-diisopropylethylamine

DMF – *N,N*-dimethylformamide

ee – enantiomeric excess

ESI – electrospray ionization

EtOAc – ethyl acetate

Et$_2$O – diethyl ether

g - gram

g – relative centrifugal force

h – hour

HCl – hydrochloric acid

HF – hydrofluoric acid

HMPA - hexamethylphosphoramide

HPLC – high pressure liquid chromatography

Hz – hertz

IR – infrared

KO^{t}Bu – potassium *tert*-butoxide

LG – leaving group

LRMS – low resolution mass spectrometry

m – multiplet

Me – methyl

MeCN – acetonitrile

MeOH – methanol

mg – milligram

MHz – megahertz

min – minute

μL – microliter

mL – milliliter

mmol – millimole

MOM – methoxymethyl

NA – not available

NaHMDS – sodium bis(trimethylsilyl)amide

NaO^{t}Bu – sodium *tert*-butoxide

NaOMe – sodium methoxide

NCI – National Cancer Institute

n-BuLi – lithium-1-butanide

NME – *N*-methylephedrine

NMR – nuclear magnetic resonance

PMB – *p*-methoxybenzyl

PPTS – pyridinium *p*-toluenesulfonate

Py. – pyridine

q – quartet

s – singlet

SAD – Sharpless asymmetric dihydroxylation

t – triplet

TBAF – *n*-tetrabutylammonium fluoride

TBTU – 2-(1H-benzotriazole-1-yl)-1,1,3,3-tetramethylaminiumtetrafluoroborate

TEMPO – 2,2,6,6-tetramethyl-1-piperidinyloxyl

THF – tetrahydrofuran

TLC – thin layer chromatography

V-ATPase – vacuolar-(H^+)-adenosine triphosphatase

Chapter 1

Design and Synthesis of a Core-Modified Oximidine Analogue

1.1 Introduction

Natural products from plants, bacteria, fungi, and marine microorganisms have been used for drug discovery campaigns for decades. Due to the unique and diverse structures, they provided lead compounds for the treatment of cancer, microbial infections, inflammation, hypercholesteremia, and tissue rejection in organ transplantation. It has been estimated that over 58% of all FDA approved drugs are derived from natural products (parent compounds, derivatives, analogues, and mimic).[1] The natural products class of macrolactones, usually originating from polyketide pathways, have been reported to possess a large spectrum of biological activity such as insecticidal, antibiotic, and anticancer. These properties account for the conformational equilibrium between preorganization and flexibility to direct the appropriate orientation of polar and non-polar groups to the biological binding pocket.[2, 3]

Macrocyclic benzolactone enamides such as salicylihalamides,[3, 4] lobatamides, [5, 6] apicularen,[7] and oximidines[8-10] show a unique cytotoxicity profile towards the NCI 60-cell line, suggesting a novel mechanism. Mammalian vacuolar ATPase (V-ATPase) enzymes have been identified as the biological target of these natural products. The natural products oximidines I and II are potent and selective anticancer agents at nanomolar concentrations. They were isolated in 1999 from the

fermentation broth of *Pseudomonas sp.* Q52002 by Hayakawa and co-workers.[8]
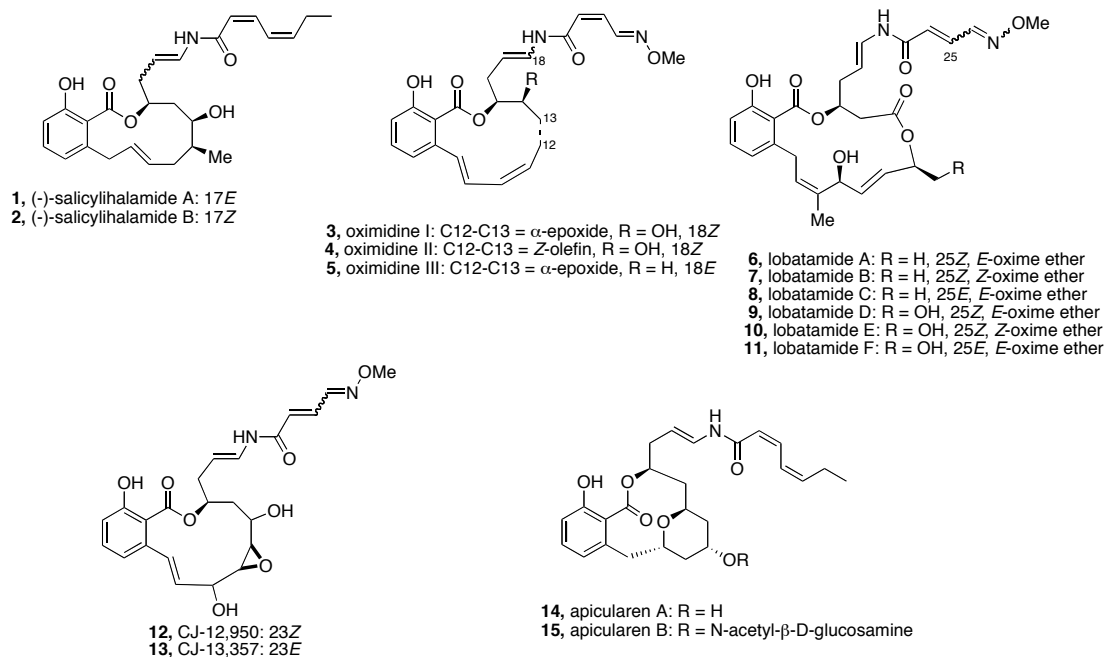
Figure 1. Macrocycle benzolactone enamide family

This class of compounds has drawn great interest in the synthetic and medicinal chemistry community due to their unique biological activity as well as intriguing molecular structure. The 12-membered macrocycle with a triene system in oximidine II, and the vinylic epoxide in oximidine I are the key synthetic challenge. Commonly used macrocyclization procedures including macrolactonization, ring closing metathesis (RCM) allowed the formation of the 12-membered ring only in modest yield.[11-13] To add to the challenge, all natural products of this class contain an acid sensitive enamide side chain.[13] A tremendous effort has been devoted to the development of new synthetic methodologies for the preparation of this class of

compounds.[11-15] A brief review of each approach and total synthesis is included in this chapter.

1.2 Previous synthetic studies of oximidines

1.2.1 The Maier Approach[11]

Maier and Scheufler reported the synthesis of a macrocycle model system lacking the conjugated diene/triene by using as key synthetic steps a sequence involving a Stille coupling[16] and a Yamaguchi macrolactonization[17], Scheme 1.
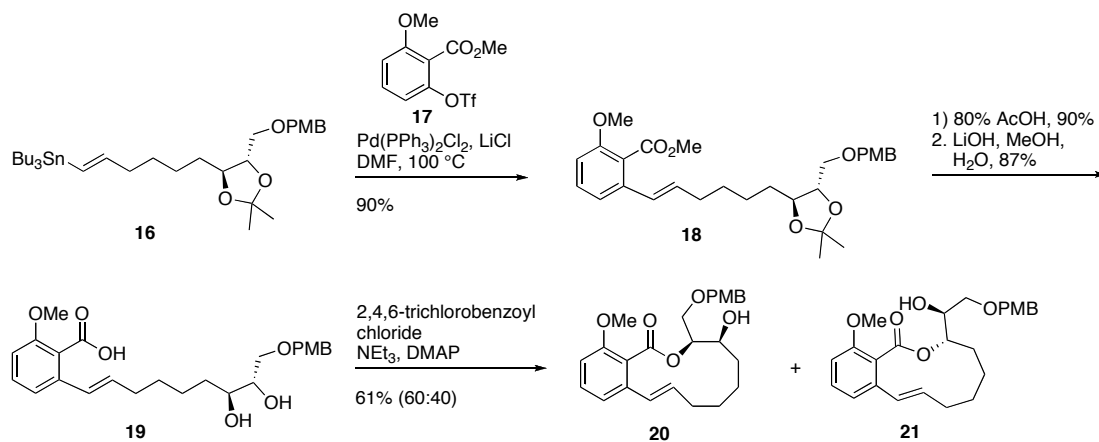
Scheme 1. Maier and Scheufler approach

The Stille coupling of vinyl stannane **16** with triflate **17** provided styrene **18**. After acetal deprotection and ester hydrolysis, the intermediate was subjected to Yamaguchi macrolactonization to provide a mixture of lactones **20** and **21** in a 3:2 ratio in a 61% combined yield.
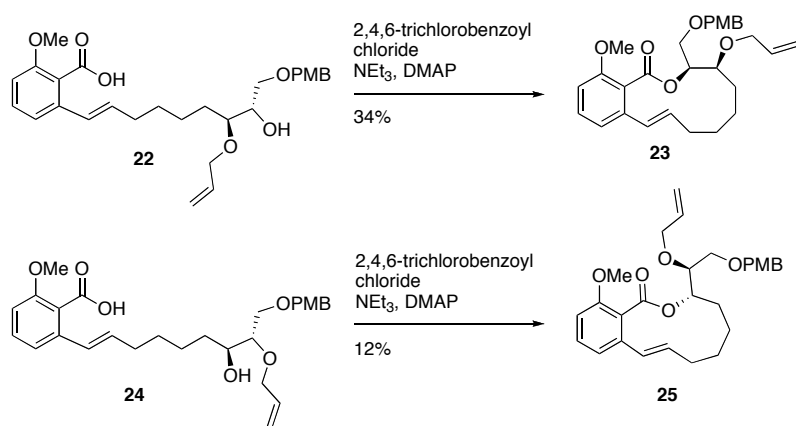
Scheme 2. Maier and Scheufler Approach for Yamaguchi macrolactonization

The preference for a 12-membered ring product, **23,** over an 11-membered ring product, **25**, was driven by both thermodynamic and kinetic factors.[18, 19] Interestingly, macrocyclization attempts with a di-protected alcohol led to much lower yield.

1.2.2 The Coleman Approach[12]

Coleman and Garg used the Miura-modified Castro-Stephens reaction[20] for the coupling of a vinyl iodide and an alkyne to form enyne or dienyne 12-membered macrocycles.[12] The reactions of the intermediates **26**, **29,** and **32** with a catalytic amount of CuI, triphenylphosphine and K$_2$CO$_3$ in DMF at 120 °C provided the desired products in modest yield; however, the epoxide lactone **35** failed to deliver the desired product, Scheme 3. This might be due to the instability of the epoxide. The resulting intermediates were subjected to Boland reduction[21] to afford the (*E,Z*)-diene **28**, **34** and (*E,Z,Z*)-triene **31** macrocycles. The modest yield for the copper-mediated macrocyclization might be due to the strain of the ring system.

Computational modeling of **30** (MMX force field) showed an out-of-plane bending of the alkyne approximately 25° from linearity.[12]
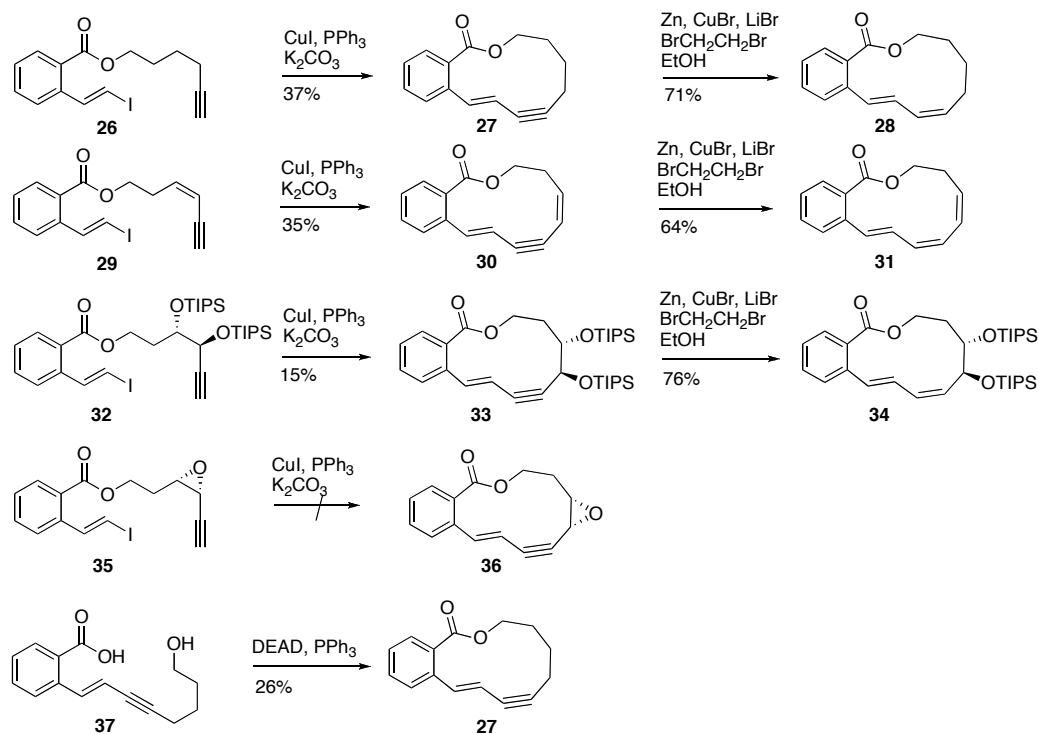
Scheme 3. Coleman and Garg approach

1.2.3 The Taylor Approach[14]

Taylor's group reported the first synthesis of the epoxide-containing macrolactone of oximidine I by using the intramolecular Horner–Wadsworth–Emmons (HWE) olefination[22-24] as the macrocyclization step.
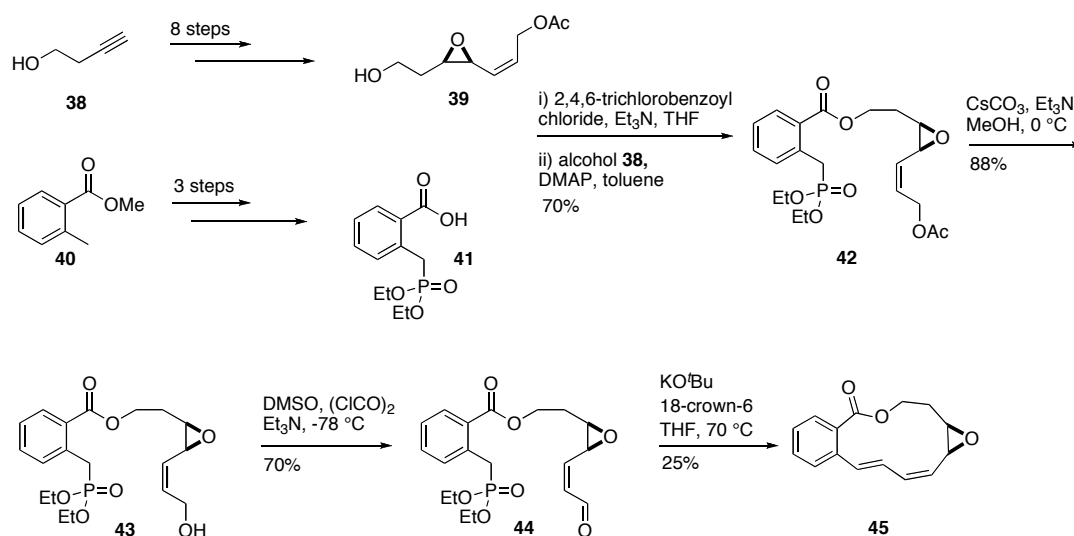
Scheme 4. Taylor approach toward the epoxy macrocycle of oximidine I

The commercially available 3-butyn-1-ol was used to prepare the *cis*-epoxy alcohol **39** in eight steps, and the phosphonate aryl acid **41** was prepared from methyl 2-methylbenzoate in three steps. After Yamaguchi-type activation of the aryl-acid **41**, the alcohol **39** was added to obtain the intermediate **42** in 70% yield. The acetate group of **42** was cleaved in the presence of $CsCO_3$ and Et_3N in MeOH at 0 °C to provide the primary alcohol **43**. Subsequent Swern oxidation furnished aldehyde **44** in good yield. The macrolactone containing epoxide **45** was obtained in 25% from the HWE intramolecular olefination using KO^tBu and 18-crown-6.

1.2.4 The Porco Synthesis of Oximidine II[13]

The first total synthesis of oximidine II was reported by Porco and Wang in 2003. The RCM[25-28] was used for the macrocycle formation of a well defined bis-

diene to construct a highly constrained triene core. The retrosynthetic analysis

revealed three major disconnections as shown in Figure 2.
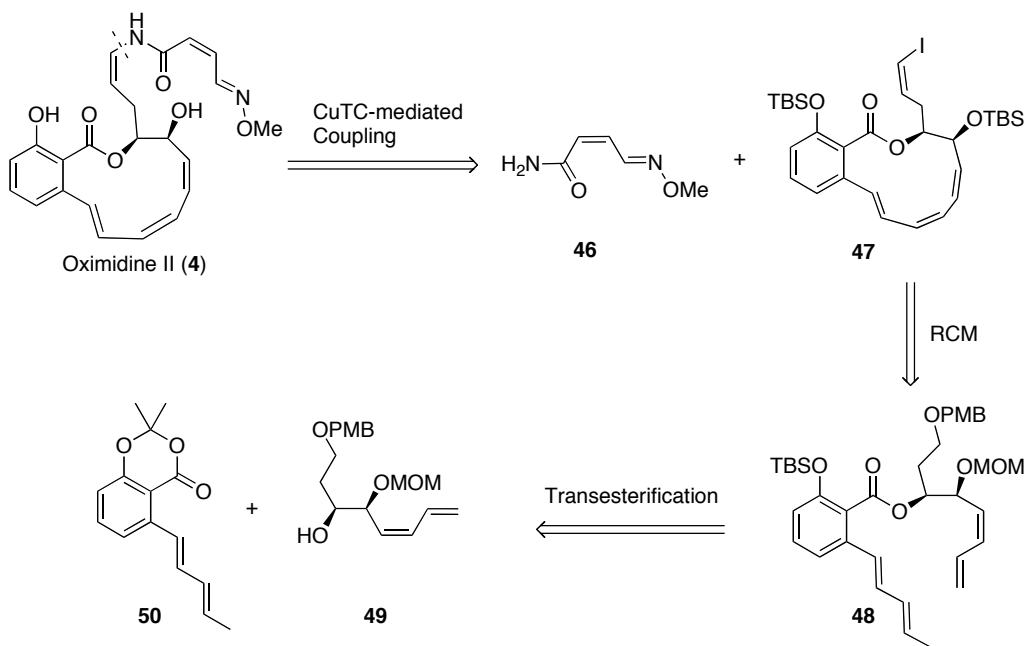
Figure 2. Porco and Wang's retrosynthetic analysis of oximidine II

Copper-mediated amidation[29] of (*Z*)-vinyl iodide **47** and amide **46** was used for the

late stage installation of the enamide side chain. The main task was to deliver the

macrocyclic triene from *bis*-diene intermediate **48** using RCM. Transesterification[30]

between salicylate **50** and diene-alcohol **49** would generate the macrocycle precursor

of *bis*-diene **48**.
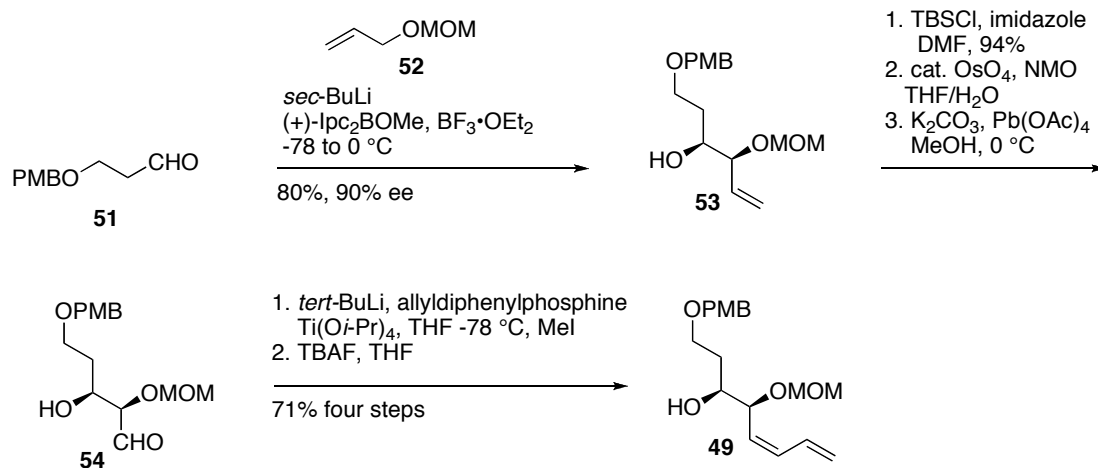
Scheme 5. Porco and Wang diene-alcohol synthesis.

Their asymmetric total synthesis began with the preparation of the diene-alcohol **49** from the enantioenriched alcohol **53**, Scheme 5. The Brown asymmetric allylation[31] of aldehyde **51** and allyl methoxymethyl ether **52** with (+)-*β*-methoxydiisopinocamphenylborane gave (*S,S*)-triol **53** as a single diastereomer with 90% ee. Silylation of the secondary alcohol **53**, followed by the dihydroxylation and *cis*-diol cleavage afforded aldehyde **54** which underwent Yamamoto's protocol[31] to obtain (*Z*)-diene and upon desilylation provided cis-diene **49**.

The diene-acetonide **50** was prepared by the homologation of (*E*)-crotonaldehyde **55** to afford dienyl stannane[32] **56** which was coupled with known triflate[33, 34] **57** under Stille coupling conditions, Scheme 6.[35] Treatment of alcohol **49** with NaHMDS followed by the addition of acetonide **50** afforded the sodium phenolate intermediate which was quenched with TBSCl to give *bis*-diene **48**.
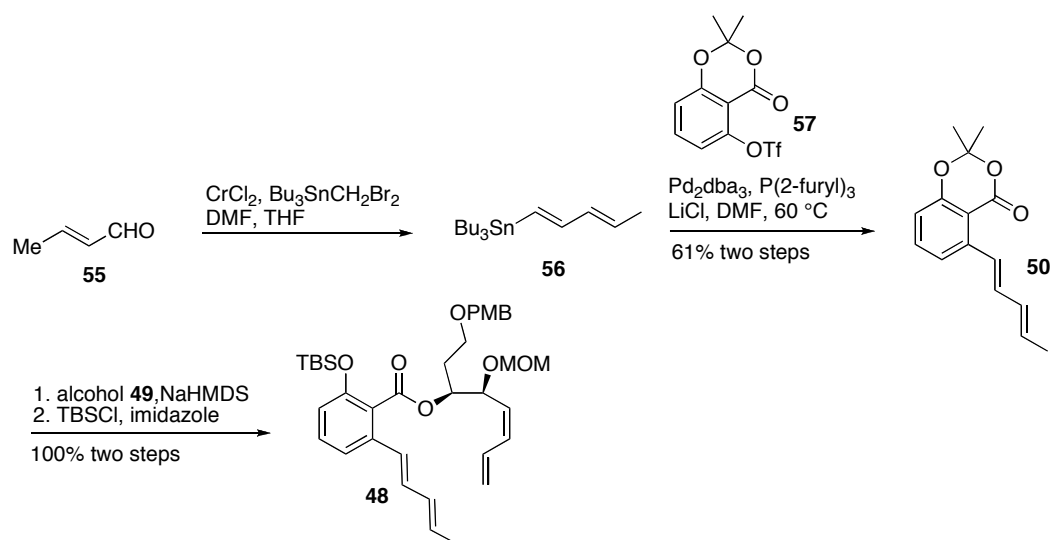
Scheme 6. Porco and Wang *bis*-diene synthesis

The TBS group was strategically placed in order to force a specific conformation which facilitates the macrocycle formation under kinetic control.[13, 36-38] In the absence of TBS, they never observed the product of macrocyclization and only oligomeric products were obtained, Scheme 7.

Scheme 7. Porco and Wang RCM approach for macrocycle triene formation

The first generation Grubbs's catalyst was ineffective under several reaction conditions while the second generation Grubbs's catalyst was able to catalyze the macrocycle formation in 48% overall yield (39% for the first cycle and 9% for the second cycle). Further experimentation showed that prolonged reaction times resulted in decomposition of both starting material and product. It is worth noting that using bis-diene **63** with Grubbs's 1st or 2nd generation catalysts led to a stable complex **64**

from the reaction of ruthenium with the trans-diene with no further progress of the reaction, Scheme 8. Thus the installation of a *trans*-methyl group on the *trans*-diene **48** was needed to force the catalyst to initiate the reaction from the *cis*-diene instead.
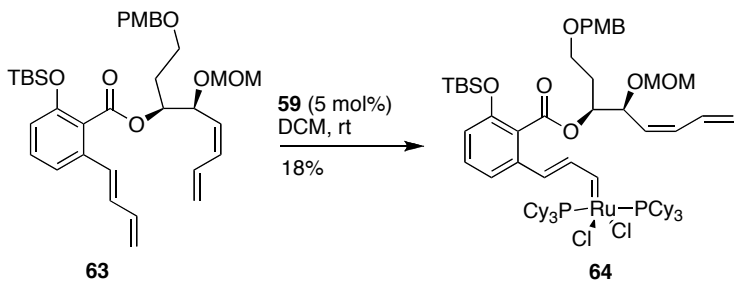
Scheme 8. Porco and Wang synthesis of the stable Ru-complex

To complete the total synthesis, the triene macrocycle **60** was subjected to DDQ oxidative cleavage of the PMB ether and the resulting alcohol was oxidized with pyridinium dichromate. The crude aldehyde was converted to the vinyl iodide **65** as a single isomer using the Stork-Zhao protocol[39] which utilizes the light sensitive iodomethyl(triphenyl)phosphonium iodide salt. Deprotection of the methoxymethyl group followed by silylation afforded (*Z*)-vinyl iodide **47**.
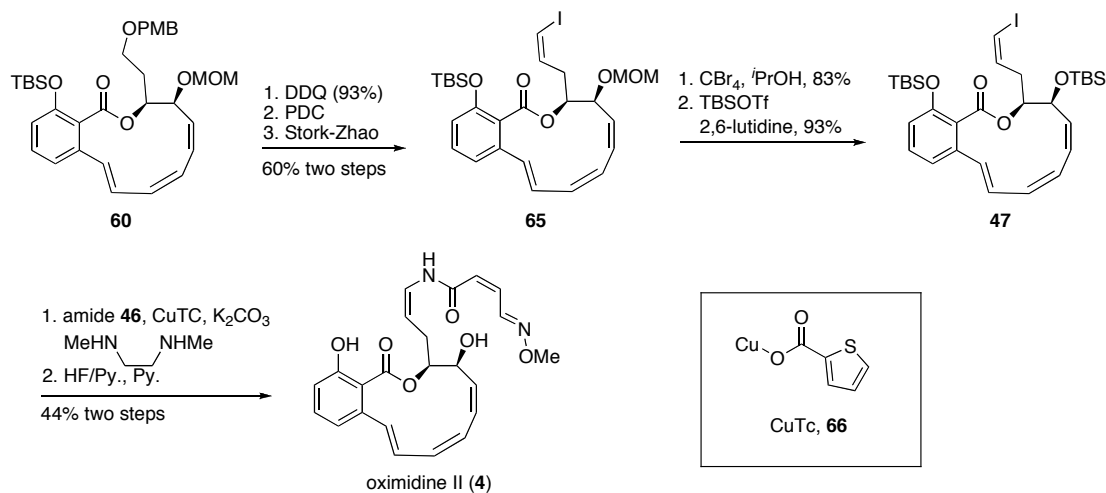
Scheme 9. Porco and Wang completion of the total synthesis of oximidine II

After several model studies, (*Z*)-vinyl iodide **47** was coupled with oxime amide **46** using a stoichiometric amount of copper (II) thiophene carboxylate (CuTC),[40] *N,N*-dimethylethylene diamine and K_2CO_3.[29] The crude amide was desilylated with a buffered solution of HF/pyridine to afford oximidine II (**4**) in 44% yield over the final two steps.

1.2.5 The Porco Synthesis of Oximidine III[41]

The synthesis of oximidine III, bearing an epoxide at C12-C13 is even more challenging as demonstrated by the model studies conducted by Coleman and Taylor.[12, 14] Porco and Wang reported the first total synthesis of oximidine III using RCM as a key step.
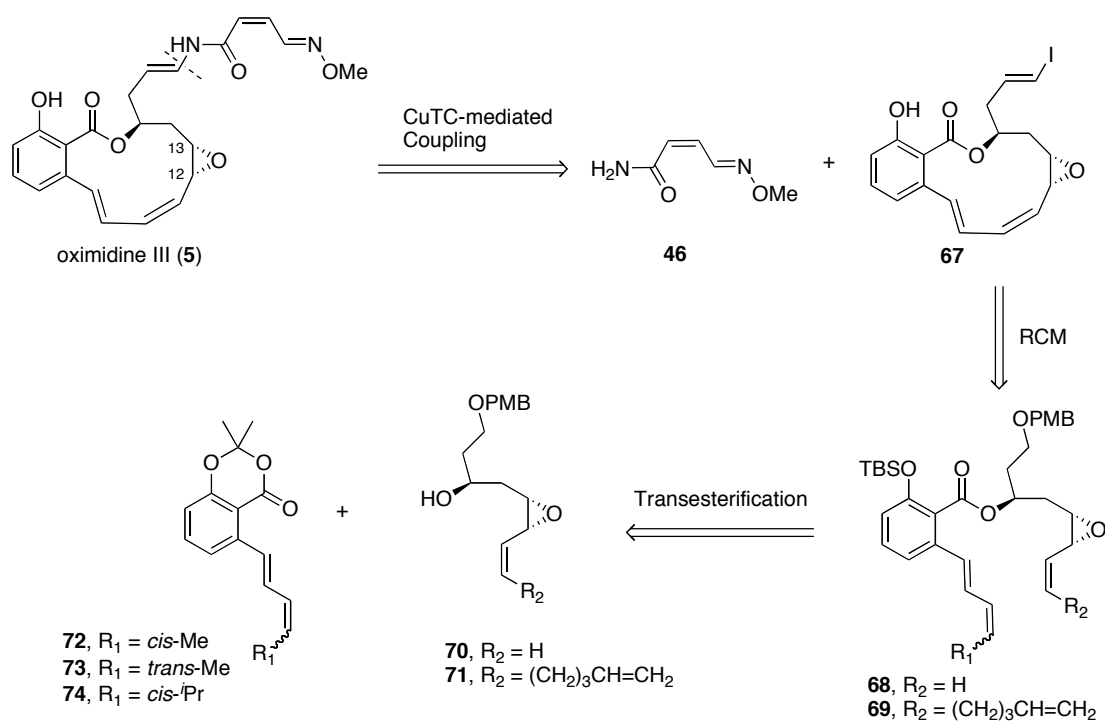
Figure 3. Porco and Wang's retrosynthetic analysis of oximidine III

The retrosynthetic analysis is a similar to the one for oximidine II, Figure 3. Based on their experience with the synthesis of oximidine II, they expected that the ruthenium would react first with the epoxy-ene terminus of the intermediate **68** to form the desired macrocycle. The synthon **69** was also considered since it would allow a Relay ring-closing metathesis (RRCM) and overcome the slow initiation step due to the presence of the vinylic epoxide.[42, 43]
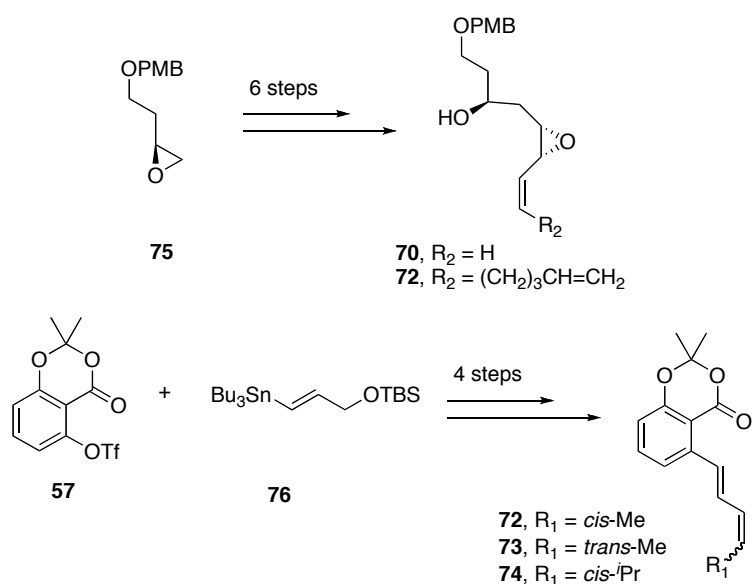
Scheme 10. Porco and Wang synthesis of alcohols and salicylates

The enantio-pure epoxide **75** was generated through a hydrolytic kinetic resolution using Jacobsen's protocol[44] and was then converted to epoxy-ene alcohol and epoxy-diene alcohol fragments **70** and **72** in six steps. The salicylate fragment **72**, **73**, and **74** were prepared in four steps starting with the coupling between triflate **57** and vinyl stannane **76**. The RCM precursors were generated from the transesterifications of the salicylates and the alcohols, followed by protection of the phenolic hydroxy group.

After extensive experimentation for both RCM and RRCM, they found that RRCM gave yields in the range of 30-71% yield when either Grubbs's 2nd generation catalyst or Hoveyda-Grubbs's 2nd generation catalyst were used. Instead, RCM occurred in 12-15% yield with both catalysts. The best result, at 71% yield, was obtained when **78** was used with Hoveyda-Grubbs's 2nd generation catalyst as shown

in Scheme 11.

77

Hoveyda-Grubbs's
2nd Generation Catalyst

RRCM, **77** (10 mol%)

71%
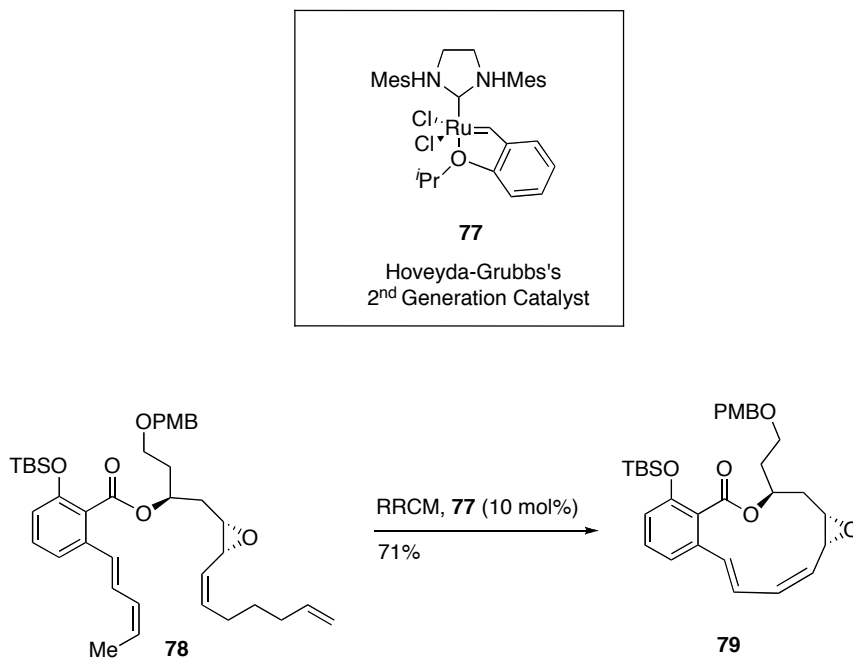
Scheme 11. Porco and Wang RRCM to provide macrocycle of oximidine III

Similar transformations, as employed for the synthesis oximidine II, were used to complete the total synthesis oximidine III.

1.2.6 The Molander Synthesis[45]

Molander and Dehmel reported a formal synthesis of oximidine II in 2004 by synthesizing triene core **80**. The initial proposal is illustrated in the retrosynthetic analysis, Figure **4**. Their success relied on a key macrolactonization step *via* intramolecular Suzuki-coupling using potassium organotrifluoroborates.[46-50]
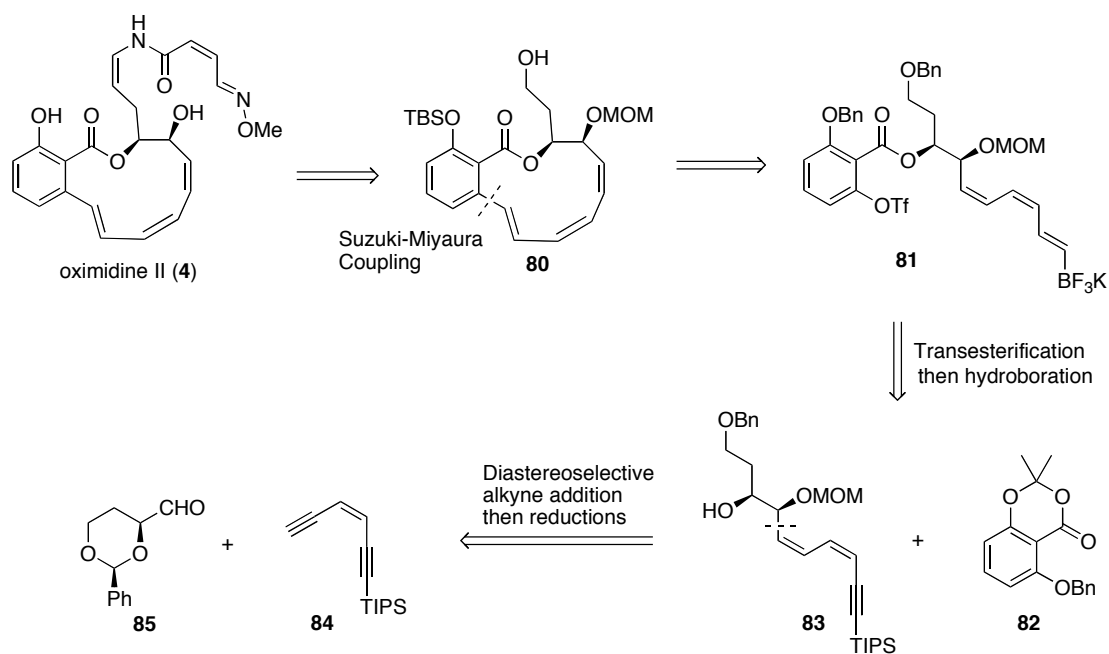
Figure 4. Molander and Dehmel's retrosynthetic analysis of oximidine II

The precursor **81** of the Suzuki macrocyclization has all required double bonds and upon reaction it will be converted into **80**, an intermediate in the Porco's total synthesis. In a similar fashion to Porco's synthesis, a transesterification will be used to couple the salicylate **82** and the alcohol **83**. The diastereoselective chelation-controlled addition of an organometallic nucleophile derived from **84** and a α-chiral aldehyde **85** would install the two stereogenic centers of the required alcohol **83**.
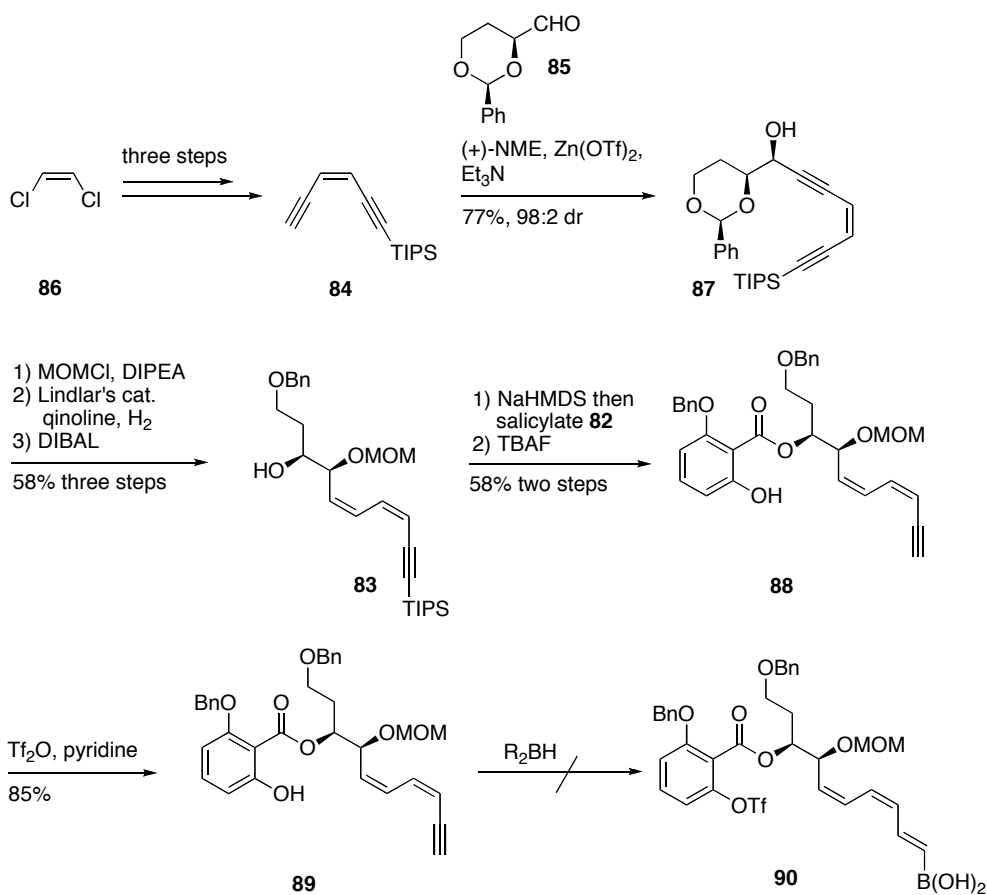
Scheme 12. Molander and Dehmel first generation approach

The synthesis began with the preparation of **84** in three steps employing a double Sonogashira coupling with *cis*-1,2-dichloroethylene.[51-53] The alcohol **87** was prepared by the addition of zinc acetylide to aldehyde[54] **85** (Carreira's protocol)[55-58] in the presence of stoichiometric (+)-*N*-methylephedrine (NME). The resulting alcohol was protected with MOMCl and the selective hydrogenation of the less hindered alkyne followed by the reductive cleavage of the benzylidene acetal (by the coordination of DIBAL to the MOM group)[59] provided selectively the secondary alcohol **83**. Base-mediated transesterification between alcohol **83** and salicylate **82**

was followed by the desilylation of TIPS group to give **88**. The resulting **88** was converted into triflate **89** uneventfully; however, after extensive efforts the hydroboration of the terminal alkyne was unsuccessful.

Therefore it was necessary to change slightly the synthetic sequence. The transesterification between salicylate **92** and alcohol **91** gave the ester **93** followed by hydroboration using Snieckus's reagent[60] to provide the precursor **95** for the macrocyclization. Optimization of the intramolecular Suzuki-Miyaura coupling gave 42% yield in two steps from alkyne **96**. To complete the formal synthesis of oximidine II, protecting group manipulations provided the triene-macrocycle **80** previously synthesized by Porco.
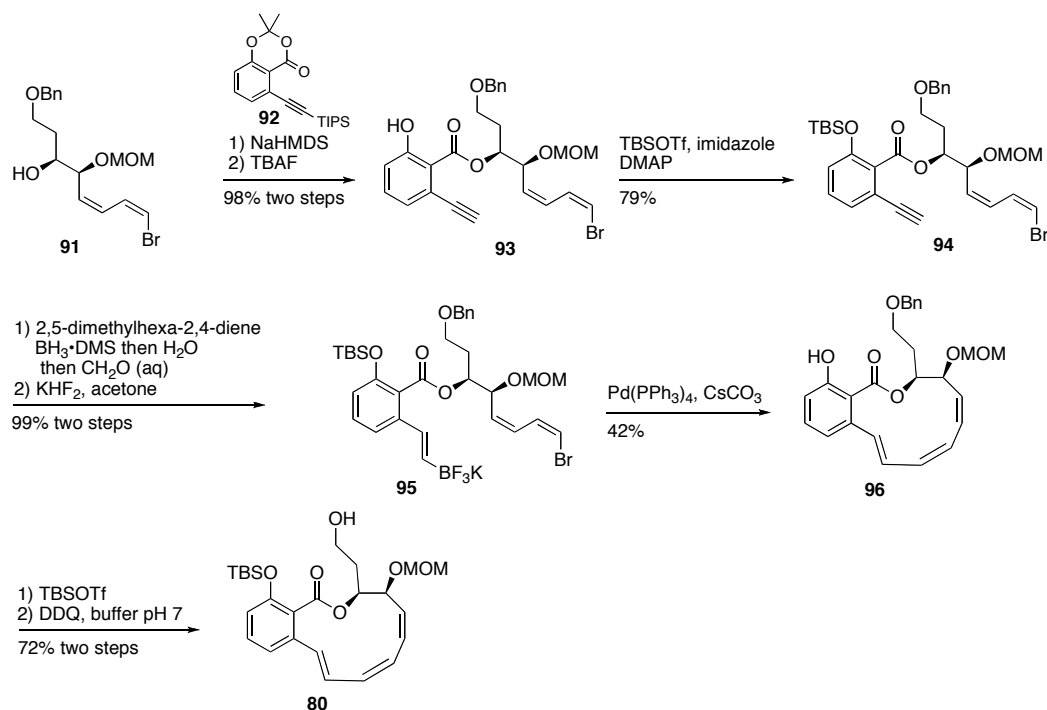
Scheme 13. Molander and Dehmel completion of the formal synthesis of oximidine II

1.2.7 The Georg Synthesis of Oximidine II[15, 61]

In 2003, Georg and co-workers reported a model study towards the synthesis of oximidine I and II using the modified Castro-Stephens conditions previously reported by Coleman and Garg for the ring closing step, in Scheme 14.[15] The reaction did not yield the expected C8-C9 *trans* double bond product, a *cis* double bond of **98** was formed as a major product instead accompanied by 3% yield of the unexpected **99** (unpublished data). A coupling constant of C8-C9 of **98** at 12 Hz and a strong nOe between C8 and C9 was observed which suggested a *Z*-olefin geometry while Coleman and Garg reported *J* value of 16 Hz consistent with an *E*-olefin.[12]
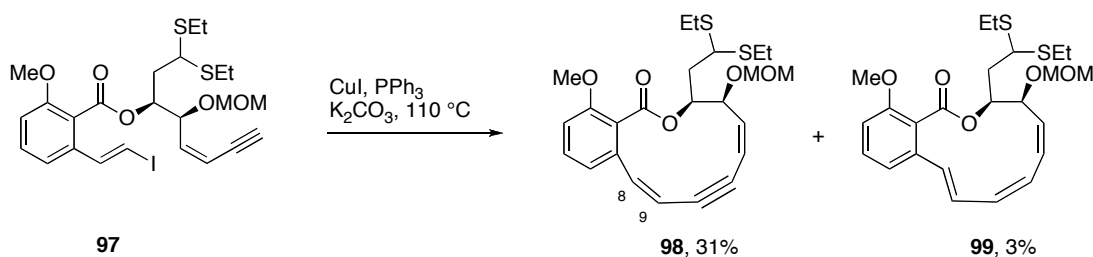
Scheme 14. Georg and Haack approach using Castro-Stephens macrocyclization

This led to the hypothesis that under Castro Stephens conditions, an *E* to *Z* isomerization of the triene occurred under the specific reaction conditions – one equivalent of **97**, 0.10 equivalents CuI, 0.20 equivalents PPh$_3$, 1.75 equivalents K$_2$CO$_3$ in 0.005 M anhydrous DMF heated at 110 °C for 26 h. However, there was no clear explanation for the formation of the triene macrocycle **99** at that time. It was

concluded that the isomerization of the desired product was governed by thermodynamic driving force. This hypothesis is supported by DFT and MP2 calculations, Figure 5.[15] The results showed that the relative energy of the alkyne containing macrocycle **100** is lower than that of **101** by 11-16 kcal/mol. Interestingly, the reduced triene **102** containing the *cis* C8-C9 double bond has higher energy than the (*E,Z,Z*)-macrocycle **103** by 2-5 kcal/mol. Furthermore, the ene-enyne macrocycle **105** with an *E* double bond at C8-C9 showed a lower energy than macrocycle **104** by 7-11 kcal/mol, in agreement with Coleman and Garg's experimental result.

100-*Z,Z*
101-*E,Z*

102-*Z,Z,Z*
103-*E,Z,Z*

104-*Z,Z*
105-*E,Z*
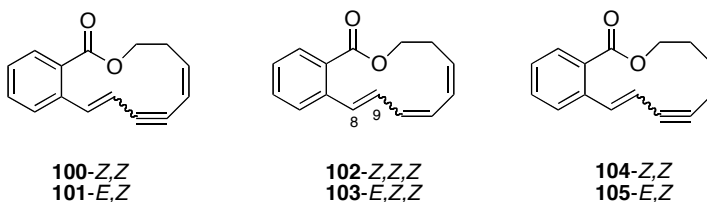
Figure 5. Georg and Haack conformational analysis

After extensive studies on the formation of the unexpected triene **99**, Georg and Schneider developed a novel copper-mediated reductive coupling under Castro-Stephens conditions, which was found to be effective towards the total synthesis of oximidine II.[61]
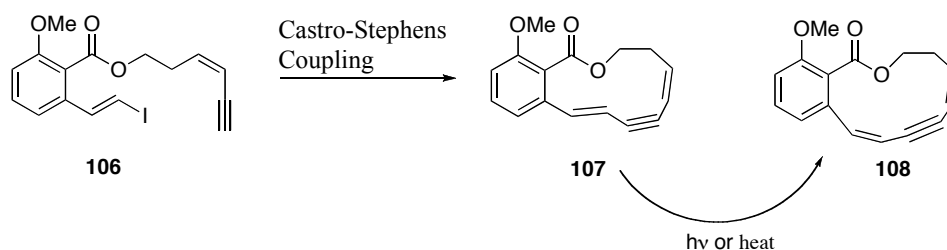
Scheme 15. Georg and Schneider Isomerization of *E* to *Z*-alkene

They observed that both *Z*- and *E*-dienyne isomer products were obtained from the treatment of **106** during the Castro-Stephens reaction in the absence of light. ^{1}H NMR studies showed that the *E*-dienyne **107** product was converted to the *Z*-dienyne **108** after 8 h in a CDCl$_3$ solution at 0 °C. This evidence suggested that the Castro-Stephens reaction is stereospecific. Reductions of dienyne **109** under the Boland reduction gave the (*E,Z,Z*)-triene **110** as predicted from computer modeling. However, there was no reduction of dienyne when a Lindlar catalyst was used.
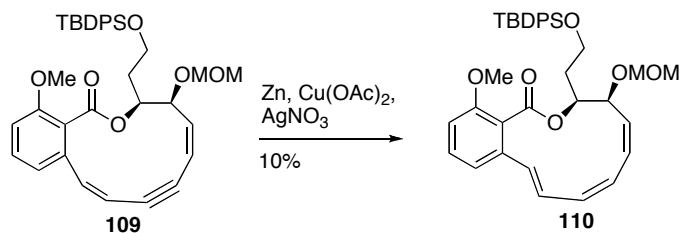
Scheme 16. Georg and Schneider Boland reductions

They proposed that the triene may be formed upon addition of a reducing agent in the presence of the copper catalyst during the Castro-Stephens coupling. Copper hydrides were considered since they are well known in the literature to reduce

alkynes to *cis*-alkenes. The *in situ* generation of Cu-H (Stryker's protocol)[62] provided the desired triene macrocycle at 31% yield, Scheme 17.
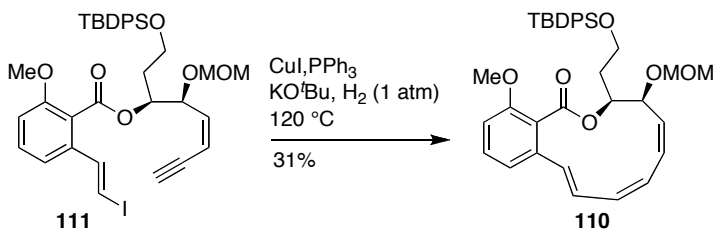
Scheme 17. Georg and Schneider *in situ* generation of Cu-H under Castro-Stephens

After considerable investigations, they discovered that sodium formate can be used as a hydride source for the copper-mediated reductive intramolecular coupling as shown in Scheme 18. As a copper source, both CuI and $Cu(OAc)_2$ are effective for the reaction.
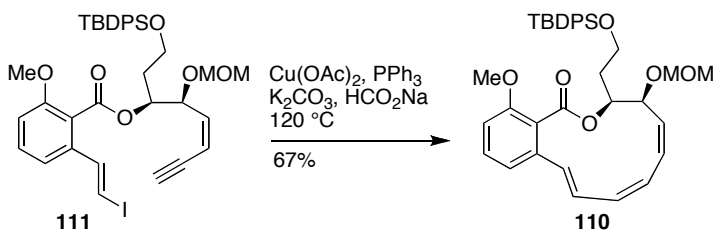
Scheme 18. Georg and Schneider reductive Castro-Stephens to provide triene core

Mechanistically, they proposed that the dienyne adduct of the Castro-Stephens reaction was coordinated to the Cu-H species forming a π-complex, preventing the isomerization of C8-C9 *E* to *Z*. The hydride transfer took place to the sp^2 carbon of

the alkyne to give a $\eta^1 \sigma$–Cu complex which can easily undergo protonolysis to give the (*E,Z,Z*)-triene, completing the catalytic cycle.
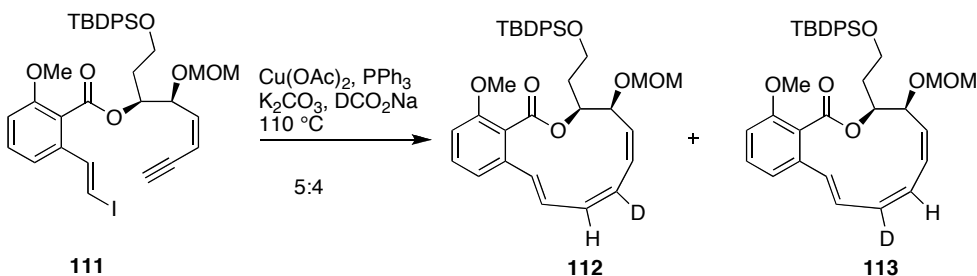
Scheme 19. Georg and Schneider deuterated-sodium formate experiments

The deuterated-sodium formate gave only mono deuterium species at either C10 or C11, Scheme 19.

Georg and Schneider applied the novel copper-mediated reductive coupling to the total synthesis of oximidine II for the formation of the requisite triene **110** as shown in the retrosynthetic analysis, Figure 6. The installation of the enamide can be done through a copper-mediated amination using Porco's protocol. The secondary alcohol could be synthesized from the commercially available 1,3-propanediol. Sharpless asymmetric dihydroxylation (SAD)[63-65] would provide the desired *cis*-diol. The Peterson olefination would provide the desired the enyne **114**.[66-68]
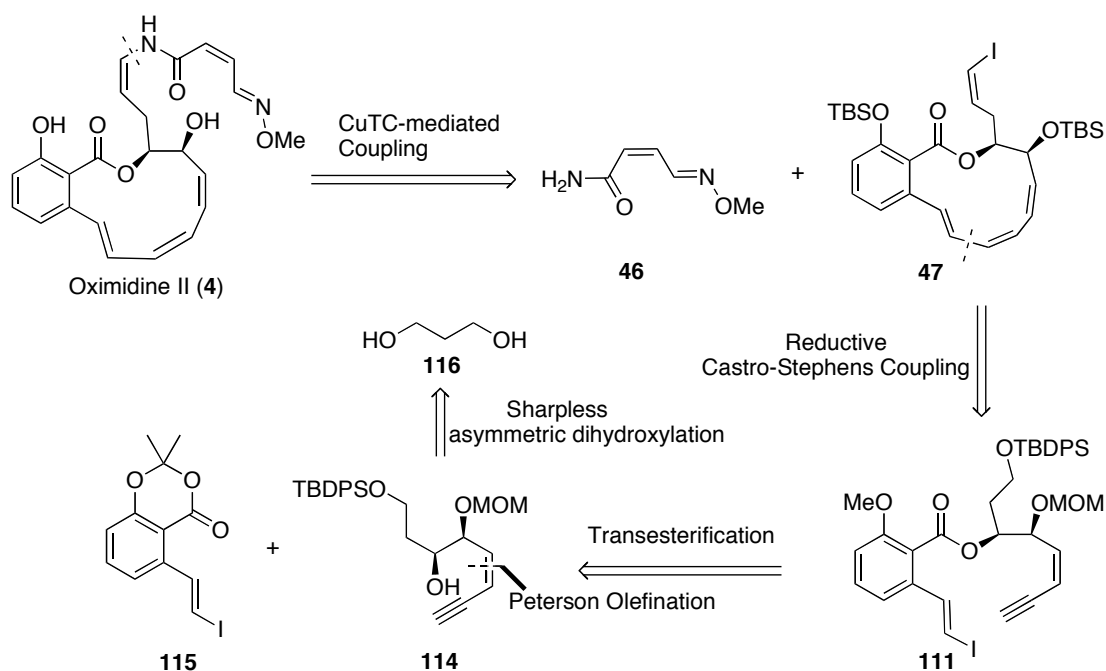
Figure 6. Georg and Schneider's retrosynthetic analysis of oximidine II

Their total synthesis began with the preparation of the secondary alcohol **114** as shown in Scheme 20. The 1,3-diol was converted to the diol **117** in five steps, involving silylation, oxidation to aldehyde, HWE Wittig homologation, and SAD. The primary alcohol **118** was obtained in five steps after protecting group manipulations. Oxidation of alcohol **118** with Dess-Martin periodinane gave aldehyde intermediate **119** and was followed with the Peterson Olefination and desilylation to provide the desired enyne **121**. After deprotection of PMB group using DDQ, secondary alcohol **114** was obtained.
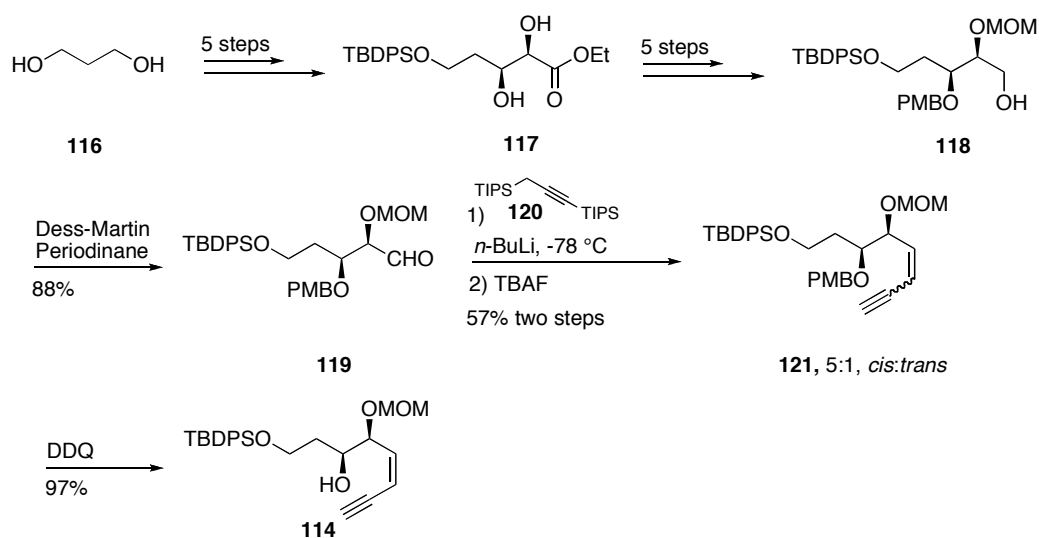
Scheme 20. Georg and Schneider synthesis of alcohol **114**

The required vinyl iodide salicylate **115** was synthesized from the known triflate **57** and vinyl(trimethyl)silane under Heck coupling conditions to provide silyl salicylate **123** (Scheme 21). Iododesilylation (Kishi's protocol)[69] led to the desired vinyl iodide **115**.
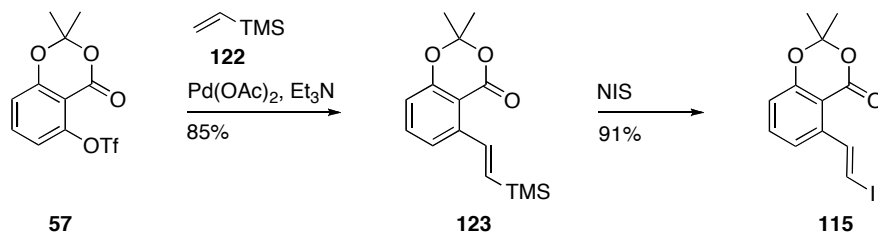
Scheme 21. Georg and Schneider synthesis of vinyl iodide salicylate **115**

The transesterification between alcohol **114** and vinyl iodide salicylate **115** followed by the *in situ* methylation gave the intermediate **111**. The reductive copper-mediated coupling of **111** gave the triene macrocycle **110**. Protecting group manipulations, oxidation and Stork-Zhao Wittig homologation gave the *Z*-vinyl iodide **47**. The two step procedure for enamide installation and desilylation gave the oximidine II.
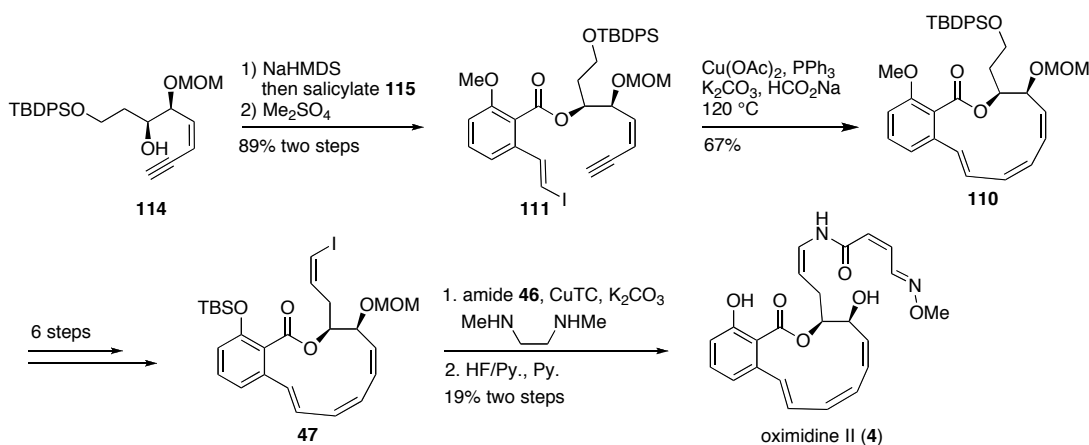
Scheme 22. Georg and Schneider completion of the total synthesis of oximidine II

1.3 Synthesis of the macrocyclic core structure of oximidine II and congeners

1.3.1 Attempt to improve of Porco and Wang's route

Due to the high cytotoxicity and selectivity of oximidine II, we aimed at exploring the Structure-Activity Relationships (SAR) of this natural product in the enamide region. The first task was to synthesize the requisite triene macrocycle **124** by applying known procedures. We hypothesized that Porco's protocol[13] could be

improved by subjecting the triene **126** to RCM, which would generate a more flexible

macrocycle as shown in our retrosynthetic analysis. The third conjugate double bond

could be introduced by oxidative cleavage of a selenium species to form the desired

triene core structure **124**.[70] The alcohol **127** would be synthesized using Molander's

protocol[45] and the salicylate[71, 72] **128** would be obtained from a known procedure.
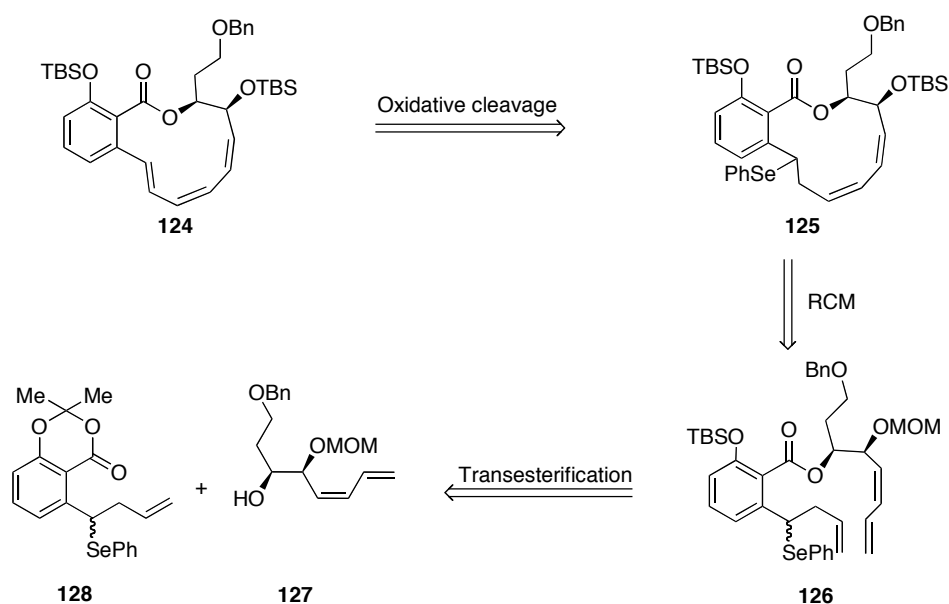
Figure 7. Retrosynthesis to improve the RCM

The synthesis of the alcohol diene **127** was adopted from Molander's

protocol[45] and started with the (*S*)-1,2,4-butanetriol to provide the desired diene in

nine steps (Scheme 23). Butanetriol was protected as 1,3-benzylacetal **130** and the

primary alcohol was oxidized to give the corresponding aldehyde (Swern oxidation).

The diastereoselective addition of the terminal alkyne to aldehyde **131** proceeded

uneventfully in the presence of (+)-NME to provide the desired diastereomer in good

yield.[45, 57] The resulting alcohol was protected with MOMCl and the following

hydrolysis of the primary acetate provided a colorless crude oil, which was then

subjected to partial hydrogenation to give cis-propargyl alcohol **132**.[45] Oxidation of

propagyl alcohol **132** with IBX provided the aldehyde which was subjected to Wittig

homologation with trimethyl phosphonium ylide to give the desired diene **133**.

Reductive cleavage of benzylidene acetal **133** with DIBAL yielded the desired

product **127** in good yield; however, TLC showed quantitative conversion to the

desired product.
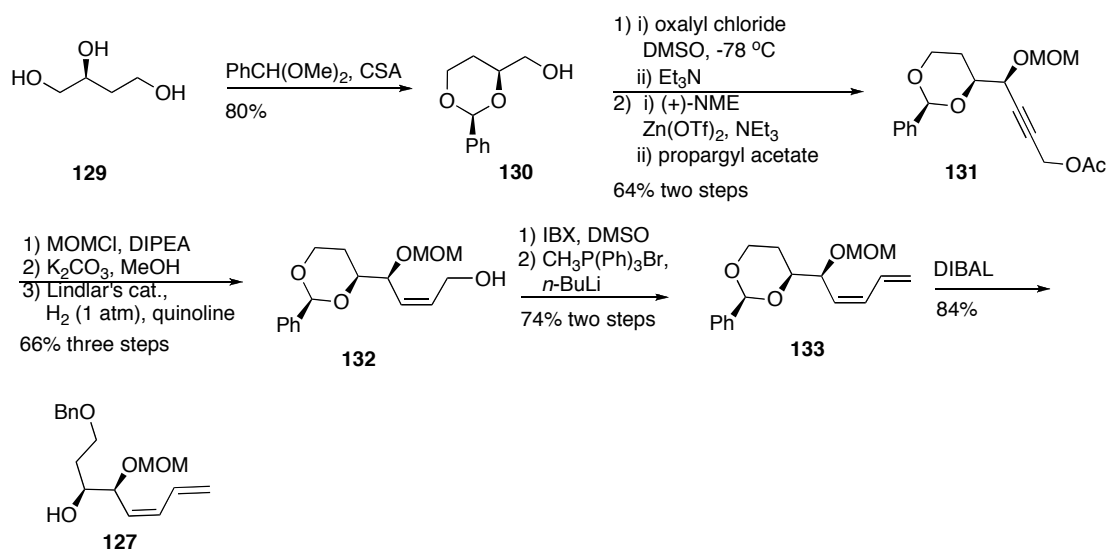
Scheme 23. Synthesis of alcohol diene **127**

The precursor of the macrocyclic core was synthesized as shown in Scheme

24. The 2,6-dihydroxybenzoic acid was treated with acetone and thionyl chloride to

give the hydroxy acetonide which was further reacted with triflic anhydride followed

by methyl cuprate coupling to afford methyl salicylate **135**.[71] The intermediate was

treated with n-BuLi and diphenyl diselenide to afford **136**.[70] The selenide was then

alkylated with allyl bromide, and the resulting intermediate was subjected to

transesterification[13] with the alcohol **127** and TBS protection to give the crucial

intermediate **126**.
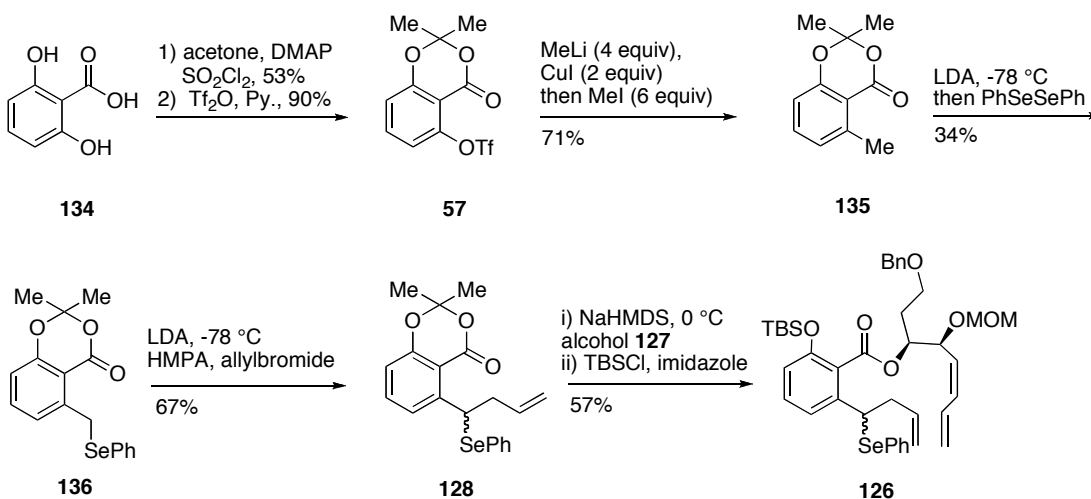
Scheme 24. Synthesis of RCM precursor

The transesterification of salicylate **50**[13] and alcohol **127**, and *in situ* silylation

with TBSCl provided the *bis*-diene **137**, Scheme 25. We assumed that the

intermediate **137** containing a benzyl protecting group should behave in a similar way

compared to Porco's intermediate carrying a PMB protecting group (**48**).
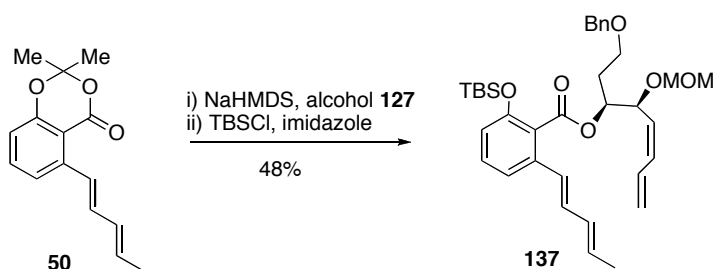
Scheme 25. Synthesis of *bis*-diene **137**

Ring closing metathesis of *bis*-diene **137** with 2nd generation Grubbs's catalyst (**59**) proceeded only with low yield, Scheme 26. Screening of other catalysts did not increase the yield of macrocycle formation. Better results were obtained when **126** was reacted with the 2nd generation Grubbs's catalyst to afford the diene product **125** in 22% yield. The following oxidative cleavage[70] occurred in 27% yield to give the identical product **124** generated during Porco's route.
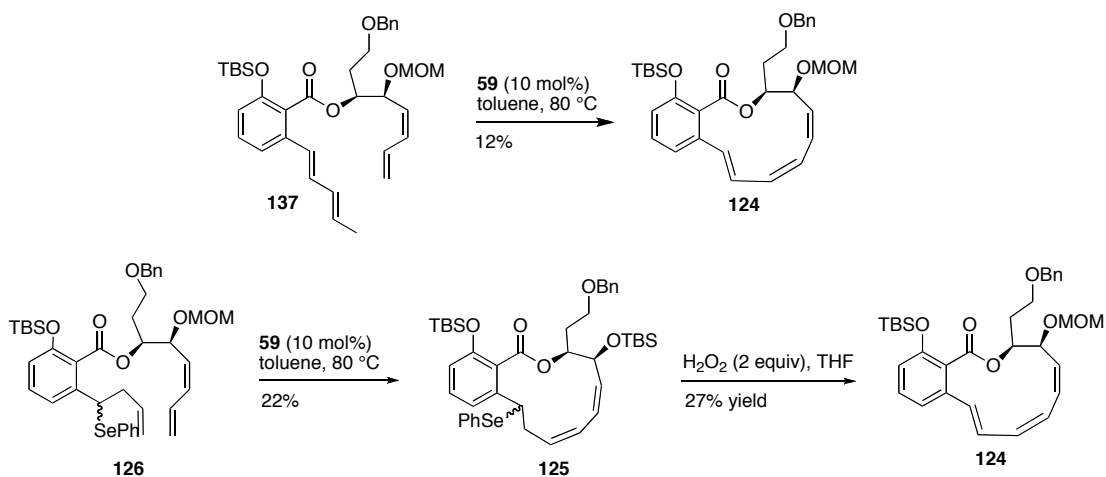
Scheme 26. Synthesis of triene core **124** using RCM

1.3.2 Synthesis of the homolog macrocyclic triene

Even though a higher yield for macrocycle formation of the diene **124** macrocycle was observed, the overall yield for triene formation was much lower than Porco's approach. Thus we decided to use Porco's protocol to prepare our desired triene **144**, homolog of **60**, as shown in Scheme 27.
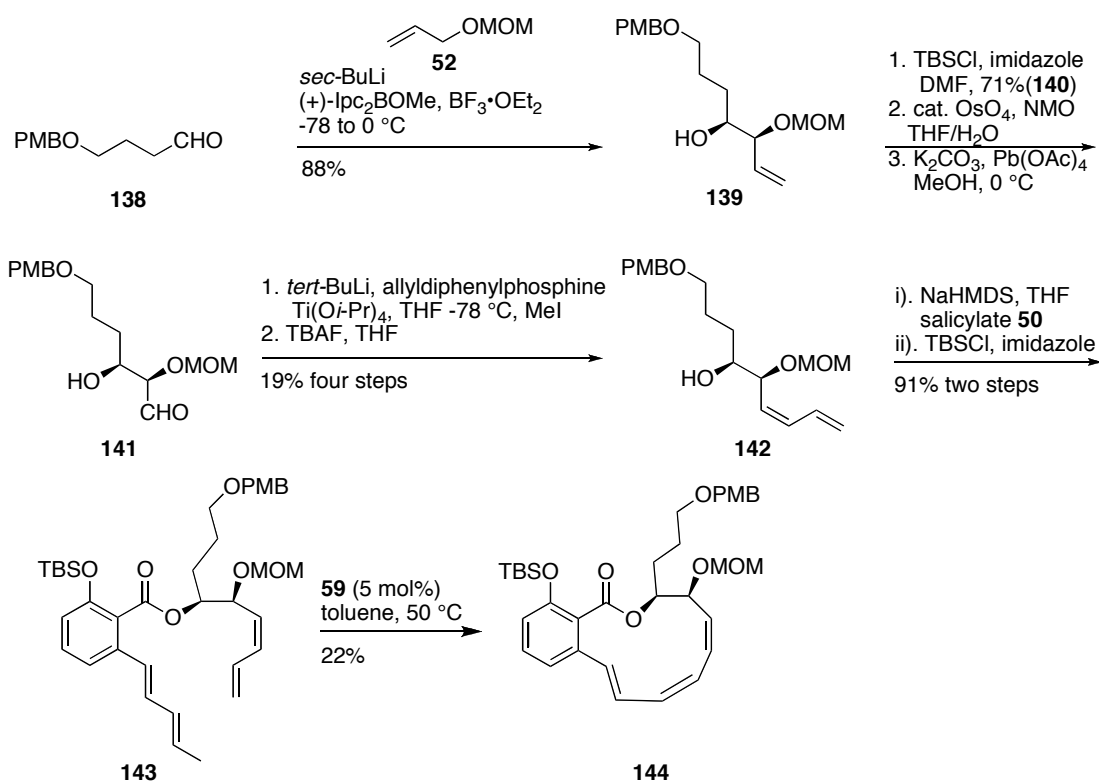
Scheme 27. Synthesis of the homolog macrocyclic triene core

The alcohol **139** was synthesized in a similar manner as described by Porco and Wang as shown in Scheme 27. The synthesis began with a Brown asymmetric allylation to provide secondary alcohol **139**.[13] The adduct **139** was silylated with

TBSCl, and subjected to dihydroxylation and oxidative cleavage to give aldehyde **141**. Using Yamamoto's protocol, the aldehyde was converted to alcohol **142**. The required alcohol **142** was obtained after the deprotection of the TBS group. The transesterification between salicylate **50** and alcohol **142** and *in situ* silylation gave the intermediate **143**. The RCM with Grubbs's 2nd generation catalyst gave the requisite triene **144** accompanied by an oligomeric product.

1.3.3 Chiral pool approach

A chiral pool approach was used to prepare alcohol **149**. The hydroxyl O-ethyl glycoside **146** was prepared from tri-*O*-acetyl-D-glucal (Glucal) in three steps using known chemistry, involving a Ferrier rearrangement[73-75] by reaction with anhydrous ethanol in the presence of tin chloride (Scheme 28).
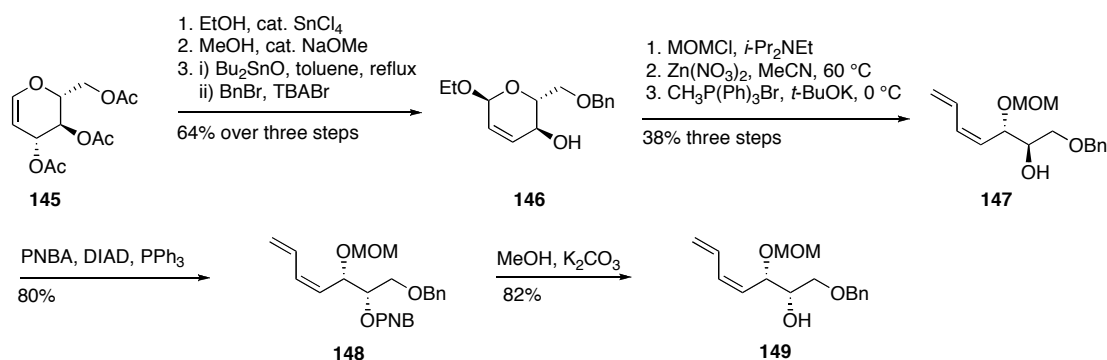
Scheme 28. Chiral pool approach to prepare alcohol **149**

After methanolysis with sodium methoxide to remove the acetyl groups, the resulting primary alcohol was protected with the benzyl group to afford a colorless oil in 64% yield over three steps with only one flash chromatography column. The resulting

hydroxyl glycoside **146** was protected with MOMCl. Hydrolysis of the ethyl acetal

group in the presence of $Zn(NO_3)_2$ revealed the hemiacetal.[76] Wittig homologation

provided a *cis*-diene **147** in 38% yield. The secondary alcohol product was subjected

to the Mitsunobu reaction[77] to install the desired configuration of the hydroxyl group.

The desired product **149** was obtained as single isomer in gram scale after the

hydrolysis of the p-nitrobenzoyl moiety in 82% yield.[78] Large-scale preparation of

diene **146** was achieved in eight steps from 20 grams of glucal.

The transesterification between alcohol **149** and salicylate **50** gave the

intermediate **150**.
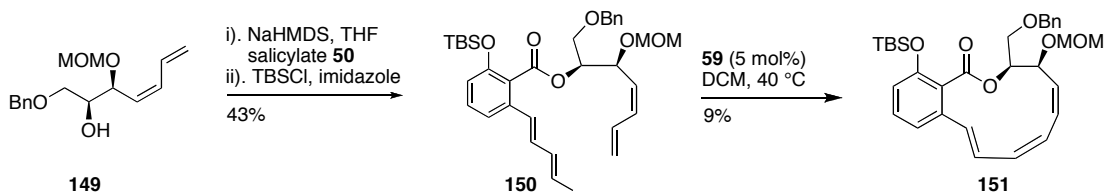
Scheme 29. Synthesis of RCM precursor

Unfortunately, the RCM with the new cis-diene gave unsatisfactory results as seen

earlier with a maximum yield of 15-17% yield by increasing the amount of the 2nd

generation Grubbs's catalyst up to 20% (Table 1).

Table 1. RCM yield with 2nd generation Grubbs's catalyst in DCM

% Catalyst	time	151, yield	amount
5%	80 min	9%	12.2 mg
15%	80 min	17%	10.9 mg
20%	80 min	11%	7.2 mg

1.3.4 Intramolecular reductive copper-mediated macrocycle formation

While we were investigating the RCM approach, the novel reductive copper-mediated macrocycle formation was developed in our lab by Georg and Schneider.[61] We decided to use this methodology for the preparation of the triene core structure of oximidine II needed for our SAR studies. We envisioned using the alcohol **153** (Scheme 30) prepared by Brown asymmetric allylation[13, 31] to produce the required alcohol **114**.[61]

The synthesis began with the Brown asymmetric allylation of aldehyde **152**, Scheme 30, to provide the desired secondary alcohol **153**. The silylation and dihydroxylation followed by oxidative cleavage gave the aldehyde **155** which was used directly for the Peterson olefination.[61] The desilylation with TBAF gave diol **157** in good yield.
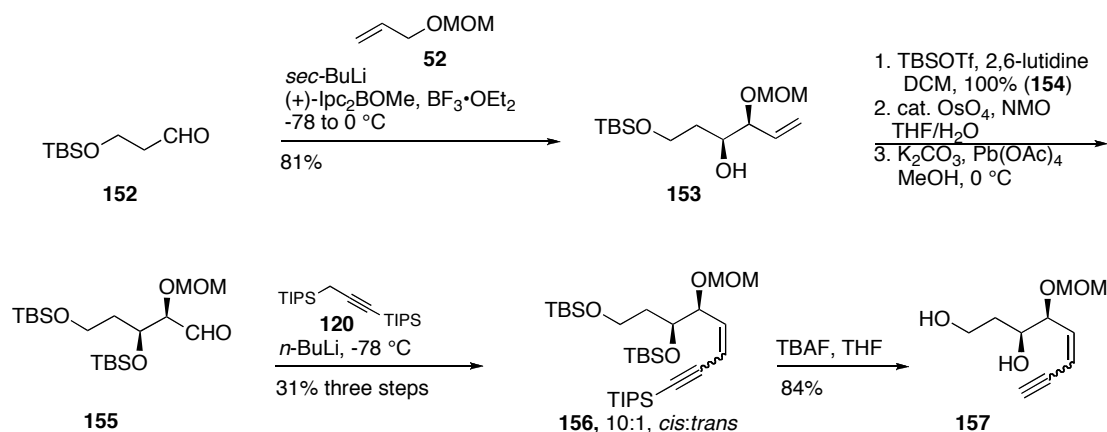
Scheme 30. Synthesis of diol **157** using Brown asymmetric allylation

The two-step procedure to propare aldehyde **155** was replaced with an ozonolysis procedure as shown in Scheme 31. After reductive work-up with dimethylsulfide, the aldehyde **155** was placed under high vacuum to give an opaque oily material which was subjected directly to Peterson olefination without further purification. The crude was subjected to desilylation with TBAF to give diol **157** in 51% over three steps. The silylation of the primary alcohol adduct gave the common intermediate **114** generated during the Georg and Schneider synthesis.
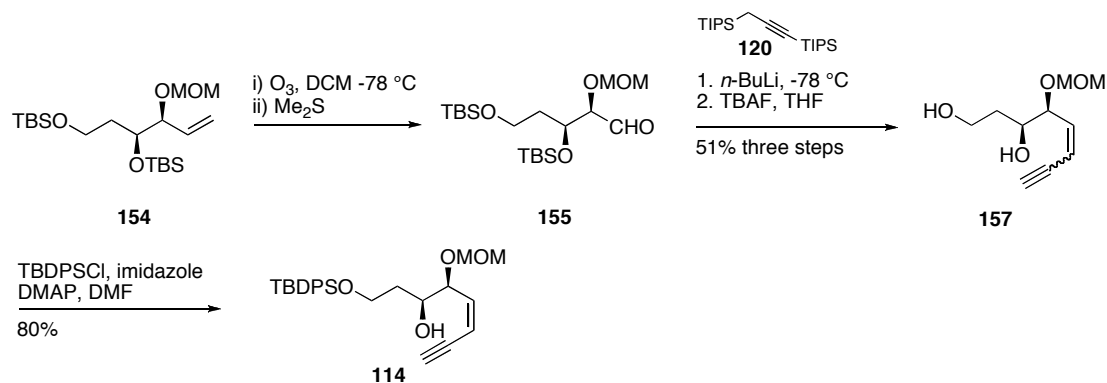
Scheme 31. Synthesis of common alcohol intermediate **114**

Transesterification product **111** was prepared according to the reported procedure, Scheme 32.[61] The intermediate **111** was subjected to the reductive copper-mediated macrocycle formation in the presence of trimethylphosphite to provide the triene macrocycle **110** in a comparable yield to the previous report, using triphenyl phosphine as a ligand.[61]
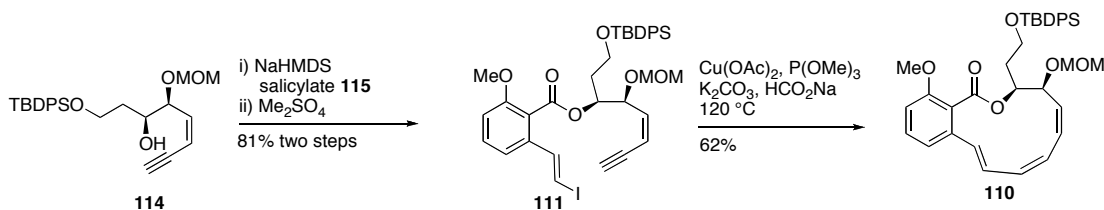
Scheme 32. Formation of the triene macrocycle

1.3.5 Simplified analogue strategy

To facilitate the preparation of oximidine analogues, we have chosen a simplified scaffold approach based on three-dimensional quantitative structure-activity relationship (3D-QSAR) analysis using the comparative molecular similarity indices analysis (CoMSIA) model reported by Georg and co-workers.[79]

A 3D-QSAR model consists of a mathematical equation describing potency as a function of 3D interactive fields around aligned training set compounds presumed to be the biologically active structures.[80, 81] This correlation is derived from a series of superimposed conformations, one for each molecule in the set that includes 3D spatial changes of interactive field values and the biological activity of molecules. The most common methods to calculate 3D descriptors are comparative molecular field

analysis (CoMFA)[82] and comparative molecular similarity indices analysis (CoMSIA).[83] Both CoMFA and CoMSIA are based on the assumption that changes in binding affinities of ligands are related to changes in molecular properties, thus correlating molecular properties with the experimental biological activity. CoMFA derives a 3D-QSAR model by systematically sampling the steric (van der Waals interactions) and electrostatic interactions (Coulombic interactions) at regularly spaced grid points surrounding a specific target protein; meanwhile, CoMSIA uses a Gaussian type function to avoid the extreme values generated by Lennard-Jones and Coulombic functions. The Gaussian function also results in smoother, less fragmented surfaces in the final model representation.[83]

The advantage of 3D-QSAR methods is that there is no need for initial active-site information and it can be used to investigate a variety of enzyme-inhibitor interactions. The 3D-QSAR can be used for the virtual screening of potential drug candidates as well as to improve the potency of existing compounds.[84, 85]

The development of 3D-QSAR of V-ATPase inhibitors was derived from the CoMSIA model by including 23 known mammalian V-ATPase inhibitors in the training set, including benzoate and benzolactone (salicylihalamides, lobatamides, lobatamide analogues, and oximidines).[79] The model showed a good correlation with bovine ATPase IC_{50} data ($R^2 = 0.968$, $Q^2 = 0.553$). It also showed reliability for prediction of human kidney V-ATPase inhibition by lobatamide compounds (R = 0.862). The electronic terms appear to dominate, with a normalized weight (0.735) nearly three times of steric (0.265). The result also showed that the lactone ring in

salicylihalamide might, in concert with the enamide double bond, play a critical compensatory role in the activity. It showed that the salicylihalamide appears to exhibit fairly optimal electrostatics; its activity may be improved by making adjustment for the steric factor. In particular, it may be possible to explore a slightly bulkier group such as ethyl or t-butyl to replace the methyl group on the lactone ring to enhance the interaction with a steric favorable region.

For our simplified core structure generation, the test scaffolds were designed based on the ease of preparation and the availability of starting material, Figure 8. We refined our proposed molecules into 3D structures using SYBYL to full molecular mechanics convergence using the Tripos Force Field[86] and Gasteriger-Marsili charges. The resulting structures were then flexibly aligned using Surflex[87] to the putatively bioactive conformation of salicylihalamide derived from the CoMSIA study of Georg and co-workers.[79] Finally, Gasteiger-Marsili charges were assigned to these resulting structures[88] and their positions and orientations within the CoMSIA field were refined via the field-alignment algorithm implemented within the QSAR/CoMSIA module of SYBYL[89] using default settings. The summarized results were obtained and analyzed by Dr. Gerald Lushington (Molecular Graphics & Modeling Laboratory, University of Kansas) shown in Table 2.

Figure 8. CoMSIA/QSAR evaluated structures

Table 2. CoMSIA/QSAR predicted IC_{50} values for V-ATPase inhibition of proposed structures using oximidines and lobatamides as controls

Molecule	predicted IC_{50} (nM)
Oximidine I, (**3**)	2.02
Oximidine II, (**4**)	1.47
Lobatamide A, (**6**)	4.91
Lobatamide B, (**7**)	4.56
Lobatamide D, (**9**)	2.28
Lobatamide E, (**10**)	2.14
Lobatamide F, (**11**)	2.09
158	0.39
159	0.16
160	0.31
161	0.40
162	0.33
163	0.28
164	0.46
165	0.58
166	1.30
167	1.55
168	1.80
169	1.71
170	0.12
171	0.21
172	0.19

The predicted IC_{50} of the proposed structures showed equipotent inhibition toward V-ATPases relative to lobatamides or oximidines. The general scaffolds of these compounds are shown in Figure 9.

Figure 9. General scaffolds of evaluated structures

Among the four, we chose scaffold **176** which can be prepared in a few steps. The retrosynthetic analysis is shown in Figure 10.

Figure 10. Retrosynthetic analysis of simplified scaffold

The ring closing metathesis is the key step that allows the formation of a macrocycle from a linear intermediate resulting from transesterification of salicylate **177** with alcohols **53**, and **139**.

The synthesis of salicylate **177** is shown in Scheme 33. The hydrostannylation of 4-pentyn-1-ol gave *trans*-vinylstannane in good yield.[90] The crude NMR showed exclusively *trans*-alkene; however, the attempt to purify the product on a silica

column led to the isomerization and low yield. This might be due to the acid sensitive nature of the vinylstannane. Parikh-Doering oxidation[91] of vinylstannane was followed by Wittig reaction to give the crucial intermediate for Stille coupling.[92] The desired salicylate **177** was obtained in 93% over four steps when palladium tetrakis was used as a catalyst while the lower yield of 52% was obtained with the $Pd_2(dba)_3$ catalyst for the Stille coupling.
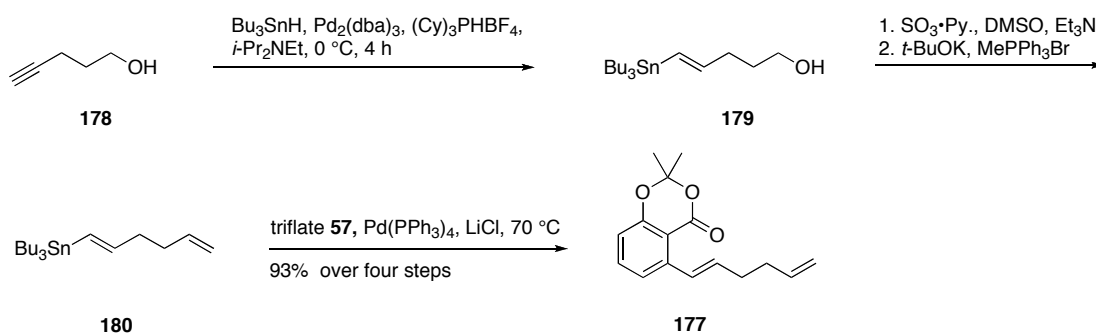
Scheme 33. Synthesis of salicylate **177**

The alcohol **53** and **139** were prepared in one step by Brown asymmetric allylation following the procedure reported by Porco's group as shown in Scheme 34.
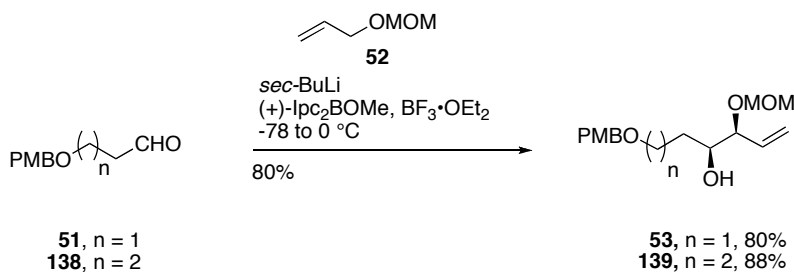
Scheme 34. Preparations of alcohols **53** and **139**

The transesterification between salicylate **177** and alcohols **53**, **139** proceeded uneventfully in the presence of NaHMDS and THF. Upon TBS protection of the phenolic hydroxyl group, intermediate **181** and **182** were subjected to RCM to yield the thermodynamically favored products **183** and **184** in 61%, and 69% yield. The two pairs of *J* coupling values at 15-16 Hz suggested the formation of *E,E*-bis-diene macrocycles **183** and **184**.

53, n = 1	**181**, n = 1	**183**, n = 1, 61%, three steps
139, n = 2	**182**, n = 2	**184**, n = 2, 61%, three steps
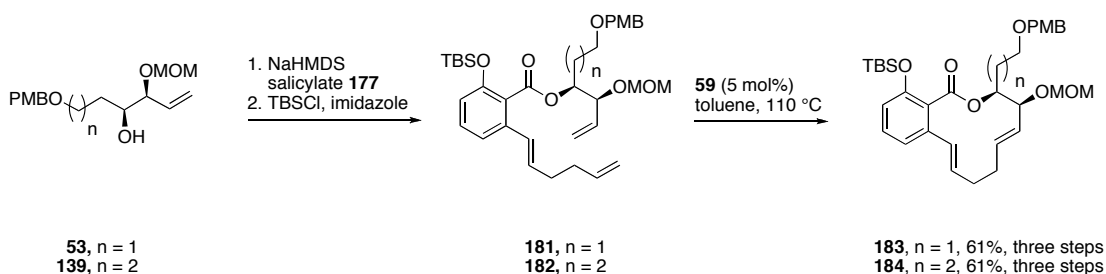
Scheme 35. Completion of the synthesis of simplified macrocycles

The attempt to deprotect the MOM group of **184** using CBr$_4$ led to the isolation of the desired product **185** and diol **186**, Scheme 36.[13] The diol **186** was recrystallized from a mixture of diethyl ether and hexanes and analyzed by X-ray crystallography. The X-ray data was obtained and analyzed by Dr. Victor Young (X-ray Crystallographic Facility, Department of Chemistry, University of Minnesota). The OTEP drawing of diol **186** (Figure 11) confirmed the structure of the desired product.
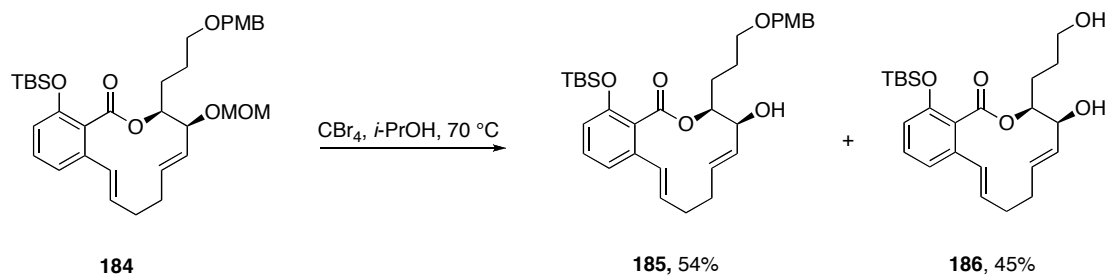
Scheme 36. Preparations of *E,E-bis*-diene-alcohol and *E,E-bis*-diene-diol
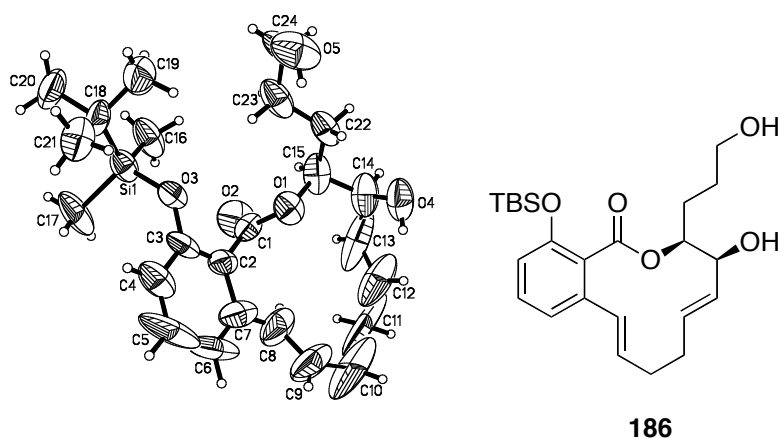
Figure 11. OTEP drawing of *E,E-bis*-diene macrocycle

1.4 Conclusion

In conclusion, we have investigated the formation of the triene macrocycle of oximidine using a RCM procedure, and the reductive copper-mediated macrocycle formation. We observed the limitation of the RCM reaction for the formation of the triene macrocycle. The chiral pool approach, using D-glucal, was explored as an alternative route to prepare the *cis*-diene for the RCM reaction. The reductive copper-mediate protocol provided a better result. Macrocycles containing a simplified triene core were designed based on CoMSIA/QSAR analysis, and prepared using the RCM

reaction. We anticipated that the change in the triene core would not affect the activity of these analogues, which would show similar potencies when compared with macrocycles containing the original oximidine core. This will be discussed further in Chapter 2.

Chapter 2

Novel Oximidine Analogues with Improved Stability as Anticancer Agents

2.1 Biological Significance of V-ATPases

V-ATPases are a class of enzymes that reguate intraorganellar acidity by translocating protons from cytoplasm to the lumen, using the energy from the hydrolysis of the ATP.[93-95] The electrochemical gradient generated from this process provides a driving force for the movement of ions and solutes into the vacuole. V-ATPases are distributed throughout eukaryotic cells and tissues, and are located on the membranes of vacuoles, lysosomes, and other components of the endo membrane systems.[96-98]

These enzymes play a crucial role for a variety of physiological functions including membrane and organellar protein sorting, neurotansmitter uptake, cellular degradations, and receptor recycling. In various intracellular compartments including endosomes, lysosomes, and secretory vesicles, V-ATPases function in processes such as receptor-mediated endocytosis,[99] intracellular targeting of lysosomal enzymes,[100] protein processing and degradation,[94] and the coupled transport of small molecules.[101]

V-ATPases are involved in acid secretion, bone degradation, homeostatis of cytoplasmic pH, and sperm maturation.[102, 103] V-ATPases present in the apical membrane of type-A renal intercalated cells play a role in maintaining the acid-base balance of kidney cells.[104] Metabolic acidosis is caused by a defect in renal acidification resulting from the mutation of human genes.[105, 106] In bone, resorption

and remodeling is conducted by osteoclasts which possess V-ATPases on their plasma membrane.[107-109] Acidification of the bone surface leads to dissolving the bone matrix and activating osteoclast-secreted acid hydrolases. The high acid production rates from metabolism in macrophages and neutrophis are neutralized by the action of V-ATPases.[98, 103]

V-ATPases have been proposed to take part in tumor metastasis by secreting lysosomal enzymes to degrade the extracellular matrix, which is essential for metastatic invasion. High glycolysis rates inside cancer cells lead to a large amount of acid production; however, an alkaline cytoplasmic pH is necessary for cancer cell survival. To survive in this harsh environment, tumor cells must upregulate V-ATPases to pump extra protons out of cellular space. Immunocytochemical experiments revealed that V-ATPases in human breast cancer cell lines are expressed more in highly metastatic than in low metastatic cells.[110]

Based on these findings, V-ATPases have attracted considerable attentions as a potential therapeutic target for anti-cancer treatment.

2.2 Structure of V-ATPases

V-ATPases are large multisubunit complexes consisting of two domains, an ATP-hydrolyic domain (V_1), made of peripherally associated subunits, and a proton-translocation domain (V_0), made of membrane-bound subunits.[97, 111] The V_1 domain (640 kDa) is comprised of eight different subunits (A-H) that control the hydrolysis of ATP. The V_0 (260 kDa) is an integral complex of six different subunits (a, c, c', c'', e, and d) which are responsible for proton translocation. The mammalian cells lack the c' subunit, Figure 12.
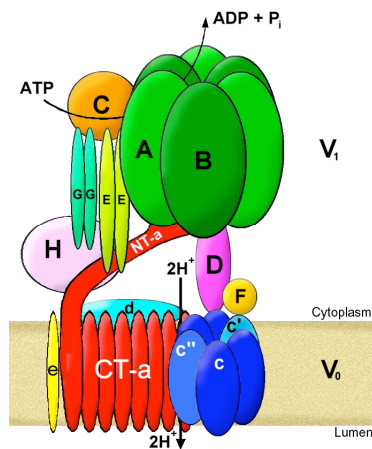
Figure 12. Schematic struture of V-ATPase

The V_1 ATP-driven rotor consists of three copies of the A and B subunits, two copies of the E and G subunits, one or two copies of subunit H and a single copy of each of the remaining subunits. The subunits A and B form a hexamer of nearly 400 kDa which serves as the ATP binding sites at one of the two types of interface of the A and B subunits. The other subunits form one of two types of stalks — peripheral

and central. They connect the V_1 and V_0 domains. The central stalk, the D subunit, functions as a rotor to couple the energy from the hydrolysis of ATP to the rotation of a ring of proteolipid subunits in V_0. [112]

Table 3. Subunit Composition of a Typical Mammalian V-ATPase[113]

Subunit	Molecular Mass (kDa)	Number of Subunits	Domain
A	70	3	V_1
B	60	3	V_1
C	40	1	V_1
D	34	1	V_1
E	33	1	V_1
F	14	1	V_1
G	13	2	V_1
H	15	1	V_1
a	100	1	V_0
d	38	1	V_0
c	16	5 or 6	V_0
c'	16	5 or 6	V_0
c"	23	1	V_0

The V_0 domain is composed of four or five copies of subunit c and a single copy of each of the remaining subunits. The complexation of proteolipid subunits (c, c', and c") forms a highly hydrophobic ring in the transmembrane region. Its subunits contain a single buried glutamate residue located in transmembrane helix-4 (TM4) of subunit c and c', and TM3 of subunit c" that are responsible for harboring the proton

to be transported across the membrane *via* reversible protonation. The subunit d, tightly bound peripheral subunit, is located on top of the proteolipid ring, providing the connection between the central stalk V_1 and V_0. It plays a role in either reversible dissociation or coupling of proton transport. The subunit a (100 kDa) has a hydrophilic N-terminal domain that is oriented toward the cytoplasmic region and a C-terminal domain that contains eight or nine transmembrane helices. The C-terminus TM7 contains arginine that is required for proton influx. The highly hydrophobic subunit e is located in the transmembrane domain.

The rotary mechanism of proton transport is driven by the proton gradient associated with ATP hydrolysis.[98] Protons enter from the cytoplasm through the hemi channel subunit a and they protonate the glutamine residues on the subunit c and c". The energy released from ATP hydrolysis allows the rotation of the rotor. This forces the realignment of the protein to allow the interaction between the protonated glutamine side chains and a crucial arginine residue in TM7. Protons are shuttled into the luminal hemi-channel of subunit a from the protonation of arginine and released into the organelle to complete the catalytic cycle.

There are three types of ATPases which differ in function, structure, and type of ions they transport, namely P-ATPases, F-ATPases and V-ATPases.[114-116] P-ATPases are found in bacteria, fungi and in eukaryotic cells. They are very different from V-ATPases and form smaller enzyme complexes. Their role is to transport different cations, Na^+, K^+, Ca^+, across membranes. From electron microscopy, F-ATPases and V-ATPases have a similar overall shape. They transport protons across

membranes and consist of distinct peripheral and integral domains that are connected by at least two stalks. However, V-ATPases show a more complex structure in the V_1 domain. F-ATPases are located mostly in mitochondria, chloroplasts, and bacterial plasma membranes, and are responsible for the synthesis of ATP. V-ATPases are found elsewhere in the cell and convert ATP to ADP to drive a catalytic cycle.

The V-ATPases have several subunit isoforms. There are at least four distinct subunit a isoforms, a1, a2, a3, a4.[117-119] The subunit isoform a3 is a component of plasma membrane V-ATPase, essential for bone resorption. It is also expressed highly in the heart and liver. The subunit isoform a4 is found in the kidney only. In human, two isoforms of subunit E are known, E_1 and E_2, but only E_1 is expressed in the testis.[120, 121] The E_1 isoform is required for acidification of luminal pH of testis-specific compartments and is involved directly in male fertility. Malfunction of V-ATPase isoforms may cause certain diseases. Mutations in the a3 isoform result in deficient bone resorption and osteoporosis.[122] In cancer, highly invasive MDA-MB231 human breast cancer cells express V-ATPases at the cell surface.[123] In contrast the poorly invasive MCF7 cell line is characterized by high expression of subunit a4 which is considered responsible for increased acidity at the cell surface. The presence of various isoforms of V-ATPases may allow for selective drug targeting.

2.3 Inhibitors of V-ATPase

The unique architectures of V-ATPases and their critical roles in living cells have drawn interest in both the scientific and medical communities. In the past two decades, much effort has been spent in the search for substrates that can specifically bind to V-ATPases. Both natural products and synthetic small molecules have been identified as V-ATPase inhibitors.

Bafilomycin A_1 (**187**) was first isolated in 1983 from *Streptomyces griseus* on the basis of its antifungal and antibacterial activity, Figure 13.[46] It was found later by Bowman *et al*. that these bafilomycins, A_1, B_1, C_1, more selectively inhibited V-ATPase than P-ATPase and had no effect on F-ATPase.[124] Another group of related macrolides was initially identified as immunosuppressive compounds. They were isolated from *Streptomyces diastatochromogenes* and named concanamycins because they inhibited the proliferation of concanavalin-A-stimulated T-cells.[125] They were found to be V-ATPase inhibitors more potent than bafilomycins.[126] Given their selectivity, bafilomycins and connamycins macrolides have been used extensively as probes to study the physiological roles of V-ATPases.

The treatment of human tumor cell lines A431 with bafilomycin A_1 showed that the inhibition of the acidification process in lysosomes prevented protein degradation.[127] A possible involvement of plasma membrane V-ATPase in cell proliferation was observed when mouse, rat, and human cell lines were treated with bafilomycin A_1 and concanamycin A1 and A4B.[128] Bafilomycin A_1 inhibited the

growth of human pancreatic cancer cells, Capan-1, through apoptosis.[129] This inhibition was observed at nanomolar concentration and was dose-dependent. The study using affinity chromatography with the immobilized bafilomycin C_1 showed that the c subunit of V_0 was the binding site.[130] This result was confirmed by the recent photoaffinity experiments of concanamycin A bearing radioactive tracer ^{125}I at C23 as shown in **192**.[131] It was found that both bafilomycins and concanamycins bind to the same site at subunit c of V_0, since the photolabeling could not replace the natural products concanamycin A and bafilomycins A_1.
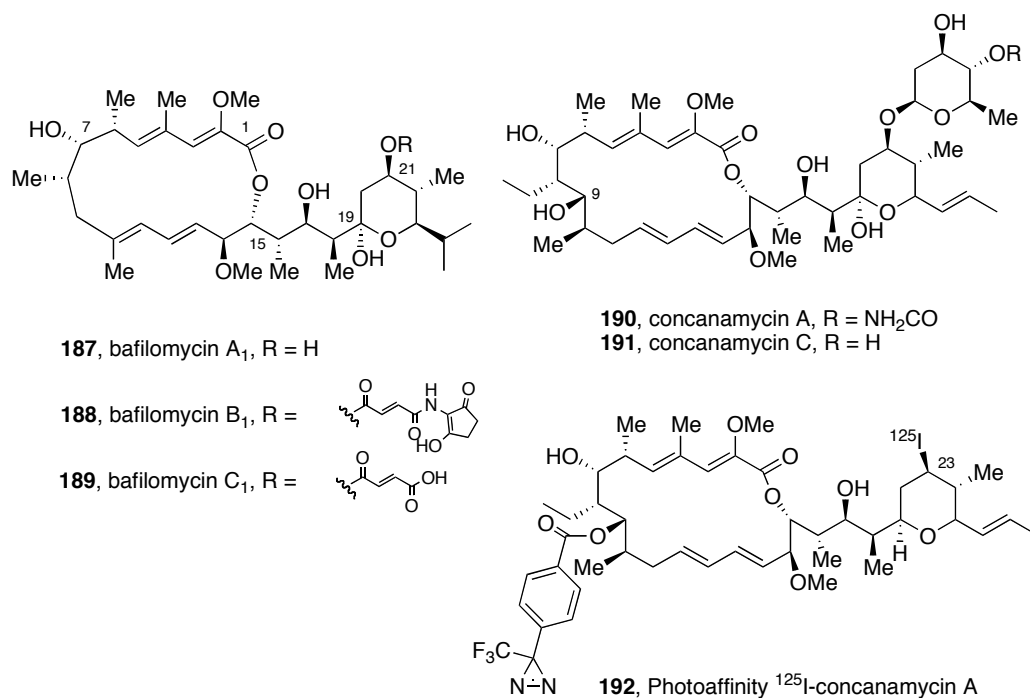
Figure 13. Bafilomycins and Concanamycins

2.3.1 SARs of Bafilomycins and Concanamycins

Extensive SARs of both concanamycins and bafilomycins have been conducted and have led to the identification of the essential structural features responsible for the biological activity. One of the structural requirements essential for the biological activity is the distinctive intramolecular hydrogen bonding between the lactone and hemiketal moieties for optimal inhibition. This is proved by the three- to four-fold loss of activity of concanamycin F analogues **194**, **195**, **196**.[132]
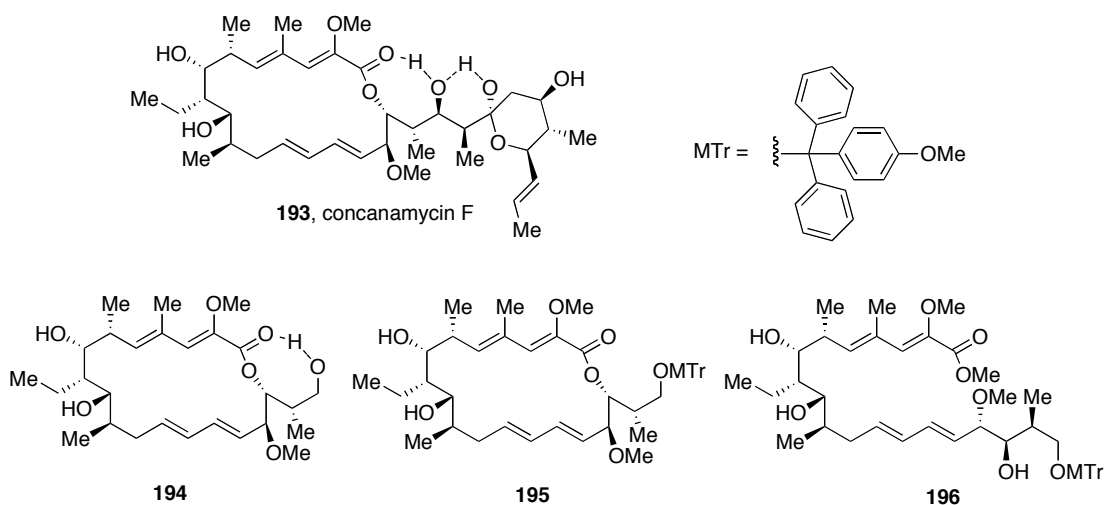
Figure 14. Analogues of Concanamycin F

The presence of a small acetyl group at C9, **199**, of concanamycin A as well as C7 and C21, **197** and **198**, of bafilomycin A₁ was tolerated while the opening of the macrocyclic ring caused a total loss of activity (Figure 15).[133] The amino analogue at C21, **198**, showed a slight improvement of selectivity.
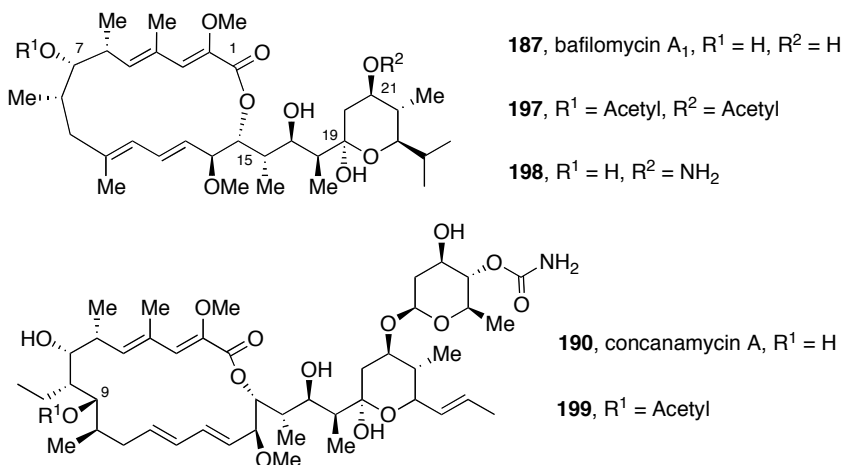
Figure 15. Analogues of bafilomycin A₁ and concanamycin A

However, the acid analogue **200** from the fragmentation of the pyran ring in bafilomycin A₁ was devoid of activity (Figure 16).[102] The sulfonamides **201** and **202** retained high potency with improvement of the selectivity. It is worth noting that the sulfonamide **201** showed a ten-fold difference between potency and toxicity, Table 4.
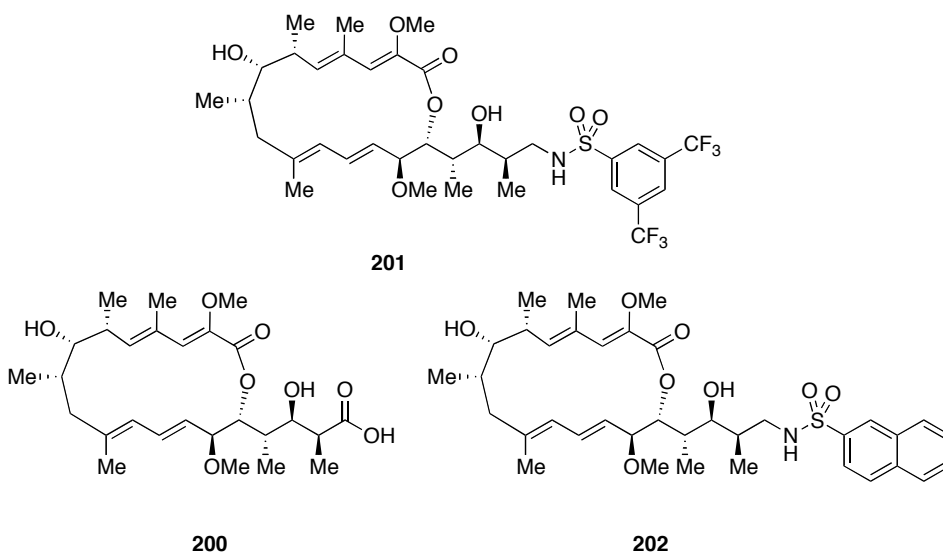
Figure 16. Acid and sulfonamide analogues of bafilomycin A₁

Table 4. Inhibition of V-ATPase and *in vivo* activity* of concanamycin C (**191**), bafilomycin A$_1$ (**186**), and analogues

Compound	V-ATPase assays, IC$_{50}$ (nM)			*In vivo* assays (mol kg^{-1})		
	Bone	Brain	Ratio	Potency	Toxicity threshold	Ratio
186	0.36	0.84	2.4	0.5	0.4	0.8
191	0.35	0.58	1.7	>0.1	0.025	<0.25
201	0.58	3.3	5.7	2.7	25	9.3
202	0.92	3.6	3.9	6.2	20	3.2

* The prevention of the retinoid-induced hypercalcaemia in thyroparathyrodectomized rats

Due to the complexity of the natural products bafilomycins and concanamycins, studies have been conducted to identify small molecules with the same critical structure feature, the C1-C7 fragment, of the complex macrolides. The new molecular bioactive entities have an indole core where the NH-group is a mimic of the C7 hydroxyl group of bafilomycins (Figure 17).[134] The lead compound **203** showed weak inhibition of chicken osteoclast V-ATPase at IC$_{50}$ 30 μM. Then systematic optimizations of the aromatic ring by addition of lipophilic and electron-withdrawing groups led to the discovery of 5,6-dichloroindole analogues **205** with an IC$_{50}$ 1.9 μM. The potency was improved when the ester was converted into the amide containing a basic nitrogen, compound **204** (IC$_{50}$ = 180 nM). The conformationally constrained piperidine derivative **206** (SB 242784) showed nanomolar inhibition of human osteoclast at 3.4 nM.[102] Recently, the indolyl analogue **207**, NiK-12192, has been reported to synergize topotecan in both topotecan sensitive and topotecan-

resistant tumor xenografts.[135] In addition, it has been reported that NiK-12192 inhibited cell migration and invasion by affecting cell motility and cell adhesion. Oral administration of NiK-12192 to mice bearing human lung tumor xenografts (NCI H460) showed a significant inhibition of metastases.[136]
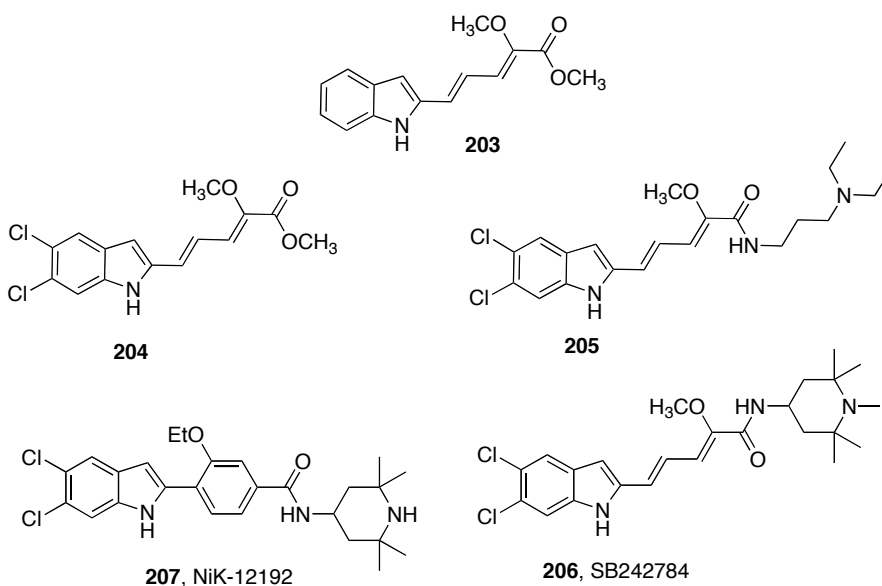
Figure 17. Small molecules mimicking bafilomycins

2.3.2 Benzolactone Enamide Family

2.3.2.1 Salicylihalamides, Oximidines, and Lobatamides

The growing family of V-ATPase inhibitors known as the benzolactone enamides contains diverse molecular features of a benzo-fused macrolactone bearing an N-acylated enamide side-chain (Figure 1). Members of this family include: (1) salicylihalamides A and B,[3, 4] (2) oximidines[8-10] I, II, and III (3) the lobatamides.[5, 6] Testing in the NCI 60-cell line panel revealed that the melanoma cell lines were the

most sensitive panel with this natural product family. Subsequent COMPARE analysis revealed that these compounds target V-ATPases.[137] The unique feature of this natural product family is their selectivity toward mammalian V-ATPases. They were shown to inhibit human kidney, liver, and osteoclast V-ATPase in membrane preparations at low- to sub-nanomolar concentrations, but were inactive against V-ATPases of fungi. In addition, the benzolactone enamide family also included CJ-13,350 and CJ-13,357,[138] isolated from fungi metabolites, and apicularen A and B, isolated from myxobacterial genus *Chondromyces*.[7]

Salicylihalamides A and B were isolated from the marine sponge *Haliclona sp.* by Boyd and co-workers in 1977 at the National Cancer Institute (NCI).[138] The isolation was hampered by the instability of the compounds in acidic media. The active compounds were identified as (-)-salicylihalamide A and (-)-salicylihalamide B. A ligand competitive assay revealed that salicylihalamides bind in a site different from the bafilomycins/concanamycins pocket.[139] This explains the unique selectivity profile of the benzolactone enamide family.

It is suspected that the benzolactone enamide members are irreversible inhibitors. The attempts to use the tritiated pentyloxy side chain analogue **208** in De Brabander's group showed only a small amount of radiolabeled V-ATPase after observing full inhibition, Figure 18. This inferred that the inhibition process might proceed from the capture of a reactive N-acyliminium ion, upon the protonation of the enamide unit, by a protein residue of V-ATPases. Then hydrolysis can take place to release the amide unit of the side chain.
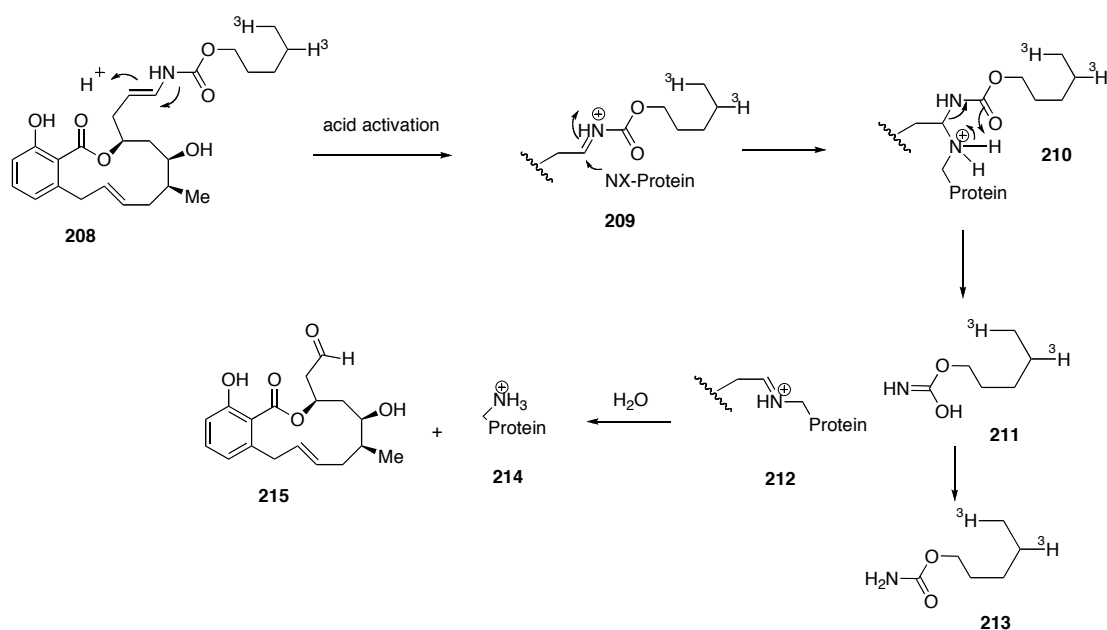
Figure 18. Proposed inhibitory process of benzolactone enamides[139]

Oximidines I, II, and III were isolated from *Pseudomonas* sp. by Hayakawa and coworkers.[8-10] These molecules inhibited the growth of oncogene-transformed cell lines of 3Y1, with adenovirus E1A, v-H-*ras*, and v-*src* oncogenes at nanomolar concentrations. By flow cytometric analysis, oximidines were found to arrest the cell cycle of *ras*- and *src*-transformed 3Y1 cells at the G1 phase and to increase the expression of p21 at protein and mRNA levels.[8, 9] Thus, it was suggested that the inhibition of V-ATPase could induce p21 expression. The same observation was found when human colon cancer cells DLD-1 were treated with the potent V-ATPase inhibitor, bafilomycin A$_1$.[140] The protein p21 plays a role in cell cycle regulation, by inhibiting cyclin-dependent kinases (Cdk) required for progression from the G1 to the S phase.[141] It is also involved in the inhibition of DNA replication by inhibiting

proliferating-cell nuclear antigen to activate DNA polymerase. The expression of the p21 protein is critical for either tumor suppressor p53-mediated G1 arrest or apoptosis. Apoptosis is defined by morphologic changes, such as condensation and margination of chromatin concomitant with cell shrinkage. Oximidine III was found to be more potent than oximidine I by three to eight folds in normal and transformed 3Y1 rat fibroblasts. This suggests a significant effect of the 14-hydroxyl group or the enamide geometry.

Lobatamides A-F have been isolated from several collections of *Aplidium* and related species; from shallow water Australian collections of *Aplidium lobatum*, from a deep water collection of *Aplidium sp.*, and from an unidentified Philippine ascidian.[5, 6] These compounds are different in oxime and $\Delta^{24\text{-}25}$ double bond geometry and hydroxylation at C30. The COMPARE analyses revealed a high correlation of their cytotoxic panels with salicylihalamide A's cytotoxic profile.[137] Their cytotoxic activities are in the low nanomolar range for sensitive cell lines and micromolar potency for resistance cell lines. Lobatamide A was also found from the extraction of *Pseudomonas sp.* cultured from an Indonesian soil sample.[142] This occurrence of the same compound in different sources suggests the possibility of their biosynthesis in the tunicates by associated microorganisms or by accumulation through dietary intake.

2.3.2.2 CJ compounds and Apicularens

It was found that an increasing level of cholesterol together with a high concentration of low-density lipoprotein (LDL) contributes to the development and progression of atherosclerosis. Thus it would be desirable to decrease the level of circulating LDL by upregulate LDL receptors. CJ-13,350 and CJ-13,357, isolated from the fungus *Mortierella verticillata* ATCC 42662, were found to enhance the expression of the LDL receptor gene in human hepatocytes.[138] Their activities in the assay were 100 nM indicating that the geometry of the oxime has little effect on the activity. These compounds showed no activity on tubulin polymerization, lysosomal pH or cholesterol synthesis.

A final pair of microbial macrolides are Apicularens A and B, which were isolated from culture extracts of the myxobacterium *Chondromyces robustus* by the Höfle group.[7] Apicularen A was highly cytotoxic for cultivated human and animal cancer cells but showed no antimicrobial activity. The *N*-acetyl-glucosamine glycoside apicularen B was distinctly less cytotoxic in micromolar concentration and showed weak activity against a few Gram-positive bacteria. The COMPARE analysis of apicularen A in the NCI-60 screen produced a profile of selective cytotoxicity similar to the salicylihalamides and lobatamides.

2.3.2.3 Related Enamide Macrocycles

A recent reported enamide-bearing polyketide of V-ATPase inhibitor, palmerolide A (**216**), was isolated from *Synoicum adareanum,* a circumpolar tunicate found in the shallow waters around Anvers Island on the Antarctic Peninsula.[143] It inhibited bovine V-ATPase at IC_{50} of 2 nM. Palmerolide A showed high selectivity toward melanoma cancer cells (e.g., UACC-62, IC_{50} = 18 nM); meanwhile, it showed a much weaker cytotoxicity by three orders of magnitude relative to other cell lines. In addition, it strongly inhibited a bovine brain V-ATPase with an IC_{50} of 2 nM.
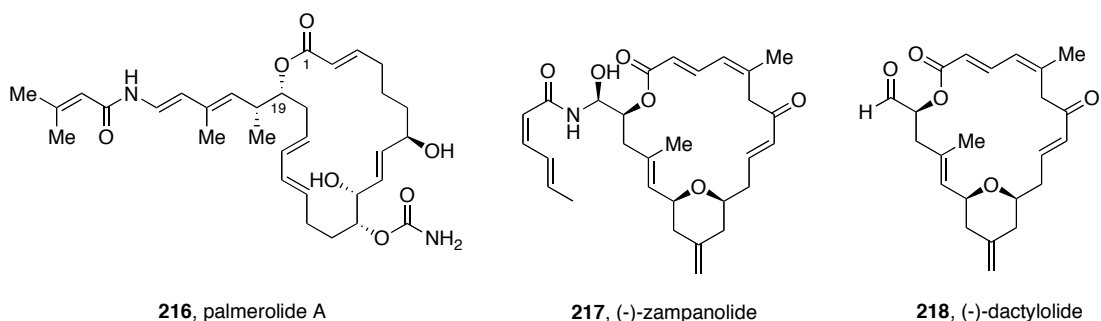
Figure 19. Related enamide macrocycles

Another hemiaminal-containing macrocycle, (-)-zampanolide (**217**), was isolated from marine sponge *Fasciospongia rimosa* collected near the island of Okinawa. The compound exhibited potent cytotoxicity at nanomolar concentrations against the P388, A549, HT29, and MEL28 cell lines.[144] The synthesized (-)-dactylolide (**218**) was found to have weak cell growth inhibition across an NCI 60-cell line screen by 2-3 orders of magnitude less than (-)-zampanolide.[145] This

illuminated the critical importance of the *N*-acyl hemiaminal side chain of the natural product for bioactivity. Even though there is no report related to V-ATPase inhibition, this evidence suggested that the hydrolyzed intermediate of the enamide moiety in the salicylihalamide family would lead to low cytotoxicity as well.
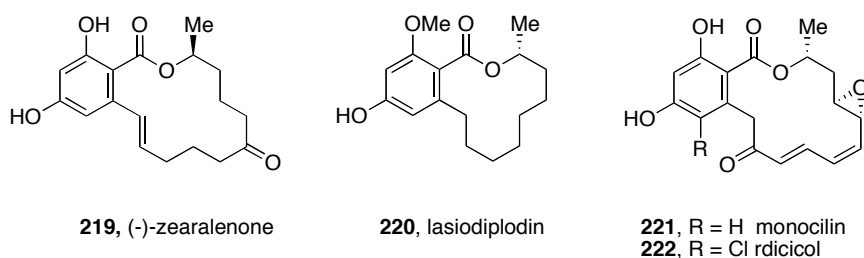
Figure 20. Benzolactone natural products

In addition, the lack of the enamide moiety in benzolactone-containing natural products such as (-)-zearalenone,[145, 146] lasiodiplodin,[147] monocillin,[148] and radicicol[148] resulted in inactivity toward V-ATPases. This infers that an enamide side-chain may be critical for binding to the biological target either for lipophilic interaction or for its role as a nucleophilic moiety as illustrated earlier.

2.3.2.4 SARs of Benzolactone Enamide Family

Extensive SARs of the benzolactone enamides have been conducted in an effort to simplify the synthesis, to define the mode of action, and the mode of binding. The first series of salicylihalamide analogues was designed the by DeBrabander's group with the aim of studying the role of the enamide side chain, Table 5.[139, 149]
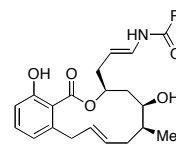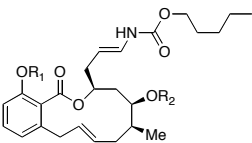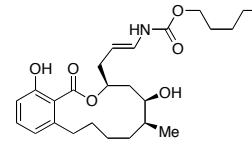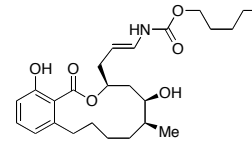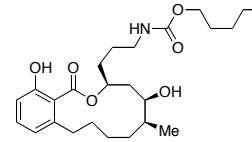
Table 5. Salicylihamide analogues and biological activity

Entry	Structure	V-ATPase IC$_{50}$ (nM)	SK-MEL-5 IC$_{50}$ (µM)	Binding Mode	Ref.
1	(-)-salicylihalamide A	< 1.0	0.06	irreversible	139, 149
2	(+)-salicylihalamide	270	NA	NA	139, 149
	R				
3	hexyl	1.0	0.38	irreversible	139, 149
4	C≡CPh	< 1.0	0.3	irreversible	139, 149
5	C≡CBu	1.0	0.3	NA	139, 149
6	O(CH$_2$)$_5$Me	1.6	0.5	irreversible	139, 149
7	S(CH$_2$)$_5$Me	1.8	0.45	NA	139, 149
8	farnesyloxy	> 1000	1.5	NA	139, 149

It is assumed that the *Z,Z*-diene moiety of the side chain might be responsible for the interaction with the V-ATPase binding pocket. The modified side chain

analogues of entry 3-7, Table 5, showed inhibitory activity equipotent with (-)-salicylihalamide A, with an irreversible binding mode toward a bovine brain V-ATPase. However, there is a limitation of the substituent group as seen from the weak inhibition of the fanesyloxy analogue (entry 8). It should be noted that the cytotoxicity of these analogues are at least ten-fold less potent than the natural product, despite their similar potency in the V-ATPase assay.
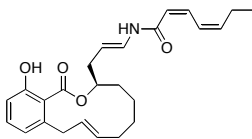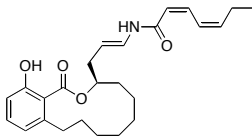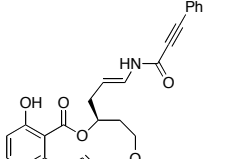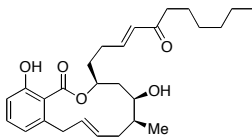
Table 6. Salicylihamide analogues and biological activity

Entry	Structure	V-ATPase IC$_{50}$ (nM)	SK-MEL-5 IC$_{50}$ (μM)	*Ref.*
1	(-)-salicylihalamide A	< 1.0	0.06	150
2	(+)-salicylihalamide	270	NA	150
3	R$_1$ = H, R$_2$ = Bz	300	1	150
4	R$_1$ = Bz, R$_2$ = H	180	> 20	150
5		3.0	8	150
6		30	> 20	150

The benzyl alcohol analogues entry 3 and 4, Table 6, are significantly less active than the parent compounds. This implies the involvement of a crucial hydrogen bonding

between salicylihalamide and the V-ATPase. The saturated macrolide analogue of entry 5 appeared to retain significant potency while the carbamide lacking the double bond of entry 6 showed a ten-fold lower activity.

Table 7. Salicylihamide analogues and biological activity
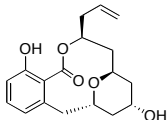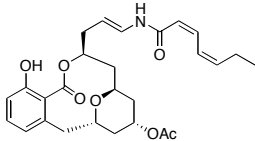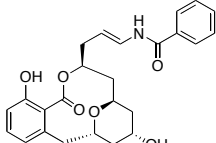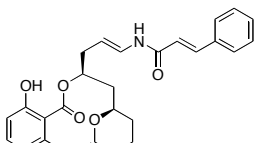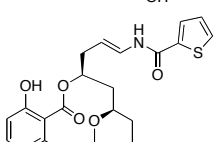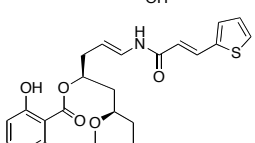
Entry	Structure	V-ATPase IC$_{50}$ (nM)	Cytoxicity	Ref.
1	(-)-salicylihalamide A	< 1.0	GI$_{50}$ = 38-81 nM	150
2	(+)-salicylihalamide	270	NA	150
3		NA	GI$_{50}$ = 110-870 nM	150
4		NA	GI$_{50}$ = 370-880 nM	150
5		4.5	IC$_{50}$ = 0.20-1.03 μM	151
6		7.5	NA	150

The simplified analogues lacking the hydroxyl and methy groups as shown in entry 3 and 4, Table 7, were about 3-10 times less potent than (-)-salicylihalamide A. This

suggested that the macrocyclic double bond is important but not critical for the activity. The ether analogue of entry 5 retained inhibition similar to the natural product, but was weakly cytotoxic. It is worth noting that the removal of substituents and the endocyclic double bond attenuates the biological activity. The α,β-unsaturated ketone derivative (entry 6) was a potent reversible inhibitor for V-ATPase inhibition. This was in agreement with the mechanistic proposal that the nucleophile intermediate is necessary for the activity of benzolactone enamide.
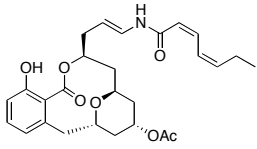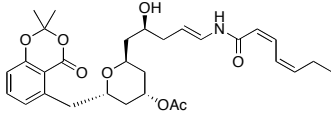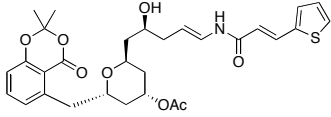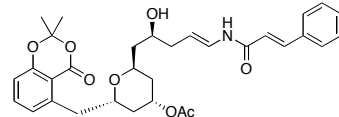
With regard to the critical role of the enamide moiety based on SARs of salicylihalamide A, several analogues of apicularen have been prepared by Maier's group and Nicolaou's group. Similar results were found in apicularen analogues. The variations in the acyl part of the enamide are tolerated with a certain chain length as observed by DeBrabander's group. The analogues of entry 5 and 7, Table 8, with short substituent groups showed weak cytostatic affects relative to their congeners, but without the enamide there is no activity (entry 3). The acetylated analogue of entry 4 showed a small change in the activity; however, the glycosidated apicularen B showed total loss of activity. The $\Delta^{17,18}$ (*Z*)-apicularen A isomer (entry 2) showed a 100-fold reduced cytotoxicity. This might suggest that *trans* geometry orchestrates the optimal orientation between the side chain and the salicylate substituents for the target binding.

Table 8. Apicularen analogues against 1A9 human ovarian carcinoma cell lines

Entry	Structure	IC$_{50}$ value	*Ref.*
1	apicularen A	0.78 ± 0.4 nM	[152]
2	$\Delta^{17,18}$ (*Z*)-apicularen A	70.7 ± 10.4 nM	[152]
3		> 20 µM, SK-MEL-5	[153]
4		3.2 nM	[152]
5		> 1500 nM	[152]
6		30.3 ± 4.6 nM	[152]
7		805.5 ± 145 nM	[152]
8		41.3 ± 5.8 nM	[152]

The intermediate open-chain analogue entries 3-5 (Table 9) showed significant potency for cell inhibitions; however, they are ten-fold less potent than their corresponding macrolides.
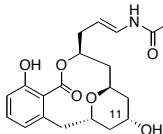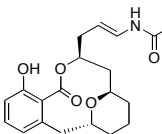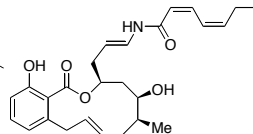
Table 9. Apicularen analogues against 1A9 human ovarian carcinoma cell lines

_____

Entry	Structure	IC_{50} value (nM)	*Ref*.

_____

Entry	Structure	IC_{50} value (nM)	*Ref*.
1	apicularen A	0.78 ± 0.4	152
2		3.2	152
3		35	152
4		357	152
5		387	152

_____

Maier's group showed that the 11-deoxy analogue, Table 10, retained cytotoxicity similarly to apicularen A and it showed better activity against drug
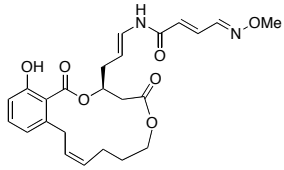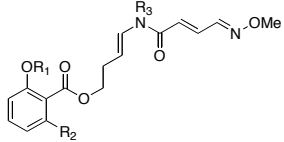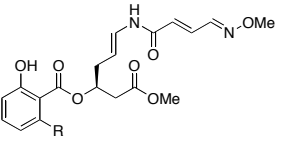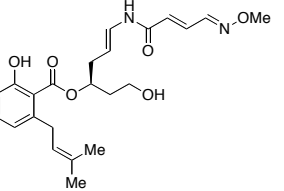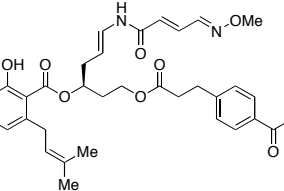
resistant cell lines than apicularen A. This observation suggested that the 11-OH is not responsible for the cytotoxicity and the inactivity of apicularen B, glycosidated at C11, might result from the steric factor.

Table 10. Cytotoxicity values of benzolactone enamides[154]

_____

Cell line	Origin	Specicies	apicularen A	11-deoxy analogue	(-)-salicylihalamide A

_____

Cell line	Origin	Specicies	apicularen A	11-deoxy analogue	(-)-salicylihalamide A
L-929	connective tissue	mouse	6.8	19	57
Y1	connective tissue	rat	2.3	8.2	23
KB-3-1	cervix carcinoma	human	2.3	7.1	6.8
KB-V1	multiple drug-re-sistant cell line	human	15.9	2.4	9.1

_____

Due to the important role of the enamide side chain, all of the simplified lobatamide analogues bear the enamide side chain as shown in Table 11. The simplified macrolide of entry 2 showed a 600-fold drop in activity, indicating that the ring size and substitution of the macrolactone are important. Salicylate compounds (entries 3 and 5) with minor modifications were found to bind weakly to V-ATPase, whereas the N-methylated analogue (entry 6) showed much less activity. Also the methylated phenol analogue (entry 4) was devoid of activity.

Table 11. Lobatamide analogues against bovine V-ATPase

_____

Entry	Structure	IC_{50} value (µM)	*Ref.*

_____

| 1 | Lobatamide C | 0.002 | 155 |

| 2 | | 1.2 | 155 |

3	$R_1 = H$, $R_2 = H$, $R_3 = H$ 25% inhibition at 20 µM; higher concentration not soluble[155]		
4	$R_1 = Me$, $R_2 = H$, $R_3 = H$	no effect	155
5	$R_1 = H$, $R_2 = Me$, $R_3 = H$	1.3	155
6	$R_1 = H$, $R_2 = H$, $R_3 = Me$	200	155

| 7 | R = Me | 0.1 | 155 |
| 8 | R = Prenyl | 0.06 | 156 |

| 9 | | 0.01 | 157 |

| 10 | | 0.1 | 157 |

_____

These results indicate the importance of both free hydroxyl and NH functionalities for hydrogen-bonding interactions. The increase of lipophilicity from a methyl group (entry 7) to a prenyl group (entry 8) showed an improvement of the activity. Interestingly, the primary alcohol of entry 9 showed high potency for V-ATPase inhibition close to the activity of natural product lobatamide c whereas the benzophenone photoaffinity labeling congener of entry 10 showed good inhibition at IC_{50} of 100 nM.[157] The benzophenone photoprobe was selected due to its stability, mild conditions required for photoactivation (350-360 nm, n $\rightarrow \pi^*$), and selectivity towards weak C-H σ-bonds.

2.3.3 Novel Oximidine Analogues with Improvement of Stability

The SARs conducted on benzolactone enamides have demonstrated that the enamide side chain is crucial for their anti-cancer activity. However, it is believed that the enamide is labile under physiological conditions. In fact, the isolation of salicylihalamides was not a straightforward process, hampered by the instability of the compounds in acidic conditions.[4] In synthetic protocols for the preparation of compounds of the benzolactone family, the enamide side chain is always installed at the end.[13, 61, 92] *Our hypothesis is that the replacement of the enamide with a stable warhead can allow the discovery of novel anti-cancer agents with improved pharmacokinetic stability.*

We chose three different warheads stable under physiological conditions that could undergo nucleophilic addition like an enamide; namely vinyl sulfone, boronic

acid and α-ketone oxadiazole, Figure 21. Based on a CoMSIA/QSAR analysis, we have designed, prepared and evaluated analogues of oximidine II possessing a modified macrocyclic structure that carries a vinyl sulfone, a boronic acid and an α-keto oxadiazole instead of the enamide side chain, Figure 21. Based on the result of the cytotoxicity of the sulfone containing macrocycle we decided to prepare the natural triene core of oximidine II and substitute the enamide side chain with a vinyl sulfone.
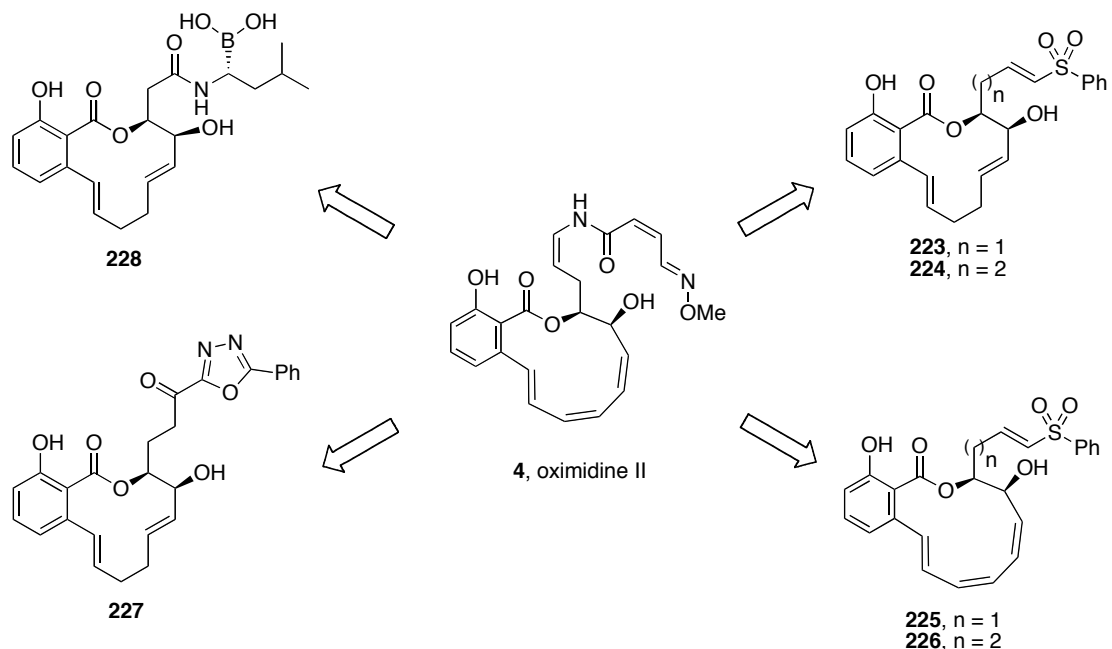
Figure 21. Oximidine II analogues with stable warheads

The ethyl spacer between the vinyl sulfone and the macrocycle was chosen to keep the same distance between the N-acyliminium moiety (generated under the acidic condition from the protonation of an enamide)[139] and the macrocycle.

However, this spacer can be tuned for length and flexibility, to optimize the biological activity of this class of analogues.

2.3.3.1 Irreversible Inhibitor

The vinyl sulfone is known to serve as an irreversible inhibitor towards cysteine proteases such as papain,[158] cruzaine,[159] cathepsin V,[160] *Staphylococcus aureus* sortase,[161] and proteasome.[162] Hanzlik and coworkers designed highly potent irreversible protease inhibitors bearing a vinyl sulfone moiety.[158] The irreversible inhibitory activity results from the formation of covalent bonds with thiol in the active site of the cysteine proteases. This could allow the investigation of the binding pocket at the molecular level.[160]

The unique property of the vinyl sulfone is that under physiological conditions it does not undergo nucleophilic addition, while once at the active site of the target, strategic hydrogen bond interactions activate the reactive site.[163] We designed this class of inhibitor, assuming that the acidic environment surrounding the V-ATPase would activate the electrophilic vinyl sulfone moiety towards Michael addition.

2.3.3.2 Reversible Inhibitor

Boronic acids have been used extensively as reversible inhibitors due to their Lewis acidity to interconvert between sp^2 and sp^3 allowing binding to nucleophiles such as alcohols and amines. In fact, boronic acids are functional groups often present in inhibitors that mimic the transition state of hydrolytic enzymes. Compounds

containing boronic acid are known to reversibly inhibit serine protease, including thrombin,[164] dipeptidyl peptidase,[165] elastase,[166] fatty acid amide hydrolase (FAAH),[167] and bortezomib (Velcade),[168] which was the first FDA approved proteasome inhibitor and is in clinical use for the treatment of multiple myeloma and mantle cell lymphoma.[169]

Even though 1,3,4-oxadiazoles are present in a wide range of biologically active molecules, including antimicrobial, anti-fungal, anti-inflammatory, and antihypertensive, the α-keto oxadiazole moiety is still under-explored in medicinal chemistry.[170-172] Recently, a series of proteasome inhibitors containing an α-keto oxadiazole warhead were reported as selective and reversible inhibitors toward human prostate cancer at subnanomolar concentrations.[173] α-Keto oxadiazole containing compounds have been developed as FAAH inhibitors.[174, 175] The crystal structures of FAAH bound to α-ketooxazoles showed the presence of a tetrahedral intermediate resulting from a covalent bond between serine and the ketone.[176]

Based on our CoMSIA/QSAR result, we believe that the designed macrocycles **183**, and **184** are valid templates for the preparation of novel active analogues. The proposed inhibitory mechanisms of these novel compounds toward the V-ATPases are illustrated in Figure 22.
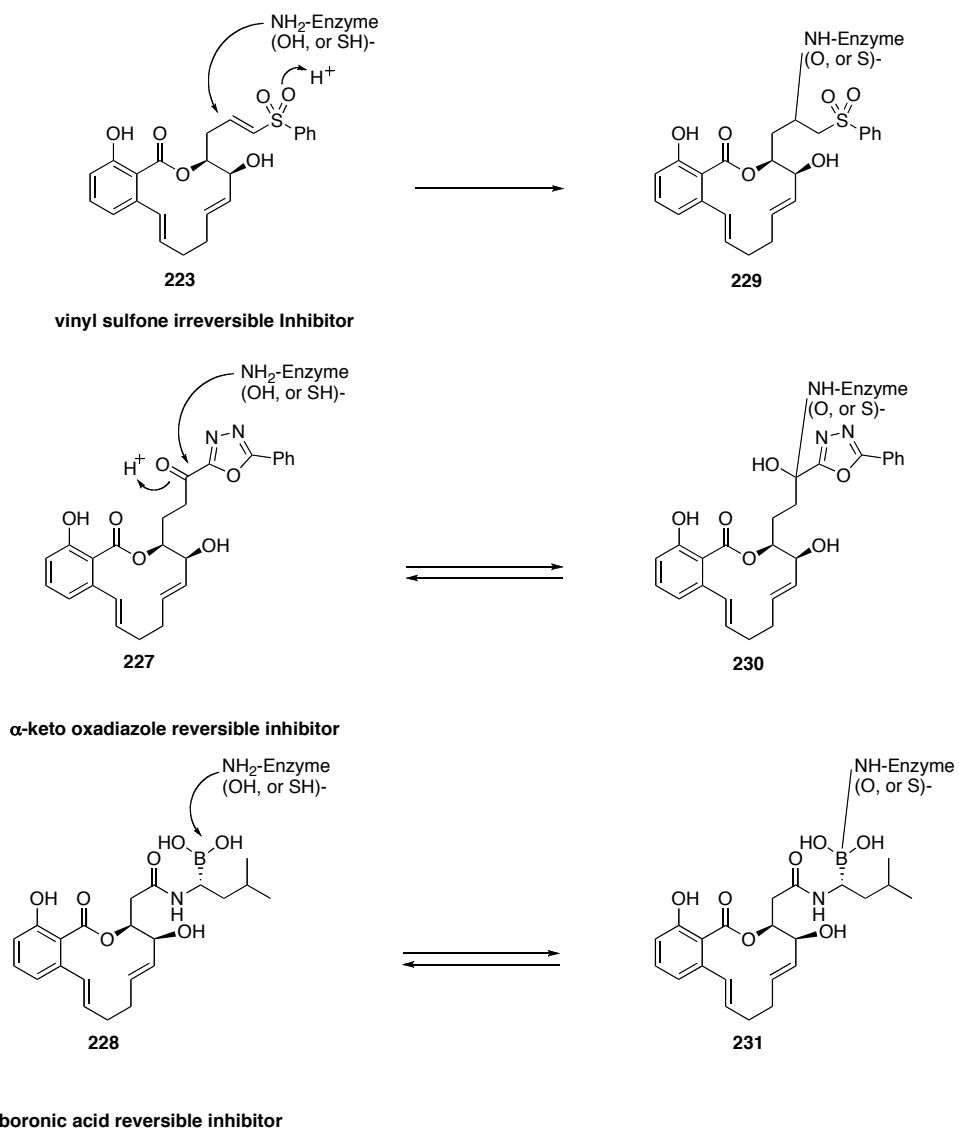
Figure 22. Proposed mechanisms of V-ATPase inhibitions by different classes of inhibitors.

2.3.4 Preparations of vinyl sulfone V-ATPase irreversible inhibitors

The novel analogues were prepared by attaching the simplified core structures described in Chapter 1 to the side chains mentioned above. For this preliminary SAR, phenyl vinyl sulfone was chosen to serve as the lipophilic moiety to interact with the

target as predicted from our CoMSIA/QSAR model. The vinyl phenylsulfone analogues were synthesized using a Horner-Wadsworth-Emmons (HWE) reaction.
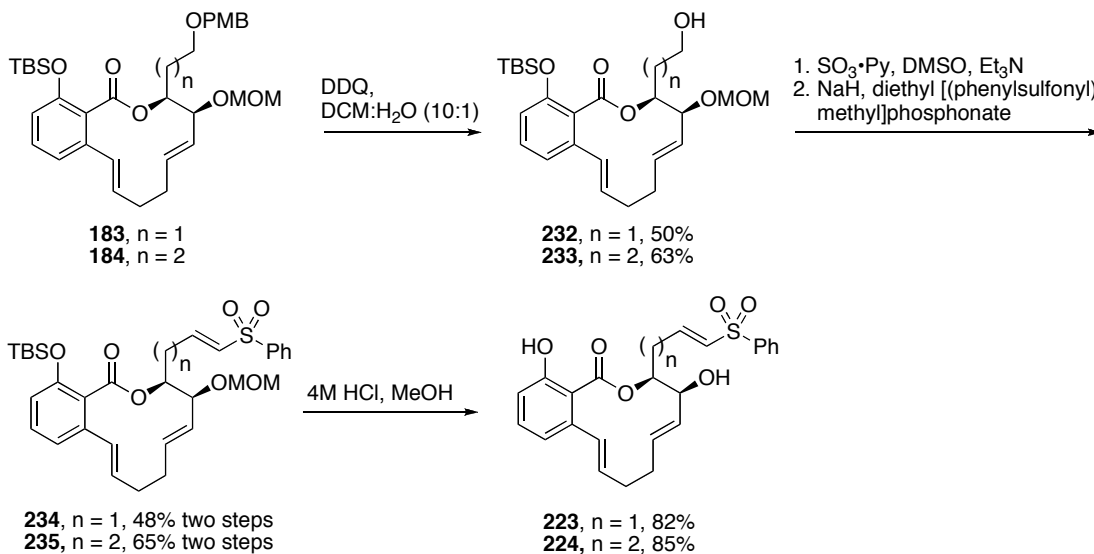
Scheme 37. Preparations of vinyl sulfone inhibitors of simplified macrocycles

Deprotection of the PMB group by oxidative cleavage with DDQ gave alcohols **232** and **233**. The resulting products were oxidized under Parikh-Doering conditions to give the aldehyde intermediates. Treatment of the HWE reagent prepared from the oxidation of commercially available diethyl [(phenylthio)-methyl]phosphonate with H_2O_2[177] with NaH and the corresponding aldehydes afforded vinyl phenylsulfones **234**, and **235** in good yield. The acidic cleavage of the MOM and TBS groups with diluted HCl provided the final vinyl phenylsulfones **223** and **224**.

Similar routes were used to prepare the vinyl phenylsulfone analogues of oximidine II. The triene macrocycle **110** was prepared using the reductive copper-

mediated macrocycle formation already mentioned in chapter 1. The deprotection of the TBDPS group using TBAF provided the corresponding alcohol **236** which underwent oxidation with PDC to afford the required aldehyde. The intermediate was treated with the HWE reagent to provide vinyl phenylsulfone **237**. The mild acidic cleavage of the MOM-ether with carbon tetrabromide (CBr$_4$) in warm *i*-PrOH gave the secondary alcohol **238**. This CBr$_4$ mixture of reagents generated a small amount of hydrobromic acid that facilitated the deprotection. Following the procedure of Georg and Schneider, treatment of aryl methyl ether **238** with BCl$_3$ gave the desired vinyl phenylsulfone inhibitor **225**.
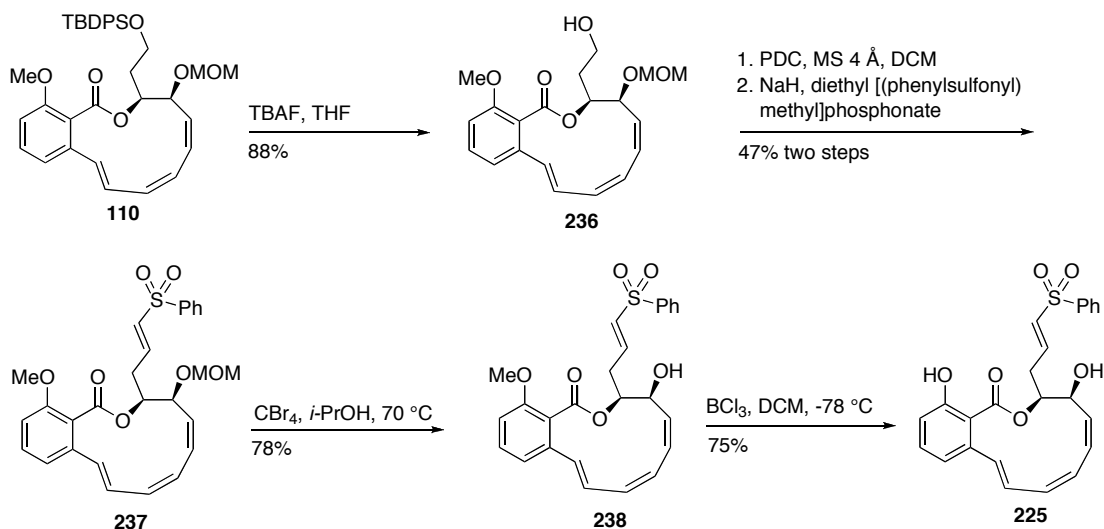
Scheme 38. Preparation of a vinyl phenylsulfone analogue of oximidine II

The synthesis of the homolog vinyl phenylsulfone **226** began with the triene macrocycle **144** generated by total synthesis using the RCM reaction as mentioned in Chapter 1. The oxidative cleavage of the PMB ether **144** using DDQ provided the

alcohol **239**. This intermediate was subjected to PDC oxidation to provide the corresponding aldehyde. The vinyl phenylsulfone **240** was obtained by treatment of HWE reagent with NaH and aldehyde. Using the previous mild acidic cleavage condition, global deprotection of both TBS and MOM ether groups provide vinyl phenylsulfone analogue **226**.
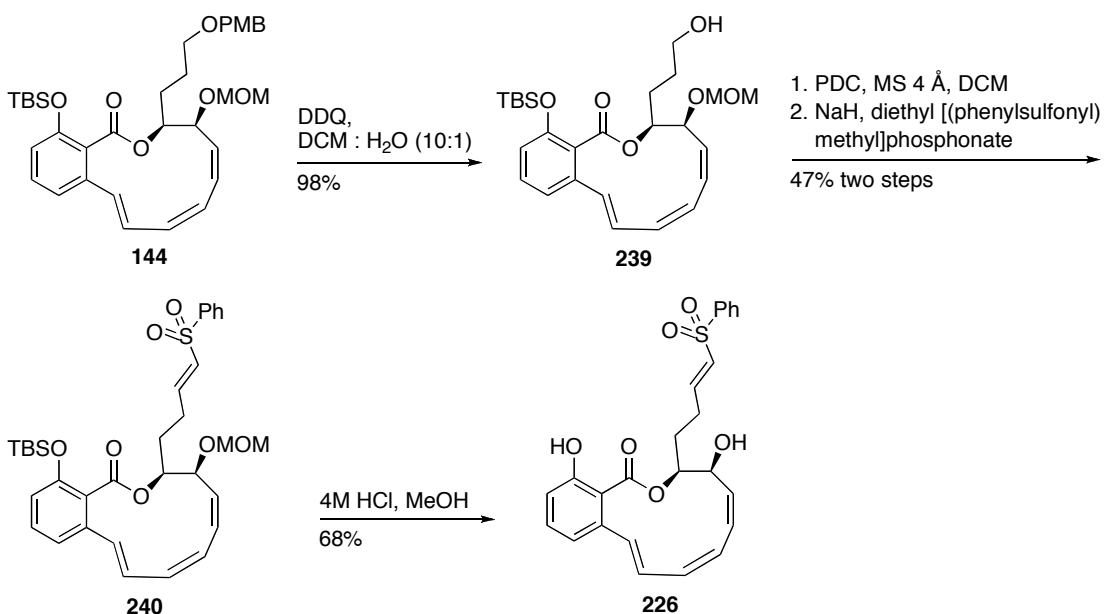
Scheme 39. Preparation of a vinyl phenylsulfone homolog analogue of oximidine II
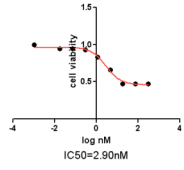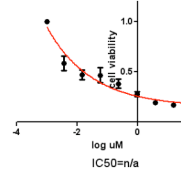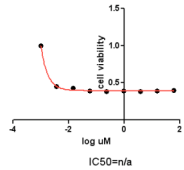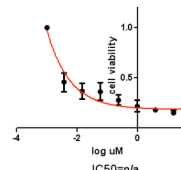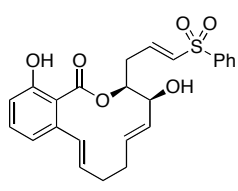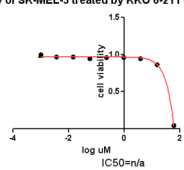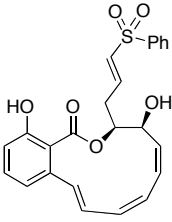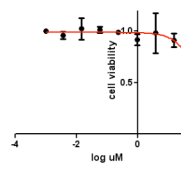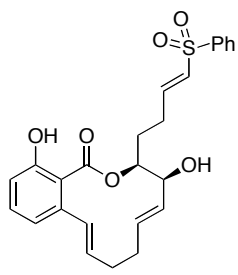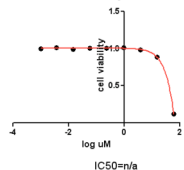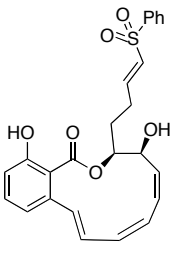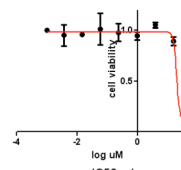
2.3.5 Biological evaluation of vinyl phenylsulfones

According to the NCI 60-cell screen, the melanoma cell lines were found to be the most sensitive to oximidine II. The cell-cytotoxic assay was conducted by Dr. Defeng Tian at the HTS laboratory, Institute for Therapeutics Discovery and Development, University of Minnesota. The SK-MEL-5 was used in our cytotoxicity

assay to evaluate the biological activity of the synthesized vinyl phenylsulfone analogues **223**, **224**, **225**, and **226**. Taxol, colchicine, oximidine I (natural product from extraction), and synthesized oximidine II (courtesy of Georg and Schneider, total synthesis) were used as positive control experiments. The result of cell inhibition of SK-MEL-5 revealed that all of our vinyl phenylsulfones were micromolar inhibitors, IC_{50} in the range of 20-60 μM; while the natural product oximidine I and the synthesized oximidine II showed an IC_{50} of about 60 nM, estimated from graph, Table 12.

However, our analogues containing the simplified core structure were equipotent to the triene core structure of the oximidine II. This result supported our hypothesis guided by CoMSIA/QSAR. The cytotoxicity of these analogues might result from the presence of the vinyl sulfone which irreversibly inhibits the enzyme. The replacement of the phenyl group at the vinyl sulfone with other substituents could improve the cytotoxicity of these inhibitors.

Table 12. Cell growth inhibition of vinyl phenylsulfone analogues

Compounds	SK-MEL-5	Compounds	SK-MEL-5
Taxol	IC50 assay of SK-MEL-5 treated by Taxol for 48 IC50=2.90nM	**Oximidine I**	IC50 assay of SK-MEL-5 treated by Oximidine for 48 IC50=n/a
Colchicine	IC50 assay of SK-MEL-5 treated by colchicine for 4 IC50=n/a	**Oximidine II**	IC50 assay of SK-MEL-5 treated by CSM11-225 for 4 IC50=n/a
223	IC50 assay of SK-MEL-5 treated by KKO 6-211 for 4 IC50=n/a	**225**	IC50 assay of SK-MEl-5 treated by KKO8-019 for 48 IC50=n/a
224	IC50 assay of SK-MEL-5 treated by KKO 7-011 for 4 IC50=n/a	**226**	IC50 assay of SK-MEL-5 treated by KKO8-015 for 48 IC50=n/a

2.3.6 Ongoing Project

Based on the comparable biological activity of the vinyl sulfones with the simplified core and the vinyl sulfones with the oximidine II triene core, we decided to use the simplified macrocycle to explore the SAR of the boronic acid and the α-keto oxadiazole. Both compounds were tested as crude products without further purification. ESI/HRMS analysis showed only one peak corresponding to the desired molecular ion. This initial task was performed to verify the activity of this class of compounds. Further studies are ongoing, including the complete characterization of these compounds.

2.3.6.1 Preparation of α-keto oxadiazole V-ATPase reversible inhibitor

The preparation of the α-keto oxadiazole began with the common intermediate alcohol **233**, Scheme 41. The phenyl moiety attached to the oxadiazole was chosen for our preliminary SARs to serve as a lipophilic portion able to bind to the enzyme. The 2-phenyl-1,3,4-oxadiazole was prepared from the condensation of phenyl hydrazide and triethylorthoformate under microwave irradiation without any solvent at 80 °C using Nafion®NR50 (a perfluorinated polymer with sulfonic acid groups) as an acidic catalyst, Scheme 40.[178]
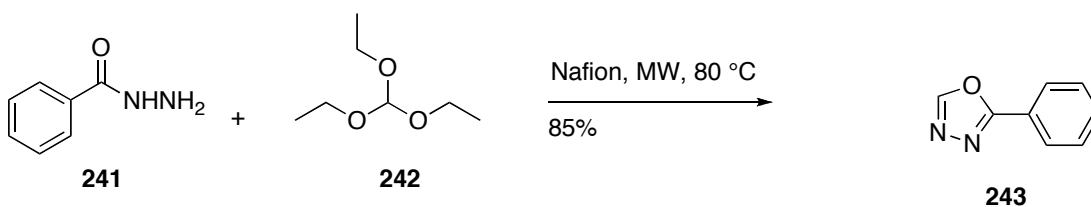
Scheme 40. Preparation of 2-phenyl-1,3,4-oxadiazole

The alcohol **233** was oxidized under Parikh-Doering conditions to give an aldehyde intermediate. The aldehyde was treated with lithiated oxadiazole to provide a diastereomeric mixture of alcohols.[173] The resulting alcohols were oxidized with DMP to provide the α-keto oxadiazole **244**. The global deprotection of TBS and MOM with 4M HCl in MeOH provided the crude product **227**.
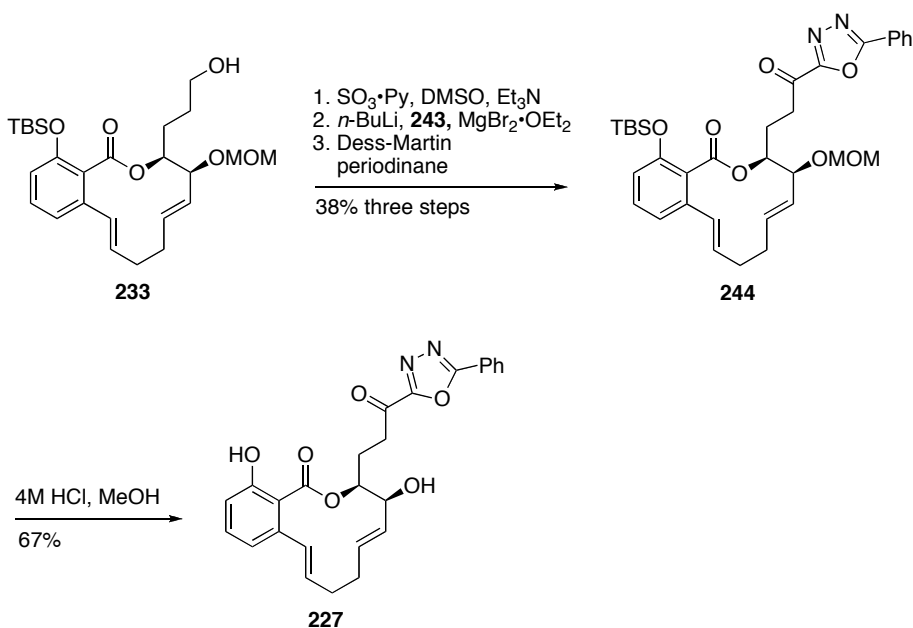
Scheme 41. Preparation of the α-keto oxadiazole analogue

2.3.6.2 Preparation of a boronic acid V-ATPase reversible inhibitor

The 3-methylbutane moiety of α-amino boronic acid **228**, Scheme 43, was assumed to promote the lipophilic interaction of the inhibitor with the binding pocket of the V-ATPase as predicted from the CoMSIA/QSAR. The analogue **228** was prepared from the coupling of the acid **250** and α-amino boronic ester **249**, Scheme

43. The asymmetric copper-catalyzed borylation on the corresponding N-butanesulfinyl aldimine of **245** (Ellman's protocol)[179] was used to prepared the required α-amino (*R*)-boronic ester **248**, Scheme 42. The butane sulfinyl was cleaved under mild acidic conditions using 4M HCl in a dioxane and methanol mixture to provide the desired α-amino boronic ester **249**.
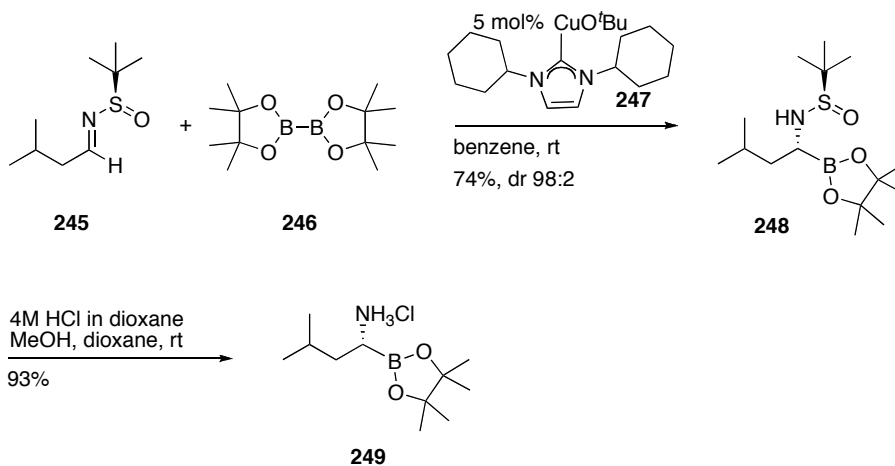
Scheme 42. Synthesis of an α-amino (*R*)-boronic ester

The oxidation of alcohol **232** with [bis(acetoxy)iodo]benzene (BAIB) and 2,2,6,6-tetramethyl-1-piperidinyloxyl (TEMPO) provided the required acid **250**.[180] The amine **249** was coupled with the acid **250** using TBTU according to the Millennium protocol, and without purification subsequently hydrolyzed under biphasic conditions utilizing *iso*-butylboronic acid as a pinacol sequestering agent to provide the desired crude boronic acid analogue **228**, Scheme 43.[168]
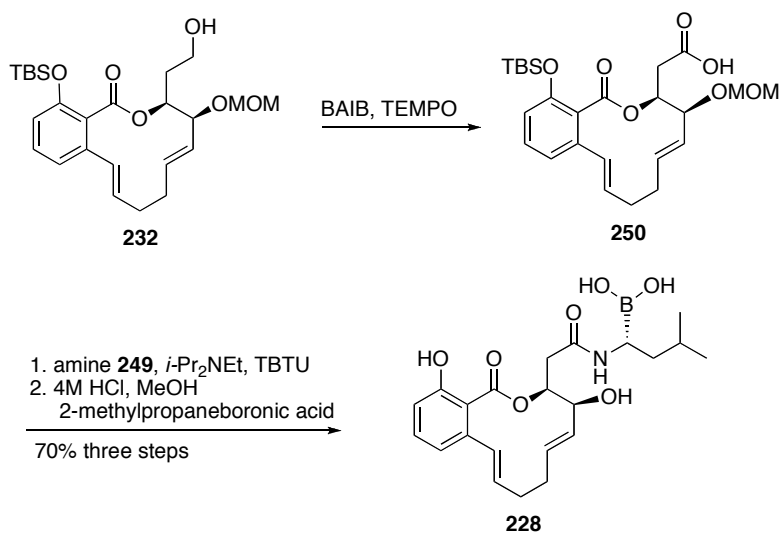
Scheme 43. Preparation of the boronic acid analogue

2.3.6.3 Biological evaluation of the vinyl sulfone, α-keto oxadiazole and boronic acid analogues

All new analogues of α-keto oxadiazole **265**, boronic acid **266**, and vinyl sulfone **261** and **262** were tested for cell growth inhibition on four human cancer cell lines using taxol and colchicine as positive controls for leukemia (HL-60), breast (MCF-7), and melanoma (SK-MEL-28 and SK-MEL-5) cell lines. The results showed that these analogues were micromolar inhibitors in vitro, greater than 20 μM, Table 13 and Table 14, except for the α-ketone oxadiazole that did not display any cytotoxicity in HL-60 cell lines (Table 13). Even though the α-keto oxadiazole analogue showed loss of cytotoxicity, it emphasized the necessity of the enamide as well as the suitable warhead architecture for biological activity. On the other hand, the loss of cytotoxicity of the α-keto oxadiazole might result from the presence of the

large phenyl group on the oxadiazole moiety. The activity of the compounds containing nucleophiles (vinyl sulfone and boronic acid) supports the proposed mechanism.

Table 13. Cell growth inhibition of leukemia HL-60 cell lines
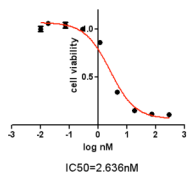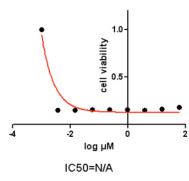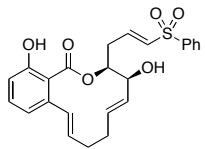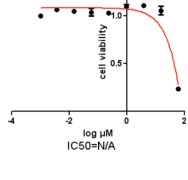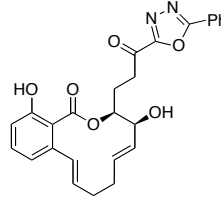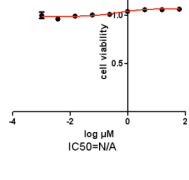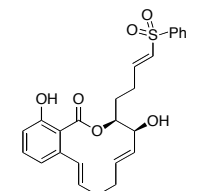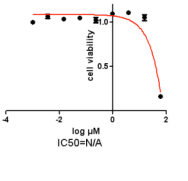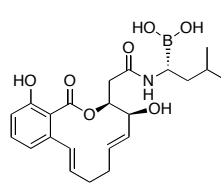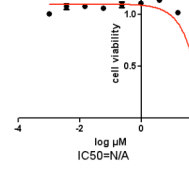
Compounds	HL-60	Compounds	HL-60
Taxol	IC50 assay of HL-60 Treated by Taxol for 48 hours IC50=2.636nM	Colchicine	IC50 assay of HL-60 Treated by colchicine for 48 IC50=N/A
223	IC50 assay of HL-60 Treated by kko-6-211 for 48 hou IC50=N/A	227	IC50 assay of HL-60 Treated by kko-7-017Cfor 4 IC50=N/A
224	IC50 assay of HL-60 Treated by kko-7-011 for 48 hours IC50=N/A	228	IC50 assay of HL-60 Treated by kko-6-245 fo IC50=N/A

Table 14. Cell growth inhibition of melanoma (SK-MEL-28 and SK-MEL-5) and breast (MCF-7) cell lines

Compounds	SK-MEL-28	SK-MEL-5	MCF-7
Taxol	IC50 assay of SK-MEL-28 treated by Taxol for IC50=n/a	IC50 assay of SK-MEL-5 treated by Taxol for 48 IC50=2.90nM	IC50 assay of MCF-7 treated by Taxol for 48 hours IC50=1.282nM
Colchicine	IC50 assay of SK-MEL-28 treated by colchicine fo IC50=n/a	IC50 assay of SK-MEL-5 treated by colchicine for IC50=n/a	IC50 assay of MCF-7 treated by Colchicine for 48 hours IC50=n/a
223	IC50 assay of SK-MEL-28 treated by KKO 6-211 fo IC50=n/a	IC50 assay of SK-MEL-5 treated by KKO 6-211 for IC50=n/a	IC50 assay of MCF-7 treated by KKO 6-211 for 48 hours IC50=n/a
224	IC50 assay of SK-MEL-28 treated by KKO 7-011 fo IC50=n/a	IC50 assay of SK-MEL-5 treated by KKO 7-011 for IC50=n/a	IC50 assay of MCF-7 treated by KKO 7-011 for 48 hours IC50=n/a
228	IC50 assay of SK-MEL-28 treated by KKO 6-245 fo IC50=n/a	IC50 assay of SK-MEL-5 treated by KKO 6-245 for IC50=n/a	IC50 assay of MCF-7 treated by KKO 6-245 for 48 hours IC50=n/a

2.4 Conclusion

In conclusion, a series of novel V-ATPase inhibitors with acid stable warheads (boronic acid, α-ketone oxadiazole, and sulfone) were designed, prepared and evaluated for their cytotoxicity. It was found that at least the simplified core structure analogues derived from CoMSIA/QSAR of vinyl phenylsulfones were equipotent to the triene core of oximidine II towards SK-MEL-5 cell lines.

The biological activity of this class of V-ATPase inhibitors could be improved since both vinyl sulfone and boronic acid are weakly cytotoxic against leukemia (HL-60), breast (MCF-7), and melanoma (SK-MEL-28 and SK-MEL-5) cells in the range of 20-60 μM. These results indicate that we are headed in the right direction for the design and preparation of more stable inhibitors of V-ATPases.

Chapter 3

Novel Endotoxin-Sequestering Compounds with Terepthalaldehyde-*bis*-Guanylhydrazone Scaffolds

3.1 Introduction

Bacteria are classified into two groups based on their appearance after treatment with the Gram stain.[181] The bacteria that stain purple when treated with the crystal violet stain are called Gram positive, while those that do not retain the violet stain and turn red or pink after the addition of a counterstain (commonly safranin) are the Gram negative bacteria. This different response to the stain is due to the composition of their cell walls. Gram-positive bacteria have a relatively thick layer of peptidoglycan surrounding their plasma membrane, whereas Gram-negative bacteria have a thin layer of peptidoglycan covered by an outer membrane.
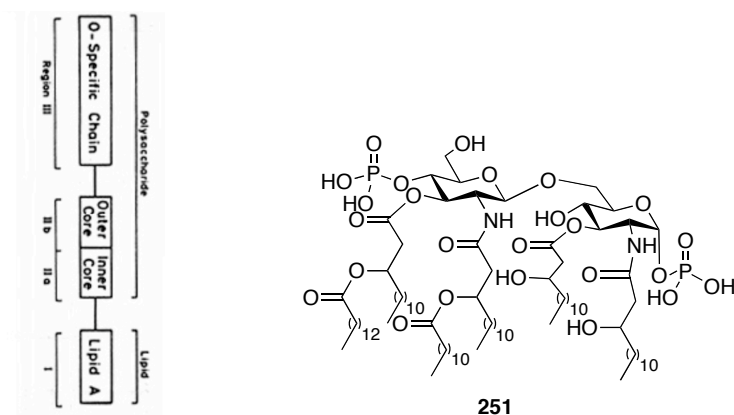
Figure 23. Schematic[182] of Lipopolysaccharide (*left*) and Lipid A (*right*)

The outer membrane of Gram-negative bacteria is composed of lipopolysaccharide (LPS), large molecules that contribute to the structural integrity of the bacteria and protect them from certain types of chemical attacks.[182]

LPS molecules are made of a lipid and a polysaccharide joined by a covalent bond. The polysaccharide includes two regions, the O-antigen, with a high level of diversity in structure and composition, and a core region, which is relatively well conserved and similar in large groups of bacteria.[182] Lipid A is a common amphipathic constituent of the LPS of all Gram-negative bacteria and is composed of a hydrophilic, negatively charged bisphosphorylated diglucosamine backbone, and a hydrophobic domain of six (*E. coli*) or seven (*Salmenella*) acyl chains in amide and ester linkages, Figure 23.[183] LPS acts as an endotoxin, and induces a strong response from the normal animal immune system.[184-186] LPS triggers the release of inflammatory cytokines, in particular TNFα, interleukin-1β and IL-6.[187, 188] It is the uncontrolled and precipitous systemic inflammatory response that ultimately results in the fatal shock syndrome characterized by endothelial damage, coagulopathy, loss of vascular tone, myocardial dysfunction, tissue hypoperfusion, and multiple organ failure.[189-191]

Despite tremendous advances in antimicrobial chemotherapy, the incidence and mortality due to Gram-negative sepsis continues to escalate worldwide.[192, 193] It is the number one cause of death in the intensive care unit, with a current estimate of at least 750,000 cases per year, and 215,00 fatalities in the United States annually.[194] The healthcare system in the United States spends about 16.7 billion dollars annually

to treat this condition.[194]

LPS is a potential drug target since it plays a prominent role in raising the immune response that causes sepsis.[185] LPS itself is chemically inert. The presence of LPS in blood, often a consequence of antibiotic therapy of preexisting bacterial infections, sets off a cascade of exaggerated host responses.[195] Thus, it would be challenging to prevent mortality from Gram-negative shock by the development of antimicrobial agents.

The total synthesis of lipid A has established that lipid A is the toxic center of LPS.[196] The receptors capable of recognizing the pathogen-associated molecular patterns are Toll-like receptors (TLRs) and scavenger receptors, thereby providing immunity against infection.[197] TLRs are on the surface of immune cells, heart muscle cells, and cells that line blood vessels. Ten members of the TLR family have been identified in humans.

LPS stimulation of mammalian cells involves several proteins including LPS binding protein (LBP), CD14, MD-2 and TLR4.[198-201] LBP protein directly binds to LPS and facilitates the association between LPS and CD14.[202] CD14 is responsible for transferring LPS to the TLR4/MD-2 receptor complex.[203] It has been shown that mutation of the TLR4 gene leads to low response to LPS.[204, 205] TLR4 requires the MD-2 protein to form a complex at the cell surface to promote the physiological recognition of LPS. This was supported by the crystal structure of the TLR4-MD-2-LPS dimerized complex at 3.1 A° resolution of the extracellular region, a leucine-rich domain.[206] The TLR4-MD-2-LPS complex is believed to play a role in   the

recruitment of specific proteins to initiate the signaling cascade. TLR signaling

involves the activation of transcription factors such as nuclear factor-κB (NF-κB) and

members of the interferon (IFN)-regulatory factor (IRF) family.[207, 208]
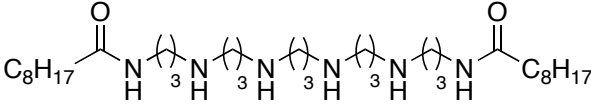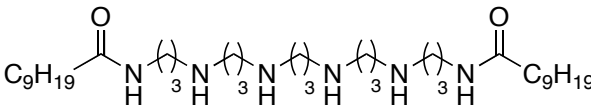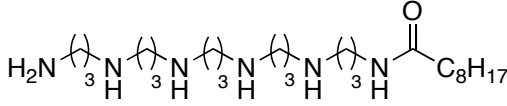
Since TLR4 is the central signaling mediator for LPS in mammals, this

finding has opened the possibilty of developing new drug targets to fight sepsis. Our

approach has been focused on neutralizing LPS in order to block the initial LPS-

signaling events by preventing the generation of cell-surface signals.[209] Polymyxin B

(PMB), a cationic amphiphilic cyclic decapeptide antibiotic isolated from *Bacillus*

polymyxa has been known to bind lipid A and to neutralize of LPS.[210] PMB also has

antimicrobial activity particularly against Gram-negative bacteria.[211] It is only

suitable for topical applications, but polymyxin B is extensively used as a standard for

experimental studies conducted to identify novel compounds able to neutralize

endotoxins.

3.2 Development of Endotoxin-Sequestering Agents

Due to the cytotoxicity of PMB, our focus is to target circulatory LPS using

small molecules.[209] The bis-anionic, amphiphilic nature of lipid A (Figure 23) enables

it to interact with a variety of bis-cationic hydrophobic ligands. We have found that

linear bis-cationic amphipathic molecules possessing terminal, protonatable cationic

groups positioned optimally (N–N distance: ~14 Å) so as to be able to

simultaneously interact with the glycosidic phosphates on lipid A as well as

appropriately positioned lipophilic moieties, enable hydrophobic interactions with the

polyacyl domain of lipid A, Table 15.[212, 213] Noteworthy examples of such molecules displaying potent *in vitro* and *in vivo* LPS-sequestering properties are acyl-polyamines which afford protection in animal models of sepsis. [209, 212-215]

Table 15. Acyl compounds for LPS neutralization[212]

Compound	ED$_{50}$ (mM)	NO IC$_{50}$ (mM)
	0.33	2.05
	0.76	1.47
	107.45	171.41
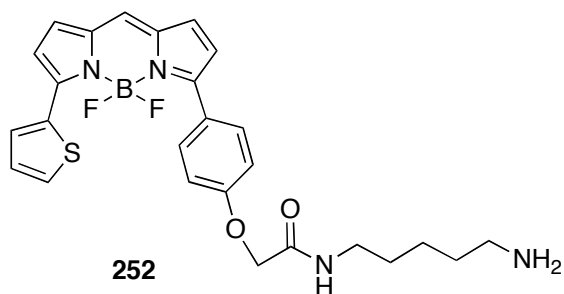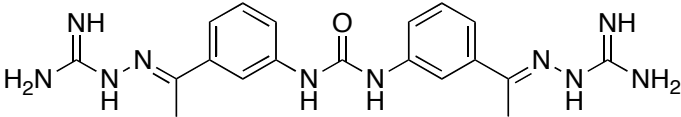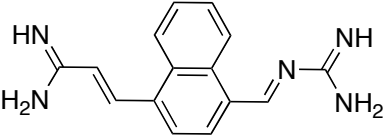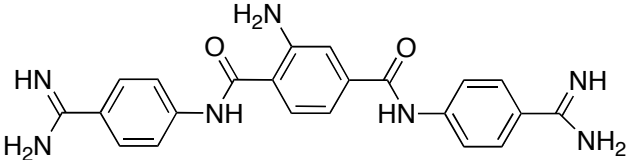
Figure 24. Bodipy-cadaverine (BC)

While members of the acylpolyamines undergo exhaustive preclinical characterization,[212] we have recently identified several bis-guanylhydrazones as potent LPS binders from an automated rapid-throughput screen on of focused libraries using the Bodipy-cadaverine (BC) displacement assay.[214, 216]

Table 16. HTS of Bodipy-cadaverine (BC) displacement assay[216]

Compound	ED$_{50}$ (mM)	NO IC$_{50}$ (mM)
	14.91	11.79
	47.74	31.95
	51.68	25.59

In silico docking of *bis*-guanylhydrazones indicates excellent charge complementarity between the guanylhydrazone moieties and lipid A phosphates, Figure 25.[217] However, binding to lipid A mediated via electrostatic interactions alone does not necessarily manifest in neutralization of endotoxicity, and we have shown that additional hydrophobic interactions with the polyacyl domain of the toxin via long-chain hydrocarbon appendages are necessary for true sequestration of the

toxin.[212, 213]
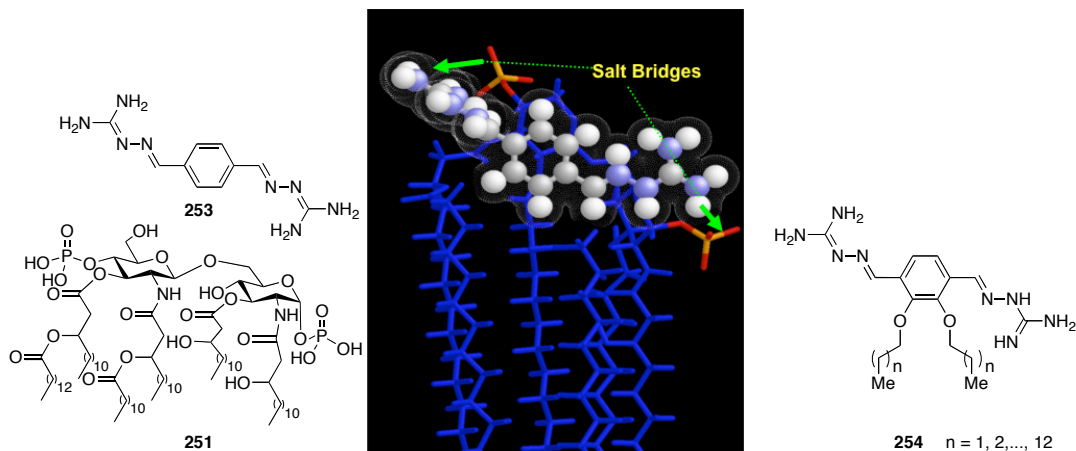
Figure 25. Salt bridges of bis-Guanylhydrazones with lipid A, *in silico* docking (SYBYL, using Surflex-Dock) and designed analogues (right)

3.2.1 Preparations of terepthalaldehyde-bis-guanylhydrazones

We now describe the syntheses and preliminary structure–activity relationships in a homologous series of bis-guanylhydrazone compounds decorated with hydrophobic functionalities, Figure 25. These first-generation compounds bind and neutralize LPS with a potency comparable to that of polymyxin B (PMB), a peptide antibiotic known to sequester LPS.

The syntheses of the target compounds are summarized in Scheme 44 and 45. 2,3-Dimethoxyterephthalaldehyde **256** was prepared according to the procedure described by Kuhnert et al.[218] by double directed ortho-lithiation of 1,2-dimethoxybenzene with *n*-BuLi/TMEDA under reflux in ether, followed by quenching with DMF in THF. Treatment of the resulting aldehyde **256** with boron

tribromide in CH$_2$Cl$_2$ afforded **257** in 86% yield.[219] The terephthalaldehydes **258a–258h** were prepared by alkylation of **257** with the respective alkyl halides.[220]

Scheme 44. Synthesis of alkylated terephthalaldehydes

The aromatic guanylhydrazones **262a–262k** were obtained by condensing the terephthalaldehydes with aminoguanidine hydrochloride in refluxing ethanol/HCl, Scheme 45.[221] Pure aminoguanylhydrazones (as HCl salts) were isolated as crystalline products after cooling to 0 °C and washing with cold ether.

Scheme 45. Synthesis of terepthalaldehyde-*bis*-guanylhydrazone analogues

3.2.2 Biological Assay

The final compounds **262a**-**262k** were tested for their ability to bind to LPS using an automated fluorescence displacement assay. The assay was performed in a three step automated sequence which included plating the compounds in serial dilution, adding LPS and BODPIY cadaverine (BC) and recording the resulting fluorescence in a plate reader at a fixed wavelength (620 nM).[222] When the test compounds bind to LPS, displacing BC, the fluorescence of LPS-bound BC is dequenched, and the intensity of light emitted is enhanced.

After we established the binding ability of the compounds to LPS and identified the most active analogues, we tested the guanylhydrazones for their biological efficacy in terms of NF-κB and Nitric oxide (NO) inhibitions.[212]

The induction of NF-κB is a key transcriptional activator of the innate immune system, leading to uncontrolled cytokine release which ultimately leads to multiple organ failure and the shock syndrome. The *in vitro* activity of our compounds was measured as IC_{50} values, since sequestering LPS in a concentration dependent manner, the tested compounds would interfere with the nuclear translocation of NF-κB. The resulting NF-κB nuclear translocation was quantified using human embryonic kidney 293 cells cotransfected with TLR4 (LPS receptor), CD14 and MD2 (co-receptors), available from InvivoGen, Inc., (HEK-Blue™, San Diego, CA) as per protocols provided by the vendor.[212]

The ability of the bisguanylhydrazone compounds to inhibit the LPS-stimulated production of nitric oxide (NO) was tested with the murine macrophage-like cell line J774.A1 (American Tissue Type Collection, Washington, D.C.), seeded in a 96-well tissue culture plate at 5×10^5 cells/well.[214] Activation of macrophages by the immune system results in the production of inducible nitric oxide synthase (iNOS) enzyme, with consequent release of nitric oxide. Following overnight culture in RPMI 1640 supplemented with L-glutamine, 10% fetal bovine serum, penicillin, and streptomycin, the cells were stimulated for 8 h with LPS alone (20 ng/ml) or LPS preincubated with graded concentrations of DOSPER, DOGS, or polymyxin B (control). The nitric oxide (NO) level was measured by the Griess assay.[223] The

mechanism is summarized as the cascade reaction of NO with oxygen under acidic condition to produce nitrite ion which was further reacted with sulfanilamide to generate diazonium species, catalyzed by nitrate reductase. The resulting diazonium intermediate was coupled with naphthylethylenediamine to produce azo compound which can be detected at 540 nM by a fluorescence spectrometer.

$$\cdot NO + 1/2O_2 \longrightarrow \cdot NO_2 \quad (1)$$

$$2\cdot NO_2 \rightleftharpoons N_2O_4 \quad (2)$$

$$N_2O_4 + H_2O \rightleftharpoons NO_2^- + NO_3^- + 2H^+ \quad (3)$$

$$\cdot NO + NO_2 \rightleftharpoons N_2O_3 \quad (4)$$

$$N_2O_3 + H_2O \longrightarrow 2NO_2^- + 2H^+ \quad (5)$$

azo compound, l_{max}: 540 nm
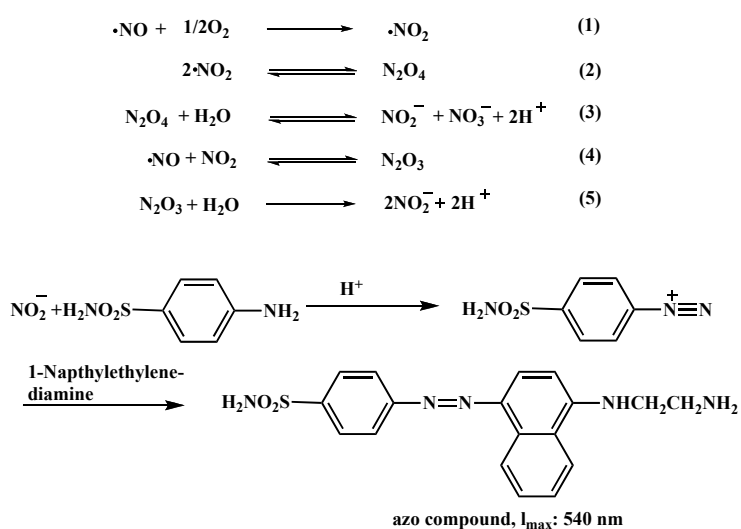
Figure 26. Greiss Assay to quantify NO production

3.2.3 Biological result[217]

The concentrations of the bis-guanylhydrazones corresponding to effective displacement of 50% of the bound fluorescent probe (ED_{50}; relative affinity of binding) and of the inhibition (IC_{50}) of nitric oxide (NO) and NF-κB are summarized in Table 17, and Figure 27. As shown in Figure 27, a relationship between the alkyl chain length and the binding affinity as well as NO and NF-κB inhibition is evident. For binding affinity, the optimal substituent appears to be C_5H_{11} while in both *in vitro* bioassays, the most favorable hydrophobic group is C_8H_{17}. This discrepancy is due to the fact that in the homogeneous fluorescent displacement assay performed in aqueous buffer the ligand must be completely soluble; increasing hydrocarbon chain length substituents results in a progressively retarded aqueous solubility, resulting in higher ED_{50} values. In the NO and NF-κB neutralization assays the presence of fetal bovine serum in the cell-culture medium ensures complete and uniform solubility and obviates this problem.[212, 215]

Table 17. Summary of binding affinity and biological activity for terepthaldehyde-

bis-guanylhydrazones **262a-262k**
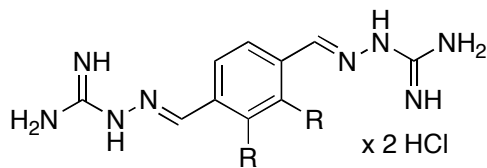
Compound	R	ED$_{50}$ (mM)	NO IC$_{50}$ (mM)	NF-kB IC$_{50}$ (mM)
Polymyxin B (Ctrl)		1.67	0.98	1.23
262a	H	34.55	24.38	164.07
262b	OH	43.68	26.39	59.14
262c	OCH$_3$	42.28	27.96	175.76
262d	OC$_2$H$_5$	22.84	4.56	35.63
262e	OC$_3$H$_7$	12.73	8.38	27.63
262f	O-allyl	29.85	9.64	61.44
262g	OC$_4$H$_9$	9.44	4.15	9.40
262h	OC$_5$H$_{11}$	7.82	3.54	10.45
262i	OC$_6$H$_{13}$	13.23	4.67	6.11
262j	OC$_8$H$_{17}$	39.48	3.45	4.50
262k	OC$_{14}$H$_{29}$	>500	14.90	190.94
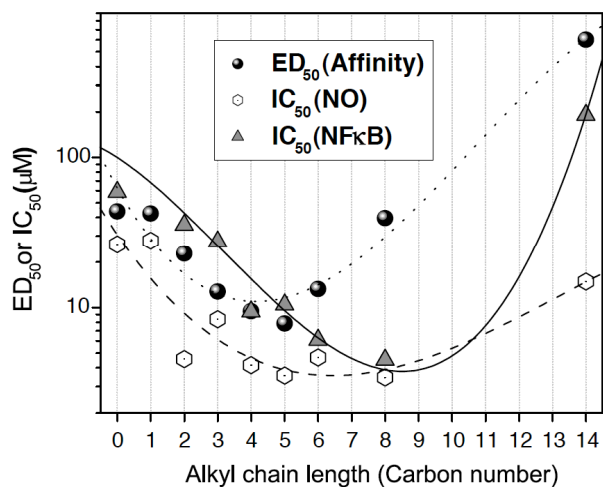
Figure 27. Relationship of alkyl chain length of **262a-262k** with binding affinity *in vitro* LPS neutralization
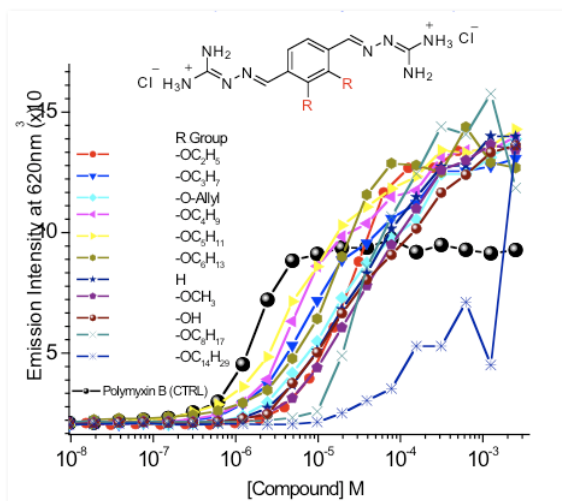
Figure 28. BC/LPS Displacement Assay

The apparent binding affinities (ED$_{50}$) of the compounds were computed from the displacement curves in Figure 28. The increasing concentration of test compounds

resulted in the enhancement of the intensity of fluorescence emission at 620 nM. The analogue with the C5 alkoxy-chain, **262h**, showed the most effective binding to LPS at 7.82 mM while its binding affinity was comparable with PMB at 1.67 mM.
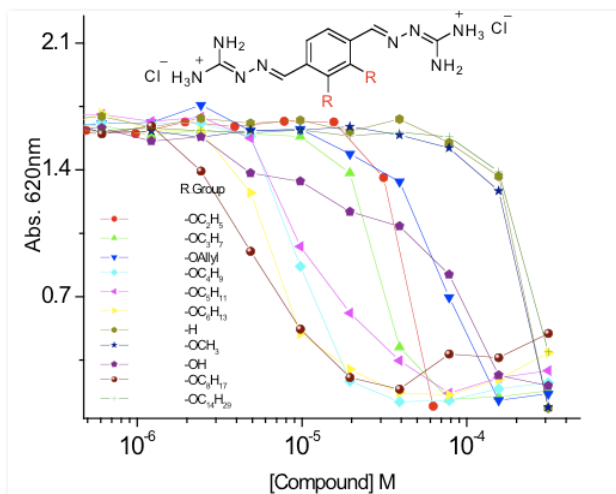
Figure 29. NF-κB Assay

The NF-κB and NO inhibition was reflected by the decrease of fluorescence emission as shown in Figures 29 and 30. The potency of compounds (IC_{50}) were computed from graphs, showing the analogue bearing the C_8H_{19} alkyl chain as the most active compound.
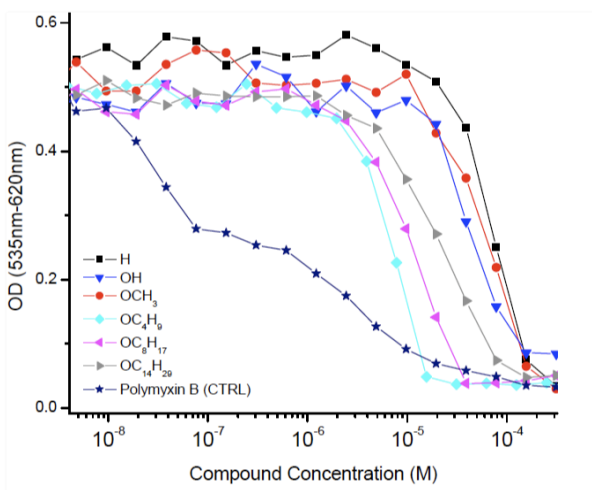
Figure 30. NO Inhibition in Murine J774 cells (Stimulus: 10 ng/ml LPS)

Given that **262j**, (R = C_8H_{17}), was the most potent compound in these biological assays (Table 17), we elected to characterize this compound in an *in vivo* D-galactosamine-primed mouse model of endotoxic shock. It is worth noting that the cytokine response to LPS in mice closely parallels that of humans,[224] and is thus a well-established confirmatory assay.[212, 214]

% Alive in Cohorts of 5 mice

Dose of **262j** (mg/25g mouse)
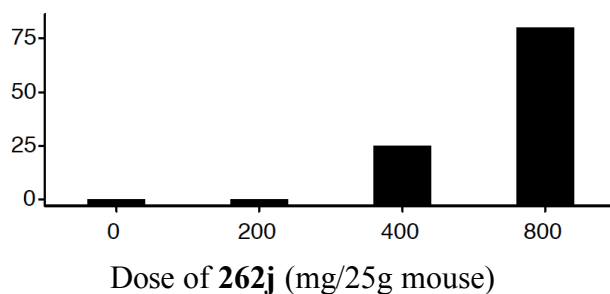
Figure 31. Dose-dependent protective effect of **262j** in a murine model of lethality induced by 200 ng LPS

The administration of graded doses of **262j** resulted in a dose-dependent decrease in lethality in mice challenged with supralethal (200 ng/mouse; LD_{100}: 100 ng/mouse) doses of LPS (Figure 31).

These results support to our strategy of incrementally converting high-affinity LPS binders to true LPS sequestrants by appending suitable hydrophobic functionalities. Further, these data would suggest that a systematic exploration of the bis-guanylhydrazone scaffold may yield useful anti-endotoxin molecules.

3.3 Conclusion

Structure-activity relationship (SAR) studies clearly indicated that modifications of the aromatic ring with long-chain alkyl groups increased potency of terepthalaldehyde-*bis*-guanylhydrazone analogues. Biological assays revealed that the most potent compound contains a C8 alkoxy-chain. Potent anti-endotoxic activity as well as the relative ease of synthesis render this class of compounds promising for further preclinical evaluation.

Chapter 4

Experimental

4.1 Materials and Methods

All reactions were performed using either standard bench top or inert atmosphere techniques. All deuterated solvents were used as purchased from Cambridge Isotope Labs. Chemical reagents were used as purchased from Aldrich, unless otherwise noted. Flash column chromatography was carried out using silica gel 60(230-400 mesh), while thin-layer chromatography (TLC) was carried out on silica gel HLF, precoated glass plates. All yields reported refer to isolated material judged to be homogeneous by TLC and NMR spectroscopy.

All reactions were performed under an atmosphere of nitrogen in overnight oven-dried glassware unless otherwise indicated. THF, DCM, toluene, Et_2O and DMF were dried and deoxygenated by passing the nitrogen-purged solvents through activated alumina columns on a solvent purification system. All other reagents and solvents were used as purchased. Reaction progress was monitored by thin layer chromatography (TLC, silica gel, 10×20 cm, 250 micron) visualizing with UV light (254 nm) or developing the plates with bluestain, anisaldehyde, or $KMnO_4$ stains.

Melting points were determined using a melting point apparatus and are uncorrected. Infrared spectra were obtained as thin films on NaCl plates using an FT-IR instrument. NMR experiments were performed on a Bruker Avance 400 MHz instrument (operating at 400.134 MHz for ^{1}H or 100.614 MHz for ^{13}C) using the

residual solvent peak as internal standard unless otherwise indicated. NMR spectra were recorded with the chemical shifts (δ) reported in relative to TMS (for ^{1}H) and CDCl$_3$ (for ^{13}C) or MeOD (for ^{13}C) as internal standards, respectively. High-resolution mass spectra were obtained utilizing the electrospray ionization technique or FAB/MS, using polyethylene glycol (PEG) as a reference compound.

4.2 Experimental Procedures

4.2.1 Chapter 1
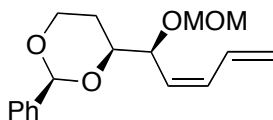
(2*S*,4*S*)-4-((*S*,*Z*)-1-(Methoxymethoxy)penta-2,4-dienyl)-2-phenyl-1,3-dioxane (133). To a flask containing alcohol[45] **132** (5.04 g, 17.1 mmol) was added DMSO (75 mL) and IBX (7.20 g, 25.7 mmol). The mixture was stirred at rt for 1 h and then diluted with Et$_2$O (400 mL) and water (400 mL). The organic layer was washed with water (5x400 mL) The organic layer was dried over MgSO$_4$ and concentrated *in vacuo* to afford a clear oil of the corresponding aldehyde. The crude aldehyde was used directly in the next step without further purification.

To a mixture of CH$_3$PPh$_3$Br (9.16 g, 25.7 mmol) in anhydrous THF (50 mL),

cooled to 0 °C under N_2 atmosphere was added dropwise a solution of *n*-BuLi in hexanes (2.5 M, 10.3 mL, 25.7 mmol). After the addition was completed, the mixture turned bright yellow. The mixture was stirred at 0 °C for 1 h, and a solution of the crude aldehyde diluted in THF (40 mL) was added dropwise over 10 min. The reaction mixture was stirred at rt for 5 h and 30 min and then quenched with water (200 mL) and extracted with Et_2O (3x200 mL). The combined organic layer was washed with brine (250 mL), dried over $MgSO_4$ and concentrated *in vacuo.* Purification on neutralized silica gel, treated with a solution of 1% Et_3N in hexanes (500 mL), (5% EtOAc in hexanes) provided 3.67 g (12.6 mmol, 74% over two steps) of *Z*-diene **133** as a colorless oil: ^{1}H NMR (400 MHz, $CDCl_3$) δ 1.47 (m, 1H), 1.86 (m, 1H), 3.37 (s, 3H), 3.96 (m, 2H), 4.28 (ddd, *J* =1.2, 5.0, 11.4 Hz, 1H), 4.63 (d, *J* = 6.8 Hz, 1H), 4.66 (m, 1H), 4.69 (d, *J* = 6.6 Hz, 1H), 5.25 (d, *J* = 10.1 Hz, 1H), 5.32 (d, *J* = 16.8 Hz, 1H), 5.35 (dd, *J* = 10.1, 10.1 Hz, 1H), 5.55 (s, 1H), 6.31 (dd, *J* =11.2, 11.7 Hz, 1H), 6.74 (td, *J* = 10.7, 16.7 Hz, 1H), 7.33 (m, 3H), 7.50 (m, 2H); ^{13}C NMR (100 MHz, $CDCl_3$) δ 129.7, 125.8, 122.9, 119.8, 119.2, 117.7, 117.2, 111.5, 92.2, 85.1, 70.1, 68.4, 64.2, 57.9, 46.5; HRMS (ESI[+]): *m/z* calc'd for $C_{17}H_{22}NaO_4^+$, 313.1410; found 313.1417.
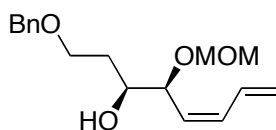
(3*S*,4*S*,*Z*)-1-(Benzyloxy)-4-(methoxymethoxy)octa-5,7-dien-3-ol (127). To a flask containing *Z*-diene **133** (100 mg, 0.34 mmol) was added anhydrous DCM (4 mL). After cooling the solution to 0 °C, DIBALH in toluene (1M, 2 mL, 2 mmol) was added dropwise and stirred for 10 min. The reaction flask was then cooled to -78 °C, prior the addition of 1:1 mixture of EtOAc and EtOH (2 mL). The mixture was stirred for 10 min before Rochelle's salt (0.5 g) was added. After the mixture was continued to stir at -78 °C for 30 min, it was warmed to rt. Filtration of the Rochelle's salt followed with an organic wash (EtOAc) to provide crude product. It was concentrated *in vacuo.* Purification on neutralized alumina, (20% EtOAc in hexanes) provided 83.9 mg (0.287 mmol, 84%) of alcohol **127** as a colorless oil:. ^{1}H NMR (400 MHz, CDCl$_3$) δ 1.73 (m, 1H), 1.82 (m, 1H), 2.92 (d, 1H), 3.39 (s, 3H), 3.67 (m, 2H), 3.79 (m, 1H), 4.40 (q, *J* = 5.6 Hz, 1H), 4.52 (s, 2H), 4.56 (d, *J* = 6.7 Hz, 1H), 4.69 (d, *J* = 6.7 Hz, 1H), 5.21 (d, *J* = 10.0 Hz, 1H), 5.30 (m, 2H), 6.29 (dd, *J* = 11.1, 11.1 Hz, 1H), 6.65 (td, *J* = 10.6, 16.8 Hz, 1H), 7.31 (m, 5H); ^{13}C NMR (100 MHz, CDCl$_3$) δ 138.3, 134.9, 131.7, 128.4, 127.7, 127.6, 127.3, 120.4, 93.7, 74.8 73.2, 71.9, 67.8, 55.6, 32.7; IR (neat, NaCl): 3512(br), 2930(br), 1620, 1510, 14460, 1350, 1120 cm^{-1}; HRMS (ESI$^+$): *m/z* calc'd for C$_{17}$H$_{24}$NaO$_4$$^+$, 315.1567; found 315.1569.
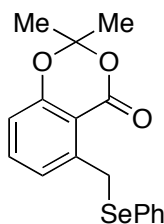
2,2-Dimethyl-5-(phenylselanylmethyl)-4*H*-benzo[*d*][1,3]dioxin-4-one (136). To a flask containing *i*-Pr$_2$NH (2.70 mL, 18.8 mmol), dissolved in anhydrous THF (50 mL) and cooled to −78 °C, was added dropwise *n*-BuLi in hexanes (2.5 M, 7.50 mL, 18.8 mmol). The resulting orange solution was stirred at −78 °C for an additional 30 min, and methyl salicylate[155] **135** (1.50 g, 7.80 mmol) dissolved in anhydrous THF (100 mL) was added dropwise. After the reaction mixture was stirred at −78 °C for 10 min, a solution of PhSeSePh dissolved in anhydrous was added dropwise. The mixture was stirred for 2 h at −78 °C and quenched by the addition of sat. NH$_4$Cl (50 mL). It was extracted with Et$_2$O (3x200 mL), washed with brine (100 mL). The organic layer was dried over Na$_2$SO$_4$ and concentrated *in vacuo*. Purification by column chromatography on silica gel (10% EtOAc in hexanes) provided 0.96 g (2.7 mmol, 35%) of phenylselenium salicylate **136** as a bright yellow oil: ^{1}H NMR (400 MHz, CDCl$_3$) δ 1.52 (s, 3H), 1.68 (s, 3H), 2.76 (t, *J* = 7.1 Hz, 2H), 4.99 (m, 2H), 5.76 (q, 1H), 6.08 (s, 1H), 6.77 (q, *J* = 3.1 Hz, 1H), 7.11 (d, *J* = 8.0 Hz, 1H), 7.21 (m, *J* = 3.5 Hz, 3H), 7.40 (m, *J* = 4.2 Hz, 3H); HRMS (ESI$^+$): *m/z* calc'd for C$_{17}$H$_{16}$NaO$_3$Se$^+$, 371.0157; found 371.0159.
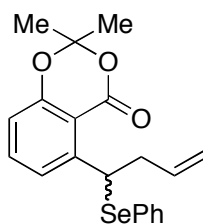
2,2-Dimethyl-5-(1-(phenylselanyl)but-3-enyl)-4*H*-benzo[*d*][1,3]dioxin-4-one

(128). To a flask containing *i*-Pr$_2$NH (0.12 mL, 0.84 mmol), dissolved in anhydrous

THF (5.0 mL) and cooled at −78 °C, was added *n*-BuLi in hexanes (2.5 M, 0.34 mL,

0.84 mmol) dropwise. The resulting orange solution was stirred at −78 °C for an

additional 30 min, and phenylselenium salicylate **136** (100 mg, 0.288 mmol)

dissolved in anhydrous THF (1.0 mL) was added dropwise. After the reaction mixture

was stirred at −78 °C for 10 min, a solution of allyl bromide (60 μL, 0.65 mmol) and

HMPA (0.16 mL, 0.92 mmol) dissolved in anhydrous THF (5.0 mL) was added

dropwise. The mixture was stirred for 30 min at −78 °C and quenched by the addition

of sat. NH$_4$Cl (15 mL). It was extracted with Et$_2$O (3x60 mL), washed with brine

(2x30 mL). The organic layer was dried over Na$_2$SO$_4$ and concentrated *in vacuo*.

Purification by column chromatography on silica gel (5% EtOAc in hexanes)

provided 73.2 mg (0.189 mmol, 66%) of alkene acetonide **128** as a bright yellow oil:

^{1}H NMR (400 MHz, CDCl$_3$) δ 1.52 (s, 3H), 1.68 (s, 3H), 2.76 (t, *J* = 7.1 Hz, 2H),

4.99 (m, 2H), 5.76 (q, 1H), 6.08 (s, 1H), 6.77 (q, *J* = 3.1 Hz, 1H), 7.11 (d, *J* = 8.0 Hz,

1H), 7.21 (m, *J* = 3.5 Hz, 3H), 7.40 (m, *J* = 4.2 Hz, 3H); ^{13}C NMR (100 MHz,

CDCl$_3$) δ 160.5, 147.5, 135.8, 135.6, 134.9, 133.2, 128.7, 127.9, 123.2, 117.1, 115.7,

111.9, 105.1, 39.9, 36.9, 36.8, 26.2, 24.8; HRMS (ESI$^+$): *m/z* calc'd for

$C_{20}H_{20}NaO_3Se^+$, 411.0470; found 411.0479.
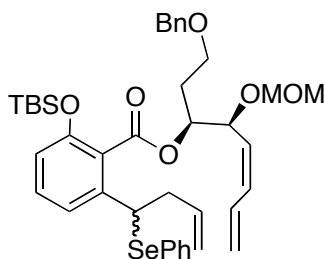
(3S,4S,Z)-1-(Benzyloxy)-4-(methoxymethoxy)octa-5,7-dien-3-yl 2-(tert-Butyldimethylsilyloxy)-6-(1-(phenylselanyl)but-3-enyl)benzoate (126). Alcohol **127** (120 mg, 0.410 mmol) was azeotroped *in vacuo* with benzene (2x3 mL), dissolved in anhydrous THF (1.0 mL) and cooled to 0 °C. NaHMDS (1.0 M, 0.90 mL, 0.90 mmol) was added dropwise. After stirring at 0 °C for 30 min, salicylate **128** (166 mg, 0.429 mmol) dissolved in distilled THF (1.0 mL) was added dropwise. The reaction was warmed to rt and stirred for 2 h, and then TBSCl (618 mg, 4.10 mmol) and imidazole (280 mg, 4.10 mmol) were added to the reaction mixture as solids. The reaction was stirred overnight, filtered through a silica gel plug and rinsed with Et_2O (10 mL) and dried over $MgSO_4$. The organic layer was concentrated *in vacuo*. Purification by column chromatography on silica gel (7% EtOAc in hexanes) provided inseparable diastereomers 173.4 mg (0.2356 mmol, 57%) of ester **126** as a bright yellow oil: ^1H NMR (400 MHz, CDC^{13}): δ 7.27-7.48 (m, 7H), 7.10-7.24 (m, 4H), 6.96 (dd, J = 14.4, 8.2 Hz, 1H), 6.68 (d, J = 8.51 Hz, 1H), 6.54-6.65 (m, 1H), 6.12-6.31 (m, 1H), 5.61-5.80 (m, 1H), 5.24-5.54 (m, 3H), 5.08-5.20 (m, 1H), 4.98(dd, J = 16.4, 8.93 Hz, 2 H), 4.63-4.84 (m, 1H), 4.57-4.65 (m, 1H), 4.42-4.57 (m, 4H), 3.62 (m, 2H), 3.28 (m, 3H), 2.60-2.86 (m, 2H), 2.10-2.25 (m, 1H), 1.82-2.04 (m, 1H),

0.97 (s, 9H), 0.22 (m, 6H); ^{13}C NMR (100.6 MHz, CDCl$_3$): δ 166.99, 166.91, 152.4,

140.5, 140.3, 138.4, 136.0, 135.5, 135.4, 135.2, 134.6, 131.7, 131.6, 129.8, 129.7,

129.2, 129.1, 128.7, 128.6, 128.4, 127.8, 127.7, 127.6, 127.5, 126.9, 126.8, 126.2,

126.1, 120.6, 120.4, 120.1, 117.6, 117.1, 117.0, 93.7, 74.7, 73.1, 73.0, 71.2, 71.1,

67.1, 67.0, 55.6, 43.2, 43.1, 41.2, 30.9, 30.8, 29.7, 25.9, 18.4, -4.11, -4.14; HRMS

(ESI$^+$): m/z calc'd for C$_{40}$H$_{52}$NaO$_6$SeSi$^+$, 759.2591; found 759.2587.
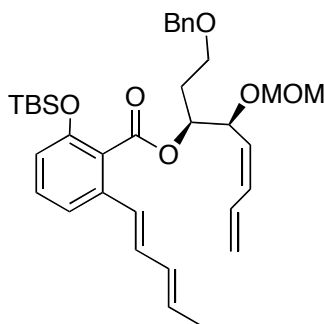
(3S,4S,Z)-1-(Benzyloxy)-4-(methoxymethoxy)octa-5,7-dien-3-yl 2-(*tert*-Butyldimethylsilyloxy)-6-((1*E*,3*E*)-penta-1,3-dienyl)benzoate (137).). Alcohol **127**

(120 mg, 0.410 mmol) was azeotroped *in vacuo* with benzene (2x3 mL), dissolved in

anhydrous THF (1.0 mL) and cooled to 0 °C. NaHMDS (1.0 M, 0.90 mL, 0.90 mmol)

was added dropwise. After stirring at 0 °C for 1 min, salicylate[13] **50** (101 mg, 0.414

mmol) dissolved in distilled THF (1.0 mL) was added dropwise. The reaction was

warmed to rt and stirred for 2 h, and then TBSCl (618 mg, 4.10 mmol) and imidazole

(279 mg, 4.10 mmol) were added to the reaction mixture as solids. The reaction was

stirred overnight, filtered through a silica gel plug and rinsed with Et$_2$O (10 mL) and

dried over MgSO$_4$. The organic layer was concentrated *in vacuo*. Purification by

column chromatography on silica gel (7% EtOAc in hexanes) provided 115.9 mg (0.1955 mmol, 48%) of ester **137** as a yellow oil: ^{1}H NMR (400 MHz, CDCl$_3$) δ ^{1}H NMR (400 MHz, CDCl$_3$) δ 0.22 (s, 6H), 0.95 (s, 9H), 1.61 (m, 1H), 1.77 (m, 1H), 1.76 (d, J = 7.0 Hz, 3H), 3.27 (s, 3H), 3.46 (m, 2H), 3.72 (dd, J = 4.8, 10.4 Hz, 1H), 3.83 (dd, J = 5.0, 10.4 Hz, 1H), 4.51 (s, 2H), 4.63 (d, J = 4.6 Hz, 1H), 4.71 (d, J = 4.5 Hz, 1H), 5.01 (dd, J = 5.8, 9.8 Hz, 1H), 5.19 (d, J = 10.0 Hz, 1H), 5.30 (tdd, J = 0.9, 6.4, 16.8 Hz, 1H), 5.34 (dd, J = 4.9, 10.7 Hz, 1H), 5.40 (t, J = 10.3 Hz, 1H), 5.80 (m, 1H), 6.04 (ddd, J = 1.3, 10.3, 14.7 Hz, 1H), 6.24 (td, J = 11.1, 14.0 Hz, 1H), 6.50 (d, J = 15.5 Hz, 1H), 6.63 (m, 3H), 7.11 (d, J = 7.0 Hz, 1H), 7.15 (dd, J = 7.92, 12.8 Hz, 1H), 7.31 (m, 5H); ^{13}C NMR (100 MHz, CDCl$_3$) δ 169.7, 152.5, 134.8, 133.4, 131.0, 131.9, 131.8, 131.6, 131.1, 129.7, 129.3, 127.7, 127.6, 127.6, 126.5, 120.3, 119.6, 117.4, 93.9, 75.0, 74.3, 72.4, 71.9, 69.9, 55.5, 55.1, 25.8, 25.8, 18.3, -4.1, -4.2; HRMS (ESI$^+$): *m/z* calc'd for C$_{35}$H$_{48}$NaO$_6$Si$^+$, 615.3112; found 615.3115.

OBn

TBSO　　O　　　　OTBS
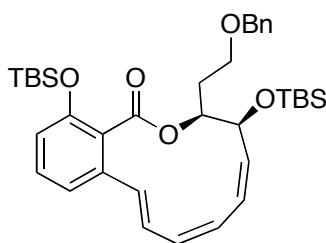
(3*S*,4*S*,5*Z*,7*Z*,9*E*)-3-(2-(Benzyloxy)ethyl)-14-(*tert*-butyldimethylsilyloxy)-4-(methoxymethoxy)-3,4-dihydro-1*H*-benzo[*c*][1]oxacyclododecin-1-one (124).

Procedure A

To a flask containing bis-diene **137** (53.9 mg, 0.0909 mmol) was added anhydrous and degassed toluene (50 mL). Ruthenium Grubbs 2nd generation catalyst (7.7 mg, 0.0091 mmol) in degassed toluene (3 mL) was added in one portion under a nitrogen atmosphere. The solution was heated at 80 °C and stirred for 17 h. The reaction mixture was allowed to cool to room temperature and filtered through a silica gel plug and was rinsed with 50% DCM in hexanes (20 mL). The combined organic layer was removed *in vacuo*. Purification by column chromatography on silica gel (5% EtOAc in hexanes) provided 4.9 mg (0.0089 mmol, 10%) of macrocyclic triene **124** as a yellow oil: ^{1}H NMR (400 MHz, CDCl$_3$) δ 0.18 (s, 3H), 0.20 (s, 3H), 0.95 (s, 9H), 2.15 (m, 1H), 2.30 (m, 1H), 3.35 (s, 3H), 350 (m, 2H), 3.82 (d, *J* = 5.0 Hz, 2H), 4.54 (s, 2H), 4.62 (s, 2H), 4.64 (dd, *J* = 3.0, 10.8 Hz, 1H), 5.55 (m, 2H), 5.85 (dd, *J* = 3.9, 10.8 Hz, 1H), 6.11 (dd, *J* = 4.1, 11.9 Hz, 1H), 6.25 (t, *J* = 11.3 Hz, 1H), 6.70 (d, *J* = 15.8 Hz, 1H), 6.77 (dd, *J* = 7.9, 13.3 Hz, 2H), 7.02 (dd, *J* = 11.4, 15.9 Hz, 1H), 7.17 (t, *J* = 7.9 Hz, 1H), 7.33 (m, 5H); ^{13}C NMR (100 MHz, CDCl$_3$) δ 168.1, 152.2,

138.4, 137.8, 132.0, 132.1, 131.1, 130.3, 129.2, 128.2, 127.4, 127.4, 127.1, 126.9, 121.2, 117.9, 93.1, 77.4, 73.2, 68.2, 67.9, 55.2, 29.0, 25.8, 18.2, -4.0, -4.5; IR (neat, NaCl): 2930, 2870, 1735, 1613, 1510, 1475, 1250, 1090 cm^{-1}; HRMS (ESI$^+$): *m/z* calc'd for C$_{32}$H$_{42}$NaO$_6$Si$^+$, 573.2643; found 573.2645.

Procedure B

To a flask containing macrocyclic selenium-diene **125** (3.3 mg, 0.0047 mmol) was added THF (0.1 mL) and 3.5% H$_2$O$_2$ (0.9 μL, 0.0094 mmol). The resulting mixture was stirred at rt for 3 h and quenced with a mixture of 2.5% NaHCO$_3$ (1 mL) and 5% Na$_2$S$_2$O$_3$ (1 mL) and then extracted with EtOAc (3x3 mL) and dried over MgSO$_4$. Purification on preparative silica-TLC (5% EtOAc in hexanes) provided 0.7 mg (0.00127 mmol, 27%) of macrocyclic triene **124** as yellow oil. The ^{1}H NMR is identical with the previous method: HRMS (ESI$^+$): *m/z* calc'd for C$_{32}$H$_{42}$NaO$_6$Si$^+$, 573.2643; found 573.2648.
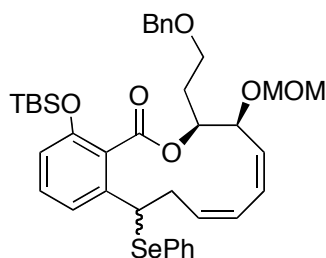
(3*S*,4*S*,5*Z*,7*Z*)-3-(2-(Benzyloxy)ethyl)-14-(*tert*-butyldimethylsilyloxy)-4-(methoxymethyl)-10-(phenylselanyl)-3,4,9,10-tetrahydro-1*H* Benzo[*c*][1]oxacyclododecin-1-one (125). To a flask containing intermediate **126** (60.4 mg, 0.0821 mmol) was added anhydrous and degassed toluene (46 mL). Ruthenium Grubbs 2nd generation catalyst (7.0 mg, 0.0082 mmol) in degassed toluene (2 mL) was added in one portion under a nitrogen atmosphere. The solution was heated at 80 °C and stirred for 17 h. The reaction mixture was allowed to cool to room temperature and filtered through a silica gel plug. It was rinsed with 50% DCM in hexanes (20 mL). The combined organic layer was removed *in vacuo*. Purification by column chromatography on silica gel (5% EtOAc in hexanes) provided 12.7 mg (0.0179 mmol, 22%) of macrocyclic selenium-diene **125** as a yellow oil: HRMS (ESI$^+$): *m/z* calc'd for C$_{38}$H$_{48}$NaO$_6$SeSi$^+$, 731.2278; found 731.2279.

OMOM

PMBO ⟍⟍⟋⟍⟋⟍ OH
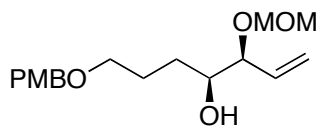
(3S,4S)-7-(4-Methoxybenzyloxy)-3-(methoxymethoxy)hept-1-en-4-ol (139). To a

flask containing 3-(methoxymethoxy)prop-1-ene (4.98 g, 48.8 mmol) dissolved in

anhydrous THF (100 mL) was added *sec*-butyllithium in cyclohexane (1.40 M, 29.0

mL, 40.7 mmol) at −78 °C dropwise. The resulting orange solution was stirred at −78

°C for an additional 30 min, and (+)-*B*-methoxydiisopinocamphenylborane (12.9 g,

40.7 mmol) dissolved in THF (100 mL) was added dropwise. After the reaction

mixture was stirred at −78 °C for 1 h, it was cooled to −90 °C (using MeOH and

liquid N_2 to prepare the cooling bath). The boron trifluoride etherate (6.80 mL, 54.1

mmol) was added dropwise. Immediately afterwards, aldehyde **138** (7.90, 40.7 mmol)

was added dropwise and the mixture kept at −90 °C for 3 h. The reaction was warmed

to rt over 18 h to give a clear colorless solution, and quenched with a mixture of 35%

H_2O_2 (30 mL) and sat. NaHCO$_3$ solution (60 mL). After stirring at rt for 30 min, the

mixture was extracted with EtOAc (3x200 mL). The combined organic extracts were

washed with brine, dried over Na$_2$SO$_4$, and concentrated *in vacuo*. Purification by

column chromatography on silica gel (30% EtOAc in hexanes) provided 11.14 g

(35.89 mmol, 88%) of alcohol **139** as a colorless oil: ^{1}H NMR (400 MHz, CDCl$_3$)

δ 1.48 (m, J = 4.9 Hz, 1H), 1.69 (m, J = 3.0 Hz, 2H), 1.83 (m, J = 3.1 Hz, 1H), 3.05

(brs, 1H), 3.39 (s, 3H), 3.48 (t, J = 6.1 Hz, 2H), 3.58 (m, 1H), 3.80 (s, 3H), 3.88 (t, J

= 7.3 Hz, 1H), 4.45 (s, 2H), 4.59 (d, J = 6.6 Hz, 1H), 4.74 (d, J = 6.6 Hz, 1H), 5.31

(d, J = 16.8 Hz, 1H), 5.32 (d, J = 10.3 Hz, 1H), 5.69 (m, 1H), 6.87 (d, J = 8.6 Hz,

2H), 7.25 (d, J = 8.5 Hz, 2H);^{13}C NMR (100 MHz, CDCl$_3$) δ 159.2, 134.6, 130.3, 129.4, 120.1, 113.8, 94.0, 81.3, 73.3, 72.6, 69.9, 55.8, 55.3, 29.5, 25.8; IR (neat, NaCl):, 3450 (br), 2950 (br), 1610, 1580, 1455, 1420, 1302, 1240 cm^{-1}; $[\alpha]_D{}^{23}$ = +44.1 (c = 1.31, CHCl$_3$); HRMS (ESI$^+$): m/z calc'd for C$_{17}$H$_{26}$NaO$_5{}^+$, 333.1672; found 333.1677.
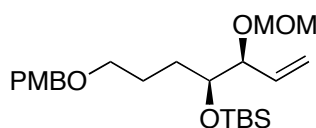
(5S,6S)-6-(3-(4-Methoxybenzyloxy)propyl)-8,8,9,9-tetramethyl-5-vinyl-2,4,7-trioxa-8-siladecane (140). To a stirred solution of alcohol **139** (3.00 g, 9.65 mmol) dissolved in anhydrous DMF (5.0 mL) were added TBSCl (10.5 g, 69.7 mmol) and imidazole (4.74 g, 69.6 mmol) as solids. The resulting mixture was heated at 75 °C for 4 h. The reaction mixture was cooled to rt and it was quenched with phosphate buffer pH 7 (100 mL). The mixture was extracted with DCM (3x100 mL). The combined organic layer was dried over Na$_2$SO$_4$ and concentrated *in vacuo*. Purification by column chromatography on silica gel (30% EtOAc in hexanes) provided 2.90 g (6.84 mmol, 71% yield) of alkene **140** as a colorless oil: ^{1}H NMR (400 MHz, CDCl$_3$) δ 0.06 (s, 3H), 0.08 (s, 3H), 0.89 (s, 9H), 1.39 (m, 1H), 1.66 (m, 3H), 3.35 (s, 3H), 3.42 (t, J = 6.5 Hz, 1H), 3.72 (ddd, J = 3.3, 4.9, 8.0 Hz, 1H), 3.80 (s, 3H), 3.99 (dd, J = 5.4, 6.5 Hz, 1H), 4.42 (s, 2H), 4.58 (d, J = 6.6 Hz, 1H), 4.67 (d, J = 6.6 Hz, 1H), 5.25 (d, J = 10.5 Hz, 1H), 5.27 (d, J = 16.7 Hz, 1H), 5.78 (m, 1H),

6.87 (t, J = 4.3 Hz, 2H), 7.25 (d, J = 8.2 Hz, 2H); ^{13}C NMR (100 MHz, CDCl$_3$) δ

159.1, 134.8, 130.8, 129.2, 117.9, 113.7, 94.6, 79.9, 74.0, 72.4, 70.3, 55.5, 55.3, 29.1,

25.9, 25.6, -4.3, -4.7; IR (neat, NaCl): 2930, 2880, 2853, 1620, 1510, 1471, 1250,

1100 cm^{-1}; $[\alpha]_D^{22}$ = +3.86 (c = 1.01, CHCl$_3$); HRMS (ESI$^+$): m/z calc'd for

C$_{23}$H$_{40}$NaO$_5$Si$^+$, 447.2537; found 447.2539.
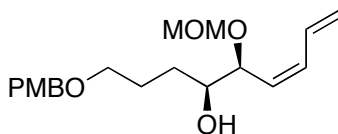
(4S,5S,Z)-1-(4-Methoxybenzyloxy)-5-(methoxymethoxy)nona-6,8-dien-4-ol (142).

To a stirred solution of alkene **140** (2.90 g, 6.84 mmol) dissolved in THF (54 mL) and

H$_2$O (27 mL) was added NMO (0.96 g, 8.2 mmol) and OsO$_4$ in toluene (1.0 M, 0.74

mL, 0.74 mmol). The resulting solution was stirred at rt for 24 h, then quenched with

a sat. Na$_2$S$_2$O$_3$ solution (20 mL) and extracted with EtOAc (3x50 mL). The combined

organic extracts were dried over Na$_2$SO$_4$ and concentrated *in vacuo*. The crude

product was dried under high vacuum for 4 h before use in the next step.

To a flask containing the crude diol was added anhydrous MeOH (60 mL) and

the reaction was cooled to 0 °C. To this mixture was added K$_2$CO$_3$ (1.54 g, 11.1

mmol) and Pb(OAc)$_4$ (3.96 g, 8.93 mmol) and the resulting solution was stirred at 0

°C for 15 min before being quenched with sat. NaHCO$_3$ (40 mL). The reaction

mixture was extracted with EtOAc (3x50 mL), and the combined organic extracts

were washed with brine (20 mL), dried over Na$_2$SO$_4$, and concentrated *in vacuo*. The

crude aldehyde was used directly in next step without further purification.

To a flask containing allyldiphenylphosphine (2.62 mL, 8.21 mmol) dissolved in anhydrous THF (30 mL) was added *tert*-butyllithium (1.70 M, 4.83 mL, 8.21 mmol) dropwise at −78 °C, and the mixture was stirred at 0 °C for 30 min. Ti(O^{i}Pr)$_4$ (2.63 mL, 8.90 mmol) was added dropwise at −78 °C, and the resulting solution was stirred for 5 min. The crude aldehyde, dissolved in THF (3.0 mL), was added over 4 min *via* syringe at −78 °C, and the mixture was stirred at −78 °C for 10 min and then at 0 °C for 1h. Methyl iodide (1.28 mL, 20.6 mmol) was added at 0 °C and the reaction mixture was stirred at rt overnight. The reaction mixture was diluted with hexanes (130 mL), filtered through a silica gel plug (13 g), washed with 20% EtOAc in hexanes (100 mL), and concentrated *in vacuo*. The resulting *cis*-diene was used directly in the next step without further purification.

The crude *cis*-diene was dissolved in anhydrous THF (18 mL) and treated with TBAF in THF (1.0 M, 10.3 mL, 10.3 mmol). The reaction mixture was stirred at rt for 25 h before being diluted with water (20 mL) and extracted with EtOAc (3x20 mL). The combined organic extracts were washed with brine (20 mL), dried over Na$_2$SO$_4$, and concentrated in *vacuo*. Purification by column chromatography on silica gel (30% EtOAc in hexanes) provided 0.43 g (1.3 mmol, 19%) of *cis*-dienol **142** as a colorless oil: ^{1}H NMR (400 MHz, CDCl$_3$) δ 1.43 (m, 1H), 1.63 (m, 1H), 1.72 (m, 1H), 1.82 (m, 1H), 2.86 (brs, 1H), 3.38 (s, 3H), 3.46 (m, 2H), 3.57 (m, 1H), 3.80 (s, 3H), 4.36 (dd, *J* = 7.10, 9.70 Hz, 1H), 4.42 (s, 2H), 4.54 (d, *J* = 6.64 Hz, 1H), 4.69 (d, *J* = 6.7 Hz, 1H), 5.27 (m, 2H), 6.29 (dd, *J* = 11.1, 11.8 Hz, 1H), 6.67 (ddd, *J* = 10.31, 11.7,

16.7 Hz, 1H), 6.86 (d, J = 8.7 Hz, 2H), 7.24 (d, J = 8.6 Hz, 2H); ^{13}C NMR (100

MHz, CDCl$_3$) δ 159.1, 134.9, 131.7, 130.6, 129.2, 127.5, 120.4, 113.7, 93.6, 74.8,

73.5, 72.4, 69.9, 55.6, 55.2, 29.6, 26.0; IR (neat, NaCl): 3430 (br), 2940 (br), 1630,

1509, 1473, 1250, 1120 cm^{-1}; $[\alpha]_D{}^{22}$ = +46.9 (c = 1.30, CHCl$_3$); HRMS (ESI$^+$): m/z

calc'd for C$_{19}$H$_{28}$NaO$_5{}^+$, 359.1829; found 359.1831.
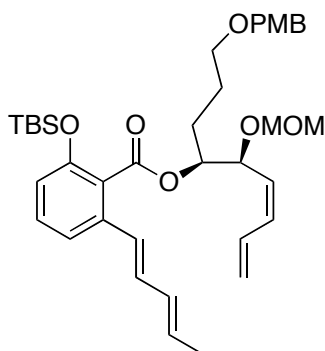
**(4S,5S,Z)-1-(4-Methoxybenzyloxy)-5-(methoxymethoxy)nona-6,8-dien-4-yl 2-
(*tert*-Butyldimethylsilyloxy)-6-((1E,3E)-penta-1,3-dienyl)benzoate (143).** Alcohol
142 (350 mg, 1.04 mmol) was azeotroped *in vacuo* with benzene (2x4 mL), dissolved
in anhydrous THF (4.0 mL) and cooled to 0 °C. NaHMDS (1.0 M, 1.98 mL, 1.98
mmol) was added dropwise. After stirring at 0 °C for 30 min, salicylate **50** (242 mg,
0.991 mmol) dissolved in distilled THF (4.0 mL) was added dropwise. The reaction
was warmed to rt and stirred for 2 h, and then TBSCl (298 mg, 1.98 mmol) and
imidazole (135 mg, 1.98 mmol) were added to the reaction mixture as solids. The
reaction was stirred overnight and then quenched by an ice-cold solution of 5% HCl
(30 mL). The mixture was extracted with Et$_2$O (2x30 mL) and the combined organic
layer was washed with 10% NaHCO$_3$ (50 mL). The organic layer was washed with

brine (30 mL), dried over MgSO$_4$ and concentrated *in vacuo*. Purification by column chromatography on silica gel (20% EtOAc in hexanes) provided 0.578 g (0.907 mmol, 91% yield) of ester **143** as a colorless oil: ^{1}H NMR (400 MHz, CDCl$_3$) δ 0.22 (s, 6H), 0.96 (s, 9H), 1.61 (m, 1H), 1.77 (m, 1H), 1.78 (d, *J* = 6.88 Hz, 3H), 1.92 (m, 1H), 3.27 (s, 3H), 3.46 (m, 2H), 3.79 (s, 3H), 4.42 (s, 2H), 4.50 (d, *J* = 6.72 Hz, 1H), 4.63 (d, *J* = 6.76 Hz, 5H), 4.72 (dd, *J* = 5.54, 9.66 Hz, 1H), 5.20 (m, 2H), 5.28 (d, *J* = 16.69 Hz, 1H), 5.39 (dd, 1H), 5.81 (m, 1H), 6.15 (dd, *J* = 10.50, 14.98 Hz, 1H), 6.27 (dd, *J* = 11.10, 11.10 Hz, 1H), 6.46 (d, *J* = 15.53 Hz, 1H), 6.69 (m, 3H), 6.86 (d, *J* = 8.60 Hz, 2H), 7.13 (m, 2H), 7.24 (d, *J* = 8.52 Hz, 2H); ^{13}C NMR (100 MHz, CDCl$_3$) δ 171.1, 167.8, 159.1, 152.5, 136.4, 134.7, 131.9, 131.7, 131.6, 131.2, 130.7, 129.6, 129.1, 126.9, 126.7, 120.4, 117.6, 117.4, 113.7, 93.4, 76.4, 72.4, 70.5, 69.7, 55.5, 55.2, 27.5, 25.8, 25.6, 25.5, 18.3, -4.1, -4.2; IR (neat, NaCl): 2950, 2873, 1720, 1565, 1505, 1440, 1280, 1100 cm^{-1}; [α]$_D^{21}$ = + 32.9 (c = 1.50, CHCl$_3$); HRMS (ESI$^+$): *m/z* calc'd for C$_{37}$H$_{52}$NaO$_7$Si$^+$, 659.3375; found 659.3381.
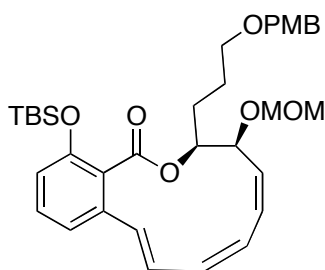
(3*S*,4*S*,5*Z*,7*Z*,9*E*)-14-(*tert*-Butyldimethylsilyloxy)-3-(3-(4-methoxybenzyloxy) propyl)-4-(methoxymethoxy)-3,4-dihydro-1*H*-benzo[*c*][1]oxacyclododecin-1-one (144). To a flask containing bis-diene **143** (100 mg, 0.157 mmol) was added

anhydrous and degassed toluene (80 mL). Ruthenium Grubbs 2nd generation catalyst (6.7 mg, 0.0079 mmol) in degassed toluene was added in one portion under a nitrogen atmosphere. The solution was heated to reflux and stirred for 60 min. The reaction mixture was allowed to cool to room temperature and DMSO (5mL) was added into the reaction flask prior to the removal of toluene *in vacuo* to obtain dark brown liquid. The crude product was loaded directly on to a silica column for combi-flash purification (0% to 10% EtOAc in hexanes) to afford 20.6 mg (0.0346 mmol, 22%) of the macrocyclic triene as a light-yellow oil: ^{1}H NMR (400 MHz, CDCl$_3$) δ 0.19 (s, 3H), 0.20 (s, 3H), 0.96 (s, 9H), 1.73 (m, 1H), 1.86 (m, 1H), 1.97 (m, 1H), 2.07 (m, 1H), 3.35 (s, 3H) , 3.49 (m, 2H), 3.80 (s, 3H), 4.52 (d, J = 6.6 Hz, 1H), 4.55 (d, J = 6.4 Hz, 1H), 4.60 (dd, J = 2.9, 10.7 Hz, 1H), 5.32 (ddd, J = 2.9, 2.88, 10.3 Hz, 1H), 5.68 (dd, J = 11.4, 11.4 Hz, 2H), 5.87 (dd, J = 4.1, 11.0 Hz, 1H), 6.18 (dd, J = 4.1, 12.0 Hz, 1H), 6.34 (t, J = 11.2 Hz, 1H), 6.64 (d, J = 16.0 Hz, 1H), 6.74 (d, J = 8.20 Hz, 1H), 6.78 (d, J = 7.7 Hz, 1H), 6.87 (d, J = 8.5 Hz, 2H), 7.01 (dd, J = 11.5, 16.01 Hz, 1H), 7.16 (dd, J = 7.9, 7.9 Hz, 1H), 7.26 (t, J = 4.3 Hz, 2H); ^{13}C NMR (100 MHz, CDCl$_3$) δ 168.4, 159.0, 152.3, 137.9, 132.2, 131.9, 131.0, 130.8, 129.9, 129.2, 129.1, 127.2, 127.1, 126.6, 121.2, 117.9; IR (neat, NaCl): 2930, 2857, 1730, 1612, 1570, 1513, 1463, 1362, 1292, 1250, 1172, 1155, 1102, 1032, 1001, 927, 863, 839, 807, 783, 753, 714, 670 cm^{-1}; $[\alpha]_D^{20}$ = -81.9 (c= 1.03, CHCl$_3$); HRMS (ESI$^+$): *m/z* calc'd for C$_{34}$H$_{46}$NaO$_7$Si$^+$, 617.2905; found 617.2907.
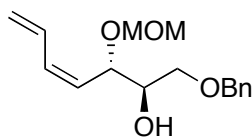
(2*R*,3*S*,*Z*)-1-(Benzyloxy)-3-(methoxymethoxy)hepta-4,6-dien-2-ol (147). To a flask containing ethyl 6-*O*-benzyl-2,3-dideoxyhex-2-enopyranoside, **146**, (11.42 g, 43.86 mmol) was added anhydrous DCM (120 mL) and cooled to 0 °C. *i*-Pr$_2$NEt (23.0 mL, 131.6 mmol) was added dropwise and stirred for 10 min. To the mixture was added MOMCl (13.4 mL, 176.4 mmol) dropwise over 40 min at 0 °C and stirred overnight. The reaction mixture was poured into a sat. NaHCO$_3$ (50 mL) and extracted with Et$_2$O (3x50 mL). The combined organic layer washed with brine (50 mL) and dried over Na$_2$SO$_4$, concentrated *in vacuo*. The crude product, a colorless oil, was used in the next step without further purification.

To a flask containing the crude product from the previous step dissolved in acetonitrile (300 mL) was added Zn(NO$_3$)$_2$•6H$_2$O (26 g, 88 mmol). The mixture was heated at 60 °C for 45 min. It was allowed to cool to rt, and then added a 1:1 mixture of sat. Na(HCO$_3$) (50 mL) and sat. Rochelle's salt (50 mL). The mixture was washed with brine, and dried over Na$_2$SO$_4$. The organic layer was concentrated *in vacuo* to afford crude pyran-2-ol as colorless oil. The crude product was used in the next step without further purification.

To a mixture of CH$_3$PPh$_3$Br (34.6 g, 96.8 mmol) in anhydrous THF (50 mL), cooled at 0 °C under a N$_2$ atmosphere, was added dropwise a solution of *t*-BuOK (9.9 g, 88 mmol) dissolved in THF (200 mL). After the addition was completed, the mixture turned bright yellow. The mixture was stirred at 0 °C for 1.5 h, and a solution

of crude pyran-2-ol diluted in THF (100 mL) was added dropwise over 10 min. The reaction mixture was stirred at 0 °C and warmed to rt overnight and then quenched with water (200 mL) and extracted with Et$_2$O (2x200 mL). The combined organic layer was washed with brine (250 mL), dried over MgSO$_4$, and concentrated *in vacuo*. Purification by column chromatography on silica gel (40% EtOAc in hexanes) provided 4.70 g (16.8 mmol, 38% over three steps) of *Z*-dienol **147** as a colorless oil: ^{1}H NMR (400 MHz, CDCl$_3$) δ 2.51 (d, *J* = 4.1 Hz, 1H), 3.34 (s, 3H), 3.55 (d, *J* = 1.2 Hz, 1H), 3.56 (s, 1H), 3.96 (m, *J* = 5.0 Hz, 1H), 4.54 (s, 2H), 4.54 (d, *J* = 6.5 Hz, 1H), 4.63 (dd, *J* = 4.1, 9.1 Hz, 1H), 4.66 (d, *J* = 6.6 Hz, 1H), 5.22 (d, *J* = 10.1 Hz, 1H), 5.30 (d, *J* = 16.8 Hz, 1H), 5.42 (dd, *J* = 10.3, 10.3 Hz, 1H), 6.32 (dd, *J* = 11.1, 11.1 Hz, 1H), 6.66 (td, *J* = 10.8, 16.8 Hz, 1H), 7.31 (m, 5H); ^{13}C NMR (100 MHz, CDCl$_3$) δ 137.9, 135.0, 131.7, 128.4, 127.8, 127.7, 126.7, 120.3, 93.7, 73.5, 72.5, 71.7, 70.8, 55.5; IR (neat, NaCl): 3520 (br), 2970 (br), 1650, 1529, 1483, 1239, 1120, 957 cm^{-1}; HRMS (ESI$^+$): *m/z* calc'd for C$_{16}$H$_{22}$NaO$_4^+$, 301.1410; found 301.1413.

OMOM
OBn
OPNB
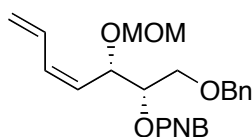
(2*S*,3*S*,*Z*)-1-(Benzyloxy)-3-(methoxymethoxy)hepta-4,6-dien-2-yl 4-Nitrobenzoate (148). To a flask containing *Z*-dienol **147** (4.70 g, 16.8 mmol) dissolved in anhydrous THF (100 mL) was added PPh$_3$ (6.61 g, 25.2 mmol). The mixture was added dropwise to a solution of DEAD and PNBA dissolved in THF (200 mL) at 0 °C. The

resulting mixture was stirred at 0 °C for 30 min, and stirred overnight at rt and concentrated *in vacuo* and loaded on a silica column. Purification by column chromatography on silica gel (30% EtOAc in hexanes) provided 5.77 g (13.5 mmol, 80%) of *Z*-diene **148** as a colorless oil: ^{1}H NMR (400 MHz, CDCl$_3$) δ 3.26 (s, 3H), 3.70 (dd, *J* = 5.5, 10.8 Hz, 1H), 3.78 (dd, *J* = 3.5, 10.8 Hz, 1H), 4.51 (m, 3H), 4.64 (d, *J* = 6.8 Hz, 1H), 4.97 (dd, *J* = 7.0, 9.6 Hz, 1H), 5.23 (d, *J* = 10.1 Hz, 1H), 5.31 (d, *J* = 7.8 Hz, 1H), 5.33 (d, *J* = 16.5 Hz, 1H), 5.43 (m, *J* = 2.3 Hz, 1H), 6.31 (dd, *J* = 11.2, 11.2 Hz, 1H), 6.71 (td, *J* = 10.5, 16.4 Hz, 1H), 7.29 (m, 5H), 8.27 (m, 4H); ^{13}C NMR (100 MHz, CDCl$_3$) δ 164.1, 150.6, 137.7, 135.6, 135.3, 131.5, 130.9, 128.3, 127.7, 127.7, 125.8, 123.5, 120.9, 93.6, 75.5, 73.3, 69.7, 68.4, 55.5; $[\alpha]_D^{21}$ = +39.5 (c = 1.24, CHCl$_3$); HRMS (ESI[+]): *m/z* calc'd for $C_{23}H_{25}NNaO_7^+$, 450.1523; found 450.1529.
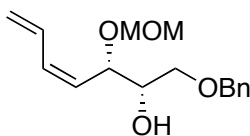
(2*S*,3*S*,*Z*)-1-(Benzyloxy)-3-(methoxymethoxy)hepta-4,6-dien-2-ol (149). To a flask containing *Z*-diene **148** (3.0 g, 7.0 mmol) dissolved in MeOH (75 mL) was added K$_2$CO$_3$ (7.5 g, 54 mmol). The mixture was stirred for 1 h at rt . The solid K$_2$CO$_3$ were filtered out using filtered paper and was rinsed with Et$_2$O (20 mL). The combined organic layer was concentrated *in vacuo* and loaded to a silica column. Purification by column chromatography on silica gel (30% EtOAc in hexanes) provided 1.60 g (5.74

mmol, 82%) of Z-dienol **149** as a colorless oil: ^{1}H NMR (400 MHz, CDCl$_3$) δ 2.81

(d, J = 4.3 Hz, 1H), 3.37 (s, 3H), 3.47 (dd, J = 5.6, 9.9 Hz, 1H), 3.59 (dd, J = 3.7, 9.9

Hz, 1H), 3.79 (m, 1H), 4.52 (s, 2H), 4.56 (d, J = 6.6 Hz, 1H), 4.63 (dd, J = 6.8, 9.8

Hz, 1H), 4.68 (d, J = 6.7 Hz, 1H), 5.21 (d, J = 10.1 Hz, 1H), 5.29 (d, J = 16.7 Hz,

1H), 5.33 (dd, J = 10.4, 10.4 Hz, 1H), 6.26 (dd, J = 11.1, 11.8 Hz, 1H), 6.69 (td, J =

10.2, 16.8 Hz, 1H), 7.29 (m, 5H); ^{13}C NMR (100 MHz, CDCl$_3$) δ 138.0, 134.7,

131.7, 128.3, 127.8, 127.6, 127.1, 120.3, 93.8, 73.5, 73.1, 72.0, 70.7, 55.6; IR (neat,

NaCl): 3545 (br), 2930 (br), 1670, 1549, 1485, 1259, 1117 cm^{-1}; $[\alpha]_D^{21}$ = + 60.3 (c

= 1.25, CHCl$_3$); HRMS (ESI$^+$): m/z calc'd for C$_{16}$H$_{22}$NaO$_4^+$, 301.1410;

found 301.1413.
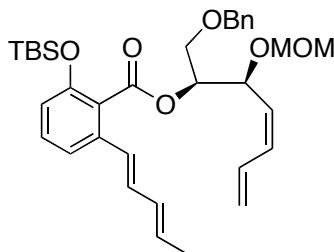
(2S,3S,Z)-1-(Benzyloxy)-3-(methoxymethoxy)hepta-4,6-dien-2-yl   2-(*tert*-
Butyldimethylsilyloxy)-6-((1E,3E)-penta-1,3-dienyl)benzoate (150). Alcohol **149**

(1.60 g, 5.74 mmol) was azeotroped *in vacuo* with benzene (2x10 mL), dissolved in

anhydrous THF (20.0 mL) and cooled to 0 °C. NaHMDS (1.0 M, 12.1 mL, 12.1

mmol) was added dropwise. After stirring at 0 °C for 30 min, salicylate **50** (1.42 g,

5.80 mmol) dissolved in distilled THF (20.0 mL) was added dropwise. The reaction

was warmed to rt and stirred for 2 h, and then TBSCl (1.82 g, 12.1 mmol) and

imidazole (0.82 g, 12.1 mmol) were added to the reaction mixture as solids. The reaction was stirred overnight, filtered through a silica gel plug and rinsed with Et_2O (40 mL) and dried over $MgSO_4$. The organic layer was concentrated *in vacuo*. Purification by column chromatography on silica gel (10% EtOAc in hexanes) provided 1.44 g (2.489 mmol, 43%) of ester **150** as a colorless oil: ^{1}H NMR (400 MHz, $CDCl_3$) δ 0.21 (s, 3H), 0.22 (s, 3H), 0.97 (s, 9H), 1.75 (d, *J* = 7.40 Hz, 3H), 3.27 (s, 3H), 3.72 (dd, *J* = 4.7, 10.4 Hz, 1H), 3.83 (dd, *J* = 5.0, 10.4 Hz, 1H), 4.52 (s, 2H), 4.63 (d, *J* = 4.6 Hz, 1H), 4.65 (d, *J* = 4.5 Hz, 1H), 4.95 (dd, *J* = 5.8, 9.8 Hz, 1H), 5.19 (d, *J* = 10.0 Hz, 1H), 5.28 (tdd, *J* = 0.9, 6.4, 16.8 Hz, 1H), 5.34 (dd, *J* = 4.9, 10.7 Hz, 1H), 5.39 (t, *J* = 10.3 Hz, 1H), 5.79 (m, 1H), 6.04 (ddd, *J* = 1.3, 10.4, 15.0 Hz, 1H), 6.24 (td, *J* = 11.1, 14.0 Hz, 1H), 6.50 (d, *J* = 15.5 Hz, 1H), 6.67 (m, 3H), 7.14 (d, *J* = 7.0 Hz, 1H), 7.15 (dd, *J* = 7.92, 12.8 Hz, 1H), 7.31 (m, 5); ^{13}C NMR (100 MHz, $CDCl_3$) δ 167.7, 152.5, 134.8, 133.4, 132.0, 131.9, 131.8, 131.7, 131.1, 129.7, 128.3, 127.7, 127.6, 127.6, 126.5, 120.3, 119.6, 117.4, 93.9, 75.0, 74.3, 73.4, 71.9, 68.9, 55.5, 25.8, 25.8, 18.3, -4.2, -4.2; IR (neat, NaCl): 2920. 2875, 1720, 1568. 1503, 1465, 1280, 1237, 1083, 985 cm^{-1}; $[\alpha]_D^{21}$ = +23.5 (c = 1.50, $CHCl_3$); HRMS (ESI^+): *m/z* calc'd for $C_{34}H_{46}NaO_6Si^+$, 601.2956; found 601.2957.
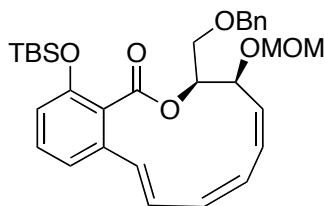
(3*S*,4*S*,5*Z*,7*Z*,9*E*)-3-(Benzyloxymethyl)-14-(*tert*-butyldimethylsilyloxy)-4-(methoxymethoxy)-3,4-dihydro-1*H*-benzo[*c*][1]oxacyclododecin-1-one (151). To a flask containing ester **150** (70 mg, 0.12 mmol) was added anhydrous and degassed DCM (65 mL). Ruthenium Grubbs 2nd generation catalyst (17 mg, 0.020 mmol) in degassed DCM (1.0 mL) was added in one portion under a nitrogen atmosphere. The solution was heated to reflux at 47 °C for 80 min. The reaction mixture was allowed to cool to room temperature and DMSO (5 mL) was added into the reaction flask. The mixture was stirred overnight, and then concentrate *in vacuo.* The crude product was loaded directly on to a silica column for combi-flash purification (0% to 10% EtOAc in hexanes) to afford 10.9 mg (0.0203 mmol, 17%) of macrocyclic triene **151** as a light-yellow oil: ^{1}H NMR (400 MHz, CDCl$_3$) δ 0.17 (s, 3H), 0.21 (s, 3H), 0.92 (s, 9H), 3.36 (s, 3H), 3.92 (d, *J* = 5.0 Hz, 2H), 4.54 (s, 2H), 4.62 (s, 2H), 4.64 (dd, *J* = 3.0, 10.8 Hz, 1H), 5.57 (m, 2H), 5.85 (dd, *J* = 3.9, 10.8 Hz, 1H), 6.13 (dd, *J* = 4.1, 11.9 Hz, 1H), 6.35 (t, *J* = 11.3 Hz, 1H), 6.65 (d, *J* = 16.0 Hz, 1H), 6.77 (dd, *J* = 7.9, 13.4 Hz, 2H), 7.02 (dd, *J* = 11.4, 16.0 Hz, 1H), 7.17 (t, *J* = 8.0 Hz, 1H), 7.33 (m, 5H); ^{13}C NMR (100 MHz, CDCl$_3$) δ 168.3, 152.5, 138.2, 138.0, 132.1, 132.1, 131.2, 130.2, 129.4, 128.3, 127.7, 127.5, 127.2, 126.9, 121.1, 117.8, 93.2, 77.4, 73.2, 68.2, 67.9, 55.5, 25.7, 18.2, -4.0, -4.5; IR (neat, NaCl): 2950, 2859, 1732, 1620, 1590, 1587, 1480, 1260, 1038 cm^{-1}; $[\alpha]_D{}^{21}$ = -78 (c = 0.50, CHCl$_3$); HRMS (ESI$^+$): *m/z* calc'd for C$_{31}$H$_{40}$NaO$_6$Si$^+$, 559.2486; found 559.2489.
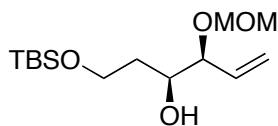
(5S,6S)-10,10,11,11-Tetramethyl-5-vinyl-2,4,9-trioxa-10-siladodecan-6-ol (153).

To a flask containing 3-(methoxymethylthoxy)prop-1-ene (4.00 g, 39.2 mmol) dissolved in anhydrous THF (80 mL) was added *sec*-butyllithium in cyclohexane (1.40 M, 23.3 mL, 32.6 mmol) at –78 °C dropwise. The resulting orange solution was stirred at –78 °C for an additional 30 min, and (+)-*B*-methoxydiisopinocamphenylborane (10.3 g, 32.6 mmol) dissolved in THF (80 mL) was added dropwise. After the reaction mixture was stirred at –78 °C for 1 h, it was cooled to -90 °C (using MeOH and liquid N_2 to prepare the cooling bath). Boron trifluoride etherate (5.45 mL, 43.4 mmol) was added dropwise. Immediately afterwards, 3-(*tert*-butyldimethylsilyloxy)propanal, **152**, (6.14 g, 32.6 mmol) was added dropwise and the mixture kept at -90 °C for 3 h. The reaction was warmed to rt over 15 h to give a clear colorless solution, and quenched with a mixture of 35% H_2O_2 (23 mL) and sat. $NaHCO_3$ solution (45 mL). After stirring at rt for 30 min, the mixture was extracted with EtOAc (3x50 mL). The combined organic extracts were washed with brine, dried over Na_2SO_4, and concentrated *in vacuo*. Purification by column chromatography on silica gel (15% EtOAc in hexanes) provided 7.64 g (26.3 mmol, 81%) of alcohol **153** as a colorless oil: ^{1}H NMR (400 MHz, $CDCl_3$) δ 0.05 (s, 6H), 0.88 (s, 9H), 1.69 (m, 2H), 3.12 (brs, 1H), 3.38 (s, 3H), 3.82 (m, 3H), 3.92 (dd, J = 6.90, 6.90 Hz, 1H), 4.59 (d, *J* = 6.64 Hz, 1H), 4.72 (d, *J* = 6.64 Hz, 1H), 5.30 (d, *J* = 15.73 Hz, 1H), 5.30 (d, *J* = 11.60 Hz, 1H), 5.74 (m, *J* = 3.54 Hz, 13H); ^{13}C NMR

(100 MHz, CDCl$_3$) δ 134.8, 119.6, 94.0, 80.9, 72.2, 61.2, 55.6, 34.9, 25.9, 18.2, -5.5,

-5.5; IR (neat, NaCl): 3450 (br), 2890 (br), 1630, 1598, 1473, 1290, 1157 cm^{-1}; [α]$_D$ ^{21}

= +61.4 (c = 1.31, CHCl$_3$); HRMS (ESI$^+$): *m/z* calc'd for C$_{14}$H$_{30}$NaO$_4$Si$^+$, 313.1806;

found 313.1809.
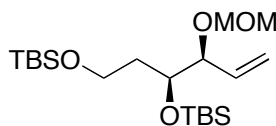
(5*S*,6*S*)-6-(*tert*-Butyldimethylsilyloxy)-10,10,11,11-tetramethyl-5-vinyl-2,4,9-

trioxa-10-siladodecane (154). Alcohol **153** (1.65 g, 5.68 mmol) was azeotroped *in*

vacuo with benzene (2x5 mL), and dissolved in anhydrous DCM (75.0 mL). To the

mixture was added 2,6-lutidine (1.32 mL, 11.36 mmol) and cooled to −78 °C. TBSOTf

(1.32 mL, 11.36 mmol) was added dropwise at −78 °C and stirred overnight while the

reaction slowly warmed to rt. The reaction mixture was quenched with cold water (2

mL) and extracted with DCM (3x30 mL). The combined organic layer was dried over

Na$_2$SO$_4$ and concentrated *in vacuo*. Purification by column chromatography on silica

gel (5% Et$_2$O in hexanes) provided 2.30 g (5.68 mmol, quantitative yield) of alkene

154 as a colorless oil: ^{1}H NMR (400 MHz, CDCl$_3$) δ 0.04 (s, 6H), 0.08 (s, 3H), 0.09

(s, 3H), 0.88 (s, 9H), 0.89 (s, 9H), 1.56 (m, 1H), 1.80 (m, 1H), 3.36 (s, 3H), 3.68 (m,

2H), 3.92 (m, 1H), 4.02 (q, 1H), 4.59 (d, *J* = 6.64 Hz, 1H), 4.67 (d, *J* = 6.60 Hz, 1H),

5.25 (d, *J* = 9.40 Hz, 1H), 5.28 (d, *J* = 16.85 Hz, 1H), 5.82 (m, 1H); ^{13}C NMR (100

MHz, CDCl$_3$) δ 134.8, 117.6, 94.7, 79.6, 70.6, 59.5, 55.4, 35.4, 25.9, 18.2, 18.1, -

4.4, -4.9, -5.3, -5.3; IR (neat, NaCl): 2968, 2945, 2849, 1608, 1520, 1469, 1246, 1093 cm^{-1}; $[\alpha]_D^{21}$ = +7.90 (c = 1.50, CHCl$_3$); HRMS (ESI$^+$): *m/z* calc'd for C$_{20}$H$_{44}$NaO$_4$Si$_2^+$, 427.2670; found 424.2675.
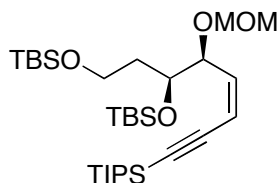
(5S,6S)-(*tert*-Butyldimethylsilyloxy)-10,10,11,11-tetramethyl-5-(4-(triisopropylsilyl) but-1-en-3-ynyl)-2,4,9-trioxa-10-siladodecane (156). To a stirred solution of alkene **154** (0.47 g, 1.16 mmol) dissolved in THF (10 mL) and H$_2$O (5 mL) was added NMO (163 mg, 1.40 mmol) and OsO$_4$ in toluene (1.0 M, 0.13 mL, 0.13 mmol). The resulting solution was stirred at rt for 41 h, then quenched with a sat. Na$_2$S$_2$O$_3$ solution (20 mL) and extracted with EtOAc (3x50 mL). The combined organic extracts were dried over Na$_2$SO$_4$ and concentrated *in vacuo*. The crude product was dried under high vacuum for 4 h before use in the next step.

To a flask containing the crude diol was added anhydrous MeOH (10 mL) and the reaction was cooled to 0 °C. To the mixture was added K$_2$CO$_3$ (0.26 g, 1.9 mmol) and Pb(OAc)$_4$ (0.67 g, 1.5 mmol) and the resulting solution was stirred at 0 °C for 15 min before being quenched with sat. NaHCO$_3$ (20 mL). The reaction mixture was extracted with EtOAc (3x20 mL), and the combined organic extracts were washed with brine (20 mL), dried over Na$_2$SO$_4$, and concentrated *in vacuo*. The crude aldehyde was used directly in next step without further purification.

To a flask containing prop-1-yne-1,3-diylbis(triisopropylsilane), **120**, (0.71 g, 2.0 mmol) was added anhydrous THF (16 mL) and cooled to -20 °C. To the resulting mixture was added *n*-BuLi in hexanes (1.6 M, 1.25 mL, 2.00 mmol) dropwise over 5 min, stirred for 30 min, and then cooled to -78 °C. The crude aldehyde dissolved in THF (11 mL) was added dropwise to the anion solution over 1.5 h. After additional stirring for 30 min, the reaction was quenched at -78 °C with saturated NH$_4$Cl solution (25 mL) and warmed to rt. The mixture was extracted with EtOAc (3x30 mL), and washed with brine. The combined organic layer was dried over MgSO$_4$ and concentrated *in vacuo*. Purification by column chromatography on silica gel (5% EtOAc in hexanes) provided 0.21 g (0.36 mmol, 31% over three steps) of the enyne product as an inseparable 10:1 *Z:E* olefin mixture, as determined by ^{1}H NMR. ^{1}H NMR (400 MHz, CDCl$_3$) δ 0.03 (s, 6H), 0.07 (s, 3H), 0.09 (s, 3H), 0.88 (s, 9H), 0.89 (s, 9H), 1.09 (s, 21H), 1.65 (m, 1H), 1.87 (m, 1H), 3.33 (s, 3H), 3.69 (m, 2H), 3.88 (m, 1H), 4.53 (dd, *J* = 5.78, 9.34 Hz, 1H), 4.58 (d, *J* = 6.36 Hz, 1H), 4.69 (d, *J* = 6.40 Hz, 1H), 5.76 (d, *J* = 11.12 Hz, 1H), 5.88 (dd, *J* = 9.32, 11.08 Hz, 1H); ^{13}C NMR (100 MHz, CDCl$_3$) δ 140.7, 113.6, 107.1, 96.9, 95.1, 78.6, 71.0, 59.7, 55.6, 36.6, 26.0, 25.9, 25.9, 25.8, 18.6, 18.6, -4.7, -4.7, -5.2, -5.3; IR (neat, NaCl): 2950, 2878, 2157, 1630, 1529, 1276, 1108, 973 cm^{-1}; [α]$_D$^{21} = +5.35 (c = 1.44 , CHCl$_3$); HRMS (ESI$^+$): *m/z* calc'd for C$_{31}$H$_{64}$NaO$_4$Si$_3$$^+$, 607.4005; found 607.4008.
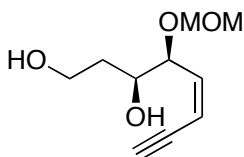
(3*S*,4*S*,*Z*)-4-(Methoxymethoxy)oct-5-en-7-yne-1,3-diol (157).

Procedure A

The eneyne **156** (110 mg, 0.188 mmol) was dissolved in anhydrous THF (18 mL), cooled to 0 °C and treated with TBAF in THF (1.0 M, 0.51 mL, 0.51 mmol). The reaction mixture was stirred at rt for 38 h before being diluted with phosphate buffer pH 7 (3 mL) and extracted with EtOAc (3x5 mL). The combined organic extracts were washed with brine (5 mL), dried over Na_2SO_4, and concentrated in *vacuo*. Purification by column chromatography on silica gel (70% EtOAc in hexanes) provided 31.5 mg (0.157 mmol, 84%) of diol **157** as a pure *Z*-enyne light yellow product:

Procedure B

A stirred solution of alkene **154** (1.40 g, 3.45 mmol) dissolved in anhydrous DCM (60 mL) was cooled to -78 °C and ozone was introduced for 3-5 min until the solution turned a deep blue color. The reaction was flushed with N_2 until the solution became colorless, and then Me_2S (13.5 mL) was added to a reaction mixture at -78 °C. The resulting mixture was stirred overnight and dried over Na_2SO_4. The organic layer was concentrated *in vacuo* to afford the aldehyde as a light yellow oil. The crude aldehyde was used directly in the next step without further purification.

To a flask containing prop-1-yne-1,3-diylbis(triisopropylsilane), **120**, (2.3 g, 6.5 mmol) dissolved in anhydrous THF (45 mL) at -20 °C was added *n*-BuLi in hexanes

(1.6 M, 4.1 mL, 6.5 mmol) dropwise over 5 min. The reaction mixture was stirred for 30 min, and then cooled to -78 °C. The crude aldehyde, dissolved in THF (11 mL), was added dropwise to the anion solution over 1.5 h. After additional stirring for 30 min, the reaction was quenched at -78 °C with saturated NH_4Cl solution (40 mL) and warmed to rt. The mixture was extracted with EtOAc (3x30 mL), and washed with brine. The combined organic layer was dried over $MgSO_4$ and concentrated *in vacuo*. The crude enyne was used directly in the next step without further purification.

The crude enyne was dissolved in anhydrous THF (30 mL), cooled to 0 °C and treated with TBAF in THF (1.0 M, 26.04 mL, 26.04 mmol). The reaction mixture was stirred at rt for 22 h before it was quenched with sat. NH_4Cl (40 mL) and extracted with EtOAc (3x40 mL). The combined organic extracts were washed with brine (20 mL), dried over Na_2SO_4, and concentrated in *vacuo*. Purification by column chromatography on silica gel (70% EtOAc in hexanes) provided 352.9 mg (1.762 mmol, 51% over three steps) of diol **157** as a pure *Z*-enyne light yellow product: ^{1}H NMR (400 MHz, $CDCl_3$) δ .74 (m, 1H), 2.85 (brs, 1H), 3.17 (d, *J* = 2.2 Hz, 1H), 3.23 (brs, 1H), 3.39 (s, 3H), 3.81 (m, 3H), 4.50 (dd, *J* = 7.1, 9.2 Hz, 1H), 4.61 (d, *J* = 6.6 Hz, 1H), 4.70 (d, *J* = 6.6 Hz, 1H), 5.73 (dd, *J* = 2.4, 11.1 Hz, 1H), 5.87 (dd, *J* = 9.0, 11.4 Hz, 1H); ^{13}C NMR (100 MHz, $CDCl_3$) δ 141.0, 113.3, 95.1, 83.4, 79.2, 78.3, 73.1, 60.9, 56.0, 34.1; IR (neat, NaCl): 3557 (br), 3300, 3078, 2953, 2870, 1635, 1463, 1298, 1107 cm^{-1}; $[\alpha]_D^{21}$ = +37.1 (c = 1.58, $CHCl_3$); HRMS (ESI$^+$): *m/z* calc'd for $C_{10}H_{16}NaO_4^+$, 223.0941; found 223.0943.

OMOM

TBDPSO

OH
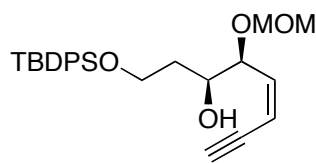
(5S,6S)-5-((Z)-But-1-en-3-ynyl)-11,11-dimethyl-10,10-diphenyl-2,4,9-trioxa-10-siladodecan-6-ol (114). To a stirred solution of diol **157** (85.0 mg, 0.424 mmol) dissolved in anhydrous DMF (2.0 mL) were added imidazole (72.0 mg, 1.06 mmol) and DMAP (3.7 mg, 0.030 mmol) as solids. To the mixture was added TBDPSCl (110 μL, 0.429 mmol) at rt, stirred overnight, and quenched with sat. NaHCO$_3$ (5 mL) , and extracted with DCM (2x5 mL). The combined organic layer was washed with brine (2 mL), dried over Na$_2$SO$_4$, and concentrated *in vacuo*. Purification by column chromatography on silica gel (20% EtOAc in hexanes) provided 149.5 mg (0.3408 mmol, 80%) of alcohol **157** as a light yellow oil: ^{1}H NMR (400 MHz, CDCl$_3$) δ 1.05 (s, 9H), 1.78 (m, 2H), 3.03 (d, 1H), 3.11 (q, 1H), 3.40 (s, 3H), 3.84 (m, 1H), 3.92 (m, 2H), 4.53 (dd, 1H), 4.63 (d, J = 6.7 Hz, 1H), 4.73 (d, J = 6.6 Hz, 1H), 5.73 (dd, J = 2.2, 11.0 Hz, 1H), 5.95 (d, J = 9.4 Hz, 1H), 5.98 (d, J = 10.2 Hz, 1H), 7.39 (m, 6H), 7.67 (m, 4H); ^{13}C NMR (100 MHz, CDCl$_3$) δ 141.7, 135.6, 135.6, 129.7, 127.7, 112.7, 95.0, 83.1, 79.3, 77.9, 71.8, 60.4, 55.9, 35.0, 26.8, 21.0; IR (neat, NaCl): 3489 (br), 3290, 3071, 2927, 2855, 1609, 1591, 1472, 1425, 1258, 1111, 1029 cm^{-1}; $[\alpha]_D^{21}$ = +39.6 (c = 1.18, CHCl$_3$); HRMS (ESI$^+$): *m/z* calc'd for C$_{26}$H$_{34}$NaO$_4$Si$^+$, 461.2119; found 461.2117.
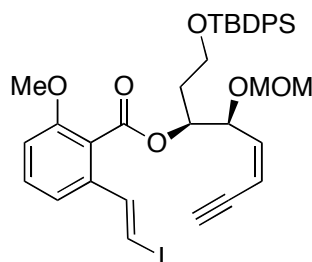
(5*S*,6*S*)-5-((*Z*)-But-1-en-3-ynyl)-11,11-dimethyl-10,10-diphenyl-2,4,9-trioxa-10-siladodecan-6-yl 2-((*E*)-2-iodovinyl)-6-methoxybenzoate (111). Alcohol **114** (550 mg, 1.25 mmol) was azeotroped *in vacuo* with benzene (2x5 mL), dissolved in anhydrous THF (15.0 mL) and cooled to 0 °C. NaHMDS (1.0 M, 2.50 mL, 2.50 mmol) was added dropwise. After stirring at 0 °C for 30 min, salicylate[61] **115** (432 mg, 1.31 mmol) dissolved in distilled THF (12.0 mL) was added dropwise. The reaction was warmed to rt and stirred for 2 h, and then Me_2SO_4 (0.52 mL, 5.5 mmol) was added. The reaction was stirred at rt for 5 h, and then quenched with phosphate buffer pH 7. The mixture was extracted with EtOAc (3x20 mL) and washed with brine (20 mL). The organic layer was dried over Na_2SO_4 and concentrated *in vacuo.* Purification by column chromatography on silica gel (10% EtOAc in hexanes) provided 735 mg (1.01 mmol, 81%) of ester **111** as a light yellow oil: ^{1}H NMR (400 MHz, $CDCl_3$) δ 1.07 (s, 9H), 2.04 (m, 2H), 3.13 (m, 1H), 3.32 (s, 3H), 3.56 (s, 3H), 3.88 (m, 2H), 4.64 (d, *J* = 6.8 Hz, 1H), 4.73 (d, *J* = 6.8 Hz, 1H), 4.82 (dd, *J* = 5.4, 9.0 Hz, 1H), 5.69 (m, 1H), 5.85 (dd, *J* = 2.6, 11.3 Hz, 1H), 6.02 (dd, *J* = 9.1, 11.0 Hz, 1H), 6.79 (d, *J* = 8.2 Hz, 1H), 6.87 (d, *J* = 14.8 Hz, 1H), 7.00 (d, *J* = 7.8 Hz, 1H), 7.28 (t, *J* = 8.6 Hz, 1H), 7.38 (m, 6H), 7.50 (d, *J* = 14.8 Hz, 1H), 7.71 (m, 4H); ^{13}C NMR (100 MHz, $CDCl_3$) δ 166.8, 156.3, 141.7, 141.0, 136.1, 135.7, 135.6, 130.4, 129.5,

127.6, 122.3, 117.5, 113.4, 110.5, 94.7, 83.8, 80.2, 79.1, 74.8, 73.1, 59.7, 55.8, 55.5, 34.1, 26.8, 19.2; IR (neat, NaCl): 3291, 3068, 2927, 2853, 1730, 1607, 1591, 1573, 1475, 1271, 1111 cm^{-1}; $[\alpha]_D^{21}$ = -4.60 (c = 3.70, CHCl$_3$); HRMS (ESI$^+$): *m/z* calc'd for C$_{36}$H$_{41}$INaO$_6$Si$^+$, 747.1609; found 747.1615.
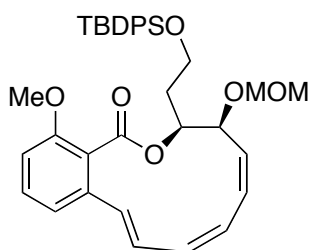

(3*S*,4*S*,5*Z*,7*Z*,9*E*)-3-(2-(*tert*-Butyldiphenylsilyloxy)ethyl)-14-methoxy-4-(methoxymethoxy)-3,4-dihydro-1*H*-benzo[*c*][1]oxacyclododecin-1-one (110). To a flask containing Cu(OAc)$_2$ (13.8 mg, 0.0760 mmol), P(OMe)$_3$ (9.0 μL, 0.076 mmol), K$_2$CO$_3$ (14.4 mg, 0.104 mmol) and NaHCO$_3$ (19.0 mg, 0.279 mmol) was added anhydrous DMF (7 mL) and stirred at 110 °C for 30 min, during which time a dark black solution formed. The intermediate **111** (50 mg, 0.0690 mmol) dissolved in DMF (7.0 mL) was added dropwise over 10 min. The reaction mixture was stirred for an additional 1 h and 15 min at 110 °C, and then cooled to rt. The mixture was diluted with Et$_2$O (5.0 mL) and sat. NH$_4$Cl (5.0 mL). The organic layer was separated, and the aqueous layer was extracted with Et$_2$O (2x5.0 mL). The combined organic layer was washed with brine (5 mL), dried over Na$_2$SO$_4$, and concentrated *in vacuo*. Purification by column chromatography on silica gel (10% EtOAc in hexanes) provided 25.7 mg (0.0429 mmol, 62%) of macrocyclic triene **110** as a light yellow

oil: ^{1}H NMR (400 MHz, CDCl$_3$) δ 1.07 (s, 9H), 2.09 (m, 1H), 2.30 (m, 1H), 3.36 (s, 3H), 3.40 (s, 3H), 3.90 (m, 2H), 4.55 (d, J = 6.5 Hz, 1H), 4.58 (d, J = 6.5 Hz, 1H), 4.63 (dd, J = 3.4, 10.8 Hz, 1H), 5.56 (dd, J = 1.78, 11.5 Hz, 1H), 5.69 (dd, J = 11.3, 11.3 Hz, 1H), 5.89 (dd, J = 4.2, 10.6 Hz, 1H), 6.18 (dd, J = 4.0, 11.9 Hz, 1H), 6.35 (dd, J = 11.3, 11.3 Hz, 1H), 6.66 (d, J = 16.0 Hz, 1H), 6.70 (d, J = 8.3 Hz, 2H), 6.79 (d, J = 7.7 Hz, 1H), 7.01 (dd, J = 11.5, 16.0 Hz, 1H), 7.23 (t, J = 8.1 Hz, 1H), 7.38 (m, 6H), 7.70 (d, J = 2.8 Hz, 4H); ^{13}C NMR (100 MHz, CDCl$_3$) δ 168.4, 156.0, 138.3, 135.5, 134.0, 133.0, 132.1, 130.8, 129.5, 129.5, 127.7, 127.6, 127.4, 123.7, 120.4, 109.2, 93.4, 74.2, 68.5, 60.6, 55.4, 55.3, 31.2, 26.8, 19.2; IR (neat, NaCl): 2930, 1732, 1572, 1468, 1427, 1271, 1111, 1030, 853, 822, 742, 703 cm^{-1}; $[\alpha]_D^{21}$ = -139 (c = 2.37, CHCl$_3$); HRMS (ESI$^+$): m/z calc'd for C$_{36}$H$_{42}$NaO$_6$Si$^+$, 621.2643; found 621.2647.
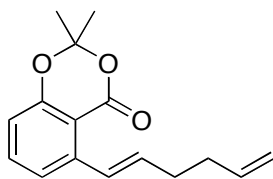
(E)-5-(Hexa-1,5-dienyl)-2,2-dimethyl-4H-benzo[d][1,3]dioxin-4-one (177). To a flask containing Pd$_2$dba$_3$ (50.3 mg, 0.0549 mmol), tricyclohexylphosphonium tetrafluoroborate (79.2 mg, 0.215 mmol) and i-Pr$_2$NEt (0.30 mL, 1.7 mmol) was added DCM (100 mL) and the resulting mixture was stirred at rt for 10 min. 4-Pentyn-1-ol (1 mL, 11 mmol) was added and the reaction mixture was cooled to 0 $^\circ$C. Bu$_3$SnH (3.45 mL, 13.0 mmol) diluted in DCM (30 mL) was added dropwise via

syringe over 15 min. The reaction was then allowed to stir at 0 °C for 4 h. The reaction mixture was condensed to approximately 30 mL of organic mixture and was used directly to the next step without any workup. The crude product showed only (*E*)-5-(tributylstannyl)pent-4-en-1-ol, identical with ^{1}H NMR and ^{13}C properties as reported by Chong.[90]

To the crude (*E*)-5-(tributylstannyl)pent-4-en-1-ol was added Et$_3$N (7.6 mL, 54 mmol) and DMSO (30 mL). The mixture was cooled to 0 °C, and SO$_3$•Py (52.0 mg, 0.324 mmol) was added in portions over 2 min. The mixture was stirred at 0 °C for 15 min, and then diluted with hexanes (100 mL) and phosphate buffer pH 7 (20 mL). The organic layer was separated, and then the aqueous layer was extracted with (3x30 mL of hexanes). The combined organic layer was concentrated *in vacuo* to afford a bright yellow crude product. The crude aldehyde was used directly in the next step without further purification.

To a mixture of CH$_3$PPh$_3$Br (8.50g, 23.8 mmol) in anhydrous THF (30 mL), cooled at 0 °C under N$_2$ atmosphere, was added dropwise a solution of *t*-BuOK (2.42 g, 21.6 mmol) over 3 min. After the addition was completed, the mixture turned bright yellow. The mixture was stirred at 0 °C for 30 min and a solution of crude aldehyde diluted in THF (30 mL) was added dropwise over 10 min. The reaction mixture was stirred at 0 °C and warmed to rt overnight, an then diluted with hexanes (100 mL) and quenched with phosphate buffer pH 7 (50 mL). The organic layer was separated and the aqueous layer was extracted with hexanes (3x100 mL), dried over NaSO$_4$ and concentrated *in vacuo* to afford crude stannyl-diene as a yellow oil. The

141

crude product was divided into four portions equally and used directly for Stille coupling in procedure A and procedure B without further purification.

Stille Coupling Procedure A

To a flask containing Pd$_2$dba$_3$ (103.0 mg, 0.1125 mmol), tri-(2-furyl)-phosphine (79.0 mg, 0.340 mmol), LiCl (475.0 mg, 11.21 mmol), and triflate **57** (731.0 mg, 2.241 mmol) was added anhydrous and degassed DMF (20 mL) and stirred at rt for 15 min under a N$_2$ atmosphere. Then the crude stannyl-diene (~ 2.7 mmol), dissolved in anhydrous and degassed DMF, was added dropwise. The resulting mixture was stirred and heated at 80 °C for 16 h, and then cooled to rt. After 10% NH$_4$OH (15 mL) was added, the mixture was extracted with hexanes (5x50 mL), washed with brine (20 mL), dried over Na$_2$SO$_4$ and concentrated *in vacuo*. Purification by column chromatography on silica gel (10% EtOAc in hexanes) provided 327.2 mg (1.267 mmol, 57%) of dienyl acetonide **177** as an opaque oil.

Stille Coupling Procedure B

To a flask containing Pd(PPh$_3$)$_4$ (129.0 mg, 0.1116 mmol), LiCl (475.0 mg, 11.21 mmol), and triflate **57** (731.0 mg, 2.241 mmol) was added anhydrous and degassed THF (10 mL) at rt under a N$_2$ atmosphere. Then the crude stannyl-diene (~ 2.7 mmol) dissolved in anhydrous and degassed DMF was added dropwise over 15 min. The resulting mixture was stirred and heated at 70 °C for 90 h, and then cooled to rt. After 10% NH$_4$OH (15 mL) was added, the mixture was extracted with hexanes

(5x50 mL), washed with brine (20 mL), dried over Na_2SO_4, and concentrated *in vacuo*. Purification by column chromatography on silica gel (10% EtOAc in hexanes) provided 538.4 mg (2.084 mmol, 93%) of dienyl acetonide **177** as an opaque oil: ^{1}H NMR (400 MHz, $CDCl_3$) δ 1.71 (s, 6H), 2.27 (m, 2H), 2.39 (m, 2H), 5.00 (dd, *J* = 1.86, 10.2 Hz, 1H), 5.08 (dd, *J* = 1.7, 17.1 Hz, 1H), 5.88 (tdd, *J* = 6.6, 10.4, 17.0 Hz, 1H), 6.23 (td, *J* = 6.8, 15.6 Hz, 1H), 6.82 (dd, *J* = 0.9, 8.1 Hz, 1H), 7.22 (d, *J* = 7.8 Hz, 2H), 7.42 (t, *J* = 8.0 Hz, 1H), 7.48 (d, *J* = 15.7 Hz, 1H); ^{13}C NMR (100 MHz, $CDCl_3$) δ 160.4, 156.8, 142.5, 138.0, 135.0, 134.6, 128.5, 121.3, 115.6, 115.0, 110.6, 105.1, 33.3, 32.5, 25.6; IR (neat, NaCl): 2990, 1735, 1598, 1467, 1320 cm^{-1}; HRMS (ESI[+]): *m/z* calc'd for $C_{16}H_{18}NaO_3^+$, 281.1148; found 281.1149.
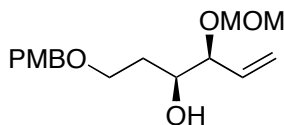
(3*S*,4*S*)-1-(4-Methoxybenzyloxy)-4-(methoxymethoxy)hex-5-en-3-ol (53). To a flask containing 3-(methoxymethoxy)prop-1-ene (1.27 g, 12.4 mmol) dissolved in anhydrous THF (25 mL) was added *sec*-butyllithium in cyclohexane (1.40 M, 7.3 mL, 10.3 mmol) at −78 °C dropwise. The resulting orange solution was stirred at −78 °C for an additional 30 min, and (+)-*B*-methoxydiisopinocamphenylborane (3.26 g, 10.3 mmol) dissolved in THF (25 mL) was added dropwise. The reaction mixture was stirred at −78 °C for 1 h, then cooled to -90 °C (using MeOH and liquid N_2 to prepare the cooling bath). The boron trifluoride etherate (1.72 mL, 13.7 mmol) was added

dropwise. Immediately afterwards, 3-(4-methoxybenzyloxy)propanal (2 g, 10.3 mmol) was added dropwise and the mixture kept at -90 °C for 3 h. The reaction was warmed to rt over 15 h to give a clear colorless solution, and quenched with a mixture of 35% H_2O_2 (12.5 mL) and sat. $NaHCO_3$ solution (20.0 mL). After stirring at rt for 30 min, the mixture was extracted with Et_2O (2x15 mL). The combined organic extracts were washed with brine, dried over Na_2SO_4, and concentrated *in vacuo*. Purification by column chromatography on silica gel (30% EtOAc in hexanes) provided 2.44 g (8.23 mmol, 80%) of alcohol **53** as a colorless oil: ^{1}H NMR (400 MHz, $CDCl_3$) δ 1.79 (m, 2H), 3.22 (brs, 1H), 3.39 (s, 1H), 3.66 (m, 2H), 3.80 (s, 3H), 3.82 (m, 1H), 3.92 (dd, J = 7.0, 7.0 Hz, 1H), 4.46 (s, 2H), 4.60 (d, J = 6.7 Hz, 1H), 4.73 (d, J = 6.7 Hz, 1H), 5.31 (d, J = 16.9 Hz, 1H), 5.31 (d, J = 11.0 Hz, 1H), 5.72 (ddd, J = 7.7, 11.4, 16.3 Hz, 1H), 6.87 (q, J = 2.9 Hz, 2H), 7.26 (t, J = 5.9 Hz, 1H); ^{13}C NMR (100 MHz, $CDCl_3$) δ 159.2, 134.4, 130.1, 129.4, 120.1, 113.8, 94.0, 81.0, 72.8, 71.8, 67.5, 55.7, 55.3, 32.4; IR (neat, NaCl): 2955 (br), 2953 (br), 1613, 1515, 1460, 1249, 1170 cm^{-1}; $[\alpha]_D^{21}$ = +50.6 (c = 1.50, $CHCl_3$), (90% ee)[13]; HRMS (ESI[+]): *m/z* calc'd for $C_{16}H_{24}NaO_5^+$, 319.1516; found 319.1518.
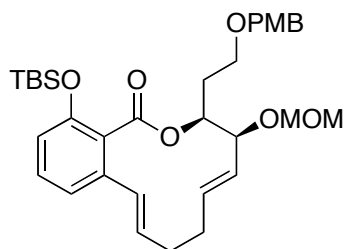
(4*S*,5*E*,9*E*)-14-(*tert*-Butyldimethylsilyloxy)-3-(2-(4-methoxybenzyloxy)ethyl)-4-

(methoxymethoxy)-3,4,7,8-tetrahydro-1*H*-benzo[*c*][1]oxacyclododecin-1-one

(183). Alcohol **53** (500 mg, 1.69 mmol) was azeotroped *in vacuo* with benzene (2x5

mL), dissolved in anhydrous THF (5.0 mL) and cooled to 0 °C. NaHMDS (1.0 M,

3.20 mL, 3.20 mmol) was added dropwise. After stirring at 0 °C for 30 min, salicylate

177 (413 mg, 1.60 mmol) dissolved in distilled THF (5.0 mL) was added dropwise.

The reaction was warmed to rt and stirred for 2 h, and then TBSCl (482 mg, 3.20

mmol) and imidazole (218 mg, 3.20 mmol) were added to the reaction mixture as

solids. The reaction was stirred overnight and diluted with hexanes (30 mL). The

mixture was filtered through a thin silica gel plug, which was rinsed with 20% Et_2O

in hexanes (2x35 mL). The combined organic layer was concentrated *in vacuo* and

azeotroped with benzene (2x5 mL). The crude ester was used directly in the next step

without further purification.

To a flask containing crude ester was added anhydrous and degassed toluene

(1L). Ruthenium Grubbs 2nd generation catalyst (50.0 mg, 0.0589 mmol) in degassed

toluene (1.0 mL) was added in one portion under a nitrogen atmosphere. The solution

was heated to reflux and stirred for 20 h. The reaction mixture was allowed to cool to

room temperature and DMSO (15 mL) was added into the reaction flask prior the

removal of toluene *in vacuo* to obtain a dark brown liquid. The crude product was loaded directly on to a silica column for combi-flash purification (0% to 20% EtOAc in hexanes) to afford 553.3 mg (0.9528 mmol, 60%) of macrocyclic diene as a light-yellow oil: ^{1}H NMR (400 MHz, CDCl$_3$) δ 0.23 (s, 3H), 0.24 (s, 3H), 0.98 (s, 9H), 2.18 (m, 4H), 2.36 (m, 2H), 3.35 (s, 3H), 3.64 (m, 2H), 3.81 (s, 3H), 4.39 (q, J = 2.6 Hz, 1H), 4.43 (d, J = 11.4 Hz, 1H), 4.51 (d, J = 11.4 Hz, 1H), 4.57 (d, J = 6.8 Hz, 1H), 4.67 (d, J = 6.8 Hz, 1H), 5.29 (td, J = 3.35, 6.7 Hz, 1H), 5.32 (dd, J = 5.5, 15.9 Hz, 1H), 5.50 (ddd, J = 5.6, 6.3, 15.9 Hz, 1H), 5.77 (td, J = 6.2, 15.9 Hz, 1H), 6.22 (d, J = 15.9 Hz, 1H), 6.68 (d, J = 8. Hz, 1H), 6.87 (q, J = 5.0 Hz, 3H), 7.13 (t, J = 7.8 Hz, 1H), 7.29 (q, J = 2.9 Hz, 2H); ^{13}C NMR (100 MHz, CDCl$_3$) δ 168.2, 159.1, 152.1, 137.6, 132.2, 131.5, 130.9, 130.6, 129.9, 129.6, 129.3, 125.7, 118.7, 117.1, 113.8, 94.9, 76.3, 75.3, 72.4, 66.6, 56.1, 55.3, 30.6, 30.6, 30.0, 25.8, 18.3, -4.0, -4.2; IR (neat, NaCl): 2910, 2857, 1730, 1613, 1600, 1565, 1505, 1463, 1250, 1160, 1033 cm^{-1}; $[\alpha]_D^{21}$ = +76.3 (c = 1.53, CHCl$_3$); HRMS (ESI$^+$): *m/z* calc'd for C$_{33}$H$_{46}$NaO$_7$Si$^+$, 605.2905; found 605.2907.
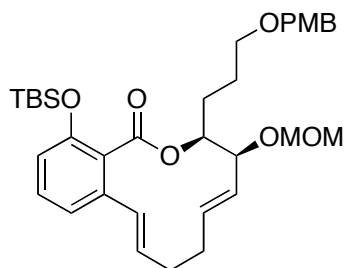
3*S*,4*S*,5*E*,9*E*)-14-(*tert*-Butyldimethylsilyloxy)-3-(3-(4-methoxybenzyloxy)propyl)-4-(methoxymethoxy)-3,4,7,8-tetrahydro-1*H*-benzo[*c*][1]oxacyclododecin-1-one

(184). Alcohol 1**39** (1.19 g, 3.83 mmol) was azeotroped *in vacuo* with benzene (2x10 mL), dissolved in anhydrous THF (15.0 mL) and cooled to 0 °C. NaHMDS (1.0 M, 7.26 mL, 7.26 mmol) was added dropwise. After stirring at 0 °C for 30 min, salicylate **177** (0.93 g, 3.63 mmol) dissolved in distilled THF (15.0 mL) was added dropwise. The reaction was warmed to rt and stirred for 2 h, and then TBSCl (1.09 g, 7.26 mmol) and imidazole (0.50 g, 7.26 mmol) were added to the reaction mixture as solids. The reaction was stirred overnight and filtered through a thin silica gel plug, which was rinsed with 20% Et$_2$O in hexanes (2x50 mL). The combined organic layer was concentrated *in vacuo* and azeotroped with benzene (2x10 mL). The crude ester was used directly in the next step without further purification.

To a flask containing crude ester was added anhydrous and degassed toluene (2L). Ruthenium Grubbs 2nd generation catalyst (98.0 mg, 0.116 mmol) in degassed toluene (3.0 mL) was added in one portion under a nitrogen atmosphere. The solution was heated to reflux and stirred for 4 h. The reaction mixture was allowed to cool to room temperature and DMSO (20 mL) was added into the reaction flask prior the

removal of toluene *in vacuo* to obtain a dark brown liquid. The crude product was loaded directly on to silica column for combi-flash purification (0% to 10% EtOAc in hexanes) to afford 1.321 g (2.212 mmol, 61%) of macrocyclic diene **184** as a light-yellow oil: ^{1}H NMR (400 MHz, CDCl$_3$) δ 0.21 (s, 3H), 0.22 (s, 3H), 0.95 (s, 9H), 1.81 (m, 3H), 2.00 (m, 1H), 2.29 (m, 4H), 3.37 (s, 3H), 3.49 (m, 2H), 3.79 (s, 3H), 4.40 (m, 1H), 4.43 (s, 2H), 4.57 (d, J = 6.8 Hz, 1H), 4.68 (d, J = 6.8 Hz, 1H), 5.17 (m, 1H), 5.32 (dd, *J* = 4.8, 15.7 Hz, 1H), 5.47 (td, *J* = 6.0, 15.7 Hz, 1H), 5.76 (td, *J* = 5.9, 15.9 Hz, 1H), 6.24 (d, *J* = 15.9 Hz, 1H), 6.67 (d, *J* = 8.2 Hz, 1H), 6.85 (t, *J* = 7.3 Hz, 3H), 7.11 (t, *J* = 8.0 Hz, 1H), 7.25 (t, *J* = 4.8 Hz, 2H); ^{13}C NMR (100 MHz, CDCl$_3$) δ 168.2, 159.1, 152.1, 137.5,132.3, 131.6, 130.7, 129.5, 129.4, 129.2, 125.8, 118.9, 117.1, 113.7, 94.9, 77.1, 75.9, 72.5, 69.9, 60.4, 56.1, 55.2, 30.6, 30.1, 27.4, 25.9, 25.8, 18.3, -4.1, -4.3; IR (neat, NaCl): 2915, 2865, 1735, 1620, 1600, 1565, 1525, 1460, 1245, 11450, 1083 cm^{-1}; $[\alpha]_D^{21}$ = +97.7 (c = 1.33, CHCl$_3$); HRMS (ESI$^+$): *m/z* calc'd for C$_{34}$H$_{48}$NaO$_7$Si$^+$, 619.3062; found 619.3065.
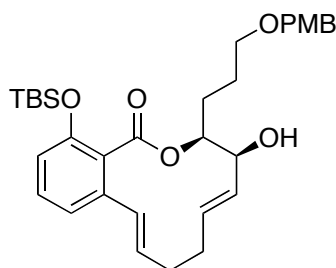
(3S,4S,5E,9E)-14-(*tert*-Butyldimethylsilyloxy)-4-hydroxy-3-(3-(4-

methoxybenzyloxy)propyl)-3,4,7,8-tetrahydro-1*H*-benzo[*c*][1]oxacyclododecin-1-

one (185). To a solution of macrocyclic diene **184** (200.0 mg, 0.3356 mmol)

dissolved in *i*-PrOH (5.7 mL) was added CBr$_4$ (398 mg, 1.20 mmol). The resulting

solution was heated to 75 °C for 4 h at which time the reaction mixture was cooled to

rt and concentrated *in vacuo*. Purification by column chromatography on silica gel

(15 % EtOAc in hexanes) provided 99.6 mg (0.180 mmol, 54%) of secondary alcohol

185 as a yellowish oil: ^{1}H NMR (400 MHz, CDCl$_3$) δ 0.18 (s, 3H), 0.22 (s, 3H), 0.95

(s, 9H), 1.86 (m, 2H), 1.97 (m, 2H), 2.23 (m, 2H), 2.34 (m, 2H), 3.50 (m, 2H), 3.80

(s, 3H), 4.30 (d, *J* = 5.1 Hz, 1H), 4.42 (s, 2H), 5.2 (t, *J* = 5.0 Hz, 1H), 5.50 (m, 2H),

5.76 (dd, *J* = 10.3, 17.2 Hz, 1H), 6.30 (d, *J* = 16.0 Hz, 1H), 6.87 (d, *J* = 4.6 Hz, 1H),

7.12 (m, 3H), 7.25 (t, *J* = 4.6 Hz, 1H), 7.26 (m, 2H); ^{13}C NMR (100 MHz, CDCl$_3$) δ

168.0, 159.0, 152.2, 137.2, 133.1, 132.7, 130.4, 130.0, 129.7, 129.4, 129.1, 125.5,

118.9, 117.2, 113.7, 77.5, 77.1, 76.8, 72.6, 71.9, 69.7, 55.3, 30.6, 29.9, 27.7, 25.9,

25.8, 18.4, -4.0, -4.2; ; IR (neat, NaCl): 3430 (br), 2935, 1733, 1460, 1350, 1250 cm^{-1};

HRMS (ESI[+]): *m/z* calc'd for C$_{32}$H$_{44}$NaO$_6$Si$^+$, 575.2799; found 575.2801.
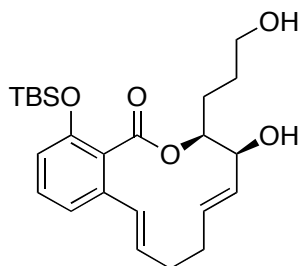
(3*S*,4*S*,5*E*,9*E*)-14-(*tert*-Butyldimethylsilyloxy)-4-hydroxy-3-(3-hydroxypropyl)-3,4,7,8-tetrahydro-1*H*-benzo[*c*][1]oxacyclododecin-1-one (186). To a solution of macrocyclic diene **184** (200.0 mg, 0.3356 mmol) dissolved in *i*-PrOH (5.7 mL) was added CBr$_4$ (398 mg, 1.20 mmol). The resulting solution was heated to 75 °C for 4 h at which time the reaction mixture was cooled to rt and concentrated *in vacuo*. Purification by column chromatography on silica gel (15 % EtOAc in hexanes) provided 64.9 mg (0.150 mmol, 45%) of diol **186** as a white solid: MP = 107-108 °C; ^{1}H NMR (400 MHz, CDCl$_3$) δ 0.19 (s, 3H), 0.20 (s, 3H), 0.94 (s, 9H), 1.43 (m, 1H), 1.46 (m, 1H), 1.80 (m, 2H), 2.22 (m, 2H), 2.36 (m, 2H), 3.58 (m, 2H), 4.15 (d, *J* = 7.9 Hz, 1H), 5.02 (t, *J* = 6.7 Hz, 1H), 5.4 (s, 2H), 5.7 (dq, *J* = 3.1, 16.0 Hz, 1H), 6.23 (d, *J* = 16.1 Hz, 1H), 6.68 (d, *J* = 8.2 Hz, 1H), 6.87 (d, *J* = 7.7 Hz, 1H), 7.16 (t, *J* = 8.0, 1H); ^{13}C NMR (100 MHz, CDCl$_3$) δ 168.0, 152.2, 136.9, 132.8, 132.4, 129.8, 129.7, 128.9, 125.5, 118.4, 117.3, 77.2, 71.7, 62.2, 30.1, 29.7, 28.7, 25.7, 25.7, 18.4, -4.0, -4.2; ; IR (neat, NaCl): 3450 (br), 3010, 2945, 2859, 1733, 1465, 1370, 1250, 1110 cm^{-1}; HRMS (ESI$^+$): *m/z* calc'd for C$_{24}$H$_{36}$NaO$_5$Si$^+$, 455.224; found 455.227.

4.2.2 Chapter 2
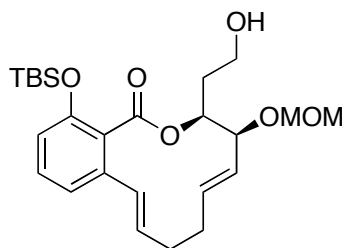
(3*S*,4*S*,5*E*,9*E*)-14-(*tert*-Butyldimethylsilyloxy)-3-(2-hydroxyethyl)-4-

(methoxymethoxy)-3,4,7,8-tetrahydro-1*H*-benzo[*c*][1]oxacyclododecin-1-one

(232). To a flask containing macrocyclic diene **183** (177.7 mg, 0.3049 mmol) was

added DCM (10.0 mL) and H_2O (1.0 mL). The mixture was cooled to 0 °C, and DDQ

(74.9 mg, 0.330 mmol) was added in one portion. The cooling bath was removed and

the reaction was stirred at rt for 1 h. The reaction mixture was diluted with sat.

$NaHCO_3$ 20 mL, and then extracted with DCM (2x20 mL). The organic layer was

washed with sat. $NaHCO_3$ (10 mL) and brine (10 mL). The crude mixture was dried

over Na_2SO_4, and concentrated *in vacuo*. Purification by column chromatography on

silica gel (30% EtOAc in hexanes) provided 70.9 mg (0.153 mmol, 50%) of alcohol

232 as a colorless oil: ^{1}H NMR (400 MHz, CDCl₃) δ 0.24 (s, 3H), 0.27 (s, 3H), 0.98

(s, 9H), 2.09 (m, 2H), 2.18 (m, 2H), 2.39 (m, 2H), 3.39 (s, 3H), 3.78 (m, 2H), 4.39 (s,

1H), 4.58 (d, *J* = 6.8 Hz, 1H), 4.69 (d, *J* = 6.8 Hz, 1H), 5.31 (d, *J* = 4.2 Hz, 1H), 5.34

(dd, *J* = 5.04, 15.8 Hz, 1H), 5.54 (td, *J* = 5.9, 15.8 Hz, 1H), 5.80 (td, *J* = 5.9, 15.9 Hz,

1H), 6.21 (d, *J* = 15.9 Hz, 1H), 6.70 (d, *J* = 8.2 Hz, 1H), 6.90 (d, *J* = 7.7 Hz, 1H), 7.14

(t, *J* = 8.0 Hz, 1H); ^{13}C NMR (100 MHz, CDCl₃) δ 169.4, 152.1, 137.5, 132.2,

131.4, 130.8, 130.1, 129.9, 125.2, 118.6, 117.2, 94.8, 77.2, 75.5, 58.8, 56.1, 34.0, 30.4, 29.8, 25.8, 18.5, -4.0, -4.1; IR (neat, NaCl): 3450 (br), 3005, 2930, 1731, 1460, 1380 cm^{-1}; $[\alpha]_D{}^{21}$ = +108 (c = 2.86, CHCl$_3$); HRMS (ESI$^+$): *m/z* calc'd for C$_{25}$H$_{38}$NaO$_6$Si$^+$, 485.2330; found 485.2335.
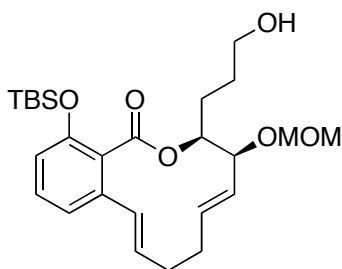
(3*S*,4*S*,5*E*,9*E*)-14-(*tert*-Butyldimethylsilyloxy)-3-(3-hydroxypropyl)-4-(methoxymethoxy)-3,4,7,8-tetrahydro-1*H*-benzo[*c*][1]oxacyclododecin-1-one (233). To a flask containing macrocyclic diene **184** (404.6 mg, 0.6779 mmol) was added DCM (15.0 mL) and H$_2$O (1.5 mL). The mixture was cooled to 0 °C, and DDQ (185.0 mg, 0.8149 mmol) was added in one portion. The cooling bath was removed and the reaction was stirred at rt for 1 h and 10 min. The reaction mixture was diluted with EtOAc 100 mL, and then washed with 10% NaHCO$_3$ solution (2x15 mL). The organic layer was washed with brine, dried over Na$_2$SO$_4$, and concentrated *in vacuo*. Purification by column chromatography on silica gel (30% EtOAc in hexanes) provided 204.5 mg (0.4290 mmol, 63%) of alcohol **233** as a colorless oil: ^{1}H NMR (400 MHz, CDCl$_3$) δ 0.22 (s, 3H), 0.22 (s, 3H), 0.96 (s, 9H), 1.71 (m, 3H), 1.87 (m, 2H), 2.00 (m, 1H), 2.22 (m, 2H), 2.34 (m, 2H), 3.39 (s, 3H), 3.69 (m, 2H), 4.42 (t, 1H), 4.58 (d, *J* = 6.8 Hz, 1H), 4.69 (d, *J* = 6.8 Hz, 1H), 5.16 (td, *J* = 3.47, 9.9 Hz,

1H), 5.33 (dd, J = 5.0, 15.7 Hz, 1H), 5.50 (td, J = 6.2, 15.1 Hz, 1H), 5.77 (td, J = 6.2,

15.9 Hz, 1H), 6.23 (d, J = 15.9 Hz, 1H), 6.67 (d, J = 8.1 Hz, 1H), 6.85 (d, J = 7.7 Hz,

1H), 7.12 (t, J = 8.0 Hz, 1H); ^{13}C NMR (100 MHz, CDCl$_3$) δ 168.4, 152.1, 137.6,

132.3, 131.8, 130.8, 129.7, 129.3, 125.6, 118.9, 117.1, 94.9, 77.2, 76.0, 62.7, 56.1,

30.6, 30.1, 28.7, 26.7, 25.7, 18.3, -4.1, -4.3; IR (neat, NaCl): 3455 (br), 3015, 2935,

1733, 1466, 1380, 1115 cm^{-1} [α]$_D$ ^{22} = +112 (c = 1.51, CHCl$_3$); HRMS (ESI$^+$): m/z

calc'd for C$_{26}$H$_{40}$NaO$_6$Si$^+$, 499.2486; found 499.2489.
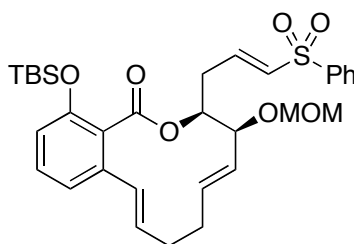
**(3S,4S,5E,9E)-14-(*tert*-Butyldimethylsilyloxy)-4-(methoxymethoxy)-3-((*E*)-3-
(phenylsulfonyl)allyl)-3,4,7,8-tetrahydro-1H-benzo[*c*][1]oxacyclododecin-1-one**
(234). To a flask containing alcohol **232** (50.0 mg, 0.108 mmol) was added DCM (0.5

mL), Et$_3$N (75.0 μL, 0.540 mmol) and DMSO (0.5 mL). The mixture was cooled to 0

°C, and SO$_3$•Py (52.0 mg, 0.324 mmol) was added in one portion. The mixture was

stirred at 0 °C for 20 min, diluted with Et$_2$O (4 mL) and phosphate buffer pH 7 (2

mL). The organic layer was separated, and then the aqueous layer was extracted with

Et$_2$O (3x4 mL). The combined organic layer was washed with sat. NH$_4$Cl (4 mL), and

then with sat. CuSO$_4$ (2x4 mL). The organic layer was concentrated *in vacuo* to

afford an opaque oil of the corresponding aldehyde. The crude aldehyde was used

directly in the next step without further purification.

To a solution of diethyl [(phenylsulfonyl)methyl]phosphonate (31.4 mg, 0.108 mmol) in anhydrous THF (1.0 mL) was added 60% NaH (5.0 mg, 0.12 mmol). The mixture was cooled to 0 °C, and was stirred for 5 min. The aldehyde in THF (1.0 mL) was added dropwise over 3 min. The mixture was stirred at 0 °C for 40 min, and then diluted with 10 % HCl (0.25 mL) and buffer pH 7 (2.0 mL). The crude mixture was extracted with EtOAc (2.0 mL). The organic layer was separated, and washed with sat. NaHCO$_3$ (1.0 mL). The organic layer was washed with brine (1.0 mL), dried over MgSO$_4$, and concentrated *in vacuo*. Purification by column chromatography on silica gel (20% EtOAc in hexanes) provided 31.0 mg (0.0518 mmol, 48%) of phenylsulfone **234** as an opaque oil: ^{1}H NMR (400 MHz, CDCl$_3$) δ 0.21 (s, 3H), 0.22 (s, 3H), 0.94 (s, 9H), 2.10 (m, 2H), 2.37 (m, 2H), 2.72 (m, 1H), 2.94 (m, 1H), 3.30 (s, 3H), 4.35 (q, J = 3.0 Hz, 1H), 4.49 (d, J = 6.7 Hz, 1H), 4.63 (d, J = 6.7 Hz, 1H), 5.08 (m, J = 2.9 Hz, 1H), 5.25 (dd, J = 6.1, 15.8 Hz, 2H), 5.52 (td, J = 6.2, 15.4 Hz, 1H), 5.75 (td, J = 6.2, 15.7 Hz, 1H), 6.12 (d, J = 15.9 Hz, 1H), 6.47 (td, J = 1.31, 15.2 Hz, 1H), 6.68 (t, J = 4.0 Hz, 1H), 6.87 (d, J = 7.7 Hz, 2H), 7.05 (td, J = 7.4, 14.9 Hz, 1H), 7.15 (t, J = 8.0 Hz, 1H), 7.56 (m, 3H), 7.88 (m, 2H); ^{13}C NMR (100 MHz, CDCl$_3$) δ 168.1, 152.0, 141.5, 140.4, 137.7, 133.4, 133.2, 132.4, 132.2, 131.0, 130.1, 129.6, 129.3, 127.7, 125.1, 118.8, 117.0, 94.6, 75.9, 75.5, 56.2, 32.3, 30.8, 30.1, 25.7, 18.2, -4.0, -4.5; IR (neat, NaCl): 2935, 1731, 1570, 1460, 1292, 1270, 1148, 1101 cm^{-1}; $[\alpha]_D^{21}$ = +100.3 (c = 1.20, CHCl$_3$); HRMS (ESI$^+$): *m/z* calc'd for C$_{32}$H$_{42}$NaO$_7$SSi$^+$, 621.2313; found 621.2317.
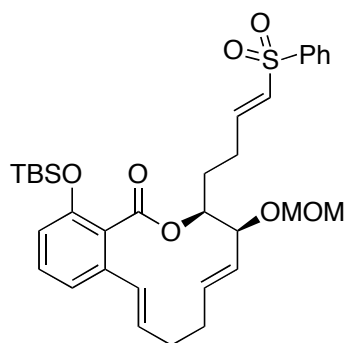
(3*S*,4*S*,5*E*,9*E*)-14-(*tert*-Butyldimethylsilyloxy)-4-(methoxymethoxy)-3-((*E*)-4-

(phenylsulfonyl)but-3-enyl)-3,4,7,8-tetrahydro-1*H*-benzo[*c*][1]oxacyclododecin-

1-one (235). To a flask containing alcohol **233** (70.3 mg, 0.147 mmol) was added

DCM (1.0 mL), Et_3N (0.15 mL, 1.07 mmol) and DMSO (1.0 mL). The mixture was

cooled to 0 °C, and SO_3•Py (73.0 mg, 0.459 mmol) was added in three portions over

3 min. The mixture was stirred at 0 °C for 30 min, and then diluted with Et_2O (2.5

mL) and phosphate buffer pH 7 (2.5 mL). The organic layer was separated, and then

the aqueous layer was extracted with Et_2O (5x1 mL). The combined organic layer

was washed with sat. NH_4Cl (5 mL), and then washed with water (2x5 mL) and sat.

$CuSO_4$ (2x5 mL). The organic layer was dried over $MgSO_4$ and concentrated *in vacuo*

to afford an opaque oil of the corresponding aldehyde. The crude aldehyde was used

directly in the next step without further purification.

To a solution of diethyl [(phenylsulfonyl)methyl]phosphonate (43.7 mg, 0.179

mmol) in anhydrous THF (2.0 mL) was added 60% NaH (6.8 mg, 0.17 mmol). The

mixture was cooled to 0 °C, and stirred for 10 min. The aldehyde in THF (1.0 mL)

was added dropwise over 3 min. The mixture was stirred at 0 °C for 40 min, and then

diluted with 10 % HCl (0.5 mL) and phosphate buffer pH 7 (4.0 mL). The crude

mixture was extracted with Et$_2$O (3x15 mL). The combined organic layer was washed with 10% NaHCO$_3$ (20.0 mL) and brine (10.0 mL), dried over MgSO$_4$, and concentrated *in vacuo*. Purification by column chromatography on silica gel (30% EtOAc in hexanes) provided 60.1 mg (0.0959 mmol, 65%) of phenylsulfone **235** as an opaque oil: ^{1}H NMR (400 MHz, CDCl$_3$) δ 0.18 (s, 3H), 0.19 (s, 3H), 0.89 (s, 9H), 1.98 (m, 2H), 2.19 (m, 2H), 2.38 (m, 4H), 3.34 (s, 3H), 4.37 (t, 1H), 4.55 (d, *J* = 6.8 Hz, 1H), 4.67 (d, *J* = 6.8 Hz, 1H), 5.09 (td, *J* = 3.4, 10.0 Hz, 1H), 5.27 (dd, *J* = 5.4, 15.6 Hz, 1H), 5.48 (td, *J* = 6.3, 15.2 Hz, 2H), 5.75 (td, *J* = 6.1, 15.9 Hz, 2H), 6.19 (d, *J* = 15.9 Hz, 1H), 6.36 (td, *J* = 1.5, 15.0 Hz, 1H), 6.67 (d, *J* = 7.7 Hz, 1H), 6.85 (d, *J* = 7.7 Hz, 1H), 7.02 (td, *J* = 6.4, 15.1 Hz, 1H), 7.13 (t, *J* = 8.0 Hz, 1H), 7.56 (m, *J* = 4.5 Hz, 3H), 7.88 (m, *J* = 2.1 Hz, 2H); ^{13}C NMR (100 MHz, CDCl$_3$) δ 168.2, 152.0, 145.8, 140.6, 137.6, 133.3, 132.5, 132.4, 130.9, 130.8, 129.8, 129.3, 128.8, 127.6, 125.3, 119.0, 117.2, 94.8, 76.2, 76.0, 56.2, 30.5, 30.1, 28.2, 27.7, 25.7, 18.3, -4.1, -4.3; IR (neat, NaCl): 2933, 1735, 1550, 1480, 1282, 1255, 1138, 1111 cm^{-1}; [α]$_D$^{22} = +90.3 (c = 2.43, CHCl$_3$); HRMS (ESI$^+$): *m/z* calc'd for C$_{33}$H$_{44}$NaO$_7$SSi$^+$, 635.2469; found 635.2471.
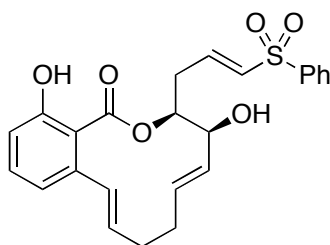
(3*S*,4*S*,5*E*,9*E*)-4,14-Dihydroxy-3-((*E*)-3-(phenylsulfonyl)allyl)-3,4,7,8-tetrahydro-1*H*-benzo[*c*][1]oxacyclododecin-1-one (223). To a flask containing phenylsulfone **234** (19.0 mg, 0.0318 mmol) was added 4M HCl in MeOH (1.0 mL). The mixture was stirred at rt for 120 h, and then concentrated *in vacuo*. Purification by column chromatography on silica gel (50% EtOAc in hexanes) provided 11.5 mg (0.0262 mmol, 82%) of the desired analogue **223** as a colorless oil: ^{1}H NMR (400 MHz, CDCl$_3$) δ 2.20 (m, 2H), 2.41 (m, 2H), 2.72 (m, 1H), 2.95 (m, 1H), 4.38 (brs, 1H), 5.27 (m, *J* = 2.4 Hz, 1H), 5.45 (dd, *J* = 5.8, 15.9 Hz, 1H), 5.62 (qd, *J* = 4.49, 15.8 Hz, 2H), 6.44 (q, *J* = 5.4 Hz, 1H), 6.52 (d, *J* = 15.8 Hz, 1H), 6.74 (d, *J* = 7.4 Hz, 1H), 6.85 (q, *J* = 3.1 Hz, 1H), 7.05 (ddd, *J* = 7.1, 8.0, 15.1 Hz, 1H), 7.30 (t, *J* = 7.9 Hz, 1H), 7.46 (m, 3H), 7.81 (q, *J* = 2.8 Hz, 2H), 10.41 (s, 1H); ^{13}C NMR (100 MHz, CDCl$_3$) δ 170.5, 161.5, 142.1, 141.7, 140.0, 135.0, 134.8, 134.3, 133.3, 133.1, 129.7, 129.2, 128.8, 127.5, 120.0, 116.3, 111.4, 75.0, 72.5, 32.4, 31.7, 29.8; IR (neat, NaCl): 3415(br), 3050, 2920, 2865, 1737, 1630, 1464, 1406, 1044 cm^{-1}; [α]$_D$ ^{21} = -35 (c = 0.58, CHCl$_3$); HRMS (ESI$^+$): *m/z* calc'd for C$_{24}$H$_{24}$NaO$_6$S$^+$, 463.1186; found 463.1193.
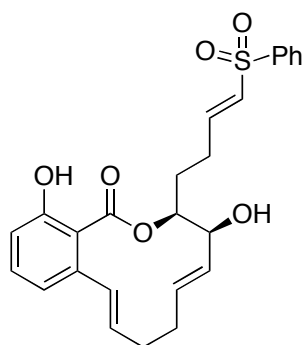
(3*S*,4*S*,5*E*,9*E*)-4,14-Dihydroxy-3-((*E*)-4-(phenylsulfonyl)but-3-enyl)-3,4,7,8-tetrahydro-1*H*-benzo[*c*][1]oxacyclododecin-1-one (234). To a flask containing phenylsulfone **235** (48.7 mg, 0.0777 mmol) was added 4M HCl in MeOH (5.0 mL). The mixture was stirred at rt for 99 h, and then concentrated *in vacuo*. Purification by column chromatography on silica gel (50% EtOAc in hexanes) provided 31.0 mg (0.0662 mmol, 85%) of the desired analogue **234** as a colorless oil: ^{1}H NMR (400 MHz, CDCl$_3$) δ 1.78 (brs, 1H), 1.91 (m, 1H), 2.20 (m, 3H), 2.40 (m, 4H), 4.33 (t, *J* = 4.8 Hz, 1H), 5.18 (m, *J* = 4.19 Hz, 1H), 5.47 (dd, *J* = 6.10, 15.6 Hz, 1H), 5.61 (m, 2H), 6.41 (d, *J* = 15.2 Hz, 1H), 6.61 (d, *J* = 15.7 Hz, 1H), 6.78 (d, *J* = 7.5 Hz, 4H), 6.86 (d, *J* = 8.3 Hz, 1H), 7.02 (td, *J* = 6.7, 14.7 Hz, 1H), 7.31 (t, *J* = 7.9 Hz, 1H), 7.57 (m, 3H), 7.88 (d, *J* = 7.9 Hz, 2H), 10.47 (s, 1H); ^{13}C NMR (100 MHz, CDCl$_3$) δ 169.7, 160.4, 144.5, 140.7, 139.4, 134.2, 133.8, 133.3, 132.3, 130.2, 128.7, 128.3, 128.0, 126.6, 119.0, 115.2, 110.6, 75.1, 71.6, 31.5, 28.7, 26.9, 26.2; IR (neat, NaCl): 3415(br), 3055, 2910, 2855, 1735, 1632, 1484, 1426, 1134 cm^{-1}; $[\alpha]_D^{21}$ = -14 (c = 0.98, CHCl$_3$); HRMS (ESI$^+$): *m/z* calc'd for C$_{25}$H$_{26}$NaO$_6$S$^+$, 477.1342; found 477.1348.
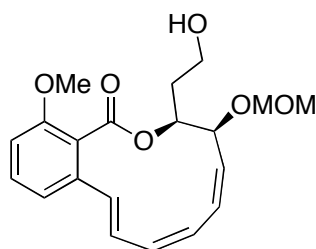
(3*S*,4*S*,5*Z*,7*Z*,9*E*)-3-(2-Hydroxyethyl)-14-methoxy-4-(methoxymethoxy)-3,4-dihydro-1*H*-benzo[*c*][1]oxacyclododecin-1-one (236). To a flask containing macrocyclic triene **110** (47.4 mg, 0.0792 mmol) was added anhydrous THF (1.0 mL), and TBAF 1 M in THF (87.0 μL, 0.0870 mmol) was added dropwise over 5 min at rt. The mixture was stirred at rt for 1.5 h, and then concentrated *in vacuo*. Purification by column chromatography on silica gel (40% EtOAc in hexanes) provided 26.6 mg (0.0694 mmol, 88%) of alcohol **235** as a colorless oil: ^{1}H NMR (400 MHz, CDCl$_3$) δ 2.18 (m, 2H), 3.37 (s, 3H), 3.84 (s, 3H), 3.90 (s, 2H), 4.53 (d, *J* = 6.4 Hz, 1H), 4.58 (d, *J* = 6.4 Hz, 1H), 4.66 (dd, *J* = 3.4, 10.8 Hz, 1H), 5.55 (ddd, *J* = 3.2, 3.2, 10.7 Hz, 1H), 5.71 (dd, *J* = 11.3, 11.3 Hz, 1H), 5.90 (dd, *J* = 3.9, 11.0 Hz, 1H), 6.21 (dd, *J* = 3.8, 11.9 Hz, 1H), 6.36 (dd, *J* = 11.3, 11.3 Hz, 1H), 6.68 (d, *J* = 15.9 Hz, 1H), 6.82 (t, *J* = 8.3 Hz, 1H), 6.99 (d, *J* = 15.9 Hz, 1H), 7.01 (d, *J* = 15.9 Hz, 1H), 7.27 (d, *J* = 5.0 Hz, 1H); ^{13}C NMR (100 MHz, CDCl$_3$) δ 168.2, 155.7, 138.5, 133.3, 132.6, 130.7, 129.9, 129.5, 127.8, 126.9, 123.3, 120.8, 109.4, 93.3, 77.3, 68.4, 61.2, 55.8, 55.5, 30.7; IR (neat, NaCl): 3432 (br), 3010, 2943,1729, 1599, 1571, 1468, 1438, 1154, 1089, 1058 cm^{-1}; [α]$_D$ [21] = -207 (c= 1.33, CHCl$_3$); HRMS (ESI[+]): *m/z* calc'd for C$_{20}$H$_{24}$NaO$_6$[+], 383.1465; found 383.1462.
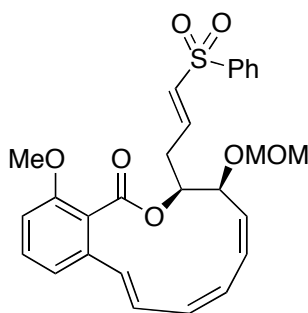
(3*S*,4*S*,5*Z*,7*Z*,9*E*)-14-Methoxy-4-(methoxymethyl)-3-((*E*)-3-

(phenylsulfonyl)allyl)-3,4-dihydro-1*H*-benzo[*c*][1]oxacyclododecin-1-one   (237).

To a flask containing alcohol **236** (25.0 mg, 0.0694 mmol) was added anhydrous

DCM (1.2 mL) and molecular sieve 4 Å (70 mg). The mixture was cooled to 0 °C,

and PDC (104.0 mg, 0.2764 mmol) was added in one portion. The cooling bath was

removed and the reaction was stirred at rt for 1.5 h The reaction mixture was diluted

with hexanes 3 mL, then filtered through a silica gel plug and rinsed with 40% EtOAc

in hexanes (20 mL). The combined organic layer was concentrated *in vacuo* to afford

an opaque oil of the corresponding aldehyde. The crude aldehyde was used directly in

the next step without further purification.

To a solution of diethyl [(phenylsulfonyl)methyl]phosphonate (22.0 mg, 0.0759

mmol) in anhydrous THF (1.0 mL) was added 60% NaH (3.4 mg, 0.086 mmol). The

mixture was cooled to 0 °C, and was stirred for 5 min. The aldehyde in THF (1.0 mL)

was added dropwise over 3 min. The mixture was stirred at 0 °C for 30 min, and then

diluted with sat. NH_4Cl (3.0 mL) and phosphate buffer pH 7 (4.0 mL). The crude

mixture was extracted with EtOAc (3x4 mL).   The combined organic layer was

washed with brine (5 mL), dried over Na_2SO_4, and concentrated *in vacuo*.

Purification by column chromatography on silica gel (30% EtOAc in hexanes) provided 17.8 mg (0.0358 mmol, 47%) of phenylsulfone **237** as an opaque oil: ^{1}H NMR (400 MHz, CDCl$_3$) δ 2.83 (m, J = 3.0 Hz, 2H), 3.33 (s, 3H), 3.95 (s, 3H), 4.49 (d, J = 6.52 Hz, 1H), 4.54 (d, J = 6.5 Hz, 1H), 4.66 (dd, J = 3.36, 10.8 Hz, 1H), 5.44 (ddd, J = 3.1, 3.1, 10.8 Hz, 1H), 5.59 (dd, J = 11.3, 11.3 Hz, 1H), 5.88 (dd, J = 3.7, 11.4 Hz, 1H), 6.2 (dd, J = 3.8, 11.8 Hz, 1H), 6.37 (dd, J = 11.3, 11.3 Hz, 1H), 6.52 (d, J = 15.2 Hz, 1H), 6.69 (d, J = 16.0 Hz, 1H), 6.83 (dd, J = 8.0, 13.8 Hz, 1H), 6.99 (dd, J = 11.7, 15.7 Hz, 1H), 7.16 (d, J = 5.5 Hz, 1H), 7.18 (d, J = 5.6 Hz, 1H), 7.21 (dd, J = 5.5, 7.8 Hz, 1H), 7.29 (t, J = 8.0 Hz, 1H), 7.57 (m, J = 7.5 Hz, 3H), 7.90 (t, J = 4.3 Hz, 2H); ^{13}C NMR (100 MHz, CDCl$_3$) δ 168.3, 156.4, 143.0, 140.6, 138.1, 133.3, 133.3, 132.8, 132.3, 131.1, 130.0, 129.9, 129.3, 127.6, 127.3, 126.0, 123.0, 120.4, 109.5, 93.3, 75.5, 68.3, 56.0, 55.6, 30.0; IR (neat, NaCl): 3012, 2945, 2842, 1732, 1635, 1572, 1469, 1318, 1305, 1105, 1087, 1059, 953, cm^{-1}; $[\alpha]_D^{20}$ = -178 (c= 0.89, CHCl$_3$); HRMS (ESI$^+$): *m/z* calc'd for C$_{27}$H$_{28}$NaO$_7$S$^+$, 519.1448; found 519.1454.
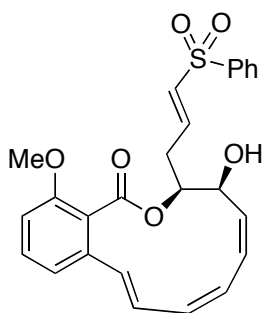
(3S,4S,5Z,7Z,9E)-4-Hydroxy-14-methoxy-3-((E)-3-(phenylsulfonyl)allyl)-3,4-dihydro-1H-benzo[c][1]oxacyclododecin-1-one (238). To a flask containing phenyl sulfone **237** (17.0 mg, 0.0359 mmol) was added *i*-PrOH (0.37 mL), and CBr₄ (48.0 mg, 0.144 mmol) in one portion. The mixture was heated at 75 °C for 2 h, and then concentrated *in vacuo*. Purification by column chromatography on silica gel (40% EtOAc in hexanes) provided 12.6 mg (0.0278 mmol, 78%) of alcohol **238** as a bright yellow oil: ¹H NMR (400 MHz, CDCl₃) δ 2.78 (m, *J* = 3.50 Hz, 1H), 2.93 (q, *J* = 7.84 Hz, 1H), 3.95 (s, 3H), 4.77 (dd, *J* = 3.2, 10.5 Hz, 1H), 5.40 (td, *J* = 2.6, 11.5 Hz, 2H), 5.76 (t, *J* = 11.22 Hz, 1H), 5.87 (dd, *J* = 3.8, 11.0 Hz, 1H), 6.10 (dd, *J* = 3.8, 11.9 Hz, 1H), 6.34 (t, *J* = 11.2 Hz, 1H), 6.52 (d, *J* = 15.2 Hz, 1H), 6.69 (d, *J* = 15.9 Hz, 1H), 6.83 (dd, *J* = 8.0, 15.0 Hz, 3H), 6.98 (dd, *J* = 11.6, 15.9 Hz, 1H), 7.18 (ddd, *J* = 5.4, 8.1, 15.1 Hz, 2H), 7.29 (t, *J* = 8.0 Hz, 1H), 7.57 (q, *J* = 10.3 Hz, 3H), 7.89 (t, *J* = 4. Hz, 2H); ¹³C NMR (100 MHz, CDCl₃) δ 168.5, 156.3, 143.1, 140.6, 138.0, 133.3, 132.8, 132.3, 131.6, 131.1, 130.1, 130.0, 129.3, 128.7, 127.6, 127.2, 122.9, 120.4, 109.6, 76.3, 65.5, 56.0, 29.3; IR (neat, NaCl): 3470, 3014, 2927, 1731, 1634, 1572, 1469, 1305, 1271, 1107, 1060, 961 cm⁻¹; [α]$_D^{20}$ = -180 (c= 0.63, CHCl₃); HRMS (ESI⁺): *m/z* calc'd for C₂₅H₂₄NaO₆S⁺, 475.1186; found 475.1181.
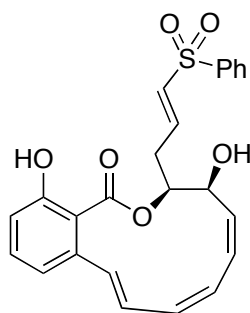
(3S,4S,5Z,7Z,9E)-4,14-Dihydroxy-3-((E)-3-(phenylsulfonyl)allyl)-3,4-dihydro-1H-benzo[c][1]oxacyclododecin-1-one (225). To a flask containing alcohol **238** (10.0 mg, 0.0221 mmol) was added anhydrous DCM (2.2 mL). The mixture was cooled to -78 °C, and BCl$_3$ 1M in DCM (0.22 mL, 0.22 mmol) was added dropwise over 1 min. The mixture was stirred at -78 °C for 10 min, and warmed to rt and stirred for 15 min. The reaction mixture was quenched with water (2 mL) and extracted with EtOAc (3x5 mL). The combined organic layer was washed with brine and dried over MgSO$_4$. The crude mixture was concentrated *in vacuo*. Purification by column chromatography on silica gel (50% EtOAc in hexanes) provided 7.2 mg (0.016 mmol, 75%) of the desired analogue **225** as a bright yellow oil: ^{1}H NMR (400 MHz, MeOD) δ 2.70 (m, 1H), 2.82 (q, 1H), 4.53 (dd, *J* = 3.32, 10.52 Hz, 1H), 5.18 (td, *J* = 2.75, 10.86 Hz, 1H), 5.69 (dd, *J* = 11.22, 11.22 Hz, 1H), 5.81 (dd, *J* = 3.94, 11.10 Hz, 1H), 5.98 (dd, *J* = 3.84, 11.92 Hz, 1H), 6.25 (dd, *J* = 11.24, 11.24 Hz, 1H), 6.56 (d, *J* = 15.97 Hz, 1H), 6.65 (m, 3H), 6.90 (dd, *J* = 11.44, 15.93 Hz, 1H), 7.08 (ddd, *J* = 7.17, 7.17, 15.15 Hz, 2H), 7.51 (m, 3H), 7.82 (m, 2H); ^{13}C NMR (100 MHz, MeOD) δ 170.8, 155.6, 145.2, 142.1, 139.4, 134.5, 133.9, 133.8, 131.6, 131.6, 131.1, 130.9, 130.5, 130.5, 130.4, 128.7, 123.1, 120.2, 115.1, 78.6, 66.3, 30.3; IR (neat,

NaCl): 3408(br), 3052, 3014, 2927, 2854, 1727, 1635, 1464, 1219, 1144, 1085, 1057 cm^{-1}; $[\alpha]_D{}^{20}$ = -133 (c= 0.36, CHCl$_3$); HRMS (ESI$^+$): *m/z* calc'd for C$_{24}$H$_{22}$NaO$_6$S$^+$, 461.1029; found 461.1037.
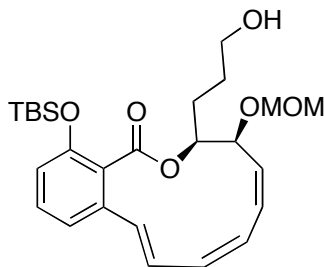
(3*S*,4*S*,5*Z*,7*Z*,9*E*)-14-(*tert*-Butyldimethylsilyloxy)-3-(3-hydroxypropyl)-4-(methoxymethyl)-3,4-dihydro-1*H*-benzo[*c*][1]oxacyclododecin-1-one (239). To a flask containing macrocyclic triene **144** (15.9 mg, 0.0274 mmol) was added DCM (1.0 mL) and H$_2$O (0.1 mL). The mixture was cooled to 0 °C, and DDQ (7.5 mg, 0.033 mmol) was added in one portion. The cooling bath was removed and the reaction was stirred at rt for 1 h. The reaction mixture was diluted with EtOAc (10 mL), and then washed with 10% NaHCO$_3$ solution (2x5 mL). The organic layer was washed with brine, dried over Na$_2$SO$_4$, and concentrated *in vacuo*. Purification by column chromatography on silica gel (30% EtOAc in hexanes) provided 12.7 mg (0.0267 mmol, 98%) of alcohol **239** as a colorless oil: ^{1}H NMR (400 MHz, CDCl$_3$) δ 0.20 (s, 3H), 0.21 (s, 3H), 0.97 (s, 9H), 1.66 (m, 2H), 1.91 (m, 2H), 3.36 (s, 3H), 3.72 (m, 2H), 4.53 (d, *J* = 6.44 Hz, 1H), 4.56 (d, *J* = 6.5 Hz, 1H), 4.61 (dd, *J* = 2.9, 10.7 Hz, 1H), 5.34 (td, *J* = 2.8, 10.3 Hz, 1H), 5.68 (dd, *J* = 11.3, 11.3 Hz, 1H), 5.87 (dd, *J* = 3.6, 11.1 Hz, 1H), 6.19 (dd, *J* = 4.1, 12.0 Hz, 1H), 6.35 (dd, *J* = 11.2, 11.2

Hz, 1H), 6.64 (d, $J = 16.0$ Hz, 1H), 6.75 (d, $J = 8.2$ Hz, 1H), 6.79 (d, $J = 7.6$ Hz, 1H), 7.01 (qd, $J = 3.9$, 16.0 Hz, 1H), 7.16 (t, $J = 8.0$ Hz, 1H); ^{13}C NMR (100 MHz, CDCl$_3$) δ 168.3, 152.3, 137.9, 132.2, 132.1, 131.1, 129.9, 129.2, 128.5, 127.2, 127.0, 121.3, 117.9, 93.2, 78.1, 69., 62.7, 55.5, 29.9, 25.8, 25.0, 18.4; IR (neat, NaCl): 3438.92(br), 2931, 2859, 1731, 1570, 1255, 1153, 1102, 1030 cm^{-1}; $[\alpha]_D^{22} = -88$ (c= 0.63, CHCl$_3$); HRMS (ESI$^+$): m/z calc'd for C$_{26}$H$_{38}$NaO$_6$Si$^+$, 497.2330; found 497.2337.
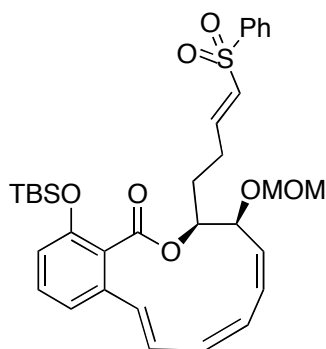
(3S,4S,5Z,7Z,9E)-14-(*tert*-Butyldimethylsilyloxy)-4-(methoxymethoxy)-3-((*E*)-4-(phenylsulfonyl)but-3-enyl)-3,4-dihydro-1*H*-benzo[*c*][1]oxacyclododecin-1-one (240). To a flask containing alcohol **239** (10.0 mg, 0.0210 mmol) was added anhydrous DCM (0.4 mL) and molecular sieve 4 Å (21 mg). The mixture was cooled to 0 °C, and PDC (32.0 mg, 0.0842 mmol) was added in one portion. The cooling bath was removed and the reaction was stirred at rt for 1.5 h. The reaction mixture was diluted with hexanes (1 mL), and then filtered through silica gel plug and rinsed with 40% EtOAc in hexanes (7 mL). The combined organic layer was concentrated *in vacuo* to afford an opaque oil of the corresponding aldehyde 6.0 mg. The crude

aldehyde was used directly in the next step without further purification.

To a solution of diethyl [(phenylsulfonyl)methyl]phosphonate (6.7 mg, 0.023 mmol) in anhydrous THF (0.3 mL) was added 60% NaH (1.0 mg, 0.026 mmol). The mixture was cooled to 0 °C, and was stirred for 5 min. The aldehyde in THF (1.0 mL) was added dropwise over 3 min. The mixture was stirred at 0 °C for 30 min, and then diluted with sat. NH_4Cl (4.0 mL) and phosphate buffer pH 7 (4.0 mL). The crude mixture was extracted with EtOAc (3x4 mL). The combined organic layer was washed with brine (5.0 mL), dried over Na_2SO_4, and concentrated *in vacuo*. Purification by column chromatography on silica gel (30% EtOAc in hexanes) provided 6.0 mg (0.0098 mmol, 47%) of phenylsulfone **240** as an opaque oil: ^{1}H NMR (400 MHz, CDCl$_3$) δ 0.17 (s, 3H), 0.19 (s, 3H), 0.93 (s, 9H), 1.97 (m, 1H), 2.11 (m, 1H), 2.37 (m, 1H), 2.63 (m, 1H), 3.30 (s, 3H), 4.47 (d, J = 6.5 Hz, 1H), 4.51 (d, J = 6.5 Hz, 1H), 4.59 (dd, J = 2.9, 10.7 Hz, 1H), 5.29 (td, J = 2.9, 10.4 Hz, 1H), 5.60 (dd, J = 11.3, 11.3 Hz, 1H), 5.87 (dd, J = 3.9, 11 Hz, 1H), 6.20 (dd, J = 4.0, 11.84 Hz, 1H), 6.33 (d, J = 11.3 Hz, 1H), 6.39 (d, J = 15.1 Hz, 1H), 6.64 (d, J = 16.0 Hz, 1H), 6.74 (d, J = 8.2 Hz, 2H), 6.79 (d, J = 7.6 Hz, 5H), 6.95 (dd, J = 11.5, 16.0 Hz, 1H), 7.05 (td, J = 6.4, 15.1 Hz, 1H), 7.17 (t, J = 8.0 Hz, 1H), 7.56 (m, 3H), 7.88 (d, J = 7.2 Hz, 2H); ^{13}C NMR (100 MHz, CDCl$_3$) δ 168.2, 152.2, 145.7, 140.6, 137.9, 133.3, 132.6, 132.2, 131.1, 130.9, 129.9, 129.4, 129.2, 127.6, 127.1, 126.4, 126.1, 121.3, 117.9, 93.1, 77.2, 68.7, 55.5, 28.5, 26.4, 25.8, 18.4, -4.0, -4.1; IR (neat, NaCl): 2930, 1731, 1570, 1463, 1292, 1252, 1148, 1101, 1027 cm^{-1}; $[\alpha]_D^{20}$ = -66 (c= 0.30, CHCl$_3$); HRMS (ESI$^+$): *m/z* calc'd for $C_{33}H_{42}NaO_7SSi^+$, 633.2313; found

633.2303.
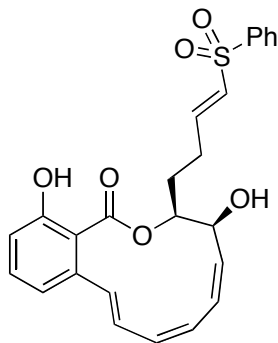
(3*S*,4*S*,5*Z*,7*Z*,9*E*)-4,14-Dihydroxy-3-((*E*)-4-(phenylsulfonyl)but-3-enyl)-3,4-dihydro-1*H*-benzo[*c*][1]oxacyclododecin-1-one (226). To a flask containing phenylsulfone **240** (6.0 mg, 0.0098 mmol) was added 4M HCl in MeOH (0.7 mL). The mixture was stirred at rt for 211 h, and then concentrated *in vacuo*. Purification by column chromatography on silica gel (60% EtOAc in hexanes) provided 3.0 mg (0.0066 mmol, 68%) of the desired analogue **226** as a colorless oil: ^{1}H NMR (400 MHz, MeOD) δ 1.87 (m, 1H), 2.03 (m, 1H), 2.38 (m, 1H), 2.48 (m, 1H), 4.48 (dd, *J* = 3.6, 10.5 Hz, 1H), 5.07 (td, *J* = 2.7, 11.8 Hz, 1H), 5.72 (dd, *J* = 11.3, 11.3 Hz, 1H), 5.81 (dd, *J* = 4.0, 11.0 Hz, 1H), 5.96 (dd, *J* = 4.0, 12.0 Hz, 1H), 6.23 (dd, *J* = 11.4, 11.4 Hz, 1H), 6.53 (d, *J* = 15.9 Hz, 1H), 6.61 (t, *J* = 7.1 Hz, 3H), 6.88 (dd, *J* = 11.5, 15.8 Hz, 1H), 6.95 (ddd, *J* = 6.1, 8.5, 14.8 Hz, 1H), 7.05 (t, *J* = 7.9 Hz, 1H), 7.51 (m, *J* = 5.0 Hz, 3H), 7.77 (m, *J* = 2.2 Hz, 2H); ^{13}C NMR (100 MHz, MeOD) δ 170.8, 155.3, 147.7, 142.1, 139.4, 134.5, 134.1, 132.9, 131.5, 131.2, 130.9, 130.8, 130.8, 130.5, 128.9, 128.5, 123.4, 120.3, 115.0, 78.6, 66.4, 28.6, 26.3; IR (neat, NaCl): 3440(br), 3060, 2950, 2854, 1730, 1640, 1457, 1115, 1070 cm^{-1}; $[\alpha]_D^{20}$ = -118 (c=

0.15, CHCl$_3$);   HRMS (ESI$^+$): *m/z* calc'd for C$_{25}$H$_{24}$NaO$_6$S$^+$, 475.1186; found 475.1186.
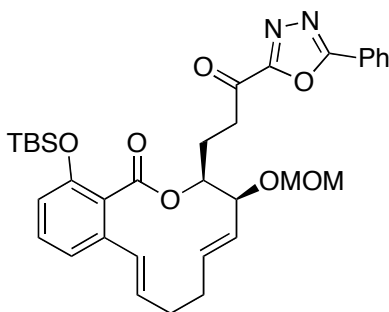
(3*S*,4*S*,5*E*,9*E*)-14-(*tert*-Butyldimethylsilyloxy)-4-(methoxymethoxy)-3-(3-oxo-3-

(5-phenyl-1,3,4-oxadiazol-2-yl)propyl)-3,4,7,8-tetrahydro-1*H*-

benzo[*c*][1]oxacyclo dodecin-1-one (244). To a flask containing alcohol **233** (70.3 mg, 0.147 mmol) was added DCM (1.0 mL), Et$_3$N (0.15 mL, 1.07 mmol) and DMSO (1.0 mL). The mixture was cooled to 0 °C, and SO$_3$.Py (73.0 mg, 0.459 mmol) was added in three portions over 3 min. The mixture was stirred at 0 °C for 30 min, and then was diluted with Et$_2$O (2.5 mL) and phosphate buffer pH 7 (2.5 mL). The organic layer was separated, and then the aqueous was extracted with Et$_2$O (5x1 mL). The combined organic layer was washed with sat. NH$_4$Cl (5 mL), and then washed with water (2x5 mL) and sat. CuSO$_4$ (2x5 mL). The organic layer was dried over MgSO$_4$ and concentrated *in vacuo* to afford an opaque oil of the desired aldehyde. The crude aldehyde was used directly in the next step without further purification.

In a different reaction flask, a solution of 2-phenyl-1,3,4-oxadiazole (43.8 mg, 0.30 mmol) was cooled with a dry ice bath and treated with a *n*-BuLi (1.6 M in

hexanes, 188 μL, 0.30 mmol). The mixture was stirred at this ambient temperature for

1 h before the addition of MgBr$_2$ diethyl etherate (77.5 mg, 0.30 mmol) as solid in

one portion. The mixture was stirred for an additional 1 h at this low temperature

before the freshly prepared aldehyde was added as a solution in THF (1 mL). The

mixture was stirred for an additional 1.5 h, and then quenched by the addition of 1M

HCl (5 mL). The organic layer was transferred to a separatory funnel and diethyl

ether was used to extract the desired crude material. The combined organic phase was

washed with 10% NaHCO$_3$, and brine and then dried over MgSO$_4$. The TLC and

crude NMR showed high conversion of the desired product. The combined organic

layer was concentrated *in vacuo,* and was used in the next step without further

purification.

The crude alcohol was dissolved in DCM and cooled to 0 °C. DMP was added

in one portion and the mixture was allowed to stir for 1 hour at 0 °C. The reaction

was quenched with phosphate buffer pH 7 (10 mL). The crude product was extracted

with diethyl acetate, washed with brine, dried over MgSO$_4$ and concentrated in vacuo.

Purification by column chromatography on silica gel (20% EtOAc in hexanes)

provided 27.6 mg (0.0446 mmol, 38% over three steps) of α-keto oxadiazole **244** as a

colorless foam. ^{1}H NMR (400 MHz, CDCl$_3$) δ 0.24 (s, 3H), 0.24 (s, 3H), 0.96 (s,

9H), 2.17 (m, 2H), 2.37 (m, 4H), 3.39 (m, 2H), 3.39 (s, 3H), 4.52 (t, *J* = 4.54 Hz, 1H),

4.58 (d, *J* = 6.76 Hz, 1H), 4.71 (d, *J* = 6.76 Hz, 1H), 5.23 (m, 1H), 5.35 (dd, *J* = 5.94,

15.67 Hz, 1H), 5.55 (td, *J* = 6.25, 15.67 Hz, 1H), 5.76 (td, *J* = 6.46, 15.85 Hz, 1H),

6.20 (d, *J* = 15.89 Hz, 1H), 6.68 (d, *J* = 8.20 Hz, 2H), 6.85 (d, *J* = 7.64 Hz, 1H), 7.12

(t, J = 7.96 Hz, 1H), 7.56 (m, 3H), 8.16 (m, 2H); ^{13}C NMR (100 MHz, CDCl$_3$) δ

186.5, 168.3, 166.3, 160.7, 152.0, 137.6, 132.8, 132.8, 132.3, 131.0, 129.8, 129.2,

129.2, 127.8, 125.4, 122.8, 118.8, 117.1, 94.7, 76.4, 76.2, 56.2, 36.1, 30.6, 30.2, 25.7,

24.3, 18.3, -4.1, -4.3;   [α]$_D$^{21} = +98.5 (c = 1.38, CHCl$_3$); HRMS (ESI$^+$): *m/z* calc'd

for C$_{34}$H$_{42}$N$_2$NaO$_7$Si$^+$, 641.2653; found 641.2659.
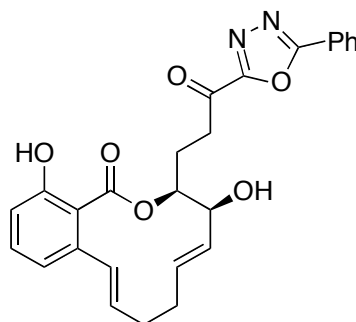
(3S,4S,5E,9E)-4,14-Dihydroxy-3-(3-oxo-3-(5-phenyl-1,3,4-oxadiazol-2-yl)propyl)-3,4,7,8-tetrahydro-1H-benzo[c][1]oxacyclododecin-1-one (227). To a flask

containing α-keto oxadiazole (20.0 mg, 0.0323 mmol) was added a solution of 4M

HCl in MeOH (5 mL). The mixture was stirred at rt for 46 h, and then washed with

diethyl ether and concentrated *in vacuo* to provide 9.97 mg (0.0216 mmol, 67%) of

desired analogue **227** as an oily white solid. HRMS (ESI$^+$): *m/z* calc'd for

C$_{26}$H$_{24}$N$_2$NaO$_6$$^+$, 483.1527; found 483.1534.

(*R*)-1-(2-((3*S*,4*S*,5*E*,9*E*)-4,14-Dihydroxy-1-oxo-3,4,7,8-tetrahydro-1*H*-benzo[*c*][1] oxacyclododecin-3-yl)acetamido)-3-methylbutylboronic Acid (228). Alcohol **232** (18.5 mg, 0.0400 mmol) was dissolved in a 1:1 mixture of MeCN/water (0.1 mL) and cooled to 0 °C, following the addition of BAIB (41 mg, 0.127 mmol) and TEMPO (1.98 mg, 0.0127 mmol). The mixture was allowed to warm to rt and stirred for 1 h, and then quenched by the addition of sat. $Na_2S_2O_3$ (1 mL), extracted with EtOAc (3 x 5 mL). The combined organic layer was dried over Na_2SO_4, and concentrated *in vacuo*. The crude product was used in the next step without further purification.

To a flask containing amine[179] **249** (10 mg, 0.040 mmol) in anhydrous DCM (0.12 mL) at 0 °C, diisopropylethylamine was added dropwise. Following the addition of the crude acid and TBTU (13.5mg, 0.0420 mmol) as solid, the mixture was stirred at 0 °C for 8 h before it was concentrated *in vacuo*. The crude was dissolved in EtOAc (2 mL) and washed with water (2 x1 mL), and brine (2 mL). The organic layer was dried over Na_2SO_4, and concentrated *in vacuo*. The crude was used in the next step by the addition of 4M HCl/MeOH (2 mL).

2-Methylpropaneboronic acid (13.4 mg, 0.131 mmol) and hexanes (0.5 mL) were added to the solution of the crude amide product. This mixture was stirred

vigorously for 90 h and the pentane layer was removed to provide 12.1 mg (0.0280 mmol, 70% over three steps) of desired analogue **228** as a colorless oil. HRMS (ESI$^+$): *m/z* calc'd for $C_{22}H_{30}BNNaO_7$, 454.2013; found 454.2019.

4.2.3 Biological Evaluation

Cytotoxicity Assay.[225]   The human cancer cell lines leukemia (HL-60), breast (MCF-7), melanoma (SK-MEL-28 and SK-MEL-5) were grown in normal RPMI 1640 culture medium containing 10% fetal bovine serum. The cells, in exponential-phase maintenance culture, were dissociated with 0.25% trypsin and harvested at 125×g for 5 min. Trypsin was removed and the cells were re-suspended in new culture medium. The cell density was adjusted to 1 x 105 and dispensed in triplicate on 96-well plates in 50 µL volumes. After incubation overnight at 37 °C under 5% CO_2, 50 µL of culture medium containing various concentrations of the test compounds was added. Paclitaxel and colchicine were used as positive controls. After 48 h incubation, the relative cell viability in each well was determined by using the AlamarBlue Assay Kit. The IC_{50} of each compound was determined by fitting the relative viability of the cells to the drug concentration using a dose-response model.

4.2.4 Chapter 3

2,3-Dihydroxyterephthalaldehyde (257).[219] To a solution of **256** (400 mg, 2 mmol) in anhydrous DCM (1 mL; at r.t.) was added dropwise a 1.0 M boron tribromide solution in anhydrous DCM (20 mL, 20 mmol). The reaction mixture was stirred for 1 h, followed by quenching of the reaction by addition of 1 M of aq. HCl (20 mL). The mixture was extracted with DCM (100 mL x 3). The combined organic extracts were washed with brine (50 mL x 2) and dried over Na_2SO_4 and the solvent was removed under reduced pressure. The resulting viscous liquid was purified by flash column chromatography (1% MeOH, 1% AcOH and DCM) on silica gel to obtain compound **257** (239 mg, 86%) as a yellowish powder. ^1H NMR (400 MHz, $CDCl_3$): δ 7.30 (s, 4H), 10.05 (s, 2H). ^{13}C NMR (100.6 MHz, $CDCl_3$): δ 122.28, 123.17, 150.86, 196.39; GC-MS (EI+) calc'd for $C_8H_6O_4$ *m/z* 166.1, found 166.1 (M)$^+$.

General Procedure for the Synthesis of 258a-258h.[220] To a solution of **2** (10 mg, 0.06 mmol) in anhydrous dimethylformamide (4 mL) were added the respective alkyl halides (25 equiv) [C_2H_5I, C_3H_7I, C_3H_5I, C_4H_9Cl, $C_5H_{11}I$, $C_6H_{13}Cl$, $C_8H_{17}Cl$, and $C_{14}H_{29}Cl$] and K_2CO_3 (67 mg, 0.48 mmol). The reaction mixture was stirred for 15 h at r.t. The reaction was quenched with water (5 mL), and the resulting solution was extracted with DCM, and the combined organic extracts were washed with brine and dried over Na_2SO_4. The resulting viscous liquids were purified by flash column chromatography (CH_2Cl_2/hexane=6:4) to obtain the terephthalaldehyde analogues

258a-258h (**258a**, R=C$_2$H$_5$; **258b**, R=C$_3$H$_7$; **258c**, R= allyl; **258d**, R=C$_4$H$_9$; **258e**,

R=C$_5$H$_{11}$; **258f**, R=C$_6$H$_{13}$; **258g**, R=C$_8$H$_{17}$; **258h**, R=C$_{14}$H$_{29}$) as oils.

2,3-Diethoxyterephthalaldehyde (258a). viscous oil; yield 49%; ^{1}H NMR (400 MHz, CDCl$_3$): δ 1.46 (t, 6H), 4.26 (q, 4H), 7.65 (s, 2H), 10.48 (s, 2H). ^{13}C NMR (100.6 MHz, CDCl$_3$): δ 15.89, 71.52, 122.99, 135.04, 156.36, 190.04; MS (FAB) calc'd for C$_{12}$H$_{14}$O$_4$ *m/z* 222.1, found 223.3 (MH)+.

2,3-Di-n-propoxyterephthalaldehyde (258b). viscous oil; yield 37%; ^{1}H NMR (500 MHz, CDCl$_3$): δ 1.09 (t, 6H), 1.84 (m, 4H), 4.09 (t, 4H), 7.63 (s, 2H), 10.46 (s, 2H). 13C NMR (125.8 MHz, CDCl$_3$): δ 10.46, 23.32, 77.21, 122.56, 134.52, 156.25, 189.61; MS (FAB) calc'd for C$_{14}$H$_{18}$O$_4$ *m/z* 250.1, found 250.1 (MH)+.

2,3-Diallyloxyterephthalaldehyde (258c). viscous oil; yield 43%; ^{1}H NMR (400 MHz, CDCl$_3$): δ 4.74 (d, *J* = 6.1 Hz, 4H), 5.34 (dd, *J* = 1.0, 10.2 Hz, 2H), 5.41 (dd, *J* = 1.3, 17.1 Hz, 2H), 5.34 (ddt, *J* = 6.1, 10.2, 16.5 Hz, 2H), 7.67 (s, 2H), 10.69 (s, 2H). ^{13}C NMR (100.6 MHz, CDCl$_3$): δ 76.13, 120.40, 123.27, 132.63, 135.05, 155.74, 189.92.

2,3-Di-n-butoxyterephthalaldehyde (258d). viscous oil; yield 63%; ^{1}H NMR (400 MHz, CDCl$_3$): δ 1.01 (t, 6H), 1.55 (m, 4H), 1.83 (m, 4H), 4.20 (t, 4H), 7.64 (s, 2H), 10.53 (s, 2H). ^{13}C NMR (100.6 MHz, CDCl$_3$): δ 14.29, 19.60, 32.48, 75.89, 122.95,

134.92, 156.68, 190.03; GC-MS (EI+) calc'd for $C_{16}H_{22}O_4$ m/z 278.3, found 278.3 (M)+.

2,3-Di-n-pentoxyterephthalaldehyde (258e). viscous oil; yield 58%; ^{1}H NMR (400 MHz, CDCl$_3$): δ 0.96 (t, 6H), 1.46 (m, 8H), 1.84 (m, 4H), 4.20 (t, 4H), 7.60 (s, 2H), 10.48 (s, 2H). ^{13}C NMR (100.6 MHz, CDCl$_3$): δ 14.41, 22.89, 28.50, 30.14, 76.20, 122.95, 134.91, 156.70, 190.06; MS (FAB) calc'd for $C_{18}H_{26}O_4$ m/z 306.2, found 307.2 (MH)$^+$.

2,3-Di-n-hexoxyterephthalaldehyde (258f). viscous oil; yield 65%; ^{1}H NMR (400 MHz, CDCl$_3$): δ 0.94 (t, 6H), 1.37 (m, 12H), 1.84 (m, 4H), 4.20 (t, 4H), 7.71 (s, 2H), 10.47 (s, 2H). ^{13}C NMR (100.6 MHz, CDCl$_3$):δ 14.42, 22.99, 26.04, 30.42, 31.99, 76.22, 122.94, 134.91, 156.70, 190.03; MS (ESI+) calc'd for $C_{20}H_{30}O_4$ m/z 334.2, found 335.2 (MH)$^+$.

2,3-Di-n-octoxyterephthalaldehyde (258g). viscous oil; yield 57%; ^{1}H NMR (400 MHz, CDCl$_3$): δ 0.91 (t, 6H), 1.35 (m, 20H), 1.84 (m, 4H), 4.20 (t, 4H), 7.61 (s, 2H), 10.47 (s, 2H). ^{13}C NMR (100.6 MHz, CDCl3): δ 14.49, 23.05, 26.38, 29.63, 29.79, 30.46, 32.19, 76.23, 122.95, 134.92, 156.69, 190.03; MS (ESI+) calc'd for $C_{24}H_{38}O_4$ m/z 390.3, found 391.3 (MH)+.

2,3-Di-n-tetradecyloxyterephthalaldehyde (258h). viscous oil; yield 56%; ^{1}H NMR (400 MHz, CDCl$_3$): δ 0.91 (t, 6H), 1.28 (m, 44H), 1.84 (m, 4H), 4.19 (t, 4H), 7.64 (s, 2H), 10.50 (s, 2H). ^{13}C NMR (100.6 MHz, CDCl$_3$): δ 14.55, 23.11, 26.39, 29.79, 29.85, 29.99, 30.02, 30.08, 30.10, 30.11, 30.12, 30.47, 32.34, 76.23, 122.94, 134.91, 156.71, 190.04; MS (ESI+) calc'd for $C_{36}H_{62}O_4$ m/z 558.5, found 559.5 (MH)+.

General Procedure for the Synthesis of 262a-262k.[221] To a hot solution of aminoguanidine hydrochloride (13.7 mg, 0.12 mmol) in EtOH (1 mL) was added a solution of the respective terephthalaldehyde (**259**, **260, 261,** and **258a-258h**) (0.5 equiv, in 0.5 mL EtOH) and conc. HCl (0.1 mL). The reaction mixture was heated up to 80 °C for 1 h, and then cooled to 0 °C. The resultant white solid HCl salts were filtered and washed with cold ether (2 mL) to give *bis*-guanylhydrazone analogues **262a-262k**. All ^{1}H and ^{13}C spectra, and mass spectral data were consonant with their corresponding structures.

262a

Terephthaldehyde-1,4-*bis*-guanylhydrazone Dihydro Dichloride (262a). yield 66%; ^{1}H NMR (500 MHz, DMSO-d_6): δ 8.10 (s, 4H), 8.21 (s, 2H). ^{13}C NMR (125.8 MHz, DMSO-d_6):δ 128.20, 135.54, 146.55, 155.69; MS (ESI+) calc'd for $C_{10}H_{14}N_8$ *m/z* 246.1, found 247.1 (MH)+.

262b

2,3-Dihydroxyterephthaldehyde-1,4-*bis*-guanylhydrazone Dihydro Dichloride (262b). yield 54%; ^{1}H NMR (500 MHz, DMSO-d_6): δ 7.49 (s, 2H), 8.45 (s, 2H). ^{13}C

176

NMR (125.8 MHz, DMSO-d$_6$): δ 117.62, 122.40, 144.07, 145.86, 155.12; MS (ESI+)

calc'd for C$_{10}$H$_{14}$N$_8$O$_2$ *m/z* 278.1, found 279.1 (MH)+.

262c

2,3-Dimethoxyterephthaldehyde-1,4-*bis*-guanylhydrazone   Dihydro   Dichloride

(262c). yield 44%; ^{1}H NMR (400 MHz, DMSO-d6): δ 3.86 (s, 6H), 7.93 (s, 2H), 8.42

(s, 2H). ^{13}C NMR (125.8 MHz, DMSO-d6): δ 61.71, 117.62, 121.30, 129.24, 141.44,

152.05, 152.24; MS (ESI+) calc'd for C$_{12}$H$_{18}$N$_8$O$_2$ *m/z* 306.2, found 307.2 (MH)+.

262d

2,3-Diethoxyterephthaldehyde-1,4-*bis*-guanylhydrazone   Dihydro   Dichloride

(262d). yield 67%; ^{1}H NMR (500 MHz, DMSO-d$_6$): δ 1.38 (t, 6H), 4.07 (q, 4H), 7.95

(s, 2H), 8.44 (s, 2H). ^{13}C NMR (125.8 MHz, DMSO-d$_6$): δ 15.28, 69.77, 121.05,

129.53, 141.70, 151.07, 155.12; MS (ESI+) calc'd for C$_{14}$H$_{22}$N$_8$O$_2$ *m/z* 334.2, found

335.2 (MH)+.

262e

2,3-Dipropoxyterephthaldehyde-1,4-*bis*-guanylhydrazone Dihydro Dichloride (262e). yield 64%; ^{1}H NMR (500 MHz, DMSO-d$_6$): δ 1.01 (t, 6H), 1.75 (m, 4H), 3.95 (t, 4H), 7.95 (s, 2H), 8.41 (s, 2H). ^{13}C NMR (125.8 MHz, DMSO-d$_6$): δ 10.42, 22.84, 75.82, 121.21, 129.50, 141.67, 151.34, 155.19; MS (ESI+) calc'd for C$_{16}$H$_{26}$N$_8$O$_2$ *m/z* 362.2, found 363.2 (MH)+.

262f

2,3-Diallyloxyterephthaldehyde-1,4-*bis*-guanylhydrazone Dihydro Dichloride (262f). yield 70%; ^{1}H NMR (500 MHz, DMSO-d$_6$): δ 4.56 (d, *J* = 6.0 Hz, 4H), 5.28 (d, *J* = 10.4 2H), 5.40 (dd, *J* = 1.3, 16.1 Hz, 2H), 6.80 (ddt, *J*= 6.0, 10.7, 16.1 Hz, 2H), 7.97 (s, 2H), 8.42 (s, 2H). ^{13}C NMR (125.8 MHz, DMSO-d$_6$): δ 74.53, 118.71, 121.28, 129.55, 133.30, 141.54, 150.61, 155.15; MS (FAB) calc'd for C$_{16}$H$_{22}$N$_8$O$_2$ *m/z* 358.2, found 359.3 (MH)+.

262g

2,3-Dibutoxyterephthaldehyde-1,4-*bis*-guanylhydrazone   Dihydro   Dichloride

(262g). yield 78%; ^{1}H NMR (500 MHz, DMSO-d$_6$): δ 0.90 (t, 6H), 1.47 (m, 4H), 1.74

(m, 4H), 4.00 (t, 4H), 8.11 (s, 2H), 8.41 (s, 2H). ^{13}C NMR (125.8 MHz, DMSO-d$_6$): δ

13.79, 18.71, 31.60, 74.06, 121.21, 129.51, 141.58, 151.34, 155.31; MS (ESI+) calc'd

for C$_{18}$H$_{30}$N$_8$O$_2$ *m/z* 390.2, found 391.2 (MH)+.

262h

2,3-Dipentoxyterephthaldehyde-1,4-*bis*-guanylhydrazone   Dihydro   Dichloride

(262h). yield 65%; ^{1}H NMR (500 MHz, DMSO-d$_6$): δ 0.90 (t, 6H), 1.39 (m, 8H),

1.76 (m, 4H), 3.96 (t, 4H), 7.94 (s, 2H), 8.40 (s, 2H). ^{13}C NMR (125.8 MHz, DMSO-

d$_6$):δ 14.27, 22.37, 27.97, 29.59, 74.83, 121.66, 129.92, 142.08, 151.81, 155.59; MS

(ESI+) calc'd for C$_{20}$H$_{34}$N$_8$O$_2$ *m/z* 418.3, found 419.3 (MH)+.

262i

2,3-Dihexoxyterephthaldehyde-1,4-*bis*-guanylhydrazone   Dihydro   Dichloride (262i). yield 66%; ^{1}H NMR (500 MHz, DMSO-d$_6$): δ 0.89 (t, 6H), 1.32 (m, 12H), 1.74 (m, 4H), 3.97 (t, 4H), 7.94 (s, 2H), 8.42 (s, 2H). 1^{13}C NMR (125.8 MHz, DMSO-d$_6$): δ 14.29, 22.42, 25.47, 29.89, 31.50, 76.22, 121.66, 129.91, 142.09, 151.81, 155.60; MS (ESI+) calc'd for C$_{22}$H$_{38}$N$_8$O$_2$ *m/z* 446.3, found 447.3 (MH)+.

262j

2,3-Dioctoxyterephthaldehyde-1,4-*bis*-guanylhydrazone   Dihydro   Dichloride (262j). yield 90%; ^{1}H NMR (500 MHz, DMSO-d$_6$): δ 0.86 (t, 6H), 1.30 (m, 20H), 1.72 (m, 4H), 3.94 (t, 4H), 7.94 (s, 2H), 8.42 (s, 2H). ^{13}C NMR (125.8 MHz, DMSO-d$_6$): δ 13.84, 22.00, 25.37, 28.57, 29.71, 29.44, 31.17, 74.39, 121.17, 129.43, 141.49, 151.33, 155.24; MS (ESI+) calc'd for C$_{26}$H$_{46}$N$_8$O$_2$ *m/z* 502.4, found 503.4 (MH)+.

262k

2,3-Ditetradecyloxyterephthaldehyde-1,4-*bis*-guanylhydrazone **Dihydro**

Dichloride (262k). yield 59%; ^{1}H NMR (500 MHz, DMSO-d$_6$): δ 0.85 (t, 6H), 1.30

(m, 44H), 1.76 (m, 4H), 3.94 (t, 4H), 7.95 (s, 2H), 8.40 (s, 2H). ^{13}C NMR (125.8

MHz, DMSO-d$_6$): δ 13.83, 22.00, 25.38, 28.63, 28.83, 28.91, 28.94, 29.46, 31.21,

74.45, 121.21, 129.43, 141.54, 151.39, 155.14; MS (ESI+) calc'd for C$_{38}$H$_{70}$N$_8$O$_2$ *m/z*

670.6, found 671.6 (MH)+.

4.2.5 Crystal structure data for 185

Data collection

REFERENCE NUMBER: 09113bs

CRYSTAL STRUCTURE REPORT for **185**

$C_{24} H_{36} O_5 Si$

185

Report prepared for:

K. Khownium / Prof. G. Georg

September 18, 2009

Victor G. Young, Jr.

X-Ray Crystallographic Laboratory

Department of Chemistry

University of Minnesota

207 Pleasant St. S.E.

Minneapolis, MN 55455

A crystal (approximate dimensions 0.45x 0.45 x 0.25mm^3) was placed onto the tip of a 0.1 mm diameter glass capillary and mounted on a CCD area detector diffractometer for a data collection at 123(2) K.[1] A preliminary set of cell constants was calculated from reflections harvested from three sets of 20 frames. These initial sets of frames were oriented such that orthogonal wedges of reciprocal space were surveyed. This produced initial orientation matrices determined from 84 reflections. The data collection was carried out using MoKα radiation (graphite monochromator) with a frame time of 60 seconds and a detector distance of 4.8 cm. A randomly oriented region of reciprocal space was surveyed to the extent of one sphere and to a resolution of 0.82 Å. Four major sections of frames were collected with 0.30º steps in ω at four different ϕ settings and a detector position of -28º in 2θ. The intensity data were corrected for absorption and decay (SADABS).[2] Final cell constants were calculated from 2990 strong reflections from the actual data collection after integration (SAINT).[3] Please refer to Table 1 for additional crystal and refinement information.

Structure solution and refinement

The structure was solved using Bruker SHELXTL[4] and refined using Bruker SHELXTL.[4] The space group I4 was determined based on systematic absences and

intensity statistics. A direct-methods solution was calculated which provided most non-hydrogen atoms from the E-map. Full-matrix least squares / difference Fourier cycles were performed which located the remaining non-hydrogen atoms. All non-hydrogen atoms were refined with anisotropic displacement parameters. All hydrogen atoms were placed in ideal positions and refined as riding atoms with relative isotropic displacement parameters. The final full matrix least squares refinement converged to $R1 = 0.1047$ and $wR2 = 0.2871$ (F^2, all data).

<div align="center">Structure description</div>

The structure is the one suggested. **This result is provided to determine the correct connectivity and relative stereochemistry only. This result is not considered publishable due to a number of factors.** The thermal ellipsoid drawing shows atoms C8 – C13 with oblate ellipsoids. This appears to be due to disordered solvent within pockets centered on the 4-fold axis. The crystal diffracted very poorly given the specimen size. Platon/Squeeze[5] was used to quantify the disordered solvent and provide a correction for the effects of diffuse scattering. 408.6Å^3, or 7.9% of the total volume was occupied by disordered solvent. 87 electrons were attributed to disordered solvent.

If a high-resolution crystal structure determination is needed for publication, then please consider recrystallization from other solvents besides DEE and hexane.

Interrupting the hydrogen bonding pattern would present an opportunity to make a new crystal form with alcohols, perhaps. Another alternative would to form a derivative with the two –OH groups. This result is certainly acceptable to the point of the determination of connectivity and relative stereochemistry, however the quality is not acceptable for the determination of absolute configuration. This was selected based on use of reference materials.

———————

[1] SMART V5.054, Bruker Analytical X-ray Systems, Madison, WI (2001).

[2] An empirical correction for absorption anisotropy, R. Blessing, *Acta Cryst.* **A51**, 33-38(1995).

[3] SAINT+ V6.45, Bruker Analytical X-Ray Systems, Madison, WI (2003).

[4] SHELXTL V6.14, Bruker Analytical X-Ray Systems, Madison, WI (2000).

[7] A. L. Spek, *Acta. Cryst.* **A46**, C34 (1990). PLATON, A Multipurpose Crystallographic Tool, Utrecht University, Utrecht, The Netherlands, A. L.Spek (2000).

Some equations of interest:

$$R_{int} = \Sigma|F_o^2 - <F_o^2>| \: / \: \Sigma|F_o^2|$$

$$R_1 = \Sigma||F_o| - |F_c|| \: / \: \Sigma|F_o|$$

$$wR2 = [\Sigma[w(F_o{}^2 - F_c{}^2)^2] / \Sigma[w(F_o{}^2)^2]]^{1/2}$$

where $w = q / [\sigma^2(F_o{}^2) + (a*P)^2 + b*P + d + e*\sin(\theta)]$

$$\text{GooF} = S = [\Sigma[w(F_o{}^2 - F_c{}^2)^2] / (n-p)]^{1/2}$$

Table 1. Crystal data and structure refinement for 09113bs.

_____

Identification code	09113bs
Empirical formula	$C_{24} H_{36} O5 Si$
Formula weight	432.62
Temperature	123(2) K
Wavelength	0.71073 Å
Crystal system	Tetragonal
Space group	I4
Unit cell dimensions	$a = 19.080(6)$ Å $\quad\quad \alpha = 90°$
	$b = 19.080(6)$ Å $\quad\quad \beta = 90°$
	$c = 14.100(9)$ Å $\quad\quad \gamma = 90°$
Volume	5133(4) Å^3
Z	8
Density (calculated)	1.120 Mg/m^3
Absorption coefficient	0.120 mm^{-1}
F(000)	1872
Crystal color, morphology	Colorless, Plate
Crystal size	0.45 x 0.45 x 0.25 mm^3
Theta range for data collection	1.51 to 26.61°
Index ranges	$-16 \leq h \leq 23, -14 \leq k \leq 23, -17 \leq l \leq 14$
Reflections collected	11480
Independent reflections	4732 [R(int) = 0.1673]
Observed reflections	2272
Completeness to theta = 26.61°	99.3%
Absorption correction	Multi-scan
Max. and min. transmission	0.97 and 0.947
Refinement method	Full-matrix least-squares on F^2

Data / restraints / parameters	4732 / 1 / 278
Goodness-of-fit on F^2	0.970
Final R indices [I>2sigma(I)]	$R1 = 0.1047$, $wR2 = 0.2609$
R indices (all data)	$R1 = 0.1674$, $wR2 = 0.2871$
Absolute structure parameter	-0.4(4)
Largest diff. peak and hole	0.473 and -0.318 e.Å^{-3}

Table 2. Atomic coordinates (x 10^4) and equivalent isotropic displacement parameters ($Å^2$x 10^3) for 09113bs. U_{eq} is defined as one third of the trace of the orthogonalized U_{ij} tensor.

	x	y	z	U_{eq}
O1	2933(2)	4969(2)	4943(4)	69(1)
C1	2255(3)	5121(4)	4919(5)	54(2)
O2	1805(3)	4691(3)	5047(6)	102(2)
C2	2121(3)	5867(4)	4789(6)	62(2)
C3	2028(3)	6121(3)	3866(7)	64(2)
C4	1903(4)	6818(4)	3748(9)	88(3)
C5	1873(6)	7270(6)	4480(20)	168(9)
C6	1980(6)	7016(8)	5448(14)	138(7)
C7	2107(4)	6332(6)	5601(9)	95(4)
C8	2233(4)	6051(8)	6496(10)	116(4)
C9	2537(5)	6352(9)	7245(10)	159(7)
C10	2706(8)	5961(16)	8145(9)	236(14)
C11	2752(14)	5175(18)	8077(17)	258(16)
C12	3236(7)	4862(10)	7392(10)	149(6)
C13	3077(9)	4405(9)	6753(13)	166(8)
C14	3527(5)	4174(5)	5984(8)	90(3)
C15	3152(4)	4245(4)	5070(7)	78(3)
O3	2076(2)	5659(2)	3149(4)	58(1)
Si1	1454(1)	5326(1)	2448(2)	65(1)
C16	1325(4)	4408(4)	2778(9)	97(4)
C17	628(3)	5843(4)	2625(11)	116(4)
C18	1792(4)	5425(4)	1222(6)	72(2)
C19	2462(5)	4985(5)	1076(9)	107(3)

C20	1238(5)	5133(6)	492(7)	103(3)
C21	1949(5)	6153(6)	941(8)	97(3)
O4	4181(3)	4491(3)	6043(6)	98(2)
C22	3637(4)	4060(4)	4317(7)	75(2)
C23	3279(4)	4021(4)	3334(8)	92(3)
C24	3755(4)	3818(4)	2559(9)	99(3)
O5	4255(3)	4353(4)	2307(7)	119(3)

_____

Table 3. Bond lengths [Å] and angles [°] for 09113bs.

_____

O(1)-C(1)	1.327(7)	C(12)-H(12A)	0.9500
O(1)-C(15)	1.454(9)	C(13)-C(14)	1.45(2)
C(1)-O(2)	1.201(7)	C(13)-H(13A)	0.9500
C(1)-C(2)	1.457(10)	C(14)-O(4)	1.389(10)
C(2)-C(3)	1.400(12)	C(14)-C(15)	1.480(14)
C(2)-C(7)	1.449(12)	C(14)-H(14A)	1.0000
C(3)-O(3)	1.345(9)	C(15)-C(22)	1.452(13)
C(3)-C(4)	1.360(10)	C(15)-H(15A)	1.0000
C(4)-C(5)	1.34(2)	O(3)-Si(1)	1.670(5)
C(4)-H(4A)	0.9500	Si(1)-C(16)	1.828(8)
C(5)-C(6)	1.47(2)	Si(1)-C(18)	1.855(10)
C(5)-H(5A)	0.9500	Si(1)-C(17)	1.876(7)
C(6)-C(7)	1.345(18)	C(16)-H(16A)	0.9800
C(6)-H(6A)	0.9500	C(16)-H(16B)	0.9800
C(7)-C(8)	1.392(16)	C(16)-H(16C)	0.9800
C(8)-C(9)	1.334(15)	C(17)-H(17A)	0.9800
C(8)-H(8A)	0.9500	C(17)-H(17B)	0.9800
C(9)-C(10)	1.51(3)	C(17)-H(17C)	0.9800
C(9)-H(9A)	0.9500	C(18)-C(21)	1.475(12)
C(10)-C(11)	1.50(4)	C(18)-C(19)	1.544(12)
C(10)-H(10A)	0.9900	C(18)-C(20)	1.577(11)
C(10)-H(10B)	0.9900	C(19)-H(19A)	0.9800
C(11)-C(12)	1.46(3)	C(19)-H(19B)	0.9800
C(11)-H(11A)	0.9900	C(19)-H(19C)	0.9800
C(11)-H(11B)	0.9900	C(20)-H(20A)	0.9800
C(12)-C(13)	1.29(2)	C(20)-H(20B)	0.9800

194

C(20)-H(20C)	0.9800		C(23)-C(24)	1.473(14)
C(21)-H(21A)	0.9800		C(23)-H(23A)	0.9900
C(21)-H(21B)	0.9800		C(23)-H(23B)	0.9900
C(21)-H(21C)	0.9800		C(24)-O(5)	1.440(9)
O(4)-H(4B)	0.8400		C(24)-H(24A)	0.9900
C(22)-C(23)	1.548(14)		C(24)-H(24B)	0.9900
C(22)-H(22A)	0.9900		O(5)-H(5B)	0.8400
C(22)-H(22B)	0.9900			

C(1)-O(1)-C(15)	119.4(5)		C(6)-C(7)-C(2)	118.1(13)
O(2)-C(1)-O(1)	122.9(7)		C(8)-C(7)-C(2)	118.5(11)
O(2)-C(1)-C(2)	124.1(6)		C(9)-C(8)-C(7)	128.8(15)
O(1)-C(1)-C(2)	112.8(5)		C(9)-C(8)-H(8A)	115.6
C(3)-C(2)-C(7)	121.3(8)		C(7)-C(8)-H(8A)	115.6
C(3)-C(2)-C(1)	118.6(6)		C(8)-C(9)-C(10)	123.1(18)
C(7)-C(2)-C(1)	120.1(9)		C(8)-C(9)-H(9A)	118.4
O(3)-C(3)-C(4)	124.1(9)		C(10)-C(9)-H(9A)	118.4
O(3)-C(3)-C(2)	117.5(6)		C(11)-C(10)-C(9)	116.9(15)
C(4)-C(3)-C(2)	118.4(8)		C(11)-C(10)-H(10A)	108.1
C(5)-C(4)-C(3)	122.8(14)		C(9)-C(10)-H(10A)	108.1
C(5)-C(4)-H(4A)	118.6		C(11)-C(10)-H(10B)	108.1
C(3)-C(4)-H(4A)	118.6		C(9)-C(10)-H(10B)	108.1
C(4)-C(5)-C(6)	119.8(12)		H(10A)-C(10)-H(10B)	107.3
C(4)-C(5)-H(5A)	120.1		C(12)-C(11)-C(10)	119(2)
C(6)-C(5)-H(5A)	120.1		C(12)-C(11)-H(11A)	107.5
C(7)-C(6)-C(5)	119.7(11)		C(10)-C(11)-H(11A)	107.5
C(7)-C(6)-H(6A)	120.2		C(12)-C(11)-H(11B)	107.5
C(5)-C(6)-H(6A)	120.2		C(10)-C(11)-H(11B)	107.5
C(6)-C(7)-C(8)	123.4(12)		H(11A)-C(11)-H(11B)	107.0

C(13)-C(12)-C(11)	126.1(14)	H(16A)-C(16)-H(16C)	109.5
C(13)-C(12)-H(12A)	117.0	H(16B)-C(16)-H(16C)	109.5
C(11)-C(12)-H(12A)	117.0	Si(1)-C(17)-H(17A)	109.5
C(12)-C(13)-C(14)	126.0(13)	Si(1)-C(17)-H(17B)	109.5
C(12)-C(13)-H(13A)	117.0	H(17A)-C(17)-H(17B)	109.5
C(14)-C(13)-H(13A)	117.0	Si(1)-C(17)-H(17C)	109.5
O(4)-C(14)-C(13)	110.7(10)	H(17A)-C(17)-H(17C)	109.5
O(4)-C(14)-C(15)	116.6(8)	H(17B)-C(17)-H(17C)	109.5
C(13)-C(14)-C(15)	109.7(8)	C(21)-C(18)-C(19)	108.0(8)
O(4)-C(14)-H(14A)	106.4	C(21)-C(18)-C(20)	107.1(7)
C(13)-C(14)-H(14A)	106.4	C(19)-C(18)-C(20)	106.0(7)
C(15)-C(14)-H(14A)	106.4	C(21)-C(18)-Si(1)	114.6(6)
O(1)-C(15)-C(22)	108.9(6)	C(19)-C(18)-Si(1)	110.9(6)
O(1)-C(15)-C(14)	109.4(8)	C(20)-C(18)-Si(1)	109.8(6)
C(22)-C(15)-C(14)	107.8(7)	C(18)-C(19)-H(19A)	109.5
O(1)-C(15)-H(15A)	110.2	C(18)-C(19)-H(19B)	109.5
C(22)-C(15)-H(15A)	110.2	H(19A)-C(19)-H(19B)	109.5
C(14)-C(15)-H(15A)	110.2	C(18)-C(19)-H(19C)	109.5
C(3)-O(3)-Si(1)	130.2(4)	H(19A)-C(19)-H(19C)	109.5
O(3)-Si(1)-C(16)	108.0(4)	H(19B)-C(19)-H(19C)	109.5
O(3)-Si(1)-C(18)	105.4(3)	C(18)-C(20)-H(20A)	109.5
C(16)-Si(1)-C(18)	112.4(5)	C(18)-C(20)-H(20B)	109.5
O(3)-Si(1)-C(17)	108.5(4)	H(20A)-C(20)-H(20B)	109.5
C(16)-Si(1)-C(17)	110.9(4)	C(18)-C(20)-H(20C)	109.5
C(18)-Si(1)-C(17)	111.3(5)	H(20A)-C(20)-H(20C)	109.5
Si(1)-C(16)-H(16A)	109.5	H(20B)-C(20)-H(20C)	109.5
Si(1)-C(16)-H(16B)	109.5	C(18)-C(21)-H(21A)	109.5
H(16A)-C(16)-H(16B)	109.5	C(18)-C(21)-H(21B)	109.5
Si(1)-C(16)-H(16C)	109.5	H(21A)-C(21)-H(21B)	109.5

C(18)-C(21)-H(21C)	109.5		C(22)-C(23)-H(23A)	108.8
H(21A)-C(21)-H(21C)	109.5		C(24)-C(23)-H(23B)	108.8
H(21B)-C(21)-H(21C)	109.5		C(22)-C(23)-H(23B)	108.8
C(14)-O(4)-H(4B)	109.5		H(23A)-C(23)-H(23B)	107.7
C(15)-C(22)-C(23)	112.6(6)		O(5)-C(24)-C(23)	113.9(7)
C(15)-C(22)-H(22A)	109.1		O(5)-C(24)-H(24A)	108.8
C(23)-C(22)-H(22A)	109.1		C(23)-C(24)-H(24A)	108.8
C(15)-C(22)-H(22B)	109.1		O(5)-C(24)-H(24B)	108.8
C(23)-C(22)-H(22B)	109.1		C(23)-C(24)-H(24B)	108.8
H(22A)-C(22)-H(22B)	107.8		H(24A)-C(24)-H(24B)	107.7
C(24)-C(23)-C(22)	113.8(7)		C(24)-O(5)-H(5B)	109.5
C(24)-C(23)-H(23A)	108.8			

_____

Symmetry transformations used to generate equivalent atoms:

Table 4.   Anisotropic displacement parameters ($Å^2 \times 10^3$)for 09113bs. The anisotropic displacement factor exponent takes the form: $-2\pi^2[\, h^2a^{*2}U_{11} + \ldots + 2\, h\, k\, a^*\, b^*\, U_{12}\,]$

	U_{11}	U_{22}	U_{33}	U_{23}	U_{13}	U_{12}
O1	45(2)	70(3)	92(4)	4(3)	6(3)	-15(2)
C1	43(3)	80(4)	38(4)	-1(3)	8(3)	-18(3)
O2	56(3)	110(4)	141(6)	-7(4)	21(3)	-31(3)
C2	36(3)	76(5)	73(6)	-25(4)	6(3)	1(3)
C3	39(3)	36(3)	118(8)	-19(4)	9(4)	3(3)
C4	67(5)	53(4)	144(9)	6(5)	6(5)	6(3)
C5	75(7)	58(6)	370(30)	-92(12)	46(12)	-8(5)
C6	77(7)	111(11)	227(18)	-111(12)	36(9)	-1(6)
C7	39(4)	135(9)	112(9)	-71(7)	16(5)	-15(4)
C8	50(5)	201(12)	98(9)	-52(9)	-8(5)	-22(6)
C9	63(6)	287(17)	128(12)	-124(12)	-4(6)	-22(7)
C10	110(10)	570(50)	29(6)	-64(14)	27(6)	-89(18)
C11	200(20)	440(40)	131(19)	-60(20)	-95(17)	-140(20)
C12	118(9)	282(16)	46(6)	22(9)	-5(7)	-85(10)
C13	159(13)	209(15)	130(13)	86(12)	-97(12)	-116(12)
C14	69(5)	105(7)	96(8)	49(6)	-15(5)	-16(5)
C15	60(4)	69(4)	106(7)	38(5)	-18(5)	-24(3)
O3	45(2)	45(2)	84(4)	-6(2)	3(2)	2(2)
Si1	42(1)	55(1)	98(2)	3(1)	-4(1)	-1(1)
C16	58(4)	55(4)	179(11)	3(5)	-25(5)	-1(3)
C17	36(3)	78(5)	233(13)	0(7)	-20(6)	12(3)
C18	61(4)	88(5)	69(5)	-1(4)	-32(4)	-7(4)
C19	105(7)	104(7)	110(9)	-21(6)	-42(6)	14(5)
C20	101(7)	139(8)	68(7)	-31(8)	-40(5)	0(5)

C21	87(6)	120(8)	84(7)	20(6)	-12(5)	-11(5)
O4	64(3)	97(4)	133(6)	16(4)	-34(3)	-9(3)
C22	57(4)	57(4)	111(7)	14(4)	1(5)	10(3)
C23	60(4)	46(4)	170(11)	2(5)	-10(6)	2(3)
C24	64(4)	49(4)	182(11)	-9(6)	35(6)	2(3)
O5	78(4)	110(5)	170(7)	-28(5)	46(5)	-21(3)

_____

Table 5.   Hydrogen coordinates (x 10^4) and isotropic displacement parameters (Å^2x 10^3)

for 09113bs.

_____

	x	y	z	U(eq)
H4A	1833	6992	3124	106
H5A	1782	7752	4364	201
H6A	1959	7333	5967	166
H8A	2083	5581	6586	139
H9A	2652	6836	7209	191
H10A	3159	6138	8389	283
H10B	2343	6079	8622	283
H11A	2879	4996	8713	309
H11B	2276	4997	7932	309
H12A	3711	5008	7421	178
H13A	2624	4201	6789	199
H14A	3606	3661	6081	108
H15A	2735	3927	5056	94
H16A	1069	4384	3380	146
H16B	1781	4179	2850	146
H16C	1055	4170	2282	146
H17A	466	5788	3281	173
H17B	266	5672	2190	173
H17C	720	6340	2498	173
H19A	2683	5114	473	160
H19B	2340	4486	1064	160
H19C	2790	5074	1597	160
H20A	1471	5031	-112	154

H20B	870	5484	391	154
H20C	1029	4702	744	154
H21A	2019	6175	253	145
H21B	2375	6311	1264	145
H21C	1556	6457	1119	145
H4B	4152	4853	6380	147
H22A	3852	3600	4463	90
H22B	4018	4412	4293	90
H23A	2890	3678	3366	111
H23B	3073	4484	3185	111
H24A	4013	3391	2749	118
H24B	3472	3701	1992	118
H5B	4239	4678	2707	179

Table 6.   Torsion angles [°] for 09113bs.

_____

C15-O1-C1-O2	4.0(11)	C12-C13-C14-O4	2.7(19)
C15-O1-C1-C2	180.0(7)	C12-C13-C14-C15	-127.4(14)
O2-C1-C2-C3	-91.5(9)	C1-O1-C15-C22	127.1(7)
O1-C1-C2-C3	92.7(7)	C1-O1-C15-C14	-115.3(7)
O2-C1-C2-C7	90.4(9)	O4-C14-C15-O1	-69.4(11)
O1-C1-C2-C7	-85.4(7)	C13-C14-C15-O1	57.5(10)
C7-C2-C3-O3	177.4(5)	O4-C14-C15-C22	48.9(11)
C1-C2-C3-O3	-0.7(8)	C13-C14-C15-C22	175.8(9)
C7-C2-C3-C4	-1.9(9)	C4-C3-O3-Si1	-72.6(8)
C1-C2-C3-C4	-180.0(6)	C2-C3-O3-Si1	108.1(7)
O3-C3-C4-C5	-178.5(8)	C3-O3-Si1-C16	-108.4(7)
C2-C3-C4-C5	0.8(11)	C3-O3-Si1-C18	131.3(7)
C3-C4-C5-C6	0.2(16)	C3-O3-Si1-C17	11.9(8)
C4-C5-C6-C7	0.0(19)	O3-Si1-C18-C21	-58.8(6)
C5-C6-C7-C8	178.2(10)	C16-Si1-C18-C21	-176.2(6)
C5-C6-C7-C2	-1.1(15)	C17-Si1-C18-C21	58.6(6)
C3-C2-C7-C6	2.1(11)	O3-Si1-C18-C19	63.8(6)
C1-C2-C7-C6	-179.9(8)	C16-Si1-C18-C19	-53.6(6)
C3-C2-C7-C8	-177.2(7)	C17-Si1-C18-C19	-178.7(6)
C1-C2-C7-C8	0.8(10)	O3-Si1-C18-C20	-179.4(5)
C6-C7-C8-C9	-31.1(16)	C16-Si1-C18-C20	63.2(6)
C2-C7-C8-C9	148.2(10)	C17-Si1-C18-C20	-61.9(7)
C7-C8-C9-C10	-173.6(11)	O1-C15-C22-C23	-68.8(8)
C8-C9-C10-C11	20(2)	C14-C15-C22-C23	172.6(6)
C9-C10-C11-C12	56(2)	C15-C22-C23-C24	-178.7(6)
C10-C11-C12-C13	-126.3(17)	C22-C23-C24-O5	-71.2(11)
C11-C12-C13-C14	169.9(19)		

202

_____

Symmetry transformations used to generate equivalent atoms:

Table 7. Hydrogen bonds for 09113bs [Å and °].

_____

D-H...A	d(D-H)	d(H...A)	d(D...A)	<(DHA)
O4-H4B...O4#1	0.84	2.01	2.601(7)	126.9
O5-H5B...O5#1	0.84	2.12	2.664(8)	121.7

_____

Symmetry transformations used to generate equivalent atoms:

#1 y,-x+1,z

Chapter 5

Bibliography

5.1 Refrences

1.   Ojima, I. Modern Molecular Approaches to Drug Design and Discovery. *Acc. Chem. Res.* **2008**, *41*, 2-3.

2.   Wessjohann, L. A.; Ruijter, E. Strategies for Total and Diversity-Oriented Synthesis of Natural Product(-Like) Macrocycles. In *Natural Product Synthesis I*, 2005; pp 137-184.

3.   Jan, R.; Florenz, S.; Martin, E. M. Synthesis of a Benzolactone Collection using Click Chemistry. *Eur. J. Org. Chem.* **2007**, *2007*, 78-87.

4.   Erickson, K. L.; Beutler, J. A.; Cardellina, J. H.; Boyd, M. R. Salicylihalamides A and B, Novel Cytotoxic Macrolides from the Marine Sponge Haliclona sp. *J. Org. Chem.* **2001**, *66*, 1532-1532.

5.   Galinis, D. L.; McKee, T. C.; Pannell, L. K.; Cardellina, J. H.; Boyd, M. R. Lobatamides A and B, Novel Cytotoxic Macrolides from the Tunicate Aplidium Lobatum. *J. Org. Chem.* **1997**, *62*, 8968-8969.

6.   McKee, T. C.; Galinis, D. L.; Pannell, L. K.; Cardellina, J. H.; Laakso, J.; Ireland, C. M.; Murray, L.; Capon, R. J.; Boyd, M. R. The Lobatamides, Novel Cytotoxic Macrolides from Southwestern Pacific Tunicates. *J. Org. Chem.* **1998**, *63*, 7805-7810.

7.   Kunze, B.; Jansen, R.; Sasse, F.; Höfle, G.; Reichenbach, H. Apicularens A and B, New Cytostatic Macrolides from Chondromyces Species (Myxobacteria):

Production, Physico-Chemical and Biological Properties. *J. Antibiot.* **1998**, *51*, 1075-1080.

8.   Kim, J. W.; Shin-ya, K.; Furihata, K.; Hayakawa, Y.; Seto, H. Oximidines I and II: Novel Antitumor Macrolides from Pseudomonas sp. *J. Org. Chem.* **1999**, *64*, 153-155.

9.   Hayakawa, Y.; Tomikawa, T.; Shin-Ya, K.; Arao, N. N., K. ; Suzuki, K. Oximidine III, a New Antitumor Antibiotic against Transformed Cells from Pseudomonas Sp. I. Taxonomy, Fermentation, Isolation, Physico-Chemical Properties and Biological Activity. *J. Antibiot.* **2003**, *56*, 899-904.

10.   Hayakawa, Y.; Tomikawa, T.; Shin-Ya, K.; Arao, N.; Nagai, K.; Suzuki, K.; Furihata, K. Oximidine III, a New Antitumor Antibiotic against Transformed Cells from Pseudomonas pp. II. Structure Elucidation. *J. Antibiot.* **2003**, *56*, 905-908.

11.   Scheufler, F.; Maier, M. E. Synthesis of a Model System for the Macrocyclic Subunit of the Oximidines. *Synlett.* **2001**, *2001*, 1221-1224.

12.   Coleman, R.; Garg, R. Stereocontrolled Synthesis of the Diene and Triene Macrolactones of Oximidines I and II: Organometallic Coupling Versus Standard Macrolactonization. *Org. Lett.* **2001**, *3*, 3487-3490.

13.   Wang, X.; Porco, J. A. Total Synthesis of the Salicylate Enamide Macrolide Oximidine II. *J. Am. Chem. Soc.* **2003**, *125*, 6040-6041.

14.   Harvey, J. E.; Raw, S. A.; Taylor, R. J. K. The First Synthesis of the Epoxide-Containing Macrolactone Nucleus of Oximidine I. *Tetrahedron Lett.* **2003**, *44*, 7209-7212.

15.   Haack, T.; Kurtkaya, S.; Snyder, J. P.; Georg, G. I. Studies toward the Synthesis of Oximidines I and II. *Org. Lett.* **2003**, *5*, 5019-5022.

16.   Scott, J. W.; Grisp, G. T.; Stille, J. K. Palladium-Catalized Coupling of Vinyl Triflates with Organostannanes: 4-tert-Butyl-1-vinylcyclohexene and 1-(4-tert-Butylcyclohexen-1-yl)-2-propen-1-one. *Org. Synth.* **1989**, *68*, 116-129.

17.   Inanaga, J.; Hirata, K.; Saeki, H.; Katsuki, T.; Yamaguchi, M. A Rapid Esterification by Means of Mixed Anhydride and Its Application to Large-ring Lactonization. *Bull. Chem. Soc. Jpn.* **1979**, *52*, 1989-1993.

18.   Illuminati, G.; Mandolini, L. Ring closure reactions of bifunctional chain molecules. *Acc. Chem. Res.* **1981**, *14*, 95-102.

19.   Casadei, M. A.; Galli, C.; Mandolini, L. Ring-closure reactions. 22. Kinetics of cyclization of diethyl (.omega.-bromoalkyl)malonates in the range of 4- to 21-membered rings. Role of ring strain. *J. Am. Chem. Soc.* **1984**, *106*, 1051-1056.

20.   Okuro, K.; Furuune, M.; Enna, M.; Miura, M.; Nomura, M. Synthesis of Aryl- and Vinylacetylene Derivatives by Copper-Catalyzed Reaction of Aryl and Vinyl Iodides with Terminal Alkynes. *J. Org. Chem.* **1993**, *58*, 4716-4721.

21.   Wilhelm, B.; Nora, S.; Christiane, S.; Martin, F. Sterospecific Syntheses and Spectroscopic Properties of Isomeric 2,4,6,8-Undecatetraenes. New Hydrocarbons from the Marine Brown Alga *Giffordia mitchellae*. Part IV. *Hel. Chim. Acta* **1987**, *70*, 1025-1040.

22.   Wadsworth, J. W. S.; Emmons, W. D. The Utility of Phosphonate Carbanions in Olefin Synthesis. *J. Am. Chem. Soc.* **1961**, *83*, 1733-1738.

23.   Horner, L. Darstellung Und Eigenschaften Optisch Aktiver, Tertiärer Phoosphine. *Pure Appl. Chem.* **1964**, *9*, 225-244.

24.   Wadsworth, J. W. S. Synthetic Applications of Phosphonyl-stabilized anions,. *Org. React.* **1977**, *25*, 73-253.

25.   Trnka, T. M.; Grubbs, R. H. The Development of $L_2X_2Ru=CHR$ Olefin Metathesis Catalysts: An Organometallic Success Story. *Acc. Chem. Res.* **2001** *34*, 18-29.

26.   Fürstner, A. Olefin Metathesis and Beyond. *Angew. Chem., Int. Ed. Engl.* **2000**, *39*, 3012-3043

27.   Schuster, M.; Blechert, S. Oefin metathesis in organic chemistry. *Angew. Chem., Int. Ed. Engl.* **1997**, *36*, 2037-2056.

28.   Grubbs, R. H.; Chang, S. Recent advances in olefin metathesis and its application in rganic synthesis. *Tetrahedron* **1998**, *54*, 4413-4450.

29.   Shen, R.; Porco, J. A. Synthesis of Enamides Related to the Salicylate Antitumor Macrolides Using Copper-Mediated Vinylic Substitution. *Org. Lett.* **2000**, *2*, 1333-1336.

30.   Bhattacharjee, A.; De Brabander, J. K. Synthesis of Side Chain Truncated Apicularen A. *Tetrahedron Lett.* **2000**, *41*, 8069-8073.

31.   Brown, H. C.; Jadhav, P. K.; Bhat, K. S. Chiral synthesis via organoboranes. 13. A highly diastereoselective and enantioselective addition of [(Z)-.gamma.-alkoxyallyl]diisopinocampheylboranes to aldehydes. *J. Am. Chem. Soc.* **1988**, *110*, 1535-1538.

208

32.   Hodgson, D. M.; Boulton, L. T.; Maw, G. N. Scope of the chromium(II)-mediated synthesis of *E*-alkenylstannanes from aldehydes and Bu$_3$SnCHBr$_2$. *Tetrahedron* **1995**, *51*, 3713-3724.

33.   Fürstner, A.; Konetzki, I. Synthesis of 2-Hydroxy-6-{[(16R)-β-DMannopyranosyloxy]Heptadecyl}Benzoic Acid, a Fungal Metabolite with GABA(A) Ion Channel Receptor Inhibiting Properties. *Tetrahedron* **1996**, *52*, 15071-15078.

34.   Alois, F.; Thorsten, D.; Oliver, R. T.; Gaetano, B. Total Synthesis of (-)-Salicylihalamide. *Chem. Eur. J.* **2001**, *7*, 5286-5298.

35.   Farina, V.; Krishnan, B. Large rate accelerations in the stille reaction with tri-2-furylphosphine and triphenylarsine as palladium ligands: mechanistic and synthetic implications. *J. Am. Chem. Soc.* **1991**, *113*, 9585-9595.

36.   Furstner, A.; Thiel, O. R.; Blanda, G. Asymmetric Synthesis of the Fully Functional Macrolide Core of Salicylihalamide: Remote Control of Olefin Geometry during RCM. *Org. Lett.* **2000**, *2*, 3731-3734.

37.   Haack, T.; Haack, K.; Diederich, W. E.; Blackman, B.; Roy, S.; Pusuluri, S.; Georg, G. I. Formal Total Syntheses of the (−)-Salicylihalamides A and B From d-Glucose and l-Rhamnose. *J. Org. Chem.* **2005**, *70*, 7592-7604.

38.   Wu, Y.; Esser, L.; De Brabander, J. K. Revision of the Absolute Configuration of Salicylihalamide A through Asymmetric Total Synthesis. *Angew. Chem. Int. Ed.* **2000**, *39*, 4308-4310.

39.   Stork, G.; Zhao, K. A Stereoselective Synthesis of (Z)-1-Iodo-1-Alkenes. *Tetrahedron Lett.* **1989**, *30*, 2173-2174.

40.   Allred, G. D.; Liebeskind, L. S. Copper-Mediated Cross-Coupling of Organostannanes with Organic Iodides at or Below Room Temperature. *J. Am. Chem. Soc.* **1996**, *118*, 2748-2749.

41.   Wang, X.; Bowman, E. J.; Bowman, B. J.; Porco, J. A., Jr. Total Synthesis of the Salicylate Enamide Macrolide Oximidine III: Application of Relay Ring-Closing Metathesis. *Angew. Chem., Int. Ed. Engl.* **2004**, *43*, 3601-3605.

42.   Hoye, T. R.; Jeffrey, C. S.; Tennakoon, M. A.; Wang, J.; Zhao, H. Relay Ring-Closing Metathesis (RRCM): A Strategy for Directing Metal Movement Throughout Olefin Metathesis Sequences. *J. Am. Chem. Soc.* **2004**, *126*, 10210-10211.

43.   Debra, J. W. Relay Ring-Closing Metathesis - A Strategy for Achieving Reactivity and Selectivity in Metathesis Chemistry. *Angew. Chem. Int. Ed.* **2005**, *44*, 1912-1915.

44.   Schaus, S. E.; Brandes, B. D.; Larrow, J. F.; Tokunaga, M.; Hansen, K. B.; Gould, A. E.; Furrow, M. E.; Jacobsen, E. N. Highly Selective Hydrolytic Kinetic Resolution of Terminal Epoxides Catalyzed by Chiral (salen)Co^{III} Complexes. Practical Synthesis of Enantioenriched Terminal Epoxides and 1,2-Diols. *J. Am. Chem. Soc.* **2002**, *124*, 1307-1315.

45.   Molander, G. A.; Dehmel, F. Formal Total Synthesis of Oximidine II Via a Suzuki-Type Cross-Coupling Macrocyclization Employing Potassium Organotrifluoroborates. *J. Am. Chem. Soc.* **2004**, *126*, 10313-10318.

46.   Molander, G. A.; Rivero, M. R. Suzuki Cross-Coupling Reactions of Potassium Alkenyltrifluoroborates. *Org. Lett.* **2002**, *4*, 107-109.

47.   Molander; G. A.; Bernardi, C. R. Suzuki-Miyaura Cross-Coupling Reactions of Potassium Alkenyltrifluoroborates. *J. Org. Chem.* **2002**, *67*, 8424-8429.

48.   Darses, S.; Genet, J. P. Potassium Trifluoro(organo)borates: New Perspectives in Organic Chemistry. *Eur. J. Org. Chem.* **2003**, *2003*, 4313-4327.

49.   Molander, G. A.; Rivero, M. R. Suzuki Cross-Coupling Reactions of Potassium Alkenyltrifluoroborates. *Org. Lett.* **2001**, *4*, 107-109.

50.   Bauer, M.; Maier, M. E. Synthesis of the Core Structure of Salicylihalamide A by Intramolecular Suzuki Reaction. *Org. Lett.* **2002**, *4*, 2205-2208.

51.   Porco, J. A.; Schoenen, F. J.; Stout, T. J.; Clardy, J.; Schreiber, S. L. Transannular Diels-Alder route to systems related to dynemicin A. *J. Am. Chem. Soc.* **1990**, *112*, 7410-7411.

52.   Lu, Y. F.; Harwig, C. W.; Fallis, A. G. Taxamycins: a new enediyne family constructed from versatile disilyl-substituted building blocks. *J. Org. Chem.* **1993**, *58*, 4202-4204.

53.   Lu, Y. F.; Harwig, C. W.; Fallis, A. G. Taxamycins: A New Enediyne Family with Synthetic and Biological Potential. *Can. J. Chem.* **1995**, *73*, 2253-2262.

54.   Pawlak, J.; Nakanishi, K.; Iwashita, T. Stereochemical Studies of Polyols from the Polyene Macrolide Lienomycin. *J. Org. Chem.* **1987**, *52*, 2896-2901.

55.   Boyall, D.; Frantz, D. E.; Carreira, E. M. Efficient Enantioselective Additions of Terminal Alkynes and Aldehydes under Operationally Convenient Conditions. *Org. Lett.* **2002**, *4*, 2605-2606.

56.   Anand, N. K.; Carreira, E. M. A Simple, Mild, Catalytic, Enantioselective Addition of Terminal Acetylenes to Aldehydes. *J. Am. Chem. Soc.* **2001**, *123*, 9687-9688.

57.   Frantz, D. E.; Fassler, R.; Carreira, E. M. Facile Enantioselective Synthesis of Propargylic Alcohols by Direct Addition of Terminal Alkynes to Aldehydes. *J. Am. Chem. Soc.* **2000**, *122*, 1806-1807.

58.   Frantz, D. E.; Fassler, R.; Tomooka, C. S.; Carreira, E. M. The Discovery of Novel Reactivity in the Development of C−C Bond-Forming Reactions: In Situ Generation of Zinc Acetylides with ZnII/R3N. *Acc. Chem. Res.* **2000**, *33*, 373-381.

59.   Sulikowski, G. A.; Lee, W.-M.; Jin, B.; Wu, B. Synthesis of the Apoptosis Inducing Agent Apoptolidin. Assembly of the C(16)−C(28) Fragment. *Org. Lett.* **2000**, *2*, 1439-1442.

60.   Alexey, V. K.; Stefan, S.; Victor, S. Di(isopropylprenyl)borane: A New Hydroboration Reagent for the Synthesis of Alkyl and Alkenyl Boronic Acids. *Angew. Chem. Int. Ed.* **2003**, *42*, 3399-3404.

61.   Schneider, C. M. Studies on Oximidine II – Total Synthesis by an Unprecedented Reductive Coupling University of Kansas, Kansas, 2009.

62. Brestensky, D. M.; Huseland, D. E.; McGettigan, C.; Stryker, J. M. Simplified, "One-Pot" Procedure for the Synthesis of [(Ph$_3$P)CuH]$_6$, a Stable Copper Hydride for Conjugate Reductions. *Tetrahedron Lett.* **1988**, *29*, 3749-3752.

63. Xu, D.; Park, C. Y.; Sharpless, K. B. Study of the Regio- and Enantioselectivity of the Reactions of Osmium Tetroxide with Allylic Alcohols and Allylic Sulfonamides. *Tetrahedron Lett.* **1994**, *35*, 2495-2498.

64. Rodney, A. F.; Pradeep, K. A Stereoselective Synthesis of Dihydrosphingosine. *Eur. J. Org. Chem.* **2000**, *2000*, 3447-3449.

65. Sharpless, K. B.; Amberg, W.; Bennani, Y. L.; Crispino, G. A.; Hartung, J.; Jeong, K. S.; Kwong, H. L.; Morikawa, K.; Wang, Z. M. The osmium-catalyzed asymmetric dihydroxylation: a new ligand class and a process improvement. *J. Org. Chem.* **1992**, *57*, 2768-2771.

66. Ager, D. J. The Peterson Reaction. *Synthesis* **1984**, *1984*, 384-398.

67. Corey, E. J.; Rucker, C. Useful Synthetic Reagents Derived from 1-Triisopropylsilylpropyne and 1,3-Bis-(Triisopropylsilyl)Propyne. Direct, Stereoselective Synthesis of Either Z or E Enynes. *Tetrahedron Lett.* **1982**, *23*, 719-722.

68. Kira, K.; Isobe, M. Acetylene Cobalt Complex and Vinylsilane Strategy in the Synthesis of Ciguatoxin (D)EF Analog. *Tetrahedron Lett.* **2000**, *41*, 5951-5955.

69. Stamos, D. P.; Taylor, A. G.; Kishi, Y. A Mild Preparation of Vinyliodides from Vinylsilanes. *Tetrahedron Lett.* **1996**, *37*, 8647-8650.

70.   Barluenga, S.; Dakas, P. Y.; Ferandin, Y.; Meijer, L.; Winssinger, N. Asymmetric Synthesis of Aigialomycin D, a Kinase-Inhibitory Scaffold. *Angew. Chem. Int. Ed.* **2006**, *45*, 3951-3954.

71.   Shen, R.; Lin, C. T.; Porco, J. A. Total Synthesis and Stereochemical Assignment of the Salicylate Antitumor Macrolide Lobatamide C1. *J. Am. Chem. Soc.* **2002**, *124*, 5650-5651.

72.   Mc Murry, J. E.; Mohanraj, S. Synthesis of arenes from phenols by coupling of aryl triflates with organocopper reagents. *Tetrahedron Lett.* **1983**, *24*, 2723-2726.

73.   Ferrier, R. J.; Prasad, N. Unsaturated carbohydrates. Part IX. Synthesis of 2,3-dideoxy-D-erythro-hex-2-enopyranosides from tri-O-acetyl-D-glucal. *J. Chem. Soc. C.* **1969**, *1969*, 570-575.

74.   Wolfgang, V.; Wolfram, F.; John, J. S.; Petra, S.-K. Molecular Structures of Tri-*O*-acetyl-D-glucal and Ethyl-4, 6-di- *O*-acetyl-2, 3-dideoxy-alpha-D-erythro-2-hexenopyranoside. *Angew. Chem., Int. Ed.* **1981**, *20*, 1042-1043.

75.   Grynkiewicz, G.; Priebe, W.; Zamojski, A. Synthesis of alkyl 4,6-di-o-acetyl-2,3-dideoxy-[alpha]-d-threo-hex-2- enopyranosides from 3,4,6-tri-o-acetyl-1,5-anhydro-2-deoxy- d-lyxo-hex-1-enitol (3,4,6-tri-o-acetyl-d-galactal). *Carbohydrate Res.* **1979**, *68*, 33-41.

76.   Vijayasaradhi, S.; Singh, J.; Singh Aidhen, I. An Efficient, Selective Hydrolysis of Terminal Isopropylidene Acetal Protection by $Zn(NO_3)_2 \cdot 6H_2O$ in Acetonitrile. *Synlett* **2000**, 110-112.

77.   Mitsunobu, O. The Use of Diethyl Azodicarboxylate and Triphenylphosphine in Synthesis and Transformation of Natural Products *Synthesis* **1981**, 1-28.

78.   Abe, H.; Aoyagi, S.; Kibayashi, C. First Total Synthesis of the Marine Alkaloids (+-)-Fasicularin and (+-)-Lepadiformine Based on Stereocontrolled Intramolecular Acylnitroso-Diels−Alder Reaction. *J. Am. Chem. Soc.* **2000**, *122*, 4583-4592.

79.   Blackman, B.; Georg, G.; Lushington, G. H. CoMSIA:QSAR Models for Vacuolar (H+) ATPase Inhibition by Selected Benzoate and Benzolactone Species *Letters in Drug Design & Discovery* **2006**, *3*, 104-107.

80.   Mervyn, S.; Philip, J. Statistical thinking and technique for QSAR and related studies. Part I: General theory. *J. Chemom.* **1993**, *7*, 455-475.

81.   Oprea, T. I.; Waller, C. L. Theoretical and practical aspects of three-dimensional quantitative structure-activity relationships. In *Review in Computational Chemistry*, Lipkowitz, K. B.; Boyd, D. B., Eds. Wiley-VCH: New York, 1997; pp 127-182.

82.   Cramer, R. D.; Patterson, D. E.; Bunce, J. D. Comparative molecular field analysis (CoMFA). 1. Effect of shape on binding of steroids to carrier proteins. *J. Am. Chem. Soc.* **1988**, *110*, 5959-5967.

83.   Klebe, G.; Abraham, U.; Mietzner, T. Molecular Similarity Indices in a Comparative Analysis (CoMSIA) of Drug Molecules to Correlate and Predict their Biological Activity. *J. Med. Chem.* **1994**, *37*, 4130-4146.

84.   Horvath, D.; Jeandenans, C. Molecular Similarity and Virtual Screening. In silico Methods to Retrieve Active Analogs in the Context of Discovering Therapeutic Compounds. *Actual Chim.* **2000**, *9*, 64-67.

85.   Leach, A. R.; Hann, M. M. The in silico world of virtual libraries. *Drug Discovery Today* **2000**, *5*, 326-336.

86.   Clark, M.; Cramer, R. D. I.; Van Opdenbosch, N. Validation of the general purpose Tripos 5.2 force field. *J. Comput. Chem* **1989**, *10*, 982-1012.

87.   Jain, A. N. Surflex: Fully Automatic Flexible Molecular Docking Using a Molecular Similarity-Based Search Engine. *J. Med. Chem.* **2003**, *46*, 499-511.

88.   Gasteiger, J.; Marsili, M. Iterative partial equalization of orbital electronegativity--a rapid access to atomic charges. *Tetrahedron* **1980**, *36*, 3219-3228.

89.   SYBYL 8.0, The Tripos Associates, St. Louis, MO. In 2007.

90.   Darwish, A.; Lang, A.; Kim, T.; Chong, J. M. The Use of Phosphine Ligands to Control the Regiochemistry of Pd-Catalyzed Hydrostannations of 1-Alkynes: Synthesis of (E)-1-Tributylstannyl-1-alkenes. *Org. Lett.* **2008**, *10*, 861-864.

91.   Parikh, J. R.; Doering, W. v. E. Sulfur trioxide in the oxidation of alcohols by dimethyl sulfoxide. *J. Am. Chem. Soc.* **1967**, *89*, 5505-5507.

92.   Nicolaou, K. C.; David, W. K.; Rachid, B.; Aurora, O.; Paraskevi, G. Total Synthesis and Biological Evaluation of (-)-Apicularen A and Analogues Thereof. *Chem. Eur. J.* **2003**, *9*, 6177-6191.

93.   Finbow, M. E.; A., H. M. The Vacuolar H-ATPase: A Universal Proton Pump of Eukaryotes. *Biochem. J.* **1997**, *324*, 697-712.

94.   Stevens, T. H.; Forgac, M. Structure, function and regulation of the vacuolar (H$^+$)-ATPase. *Annu. Rev. Cell Dev. Biol.* **1997**, *13*, 779-808.

95.   Nelson, N.; Harvey, W. R. Vacuolar and Plasma Membrane Proton-Adenosinetriphosphatases. *Physiol. Rev.* **1999**, *51*, 361-385.

96.   Lafourcade, C. l.; Sobo, K.; Kieffer-Jaquinod, S.; Garin, J. R.; van der Goot, F. G. Regulation of the V-ATPase Along the Endocytic Pathway Occurs through Reversible Subunit Association and Membrane Localization. *PLoS ONE* **2008**, *3*, e2758.

97.   Nishi, T.; Forgac, M. The Vacuolar (H$^+$)-ATPases - Nature's Most Versatile Proton Pumps. *Nature Rev. Mol. Cell Biol.* **2002**, *3*, 94-103.

98.   Forgac, M. Vacuolar ATPases: Rotary Proton Pumps in Physiology and Pathophysiology. *Nat. Rev. Mol. Cell Biol.* **2007**, *8*.

99.   Brown, M. S.; Anderson, R. G. W.; Goldstein, J. L. Recycling receptors: The round-trip itinerary of migrant membrane proteins. *Cell* **1983**, *32*, 663-667.

100.   Mellman, I. The importance of being acid: the role of acidification in intracellular membrane traffic. *J. Exp. Biol.* **1992**, *172*, 39-45.

101.   Gruenberg, J.; van der Goot, F. G. Mechanisms of Pathogen Entry through the Endosomal Compartments. *Nature Rev. Mol. Cell Biol.* **2006**, *7*, 495-504.

102.   Farina, C.; Gagliardi, S. Selective inhibitors of the osteoclast vacuolar proton ATPase as novel bone antiresorptive agents. *Drug Discovery Today* **1999**, *4*, 163-172.

103.   Hinton, A.; Bond, S.; Forgac, M. V-ATPase Functions in Normal and Disease Processes. *Pflügers Arch. Eur. J. Physiol.* **2009**, *457*, 589-598.

104.   Wieczorek, H.; Brown, D.; Grinstein, S.; Ehrenfeld, J.; Harvey, W. R. Animal Plasma Membrane Energization by Proton-Motive V-ATPases. *Bioessays* **1999**, *21*, 637-648.

105.   Brown, D.; Breton, S. H(+)V-ATPase-dependent luminal acidification in the kidney collecting duct and the epididymis/vas deferens: vesicle recycling and transcytotic pathways. *J. Exp. Biol.* **2000**, *203*, 137-145.

106.   Smith, A. N.; Skaug, J.; Choate, K. A.; Nayir, A.; Bakkaloglu, A.; Ozen, S.; Hulton, S. A.; Sanjad, S. A.; Al-Sabban, E. A.; Lifton, R. P.; Scherer, S. W.; Karet, F. E. Mutations in ATP6N1B, encoding a new kidney vacuolar proton pump 116-kD subunit, cause recessive distal renal tubular acidosis with preserved hearing. *Nat. Genet.* **2000**, *26*, 71-75.

107.   Baron, R.; Neff, L.; Louvard, D.; Courtoy, P. J. Cell-mediated extracellular acidification and bone resorption: evidence for a low pH in resorbing lacunae and localization of a 100-kD lysosomal membrane protein at the osteoclast ruffled border. *J. Cell Biol.* **1985**, *101*, 2210-2222.

108.   Blair, H. C.; Teitelbaum, S. L.; Ghiselli, R.; Gluck, S. Osteoclastic bone resorption by a polarized vacuolar proton pump. *Science* **1989**, *245*, 855-857.

109.   Gelb, B. D.; Shi, G.-P.; Chapman, H. A.; Desnick, R. J. Pycnodysostosis, a Lysosomal Disease Caused by Cathepsin K Deficiency. *Science* **1996**, *273*, 1236-1238.

110.   Sennoune, S. R.; Bakunts, K.; Martinez, G. M.; Chua-Tuan, J. L.; Kebir, Y.; Attaya, M. N.; Martinez-Zaguilan, R. Vacuolar H$^+$-ATPase in human breast cancer cells with distinct metastatic potential: distribution and functional activity. *Am. J. Physiol. Cell Physiol.* **2004**, *286*, C1443-1452.

111.   Wilkens, S.; Forgac, M. Three-dimensional Structure of the Vacuolar ATPase Proton Channel by Electron Microscopy. *J. Biol. Chem.* **2001**, *276*, 44064-44068.

112.   Stock, D.; Leslie, A. G.; Walker, J. E. Molecular Architecture of the Rotary Motor in ATP Synthase. *Science* **1999**, *286*, 1700-1705.

113.   Beutler, J. A.; McKee, T. C. Novel Marine and Microbial Natural Product Inhibitors of Vacuolar ATPase. *Curr. Med. Chem.* **2003**, *10*, 787-796.

114.   Nelson, D. L.; Cox, M. M. *Lehninger Principles of Biochemistry.* 3rd ed.; Worth Publishers: New York, NY, 2000.

115.   Kane, P. M. Regulation of V-ATPases by reversible disassembly. *FEBS Lett.* **2000**, *469*, 137-141.

116.   Meier, T.; Polzer, P.; Diederichs, K.; Welte, W.; Dimroth, P. Structure of the Rotor Ring of F-Type Na$^+$-ATPase from Ilyobacter tartaricus. *Science* **2005**, *308*, 659-662.

117.   Nishi, T.; Forgac, M. Molecular Cloning and Expression of Three Isoforms of the 100-kDa a Subunit of the Mouse Vacuolar Proton-translocating ATPase. *J. Biol. Chem.* **2000**, *275*, 6824-6830.

118.   Smith, A. N.; Finberg, K. E.; Wagner, C. A.; Lifton, R. P.; Devonald, M. A. J.; Su, Y.; Karet, F. E. Molecular Cloning and Characterization of Atp6n1b : A

Novel Fourth Murine Vacuolar H$^+$-ATPase a-Subunit Gene. *J. Biol. Chem.* **2001**, *276*, 42382-42388.

119. Pietrement, C.; Sun-Wada, G. H.; Da Silva, N.; McKee, M.; Marshansky, V.; Brown, D.; Futai, M.; Breton, S. Distinct Expression Patterns of Different Subunit Isoforms of the V-ATPase in the Rat Epididymis. *Biol. Reprod.* **2006**, *74*, 185-194.

120. Imai-Senga, Y.; Sun-Wada, G.-H.; Wada, Y.; Futai, M. A human gene, ATP6E1, encoding a testis-specific isoform of H$^+$-ATPase subunit E. *Gene* **2002**, *289*, 7-12.

121. Sun-Wada, G.-H.; Imai-Senga, Y.; Yamamoto, A.; Murata, Y.; Hirata, T.; Wada, Y.; Futai, M. A Proton Pump ATPase with Testis-specific E1-Subunit Isoform Required for Acrosome Acidification. *J. Biol. Chem.* **2002**, *277*, 18098-18105.

122. Ochotny, N.; Van Vliet, A.; Chan, N.; Yao, Y.; Morel, M.; Kartner, N.; von Schroeder, H. P.; Heersche, J. N. M.; Manolson, M. F. Effects of Human a3 and a4 Mutations That Result in Osteopetrosis and Distal Renal Tubular Acidosis on Yeast V-ATPase Expression and Activity. *J. Biol. Chem.* **2006**, *281*, 26102-26111.

123. Hinton, A.; Sennoune, S. R.; Bond, S.; Fang, M.; Reuveni, M.; Sahagian, G. G.; Jay, D.; Martinez-Zaguilan, R.; Forgac, M. Function of a Subunit Isoforms of the V-ATPase in pH Homeostasis and in Vitro Invasion of MDA-MB231 Human Breast Cancer Cells. *J. Biol. Chem.* **2009**, *284*, 16400-16408.

124. Bowman, E. J.; Siebers, A.; Altendorf, K. Bafilomycins: A Class of Inhibitors of Membrane Atpases from Microorganisms, Animal Cells, and Plant Cells. *Proc. Natl. Acad. Sci. U.S.A.* **1988**, *85*, 7972-7976.

125.   Kinashi, H.; Someno, K.; Sakaguchi, K. Isolation and Characterization of Concanamycins A, B, and C. *J. Antibiot.* **1984**, *38*, 1333-1343.

126.   Woo, J.-T.; Shinohara, C.; Sakai, K.; Saumi, K.; Endo, A. Isolation, Characterization and Biological Activities of Concanamycins as Inhibitors of Lysosomal Acidification. *J. Antibiot.* **1992**, *45*, 1108-1116.

127.   Yoshimori, T.; Yamamoto, A.; Moriyama, Y.; Futai, M.; Tashiro, Y. Bafilomycin A1, a specific inhibitor of vacuolar-type H(+)-ATPase, inhibits acidification and protein degradation in lysosomes of cultured cells. *J. Biol. Chem.* **1991**, *266*, 17707-17712.

128.   Tsukasa, M.; Tamotsu, Y.; Nobuhiro, H.; Yutaka, T. Inhibitors of vacuolar-type H^+-ATPase suppresses proliferation of cultured cells. *J. Cell Physiol.* **1993**, *157*, 445-452.

129.   Tetsuo, O.; Hajime, A.; Fumio, F.; Sachio, F.; Hirohisa, K.; Masato, K.; Takukazu, N.; Koichi, M.; Kazuyoshi, K.; Masayuki, N.; Yukisato, K.; Tadashi, T.; Shoji, O. Bafilomycin A_1 induces apoptosis in the human pancreatic cancer cell line Capan-1. *J. Pathol.* **1998**, *185*, 324-330.

130.   Rautiala, T. J.; Koskinen, A. M. P.; Vaananen, H. K. Purification of Vacuolar ATPase with Bafilomycin C1 Affinity Chromatography. *Biochem. Biophys. Res. Commun.* **1993**, *194*, 50-56.

131.   Huss, M.; Ingenhorst, G.; König, S.; Gaßel, M.; Dröse, S.; Zeeck, A.; Altendorf, K.; Wieczorek, H. Concanamycin A, the Specific Inhibitor of V-ATPases, Binds to the Vo Subunit c. *J. Biol. Chem.* **2002**, *277*, 40544-40548.

132.   Yoshimoto, Y.; Jyojima, T.; Arita, T.; Ueda, M.; Imoto, M.; Matsumura, S.; Toshima, K. Vacuolar-type H^+-ATPase inhibitory activity of synthetic analogues of the concanamycins: Is the hydrogen bond network involving the lactone carbonyl, the hemiacetal hydroxy group, and the C-19 hydroxy group essential for the biological activity of the concanamycins? *Bioorg. Med. Chem. Lett.* **2002**, *12*, 3525-3528.

133.   Droese, S.; Bindseil, K. U.; Bowman, E. J.; Siebers, A.; Zeeck, A.; Altendorf, K. Inhibitory effect of modified bafilomycins and concanamycins on P- and V-type adenosinetriphosphatases. *Biochemistry* **2002**, *32*, 3902-3906.

134.   Gagliardi, S.; Nadler, G.; Consolandi, E.; Parini, C.; Morvan, M.; Legave, M.-N.; Belfiore, P.; Zocchetti, A.; Clarke, G. D.; James, I.; Nambi, P.; Gowen, M.; Farina, C. 5-(5,6-Dichloro-2-indolyl)-2-methoxy-2,4-pentadienamides: Novel and Selective Inhibitors of the Vacuolar H+-ATPase of Osteoclasts with Bone Antiresorptive Activity. *J. Med. Chem.* **1998**, *41*, 1568-1573.

135.   Petrangolini, G.; Supino, R.; Pratesi, G.; Bo, L. D.; Tortoreto, M.; Croce, A. C.; Misiano, P.; Belfiore, P.; Farina, C.; Zunino, F. Effect of a Novel Vacuolar-H^+-ATPase Inhibitor on Cell and Tumor Response to Camptothecins. *J. Pharmacol. Exp. Ther.* **2006**, *318*, 939-946.

136.   Supino, R.; Petrangolini, G.; Pratesi, G.; Tortoreto, M.; Favini, E.; Bo, L. D.; Casalini, P.; Radaelli, E.; Croce, A. C.; Bottiroli, G.; Misiano, P.; Farina, C.; Zunino, F. Antimetastatic Effect of a Small-Molecule Vacuolar H^+-ATPase Inhibitor in in Vitro and in Vivo Preclinical Studies. *J. Pharmacol. Exp. Ther.* **2008**, *324*, 15-22.

137.   Boyd, M. R.; Farina, C.; Belfiore, P.; Gagliardi, S.; Kim, J. W.; Hayakawa, Y.; Beutler, J. A.; McKee, T. C.; Bowman, B. J.; Bowman, E. J. Discovery of a Novel Antitumor Benzolactone Enamide Class That Selectively Inhibits Mammalian Vacuolar-Type (H$^+$)-ATPases. *J. Pharmacol. Exp. Ther.* **2001**, *297*, 114-120.

138.   Dekker, K. A.; Aiello, R. J.; Haria, H.; Inagaki, T.; Sakakibara, T.; Suzuki, Y.; Thompson, J. F.; Yamauchi, Y.; Kojima, N. Novel Lactone Compounds from Mortierela Verticillata That Induce the Human Low Density Lipoprotein Receptor Gene: Fermentation, Isolation, Structural Elucidation and Biological Activities. *J. Antibiot.* **1998**, *51*, 14-20.

139.   Xie, X.-S.; Padron, D.; Liao, X.; Wang, J.; Roth, M. G.; De Brabander, J. K. Salicylihalamide A Inhibits the V0 Sector of the V-ATPase through a Mechanism Distinct from Bafilomycin A1. *J. Biol. Chem.* **2004**, *279*, 19755-19763.

140.   Kawada, M.; Usami, I.; Ohba, S.-i.; Someno, T.; Kim, J. W.; Hayakawa, Y.; Nose, K.; Ishizuka, M. Hygrolidin induces p21 expression and abrogates cell cycle progression at G1 and S phases. *Biochem. Biophys. Res. Commun.* **2002**, *298*, 178-183.

141.   Kagawa, S.; Fujiwara, T.; Hizuta, A.; Yasuda, T.; Zhang, W.-W.; Roth, J. A.; Tanaka, N. p53 expression overcomes p21-[WAF1/CIP1]-mediated G1 arrest and induces apoptosis in human cancer cells. *Oncogen* **1997**, *15*, 1903-1909.

142.   Suzumura, K.-i.; Takahashi, I.; Matsumoto, H.; Nagai, K.; Setiawan, B.; Rantiatmodjo, R. M.; Suzuki, K.-i.; Nagano, N. Structural Elucidation of YM-75518,

A Novel Antifungal Antibiotic Isolated from Pseudomonas sp. Q38009. *Tetrahedron Lett.* **1997**, *38*, 7573-7576.

143.   Diyabalanage, T.; Amsler, C. D.; McClintock, J. B.; Baker, B. J. Palmerolide A, a Cytotoxic Macrolide from the Antarctic Tunicate Synoicum adareanum. *J. Am. Chem. Soc.* **2006**, *128*, 5630-5631.

144.   Tanaka, J.-i.; Higa, T. Zampanolide, a new cytotoxic marcrolide from a marine sponge. *Tetrahedron Lett.* **1996**, *37*, 5535-5538.

145.   Ding, F.; Jennings, M. P. Total Synthesis of (−)-Dactylolide and Formal Synthesis of (−)-Zampanolide via Target Oriented β-C-Glycoside Formation. *J. Org. Chem.* **2008**, *73*, 5965-5976.

146.   Martin, P. M.; Horwitz, K. B.; Ryan, D. S.; McGuire, W. L. Phytoestrogen Interaction with Estrogen Receptors in Human Breast Cancer Cells. *Endocrinology* **1978**, *103*, 1860-1867.

147.   Leet, K.-H.; Hayashi, N.; Okano, M.; Hall, I. H.; Wu, R.-Y.; McPhailti, A. T. Lasiodiplodin, a potent antileukemic macrolide from Euphorbia splendens. *Phytochem.* **1982**, *21*, 1119-1121.

148.   Wicklow, D. T.; Joshi, B. K.; Gamble, W. R.; Gloer, J. B.; Dowd, P. F. Antifungal Metabolites (Monorden, Monocillin IV, and Cerebrosides) from Humicola fuscoatra Traaen NRRL 22980, a Mycoparasite of Aspergillus flavus Sclerotia. *Appl. Environ. Microbiol.* **1998**, *64*, 4482-4484.

149.   Wu, Y.; Liao, X.; Wang, R.; Xie, X.-S.; De Brabander, J. K. Total Synthesis and Initial Structure−Function Analysis of the Potent V-ATPase Inhibitors

Salicylihalamide A and Related Compounds. *J. Am. Chem. Soc.* **2002**, *124*, 3245-3253.

150.   Smith, A. B.; Zheng, J. Total synthesis of (-)-salicylihalamide A and related congeners. *Tetrahedron* **2002**, *58*, 6455-6471.

151.   Lebreton, S.; Xie, X.-S.; Ferguson, D.; De Brabander, J. K. Ring-closing metathesis: a powerful tool for the synthesis of simplified salicylihalamide-based V-ATPase inhibitors. *Tetrahedron* **2004**, *60*, 9635-9647.

152.   Nicolaou, K. C.; David, W. K.; Rachid, B.; Aurora, O.; Paraskevi, G. Total Synthesis and Biological Evaluation of (-)Apicularen A and Analogues Thereof. *Chem. Eur. J.* **2003**, *9*, 6177-6191.

153.   Bhattacharjee, A.; Seguil, O. R.; De Brabander, J. K. Total synthesis and biological evaluation of apicularen A and synthetic analogs. *Tetrahedron Lett.* **2001**, *42*, 1217-1220.

154.   Andreas, F. P.; Florenz, S.; Martin, E. M. Synthesis and Biological Evaluation of Apicularen A Analogues. *Eur. J. Org. Chem.* **2005**, *2005*, 1865-1875.

155.   Shen, R.; Lin, C. T.; Bowman, E. J.; Bowman, B. J.; Porco, J. A. Synthesis and V-ATPase Inhibition of Simplified Lobatamide Analogues. *Org. Lett.* **2002**, *4*, 3103-3106.

156.   Shen, R.; Lin, C. T.; Bowman, E. J.; Bowman, B. J.; Porco, J. A. Lobatamide C: Total Synthesis, Stereochemical Assignment, Preparation of Simplified Analogues, and V-ATPase Inhibition Studies. *J. Am. Chem. Soc.* **2003**, *125*, 7889-7901.

157.	Shen, R.; Inoue, T.; Forgac, M.; Porco, J. A. Synthesis of Photoactivatable Acyclic Analogues of the Lobatamides. *J. Org. Chem.* **2005**, *70*, 3686-3692.

158.	Liu, S.; Hanzlik, R. P. Structure-activity relationships for inhibition of papain by peptide Michael acceptors. *J. Med. Chem.* **2002**, *35*, 1067-1075.

159.	Engel, J. C.; Doyle, P. S.; Hsieh, I.; McKerrow, J. H. Cysteine Protease Inhibitors Cure an Experimental Trypanosoma cruzi Infection. *J. Exp. Med.* **1998**, *188*, 725-734.

160.	Somoza, J. R.; Zhan, H.; Bowman, K. K.; Yu, L.; Mortara, K. D.; Palmer, J. T.; Clark, J. M.; McGrath, M. E. Crystal Structure of Human Cathepsin V. *Biochemistry* **2000**, *39*, 12543-12551.

161.	Frankel, B. A.; Bentley, M.; Kruger, R. G.; McCafferty, D. G. Vinyl Sulfones: Inhibitors of SrtA, a Transpeptidase Required for Cell Wall Protein Anchoring and Virulence in Staphylococcus aureus. *J. Am. Chem. Soc.* **2004**, *126*, 3404-3405.

162.	Mc Cormack, T.; Baumeister, W.; Grenier, L.; Moomaw, C.; Plamondon, L.; Pramanik, B.; Slaughter, C.; Soucy, F.; Stein, R.; Zühl, F.; Dick, L. Active Site-directed Inhibitors of Rhodococcus 20 S Proteasome. *J. Biol. Chem.* **1997**, *272*, 26103-26109.

163.	Palmer, J. T.; Rasnick, D.; Klaus, J. L.; Bromme, D. Vinyl Sulfones as Mechanism-Based Cysteine Protease Inhibitors. *J. Med. Chem.* **2002**, *38*, 3193-3196.

164.	Kettner, C.; Mersinger, L.; Knabb, R. The selective inhibition of thrombin by peptides of boroarginine. *J. Biol. Chem.* **1990**, *265*, 18289-18297.

165.   Snow, R. J.; Bachovchin, W. W.; Barton, R. W.; Campbell, S. J.; Coutts, S. J.; Freeman, D. M.; Gutheil, W. G.; Kelly, T. A.; Kennedy, C. A. Studies on Proline Boronic Acid Dipeptide Inhibitors of Dipeptidyl Peptidase IV: Identification of a Cyclic Species Containing a B-N Bond. *J. Am. Chem. Soc.* **1994**, *116*, 10860-10869.

166.   Kinder, D. H.; Katzenellenbogen, J. A. Acylamido boronic acids and difluoroborane analogs of amino acids: potent inhibitors of chymotrypsin and elastase. *J. Med. Chem.* **1985**, *28*, 1917-1925.

167.   Minkkilä, A.; Saario, S. M.; Käsnänen, H.; Leppänen, J.; Poso, A.; Nevalainen, T. Discovery of Boronic Acids as Novel and Potent Inhibitors of Fatty Acid Amide Hydrolase. *J. Med. Chem.* **2008**, *51*, 7057-7060.

168.   Millennium Pharmaceuticals, Inc. Synthesis of Boronic Ester and Acid Compounds. World Intellectual Property Organization 097809, October 20, 2005.

169.   Borissenko, L.; Groll, M. 20S Proteasome and Its Inhibitors: Crystallographic Knowledge for Drug Development. *Chem. Rev.* **2007**, *107*, 687-717.

170.   Tully, W. R.; Gardner, C. R.; Gillespie, R. J.; Westwood, R. 2-(Oxadiazolyl)- and 2-(thiazolyl)imidazo[1,2-a]pyrimidines as agonists and inverse agonists at benzodiazepine receptors. *J. Med. Chem.* **2002**, *34*, 2060-2067.

171.   Chen, C.-y.; Senanayake, C. H.; Bill, T. J.; Larsen, R. D.; Verhoeven, T. R.; Reider, P. J. Improved Fischer Indole Reaction for the Preparation of N,N-Dimethyltryptamines: Synthesis of L-695,894, a Potent 5-HT1D Receptor Agonist. *J. Org. Chem.* **2002**, *59*, 3738-3741.

172.	Holla, B. S.; Gonsalves, R.; Shenoy, S. Synthesis and antibacterial studies of a new series of 1,2-bis(1,3,4-oxadiazol-2-yl)ethanes and 1,2-bis(4-amino-1,2,4-triazol-3-yl)ethanes. *Eur. J. Med. Chem.* **2000**, *35*, 267-271.

173.	Rydzewski, R. M.; Burrill, L.; Mendonca, R.; Palmer, J. T.; Rice, M.; Tahilramani, R.; Bass, K. E.; Leung, L.; Gjerstad, E.; Janc, J. W.; Pan, L. Optimization of Subsite Binding to the β5 Subunit of the Human 20S Proteasome Using Vinyl Sulfones and 2-Keto-1,3,4-oxadiazoles: Syntheses and Cellular Properties of Potent, Selective Proteasome Inhibitors. *J. Med. Chem.* **2006**, *49*, 2953-2968.

174.	Guimaraes, C. R. W.; Boger, D. L.; Jorgensen, W. L. Elucidation of Fatty Acid Amide Hydrolase Inhibition by Potent α-Ketoheterocycle Derivatives from Monte Carlo Simulations. *J. Am. Chem. Soc.* **2005**, *127*, 17377-17384.

175.	Seierstad, M.; Breitenbucher, J. G. Discovery and Development of Fatty Acid Amide Hydrolase (FAAH) Inhibitors. *J. Med. Chem.* **2008**, *51*, 7327-7343.

176.	Mileni, M.; Garfunkle, J.; DeMartino, J. K.; Cravatt, B. F.; Boger, D. L.; Stevens, R. C. Binding and Inactivation Mechanism of a Humanized Fatty Acid Amide Hydrolase by α-Ketoheterocycle Inhibitors Revealed from Cocrystal Structures. *J. Am. Chem. Soc.* **2009**, *131*, 10497-10506.

177.	Enders, D.; von Berg, S.; Jandeleit, B. Diethyl [(pheneylsulfonyl)methyl]phosphonate. *Org. Synth.* **2002**, *78*, 169-171.

178.   Polshettiwar, V.; Varma, R. S. Greener and rapid access to bio-active heterocycles: one-pot solvent-free synthesis of 1,3,4-oxadiazoles and 1,3,4-thiadiazoles. *Tetrahedron Lett.* **2008**, *49*, 879-883.

179.   Beenen, M. A.; An, C.; Ellman, J. A. Asymmetric Copper-Catalyzed Synthesis of α-Amino Boronate Esters from N-tert-Butanesulfinyl Aldimines. *J. Am. Chem. Soc.* **2008**, *130*, 6910-6911.

180.   Epp, J. B.; Widlanski, T. S. Facile Preparation of Nucleoside-5'-carboxylic Acids. *J. Org. Chem.* **1998**, *64*, 293-295.

181.   Beveridge, T. J. Use of the gram stain in microbiology. *Biotech. Histochem* **2001**, *76*, 111-118.

182.   Rietschel, E. T.; Kirikae, T.; Schade, F. U.; Mamat, U.; Schmidt, G.; Loppnow, H.; Ulmer, A. J.; Zahringer, U.; Seydel, U.; Di Padova, F. Bacterial endotoxin: molecular relationships of structure to activity and function. *FASEB J.* **1994**, *8*, 217-225.

183.   Rietschel, E. T.; Brade, L.; Lindner, B.; Zähringer, U. Biochemistry of lipopolysaccharides. In *Bacterial endotoxic lipopolysaccharides, vol. I. Molecular biochemistry and cellular biology*, Morrison, D. C.; Ryan, J. L., Eds. CRC Press: Boca Raton: 1992; pp 1-41.

184.   da Silva, A. M. T.; Kaulbach, H. C.; Chuidian, F. S.; Lambert, D. R.; Suffredini, A. F.; Danner, R. L. Shock and Multiple-Organ Dysfunction after Self-Administration of Salmonella Endotoxin. *N. Engl. J. Med.* **1993**, *328*, 1457-1460.

185.   Janeway Jr, C. A.; Medzhitov, R. Innate immune recognition. *Annu. Rev. Immunol* **2002**, *20*, 197-216.

186.   Rietschel, E. T.; Brade, H.; Brade, L.; Brandenburg, K.; Schade, U. F.; Seydel, U.; Zähringer, U.; Galanos, C.; Lüderitz, O.; Westphal, O.; Labischinski, H.; Kusumoto, S.; Shiba, T. Lipid A, the endotoxic center of bacterial lipopolysaccharides: Relation of chemical structure to biological activity. Progress in clinical and biological research. In *Progress in clinical and biological research*, New York, NY, 1987; Vol. 231, pp 25-53.

187.   Simpson, J. L.; Grissell, T. V.; Douwes, J.; Scott, R. J.; Boyle, M. J.; Gibson., P. G. Innate immune activation in neutrophilic asthma and bronchiectasis. *Thoarax* **2007**, *62*, 211-218.

188.   Dinarello, C. A. Cytokines as mediators in the pathogenesis of septic shock. *Curr. Top. Microbiol. Immunol.* **1996**, *216*, 133-165.

189.   Wendel, M.; Paul, R.; Heller, A. R. Lipoproteins in inflammation and sepsis. II. Clinical aspects. *Intensive. Care Med.* **2007**, *33*, 25-35.

190.   Rocke, D.; Gaffin, S.; Wells, M.; Koen, Y.; Brocke-Utine, J. Endotoxemia associated with cardiopulmonary bypass. *J. Thorac. Cardiovasc. Surg.* **1987**, *93*, 832-837.

191.   van Deventer, S.; ten Cate, J.; Tygat, G. Intesinal endotoxemia-Clinical significance. *Gastroenterology* **1998**, *94*, 825-831.

192.	Martin, G. S.; Mannino, D. M.; Eaton, S.; Moss, M. The epidemiology of sepsis in the United States from 1979 through 2000. *N. Engl. J. Med.* **2003**, *348*, 1546-1554.

193.	Danai, P.; Martin, G. S. Epidemiology of sepsis: recent advances. *Curr. Infect. Dis. Rep.* **2005**, *7*, 329-334.

194.	Angus, D. C.; Wax, R. S. Epidemiology of sepsis: an update. *Crit. Care Med.* **2001**, *29*, S109-S116.

195.	Bone, R. C. Gram-negative sepsis: a dilemma of modern medicine. *Clin. Microbiol. Rev.* **1993**, *6*, 57-68.

196.	Galanos, C.; Lüderitz, O.; Rietschel, E. T.; Westphal, O.; Brade, H.; Brade, L.; Freudenberg, M. A.; Schade, U. F.; Imoto, M.; Yoshimura, S.; Kusumoto, S.; Shiba, T. Synthetic and natural *Escherichia coli* free lipid A express identical endotoxic activities. *Eur. J. Biochem.* **1985**, *148*, 1-5.

197.	Means, T. K.; Golenbock, D. T.; Fenton, M. J. Structure and function of Toll-like receptor proteins. *Life Sci.* **2000**, *68*, 241-258.

198.	Medzhitov, R.; Preston-Hurlburt, P.; Janeway, C. A. A human homologue of the Drosophila Toll protein signals activation of adaptive immunity. *Nature* **1997**, *388*, 394-397.

199.	Gioannini, T.; Weiss, J. Regulation of interactions of Gram-negative bacterial endotoxins with mammalian cells. *Immunol. Res.* **2007**, *39*, 249-260.

200.	Miyake, K. Innate immune sensing of pathogens and danger signals by cell surface Toll-like receptors. *Semin. Immunol.* **2007**, *19*, 3-10.

201.   Schumann, R. R.; Leong, S. R.; Flaggs, G. W.; Gray, P. W.; Wright, S. D.; Mathison, J. C.; Tobias, P. S.; Ulevitch, R. J. Structure and function of lipopolysaccharide binding protein. *Science* **1990**, *249*, 1429-1431.

202.   Wright, S. D.; Tobias, P. S.; Ulevitch, R. J.; Ramos, R. A. Lipopolysaccharide (LPS) binding protein opsonizes LPS-bearing particles for recognition by a novel receptor on macrophages. *J. Exp. Med.* **1989**, *170*, 1231-1241.

203.   Wright, S. D.; Ramos, R. A.; Tobias, P. S.; Ulevitch, R. J.; Mathison, J. C. CD14, a receptor for complexes of lipopolysaccharide (LPS) and LPS binding protein. *Science* **1990**, *249*, 1431-1433.

204.   Qureshi, S. T.; Lariviere, L.; Leveque, G.; Clermont, S.; Moore, K. J.; Gros, P.; Malo, D. Endotoxin-tolerant Mice Have Mutations in Toll-like Receptor 4 (Tlr4). *J. Exp. Med.* **1999**, *189*, 615-625.

205.   Poltorak, A.; He, X.; Smirnova, I.; Liu, M.-Y.; Huffel, C. V.; Du, X.; Birdwell, D.; Alejos, E.; Silva, M.; Galanos, C.; Freudenberg, M.; Ricciardi-Castagnoli, P.; Layton, B.; Beutler, B. Defective LPS Signaling in C3H/HeJ and C57BL/10ScCr Mice: Mutations in Tlr4 Gene. *Science* **1998**, *282*, 2085-2088.

206.   Park, B. S.; Song, D. H.; Kim, H. M.; Choi, B.-S.; Lee, H.; Lee, J.-O. The structural basis of lipopolysaccharide recognition by the TLR4-MD-2 complex. *Nature* **2009**, *458*, 1191-1195.

207.   Kirschning, C. J.; Wesche, H.; Merrill Ayres, T.; Rothe, M. Human Toll-like Receptor 2 Confers Responsiveness to Bacterial Lipopolysaccharide. *J. Exp. Med.* **1998**, *188*, 2091-2097.

208. O'Neill, L. A. J.; Bowie, A. G. The family of five: TIR-domain-containing adaptors in Toll-like receptor signalling. *Nat. Rev. Immunol.* **2007**, *7*, 353-364.

209. David, S. A. Towards a rational development of anti-endotoxin agents: novel approaches to sequestration of bacterial endotoxins with small molecules. *J. Mol. Recognit.* **2001**, *14*, 370-387.

210. Rifkind, D. Prevention by polymyxin B of endotoxin lethality in mice. *J. Bacteriol.* **1967**, *93*, 1463-1464.

211. Danner, R. L.; Joiner, K. A.; Rubin, M.; Patterson, W. H.; Johnson, N.; Ayers, K. M.; Parrillo, J. E. Purification, toxicity, and antiendotoxin activity of polymyxin B nonapeptide. *Antimicrob. Agents Chemother.* **1989**, *33*, 1428-1434.

212. Miller, K. A.; Suresh Kumar, E. V. K.; Wood, S. J.; Cromer, J. R.; Datta, A.; David, S. A. Lipopolysaccharide Sequestrants: Structural Correlates of Activity and Toxicity in Novel Acylhomospermines. *J. Med. Chem.* **2005**, *48*, 2589-2599.

213. Burns, M. R.; Jenkins, S. A.; Kimbrell, M. R.; Balakrishna, R.; Nguyen, T. B.; Abbo, B. G.; David, S. A. Polycationic Sulfonamides for the Sequestration of Endotoxin. *J. Med. Chem.* **2007**, *50*, 877-888.

214. David, S. A.; Silverstein, R.; Amura, C. R.; Kielian, T.; Morrison, D. C. Lipopolyamines: Novel Antiendotoxin Compounds That Reduce Mortality in Experimental Sepsis Caused by Gram-Negative Bacteria. *Antimicrob. Agents Chemother.* **1999**, *43*, 912-919.

215.   Burns, M. R.; Wood, S. J.; Miller, K. A.; Nguyen, T.; Cromer, J. R.; David, S. A. Lysine-spermine conjugates: hydrophobic polyamine amides as potent lipopolysaccharide sequestrants. *Bioorg. Med. Chem.* **2005**, *13*, 2523-2536.

216.   Wood, S. J.; Miller, K. A.; David, S. A. Anti-Endotoxin Agents. 2. Pilot High-Throughput Screening for Novel Lipopolysaccharide-Recognizing Motifs in Small Molecules *Comb. Chem. High Throughput Screen.* **2004**, *7*, 733-743.

217.   Khownium, K.; Wood, S. J.; Miller, K. A.; Balakrishna, R.; Nguyen, T. B.; Kimbrell, M. R.; Georg, G. I.; David, S. A. Novel endotoxin-sequestering compounds with terephthalaldehyde-bis-guanylhydrazone scaffolds. *Bioorg. Med. Chem.* **2006**, *16*, 1305-1308.

218.   Kuhnert, N.; Rossignolo, G. M.; Lopez-Periago, A. The synthesis of trianglimines: on the scope and limitations of the [3 + 3] cyclocondensation reaction between (1R,2R)-diaminocyclohexane and aromatic dicarboxaldehydes. *Org. Biomol. Chem.* **2003**, *1*, 1157-1170.

219.   Akine, S.; Taniguchi, T.; Nabeshima, T. Synthesis and crystal structure of a novel triangular macrocyclic molecule, tris(H2saloph), and its water complex. *Tetrahedron Lett.* **2001**, *42*, 8861-8864.

220.   van Otterlo, W. A. L.; Ngidi, E. L.; de Koning, C. B. Sequential isomerization and ring-closing metathesis: masked styryl and vinyloxyaryl groups for the synthesis of benzo-fused heterocycles. *Tetrahedron Lett.* **2003**, *44*, 6483-6486.

221. Ulrich, P.; Cerami, A. Trypanocidal 1,3-arylene diketone bis(guanylhydrazones). Structure-activity relationships among substituted and heterocyclic analogs. *J. Med. Chem.* **1984**, *27*, 35-40.

222. Wood, S. J.; Miller, K. A.; David, S. A. Anti-Endotoxin Agents. 1. Development of a Fluorescent Probe Displacement Method Optimized for the Rapid Identification of Lipopolysaccharide-Binding Agents. *Comb. Chem. High Throughput Screen.* **2004**, *7*, 239-249.

223. Green, L. C. W., D. A.; Glogowski, J.; Skipper, P. L.; Wishnok, J. S.; Tannenbaum, S. R. Analysis of nitrate, nitrite and [^{15}N]nitrate in biological fluids. *Anal. Biochem.* **1982**, *126*, 131-138.

224. Copeland, S.; Warren, H. S.; Lowry, S. F.; Calvano, S. E.; Remick, D.; the, I.; the Host Response to Injury, I. Acute Inflammatory Response to Endotoxin in Mice and Humans. *Clin. Diagn. Lab. Immunol.* **2005**, *12*, 60-67.

225. Tian, D.; Das, S. G.; Doshi, J. M.; Peng, J.; Lin, J.; Xing, C. sHA 14-1, a stable and ROS-free antagonist against anti-apoptotic Bcl-2 proteins, bypasses drug resistances and synergizes cancer therapies in human leukemia cell. *Cancer Lett.* **2008**, *259*, 198-208.